PRODUCTION, CHARACTERIZATION AND SI ENGINE PERFORMANCE EVALUATION OF PALM BUNCH BIOETHANOL

BY

LOVELYN NGOZI ONUOHA (B.Eng, M.Eng.)
REG. No. 20144918898

A THESIS SUBMITTED TO THE POSTGRADUATE SCHOOL, FEDERAL UNIVERSITY OF TECHNOLOGY, OWERRI, NIGERIA.

IN PARTIAL FULFILMENT OF THE REQUIREMENTS FOR

THE AWARD OF THE DEGREE OF DOCTOR OF

PHILOSOPHY (PhD) IN ENERGY AND POWER ENGINEERING

SEPTEMBER, 2018

PRODUCTION, CHARACTERIZATION AND SI ENGINE PERFORMANCE EVALUATION OF PALM BUNCH BIOETHANOL

BY

LOVELYN NGOZI ONUOHA (B.Eng, M.Eng.)
REG. No. 20144918898

A THESIS SUBMITTED TO THE POSTGRADUATE SCHOOL, FEDERAL UNIVERSITY OF TECHNOLOGY, OWERRI, NIGERIA.

SUPERVISORS:

ENGR. PROF. O.M.I. NWAFOR

ENGR. DR. J. O. IGBOKWE

ENGR. DR. B. OKAFOR

SEPTEMBER, 2018

DECLARATION

I, LOVELYN NGOZI ONUOHA (20144918898), declare this that the work in this thesis represents my original work and has not been previously submitted elsewhere or in this University for the award of degree.

CERTIFICATE

We hereby certify that this research, "Production, Characterization and SI Engine Performance Evaluation of Palm Bunch Bioethanol" is original work of LOVELYN NGOZI ONUOHA (20144918898) and has not been submitted elsewhere for the award of any degree.

Signature..... Date 05/11/18

Engr. Prof. O.M.I. Nwafor
Supervisor,

Signature..... Date 05/11/18

Engr. Dr. J.O. Igbokwe
Supervisor,

Signature..... Date 05/11/2018

Engr. Dr. B. Okafor
Supervisor,

Signature..... Date 05/11/18.

Engr. Dr. G. O. Osueke
Head of Department,

Signature..... Date 17/12/18

Engr. Prof. G.I. Nwandikom
Dean of School of Engineering and Engineering Technology

Signature..... Date .....

Prof. (Mrs.) Nnenna N. Oti
Dean of Post Graduate School

Signature..... Date .....

External Examiner

DEDICATION

This work is dedicated specially to my beloved father Elder Hillary Onuoha Osuji

and Dearest mum, Mrs.Virginia A. Onuoha.

ACKNOWLEDGEMENT

I am most grateful to the Almighty GOD who sustained my willing power to endure during hard and trying periods. Thank you, Almighty GOD.

To my beloved father, I am grateful for your providing me with the fertile ground for my development. You are a model indeed.

I am grateful to my supervisors, Prof. O.M.I. Nwafor, Engr. Dr. J. O. Igbokwe and Engr. Dr. B. Okafor who despite their stream of schedules attended to my work with constructive criticism and careful suggestions. Words are not enough to express my gratitude and appreciation.

To my HOD, Engr. Dr. G. Osueke, my Co-ordinator, Engr. Dr. O. Obiukwu, all the lecturers and other members of staff in the Department of Mechanical Engineering, FUTO, I express my appreciation for all the assistance rendered to me in the course of this study.

My special thanks go to my friends, brothers and sisters for their prayers and sacrifice; to my counselors, Prof. A. T. Suleiman, of Bayero University Kano, Mrs Chinyere Ujah, of DCLM, Prof. N. N. Aviara, of University of Maiduguri, Mr O. Elom, Prof. E. Ofodile, of Paul University, Awka, Anambra State, for the stimulating guidance, constant encouragement and suggestions throughout the process of the work.

To my course mates, Olisaemeka Nwufo, Jerry Azubuike, Boniface Ibe, Godswill Nwaji, Micheal, Chibuike and Chidi Nwaiwu, I say thank you for your goodness throughout this period.

Thank you all!

TABLE OF CONTENTS

LIST OF TABLES

LIST OF FIGURES

LIST OF PLATES

NOMENCLATURE

Symbol	Definition	Unit
A	Absorbance	Nm
a	cylinder bore	mm
BMEP	Brake mean effective pressure	bar
BP	Brake power	kW
BSFC	Brake specific fuel consumption	Kg/kW-h
BTE	Brake thermal efficiency	%
CR	Compression ratio	Dimensionless
FCR	Fuel consumption rate	Kg/h
FP	Frictional power	kW
HVF	heating value of fuel	kJ/kg
N	Engine speed	RPM
T	Torque	N
t	time	s
T_a	Ambient temperature	^{0}C
V_c	clearance volume	mm^3
V_f	Volume of fuel	mm^3
VI	Viscosity Index	dimensionless
w	Weight, Load	kg
ρ	density	Kg/m^3
μ	viscosity	m^2/s

ABSTRACT

This study investigates bioethanol production from waste palm bunch. This project falls under the focus category of waste to energy as it addressed issues relating to conversion of waste which poses a disposal burden to energy. Physical properties of the feedstock which was collected from Siat Nigeria Limited Ubima, Rivers State were determined to consist of 57.44 % cellulose, 16.89 % hemicelluloses, 15.87 % lignin and 5.57 % ash. The raw material was prepared by physical pretreatment, chemical hydrolysis, fermentation and distillation to obtain bioethanol fuel. The presence of bioethanol and its optimum preparation condition were established from a preliminary experiment in the laboratory. The physical pretreatment which is the most critical step being labour intensive reduced the feedstock size to 850 microns. Hydrolysis carried out with H_2SO_4 on 200 g of the pretreated raw material gave optimum yield of 27 g/L xylose and 49 g/L glucose with 1.2 % acid load for 30 minutes at 160 ^{0}C, giving a total sugar yield of 76 g/L. Fermentation of the optimum hydrolyzate with S. cereviasea for 72 hours at room temperature gave optimum bioethanol yield of 32 g/L. A charcoal fueled distiller of 20 L feed/h loading capacity, 8.95 kW reactor power rating was fabricated based on the preliminary data. The distiller was used to distill bioethanol from the optimum fermentate, at 75 % combustion efficiency. 817 ml of bioethanol was obtained in 115 minutes at actual combustion efficiency of 55 % and power rating of 12.2 kW. The distiller has high flexibility of handling various boiler feed using different biomass solid fuel in the reactor. The produced bioethanol elemental analysis conforms to ASTM D4806. Fuel blends of the bioethanol with pure petrol were characterized based on ASTM D4814. At 15 ^{0}C, density of pure petrol increased from 744.73 kg/m^3 to 782.5 kg/m^3 with increase in bioethanol while E100 has 791.13 kg/m^3. Octane number of pure petrol increased with increase in bioethanol in the blends. Flash point of all the blends is below 15 ^{0}C making them susceptible to ignition and has the chance of flammability hazard. The vapour pressure of pure petrol increased with 10 % bioethanol but decreased with increase in bioethanol from 20 %. Bioethanol content above 10 % increased viscosity of pure petrol. Calorific value of pure petrol was decreased with increase in bioethanol percentage in the blends. The suitability of the fuel blends as SI engine fuels were studied at full, 3/4 and 1/2 engine loads; and at 2500 rpm, 3000 rpm and 3500 rpm engine speeds. The performance evaluation was carried out in a single cylinder, four strokes, air cooled Petrol Engine. The performance characteristics observed showed that, blending pure petrol with the bioethanol increases the brake power, brake specific fuel consumption and brake thermal efficiencies. The engine performance results recommend blending pure petrol with 10 – 30 % of the bioethanol. Thus, the need of bioethanol for energy sector could be met by using Nigerian waste palm bunch as raw material.

Keywords: *Waste Palm bunch, Bioethanol, Distiller and Engine performance.*

CHAPTER ONE

INTRODUCTION

1.1 Background of the Study

The standard of living of the people of any country is considered to be directly proportional to the energy consumption of its people (Peter & Gbenga, 2007). The disparity one feels from country to country arises from the extent of accessible energy for the citizens of each country. Fossil fuels particularly oil, coal and natural gas have been providing over 90 % of world's energy demands mainly because they are readily available and convenient to use (Ashish & Mohapatra 2013). The geographical non equi-distribution of this source and also the ability to acquire, control the production and supply of this energy source have given rise to many issues and also disparity in the standard of living. Upon this these resources are not renewable and will eventually deplete (Ganesan & Elango 2013), the readily accessible reserves may well get exhausted by 2030 (Helma 2013, Tan et. al., 2014). Fossil fuels have high energy intensity and have heralded technological progress but its lead to air pollution, acid rain, increasing levels of tropospheric ozone, depletion of stratospheric ozone, greenhouse effect and thereby global warming which are serious environmental threats and harmful to human health (Scott 2013, Siddegowda & Venkatesh 2013). Six greenhouse gases have been identified under the Kyoto Protocol to include Carbon dioxide ($C0_2$), Methane (CH_4), Nitrous oxide (N_20), Hydrofluorocarbons (HFCs), Perfluorocarbons (PFCs) and Sulphur hexafluoride (SF_6), as listed in Annex A of the Koyoto Protocol. The current trajectory of fossil fuel use and its related emission of these greenhouse gases are unsustainable (IEA 2008); the environment is in threat by exploration of oil. Presently, in Nigeria there are over 11 oil companies operating 1,481 wells from 159 oil fields in the Niger Delta producing 2.7 million barrels of crude oil each day and flaring about 17 billion cubic meters of associated gas, spewing 2,700 tons of particulates, 160 tons of sulphur oxides, 5,400 tons of carbon monoxide, 12 and 3.5 million tons of methane and carbon dioxide, respectively, in the process (Peter & Gbenga, 2007). Dheeraj et. al., (2014) reported that the contribution to global anthropogenic emissions from transportation amounts to 21% of CO_2, 37% of Nox, 19% of volatile organic compounds (VOCs), 18% of CO and 14% of black carbon, the main source of carbonyls and VOCs result directly from incomplete combustion of fossil fuel such as vehicle exhausts and biomass burning. The continual and increasing energy demand of the world, advances in technology,

uneven distribution around the globe and non renewability of fossil fuels in addition to the rising costs of its resulting pollution led to desire for an alternative or a fuel additive which led to the increasing demand for biofuels (Ferreira et al., 2010). Thus, there is need for fuels from renewable energy sources, clean air and improving engine efficiency which can be achieved with fuels of high compression tolerance, higher latent heat of vaporization, higher anti-knocking characteristics and better combustion (Ganesan & Elango, 2013, Helma, 2013, Dheeraj et. al., 2014). The renewable feedstock is to be abundant in nature and competes not with human food supply hence; utilizing renewable agricultural wastes is of great benefit as the disposal problems of such wastes are then eliminated while energy and environmental advantages are gained against their direct combustion which causes air pollution. According to the experts programs of the World Committee of Energy Council, it is predicted that in 2070 the contribution of renewable energy to the total world energy balance will be about 60 % (Wladyslaw et al., 2008, UNDP 2007). World ethanol production for transport fuel tripled between 2000 and 2007 from 17 billion to more than 52 billion liters and reached 84.6 billion liters in 2011, with United States as the top producer (52.6 billion liters), accounting for 62.2 % of global production, followed by Brazil with (21.1 billion liters) (Hossein et. al., 2006, Steenblik 2007). Owing to its widespread availability, biorenewable fuel technology will potentially result to more employment than fossil-fuel-based technology (Demirbas 2006, Shyam et. al., 2012, Karl et. al., 2005). Due to high-energy values, ethanol is the most promising future biofuel (Veronica et al., 2010, Ferreira et al., 2010). Generally, modernizing biomass energy production however faces a variety of challenges which include technical problems, resource availability, environmental impacts, and economic feasibility **(**Antonia et al., 2000). In spite this limitation, the market of ethanol for fuel is increasing. Its energy content is about 70 % of that of petrol (Pradeep and Samir, 2011). Its reduction in greenhouse gas emission is an added value. With advancement in science and technology, the benefits derivable from bioethanol have continued to multiply; medically, ethanol is sleep inducing; Pharmaceutical; it is use in preparing cough syrups and antiseptics. Raw materials; it is use as a solvent in the manufacture of varnishes and perfumes; as explosives, detergents, germicide, anti-freeze in automobile radiators, versatile intermediate for organic chemicals e.g. acetaldehyde, ethylene, glycol, dyes, cleaning solution etc. It is used in preparing alcoholic beverages also, as a preservative for biological specimens. Bioethanol is unique amongst

today's sustainable fuel options; in that it can be used in internal combustion engines and also as a perfect fuel source for hydrogen fuel cell.

The enormous advantages of ethanol and other biofuels have geared researches towards the production of biofuel from various renewable organic raw materials like corn, cassava, palm oil etc. However, in an attempt to save the food chain and to reduce the inflation of food prices caused by biofuels from agricultural feed, researches are being directed to the production of biofuels from agricultural waste e.g. lignocelluloses like sugar cane baggase, palm bunch etc., which constitutes approximately 50 % of land produced biomass (Ganesan & Elango 2013, Thallada et al., 2011). It is estimated that ethanol produced from the world's agriwaste and forest residues could replace 32 % of global petrol consumption (Leland, 2005). Thus, implementation of efficient bioethanol production from lignocellulose can be a breakthrough in the fuel market or world's energy portfolio (Piotr et al., 2007; Leland, 2005). Currently, there are not many biomasses to ethanol plants in commercial operation in Nigeria, thus, the real or perceived risks will only be addressed when several plants are in successful operation. As the technology matures, however, producing ethanol from lignocellulosic wastes will become more competitive with other means. Palm bunch is a lignocellulosic agricultural waste that remains after the removal of palm fruits from the bunch. In Nigeria, the quantities of palm bunch available in palm oil producing states are high; thus converting these to bioethanol fuel would have a significant positive economic impact on the nation. Also the use of local feed stocks from Nigeria would enhance both the grower's and the nation's economy by partially augmenting fuel exports. The utilization of lignocellulosic biomass for bioethanol production necessitates the large-scale production techniques to be cost effective and environmentally sustainable. Although extensive studies have been carried out using food crops as feedstock to meet the future challenges of bioenergy generation, attention is still required in the conversion of lignocellulosic biomass to bioethanol. The yield and fuel properties of bioethanol from Nigerian palm bunch, and factors that affects them is yet to be extensively studied. Also the produced bioethanol fuel adaptability to the existing engines still needs to be guaranteed. This study will produce bioethanol from waste palm bunch and investigate its fuel properties and adaptability in existing spark ignition engines. It proposes achieving commercial lignocellulosic biofuel production in Nigeria, to gradually reduce the nation's dependence on petrol, and precipitate sustainable domestic jobs.

1.2 Statement of the Problem

There are increasing costs of fossil fuels; also its finite nature, environmental threat-pollution, and the need to increase engine life and efficiency have been a problem to the world. These problems call for alternative energy sources. The required alternative energy sources need to have some desirable characteristics such as low cost, abundance / availability, conveniently usable, clean combustion, and renewable nature, economically transportable and socially compatible. Though alternative energy sources such as solar, wind, tidal, ocean, geothermal etc. are available in plenty and environmental compatible, their harnessing are still poor due to drawbacks such as productive cost and unfeasible technological know-how. Thus, this search for alternative energy sources led to this research to produce bioethanol. Bioethanol can be considered as the only conceivable energy source that is an ideal fuel of the future because of its non-polluting, high compression resistance and renewable nature. Little work has been done towards lignocellulosic biofuel production and usage in Nigeria. Hence, working out the technical and economic feasibility of lignocellulosic biofuel by this research is of major importance. This report proposes achieving commercial lignocellulosic bioethanol production in Nigeria, to gradually reduce the nation's dependence on petrol, reduce environmental pollution while at the same time create a commercially viable industry that can precipitate sustainable domestic jobs.

1.3 Objectives of the Study

The main objective of this study is to produce, characterize and evaluate the SI engine performance of bioethanol from Nigerian waste palm bunch.

The specific objectives are to:

(i) Fabricate a distiller for the waste palm bunch broth distillation.

(ii) Produce bioethanol fuel from the waste palm bunch using the fabricated distiller.

(iii) Characterize the produced bioethanol fuel using ASTM standard.

(iv) Carry out performance evaluation of the produced bioethanol fuel on spark ignition engine.

1.4 Significance of the Study

This study will produce bioethanol fuel from biomass waste, which could be conveniently used in spark ignition engine and produce to exportable level. The quality of the environment improves; as combustion is improved, carbon monoxide emissions will be reduced, lead and other carcinogens (cancer causing agents) are removed from petrol. The engine overall efficiency will increase due to higher latent heat of vaporisation and higher anti-knocking characteristics of the fuel. These ensure reduction of heat loss and higher air-fuel mixture compression respectively and, consequently, better thermal efficiency, potential energy efficiency and performance gain. The study will also produce a distiller for biofuel production. The project falls under the focus category of second generation energy production as it addresses issues relating to conversion of waste which poses a disposal burden to energy. Converting lignocellulosic waste organic farm produce to a high quality fuel would provide an economic opportunity for Nigeria. The target beneficiaries are transporters, car owners, organizations, homes, the nation and world at large.

1.5 Scope of the Study

In the course of this study, the chosen waste organic raw material for the production of bioethanol fuel is Nigerian waste palm bunch. The scope is the production of bioethanol fuel from the waste palm bunch, distilled with the fabricated distiller; the product fuel will be characterized using ASTM standard after which its performance in a spark ignition engine will be evaluated without considering the engine emission. Finally, analysis of the results will be carried out.

CHAPTER TWO

LITERATURE REVIEW

2.1 Biofuels

Biofuels shall mean fuel ethanol and biodiesel and other fuels e.g. biohydrogen made from biomass and primarily used for automotive, thermal and power generation, according to quality specifications set by the American Society for Testing and Materials (ASTM), the Environmental Protection Agency (EPA), state regulatory agencies and their own company standards. Biodiesel is the product obtained when a vegetable oil or animal fat is chemically reacted with an alcohol to produce mono alkyl esters of fatty acid (van et. al., 2004). Bioethanol is produced from any biological feedstock that contains sugar or materials that can be converted into sugar such as starch or cellulose (Kristina et. al., 2008). Biohydrogen is mainly produced from biomass using bacterial micro organisms and from water by bio-photolysis (Hema 2013). Organic wastes frequently contain sugar or sugar polymers. It is not however easy to obtain organic wastes containing organic acids as the main components. Fermentative bacteria metabolize sugars to produce hydrogen gas and organic acids, but are incapable of further breaking down the organic acids formed, proposing the use of hybrid system (involving photosynthetic and fermentative bacteria) for the conversion of organic acids to hydrogen (Hema 2013). Theoretically, one mole of glucose can be converted to 12 moles of hydrogen using photosynthetic bacteria capable of capturing light energy in such a combined system. Bioethanol has a higher octane number with broader flammability limit, higher flame speeds, and higher heats of vaporization than petrol. As a result, it will lead to higher compression ratio, shorter burn time, and leaner burn (Dias de Oliveira et al, 2005). This sparks the interest of using bioethanol as a long term solution for transportation fuel.

2.2 Ethanol

Ethanol, CH_3CH_2OH, is an alcohol, a group of organic chemical compounds whose molecules contain a hydroxyl group, –OH, bonded to a carbon atom. Ethanol also known as ethyl alcohol or grain alcohol is a colorless, volatile and flammable liquid. It has a somewhat sweet flavor in dilute aqueous solution and a burning taste in more concentrated solutions (Alvydas et. al., 2003). Table 2.1 gives properties of fuels from literatures.

Table 2.1: Properties of Fuels from Literatures (NIOSH, Siddegowda & Venkatesh (2013), Ullmann 1990, Ashish & Deshmukh 2012, DOE, Anderson et al, 2012)

Properties	**Petrol**	**Diesel**	**LPG**	**Ethanol**
Chemical formula	mCnH2n	C_{10-21} HC	C_3H_8	C_2H_5OH
Molecular weight (kg/kmol)			44.1	46.07
Flash Point	-45°F, 25^{0}C	52^{0}C		-5°F, 13 ^{0}C
Stoichiometric A/F ratio	14.7	15	15.6	9
Ignition limits (A/F ratio)	6 - 22			3.5 - 17
Ignition Temperature	530–853°F≈300^{0}C	316^{0}C		793°F, 420 ^{0}C
Cetane number	10-20	55		8
Octane number: RON	90 -100	03	106 -130	102 -130
MON	80 - 92		89 -103	89 - 96
Blending RON	90 -100			112 -120
Blending MON	80 - 92			95 -106
Specific Gravity at 15^{0}C	0.72 – 0.76 k g/l	0.84 k g/l	0.53 kg/l	0.79 kg/l
Vapor Density	3 – 4			1.49
Vapor Pressure	60 - 90 (kPa)			19.3 (kPa)
Heat of vaporization	0.36 (MJ/kg)	115Btu/lb		0.92 (MJ/kg)
Lower Calorific value	43000 kJ/kg	46500 kJ/kg	46100	29,895 kJ/kg
Upper Calorific value	47300 kJ/kg	42.52(MJ/kg)	kJ/kg	29,964 kJ/kg
Kinematic Viscosity 20°C	0.4 - 0.8 (mm^2/s)	2.97 at 4^{0}C		1.52 (mm^2/s)
Energy content	34.8 MJ/L	38.6 MJ/L 45.4	25.3MJ/L	21.2 MJ/L 26.8
	44.4 MJ/kg	MJ/kg	55 MJ/kg	MJ/kg
Boiling Point	30 - 225 ^{0}C	125 – 400 ^{0}C	-44 ^{0}C	78.39 ^{0}C
Freezing point	-107.4 ^{0}C			-117.2 ^{0}C
Melting point				-114.15 ^{0}C
Flammable Range: LEL	1.4		4.1	4.3
(%vol) UEL	7.6		74.5	19
Flame speed	52.58 m/s		48 m/s	
Water Solubility	None	insoluble		Completely

LPG: Liquified petroleum gas.

Low freezing point of ethanol made it a useful fluid in thermometers for temperatures <40°C, the freezing point of mercury, and for other low-temperature purposes, such as for antifreeze in automobile radiators. Having a vapor density of 1.49, ethanol is heavier than air. Consequently, its vapor does not rise, similar to vapor from petrol, which seeks lower altitudes. With specific gravity of 0.79, ethanol is lighter than water but being hydrophilic unlike petrol, it thoroughly mixes easily with water. So, while it is possible to dilute ethanol to a condition where it no longer supports combustion, it is not practical in the field as it requires copious amounts of water (Chevron, 2004). Even at 5 parts water to 1 part ethanol, it will still burn. However, water in ethanol–water mixture reduces the mass burning rate due to increase in the boiling point and latent heat of vaporization (Alvydas et. al., 2003).

In comparison with commercial petrol, ethanol has higher density, higher octane number and is less toxic than petrol. Interestingly, ethanol and some ethanol blends can conduct electricity while petrol does not and is considered an electrical insulator. Like petrol, ethanol's greatest hazard as a motor fuel component is its flammability (RFA, 2010). It has a wider flammable range than petrol (Lower Explosive Limit is 3.3% and Upper Explosive Limit is 19%). In a pure form, ethanol does not produce visible smoke and has a hard-to-see blue flame. Ethanol and petrol mix readily with minimal agitation. Since ethanol has a greater affinity for water than it does for petrol, even at high concentrations of ethanol, minimal amounts of water will draw the ethanol out of the blend away from the petrol. Thus, over time, without agitation, petrol will be found floating on a layer of an ethanol/water solution i.e. phase separation. Phase separation can occur in fuel storage systems where water is known to be present (De-Menezes et. al., 2006, Shi et. al., 2005).

2.3 Ethanol Background

Bioethanol is produced from any biological feedstock that contains sugar or materials that can be converted into sugar such as starch or cellulose. There is currently no international standard for bioethanol, but many countries have their own standards or guidelines for fuel content and properties (Kristina et. al., 2008). Ethanol production, traces back as far as the days of Noah who was believed to have built himself a vineyard in which he grew grapes that he fermented into some sort of alcoholic beverages. The ancient Egyptians produced alcohol by naturally fermenting vegetative materials. Also in ancient times, the Chinese discovered

the art of distillation, which increases the concentration of alcohol in fermented solutions. Ethanol was first prepared synthetically in 1826, through the independent effort of Henry Hennel in Britain and S.G Serullas in France (Yanuandri et. al. 2014, Tan et. al., 2014). Michael Faraday prepared ethanol by the acid-catalyzed hydration of ethylene in 1828, in a process similar to that used for industrial synthesis of ethanol today (Boullanger 1924). In 1940s the first fuel ethanol plant was built in the U.S. in Omaha, Nebraska, to produce fuel for the army and for regional fuel blending (John 2006). Major quantities were not manufactured until the 1970s due to low cost of petrol between 1940s and 1970s, however the ethanol industry began to remerge when ethanol was used as a fuel extender during petrol shortages caused by the OPEC oil embargoes in 1973 (Nebraska, 2011, Antoni 2003, Wikipedia 2014d, John 2006). At that time petrol (gasoline) containing ethanol was called "gasohol". Later, when petrol was more plentiful, ethanol-petrol blend was introduced to increase the octane rating and the name "gasohol" was dropped in favor of names reflecting the higher octane levels, "E10 Unleaded" and "super unleaded" are examples of names used today. World Ethanol Market (2006), estimated petrol consumption in Nigeria is 30 million liters per day, consequently the use of E10 would require 3 million liters of ethanol per day. Nigeria under Nigerian Bio-fuel Policy and Incentives established a policy with the objective to firmly establish a thriving fuel ethanol industry utilizing agricultural products as a means of improving the quality of automotive fossil-based fuels in Nigeria (Antoni 2003). The Policy links the agricultural and energy sector, with the underlying aim of stimulating development in the agricultural sector.

First generation of ethanol used food crops to produce bioethanol. These food crops include corn, sugar cane, wheat, barley, rice, cassava etc. Table 2.2 presents the bioethanol fuelprograms in some countries. It reveals the efforts of different countries to promote bioethanol production.

Table 2.2: Bioethanol Fuel Programs in some Countries (Oscar & Carlos 2008, Antoni 2000)

Country	Feedstock	% bioethanol in petrol blends (v/v)	Remarks
Brazil	Sugar cane	24	ProAlcool program; hydrous ethanol is also used as fuel instead of gasoline
USA	Corn	10	Oxygenation of petrol is mandatory in dirtiest cities; tax incentives; some states have banned MTBE; 85% blends are also available
Canada	Corn, wheat, barley	7.5-10	Tax incentives; provincial programs aimed to meet Kyoto Protocol
Colombia	Sugar cane	10	Began in November 2005; total tax exemption
Spain	Wheat, barley		Ethanol is used for ETBE production; direct gasoline blending is possible
France	Sugar beet, wheat, corn	-	Ethanol is used for ETBE production; direct gasoline blending is possible
Sweden	wheat	-	85% blends are also available; there is no ETBE production
China	Corn, wheat		Trial use of fuel ethanol in central and north-eastern regions
India	Sugar cane	5	Ethanol blends are mandatory in 9 states
Thailand	Cassava, rice sugar cane,	10	All petrol stations in Bangkok must sell ethanol blends; ethanol blends will be mandatory from 2007

By using food crops, first generation of ethanol has been competing with food (Ruth 2008, Koonin 2006, Anjan 2013). According to Regmi et al (2001), a 1% increase in food prices causes an average of 0.75% decline in food consumption in developing countries. In addition to reducing caloric intake as food prices increase, low-income people also switch to less nutritious food (Von Braun 2007, Raneses et.al., 1998). For example Nigeria Global Bio-fuels limited invested about US$ 21 million in the sorghum to ethanol fuel production project (Philip and Mary, 2011). The fund will cover the purchase of about 10,000 hectares of virgin

land (forests and grasslands) covering seven states (Osun, Oyo, Kwara, Ondo, Ekiti, Niger and Kogi) in Nigeria and seven ethanol plants in each of the seven states, to produce about 1 million litres of ethanol per plant on a daily basis. Major players in the Energy sector see this as a distraction because there is no doubt that the sorghum feedstock for the biofuels plants will compete with production of food crops in the proposed state, thereby exacerbating hunger in the nation. Nigeria, failed with its policies to achieve E10 in 2010 because it adopts the use of staple foods (Phillips et al., 2011). Some of the bioethanol plant in Nigeria is given in table below Table 2.3.

Table 2.3: Bioethanol Plants in Nigeria (Phillips and Mary 2011)

Name of Company	**Plant Location**	**Feed stock**	**Feed stock yield**
Dura Clean	Bacita	Molasses/Cassava	4.4 (million ltr / yr)
AADL	Sango Ota	Cassava	10.9 "
CrowNek	Ekiti	Cassava	64.0 "
BV Energy Company	Bayelsa	Cassava	75.0 "
Akoni	Lagos	Cassava	53.0 "

Fuel bioethanol production has increased remarkably because many countries look for reducing oil imports, boosting rural economies and improving air quality (Ruth 2008). Nigeria is the largest producer of cassava in the world, but more than 90 % of cassava produced is used for domestic food consumption; so one major view shared by many on Nigeria bioethanol blend is her capacity to prevent food crises while achieving energy security.

The second generation of bioethanol is based on lignocellulosic agricultural wastes and forest residue (Yanuandri et. al. 2014, Lynd et al., 2009, Antoni 2003) which takes the pressure off of food crops and is less expensive than first generation feedstocks (Somerville 2006, Ruth 2008, Koonin 2006). Biomass feedstocks have a reduced contribution to greenhouse effect compared to fossil fuels, at least if it is produced in a sustainable way not leading to any deforestation (Grassi and Allan, 2007). Feedstocks were compared with respect to several social objectives as presented in Table 2.4. Cellulosic biomass is the best candidate for large-scale energy production in the long term among the feedstock types reported. This is because

of its potential in low fuel-production price, large-scale production, environmental, socioeconomic and political benefit effects (Lynd et al., 2009, Grassi and Allan, 2007; Hall, 1997). Thus, countries are shifting to second generation of bioethanol.

Table 2.4: Comparison of Feedstocks with Respect to Several Social Objectives (Lynd et al., 2009).

Feedstock Type	A) Large-Scale Production	B) Rural Economic Development	C) Petroleum Displacement	D) Fossil Fuel Displacement/ GHG Reduction	E) Soil Fertility & Agricultural Ecology	F) Low-Cost Fuels (Feedstock & Conversion)
	(Per unit Total)	(Now Future)	(Per unit Total)	(Per Unit Total)		(Now Future)
Cellulosic	•••• ••••	•• •••••	••••• •••••	••••• •••••	•••••	•• •••••
Starch rich	•••• ••	•••• •••	••••• •••	••• ••	••	••• •••
Sugar rich	••• ••	•••• •••	••••• •••	••••• ••••	••••	••• •••

Ratings: ••••• Excellent; •••• Very good; ••• Good; •• Fair; • Poor.

In the case of energy cogeneration/energy balance, cellulosic biomass is also an attractive alternative; because it is largely available and able to recycle part of CO_2 emitted during its planting cycle (Bourne 2007). Lignocellulosic feedstocks have the best well-to-wheel assessment, considering its abundance, low cost and high polysaccharides (cellulose and hemicellulose) content (Fujii et al., 2009). However, order of conversion costs using current technology is the opposite of that of feedstock purchase cost: cellulosic biomass > corn > sugarcane (Antoni 2003, Ashish M. and Mohapatra S. 2013). Taking both purchase price and current conversion technology into account, the near-term fuel cost is sugarcane ethanol < corn ethanol < cellulosic ethanol, whilst in the long term, incorporating advanced technological improvements, the projected selling price of cellulosic ethanol is less than the purchase cost of the other feedstocks considered (Lynd et al., 2009).

In the move from first to second generation, the U.S National Renewable Energy Laboratory (NREL) in 2002 published a detailed report documenting a process design and economic analysis for the biochemical conversion of lignocellulosic biomass (corn stover) to ethanol. The design makes use of dilute acid pretreatment followed by enzymatic saccharification and

cofermentation with recombinant *Zymomonas mobilis.* This design is not optimized; rather, it represents one technology package. Although experimentally verified data are contained in the report, it serves a more important function—to set the technological targets necessary for attaining U.S. Department of Energy (DOE) cost goals. The report still serves as the basis for the 2012 DOE goals (Andy Aden, 2008). Mabee and Saddler, (2010) reported the potential of Canada to meet as much as 50% of its demand for gasoline with the wide range of residual lignocellulosic feedstocks currently available. Winrock International India initiated the formation of an "Ethanol Coalition of India" in 2000 to promote the development of fuel ethanol (Rajeev et. al., 2010, Karl et. al., 2005). Carlos et al., (2010) and Karl et. al., (2005) reported that ethanol yield per hectare of sugarcane in Brazil presently is 6000 L/ha, and could reach 10,000 L/ha, if 50% of the produced bagasse would be converted to ethanol (Hossein et. al., 2006). As the world's most exciting oil palm industry cluster, Malaysia generates a great deal of lignocellulosic waste, it is working hard to solve its challenges such as immature policies, to convert these wastes to fuel ethanol (Chun et al., 2010, Norhisam et. al., 2011, Tan et. al., 2014). Efforts to identify new suitable biomass resources for cellulosic ethanol production are ongoing and intensive in many countries. In 2001 the Chinese State Development Commission launched an ethanol program and after careful consideration issued quality standards for denatured ethanol and ethanol blended gasoline; Beijing (China) also organised a World fuel ethanol congress (Karl et. al., 2005, Fang et. al., 2010). Aquatic biomasses including macroalgae and plantation wastes have been found to have great potential as feedstocks for the production of cellulosic ethanol in Korea; cellulosic ethanol is expected to be in supply from 2020 and its use will have effectively reduced Korea's total gasoline consumption by 10% by 2030 (Jun-Seok et al., 2010). In 2002 Thailand hosted the 14th International Symposium on Alcohol Fuels (ISAF), entitled "The Role of Alcohol Fuels in Meeting the Energy, Environmental and Economic Needs of the 21st Century" (Karl et. al., 2005). The policy instruments of Europe is expected to explicitly reward the higher value of lignocellulosic ethanol compared to first the generation ethanol and petrol (Edgard 2010). In 2004, the ethanol production capacity in Australia amounted to 135 000m^3 (Karl et. al., 2005). In 2015, production of second-generation biodiesel in Chile is mandated to be fundamentally based on forestry residues using Fischere Tropsch processes (Garcia et. al., 2010).

Apart from agricultural feed and cellulosic biomass other feed stock in the production of bioethanol that constitutes the third generation includes: Algae: rather than grow algae, harvest and ferment it, the algae grow in sunlight and produce ethanol directly which is removed without killing the algae (Bourne 2007, Ruth 2008). However biofuel consumption is still relatively low. This is due to low technical implementation and unfavourable pricing which makes industry reluctant to invest.

2.3.1 Synthetic Ethanol

There are two types of produced ethanol namely fermentative and synthetic ethanol (Ganesan & Elango 2013). Fermentation ethanol is mainly produced for fuel, though a small share is used by the beverage industry and the industrial application. Synthetic ethanol is commercially prepared from ethylene by the direct reaction of extremely pure water with ethylene gas (Ganesan & Elango 2013). This process, called direct hydration, is generally considered environmentally and technically the best commercial method for obtaining a consistently high quality ethanol product. The primary chemical reaction for this process occurs when water vapor and ethylene are combined at elevated pressure and temperature and are passed over the surface of a catalyst support impregnated with phosphoric acid. The main reaction yields a dilute crude ethanol. This ethanol is then separated from unreacted ethylene, which is recycled, and is concentrated and purified through a series of distillation towers (Ullmann 1990). The chemical reaction to produce ethanol from ethylene is as follows:

$$CH_2 = CH_2(g) + H_2O(g) \xrightarrow{(catalyst\ )} CH_3CH_2OH\ (g) \qquad \Delta H = -43.4kJ \qquad (2.1)$$

Ethylene water Ethanol

2.4 Lignocellulose

Lignocelluloses are composed of cellulose, hemicelluloses, lignin, extractives, and several inorganic materials (Thallada et al., 2011, Taherzadeh and Karimi 2007, James and John, 2001, Ferreira et al., 2010). The cellulose, hemicellulose, lignin, ash and soluble substances called extractivess in lignocelluloses biomass makes ethanol production more difficult. Cellulose and hemicellulose make two-thirds to three-quarters of the dry weight of most biomass materials. Cellulose as described by biologist and chemists is a complex carbohydrate, a linear polysaccharide polymer with glucose monosaccharide units (300 to

over 10, 000units with the formula $(C_6H_{10}O_5)n$, (Wikipedia 2014, IFQC, 2004, Bodîrlău et al., 2007). Figure 2.1 shows the structure of cellulose.

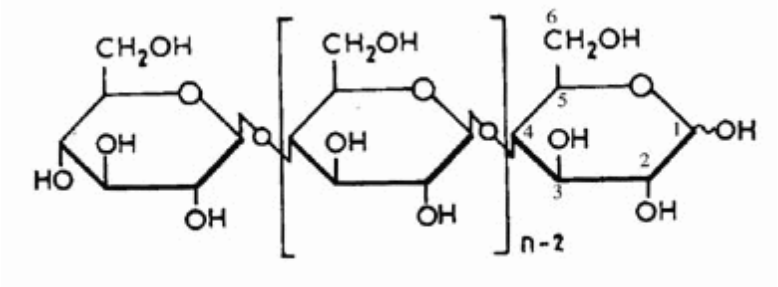

Figure 2.1: Structure of Cellulose (Wikipedia 2014)

Cellulose is a polymer of glucose and is difficult to break down into glucose because of its crystalline structure. The degree of polymerization (DP) of native cellulose is calculated with Equation 2.2 according to Bodîrlău et al., (2007).

$$DP = \frac{molecular\ weight\ of\ cellulose}{molecular\ weight\ of\ one\ glucose\ unit} \qquad (2.2)$$

The following are the basic properties of cellulose (Wikipedia 2014):

1. It is tasteless and odorless.

2. It is insoluble in water and most organic solvents.

3. It is hydrophilic and biodegradable.

4. It can be broken down chemically into its glucose units by treating.

5. Very high tensile strength-this strength is important in cell walls, where they are meshed into a carbohydrate matrix, conferring rigidity to plant cells.

6. Cellulose is hard to digest because it has a beta 1.4 glycosidic linkage.

Unlike cellulose, hemicelluloses consist of different monosaccharide units (sugars) including the six-carbon sugars glucose, galactose, and mannose, and the five-carbon sugars arabinose and xylose. The polymer chains of hemicelluloses are short-branched and amorphous and are easily broken down into its individual sugars. Owing to the amorphous morphology,

hemicelluloses are partially soluble in water (Demirbas, 2008). Hemicelluloses are able to bind to cellulose by multiple hydrogen bonds and to bind to lignin by covalent bonds.

Lignin is a complex three-dimensional hydrophobic network of phenylpropanoid units that acts as glue to hold the cellulose and hemicelluloses together (Sjöström, 1993, Higuchi, 1985). Lignin has been recognized not only to give mechanical strength or rigidity to a plant (Chabannes et al., 2001), but also to prevent the invasion by pathogens and pests (Sarkanen and Ludwig, 1971). It is currently viewed as a source of fuel to provide steam and power to run the ethanol plant. The solubility of lignin is highly variable (FAO, 2002).

Extractives in lignocelluloses refer to the organic substances which have low molecular weight and are soluble in neutral solvents. Resins, fats, waxes, fatty acids and alcohols, phenolics, phytosterols, salts, minerals, and other compounds are categorized as extractives. Moreover, the residue remaining after ignition (dry oxidation at 575± 25˚C) of lignocellulosic biomass is ash, which is composed of minerals such as silicon, aluminum, calcium, magnesium, potassium, and sodium (Lee et al., 2007). Extractives can have an economic value depending on their characteristics and cost of recovery.

The amount of agriwaste available depends upon the level of waste component of a crop which in turn depends upon the nature and structure of the plant, agricultural operations carried out and the volume of production in a particular area. Ethanol produced from lignocellulosic feedstock is expected to become mature in the space of 5-10 years and partly replace first-generation ethanol. Research is going on in several countries with the aim of improving the efficiency and economic performance of various pathways.

2.4.1 Waste Palm Bunch Lignocellulose

Palm oil and cassava are the most important agricultural commodities in Nigeria and play a significant role in the country's development. The palm oil sector globally, produces tons of Crude Palm Oil (CPO) and Palm Kernel Oil (PKO). CPO has many applications in the food industry e.g., cooking oil, and the non-food industry. e.g., biofuel; while PKO is a common ingredient in processed foods, soaps and personal care products. The average yield of palm oil ranges higher than those of soybean oil, rapeseed oil and sunflower oil with the same land area. Table 2.5 shows the major producers of palm oil. However, residues such as fibre, shell, fronds, palm kernel cake, palm oil mill effluent (POME) and waste palm bunch (WPB) are

also produced during the CPO and PKO extraction process (Yusoff 2006). Currently, palm oil mills typically use the shell and the drier part of the fibre product stream, rather than waste palm bunch, to fuel their boilers, as the raw waste palm bunch contain nearly 60% water.

Table 2.5: Major Producers of Palm Oil in Thousand Tonne (2007-2011), (Oil World, 2012)

Countries	2007	2008	2009	2010	2011
Indonesia	16.800	19.200	21.000	21.000	22.100
Malaysia	15.823	17.735	17.566	16.993	18.880
Thailand	1.020	1.300	1.310	1.380	1.830
Nigeria	835	830	870	885	900
Colombia	780	778	802	753	765
Ecuador	385	418	448	380	460
Others	2.905	3.045	3.107	3.367	4.159
Total	38.548	43.306	45.103	44.758	49.094

Palm oil industry is striving towards quality and environmental conservation through a 'sustainable development and cleaner technology' approach through the requirements of Environmental Quality Act (EQA) and the specific regulations governing the management of CPO mills. Sustainable industrial development means that products that contribute to economic activity satisfy human needs and support or enhance quality of life need to be produced with reduced consumption of materials and with reduced environmental damage (Azapagic & Perdan, 2010).

The present practices in CPO mill are still insufficient for full compliance of regulatory requirements in terms of combustion, fly ash and energy conservation (Yusoff, 2006) because the annual production volume exceeds the conversion process. The surplus biomass ends up being discarded in open areas or burnt; generating pollutant gases (Yong *et al*, 2007). Decomposition is a problem when the wastes are disposed within limited open spaces and in catchment ponds. The option of incinerating WPB is restricted by Department of Environment (DOE) within the confines of EQA (Yusoff, 2006). Palm biomass is generally composed of lignin, cellulose and hemicelluloses (Thiam & Bhatia 2008). Growing interest in alternative energy provides great potential for use of the lignocellulosic WPB as renewable energy for biofuel production. It can be converted to biofuels through thermo-chemical or

biological conversion. A summary of waste palm bunch conversion technology is illustrated in Figure 2.2.

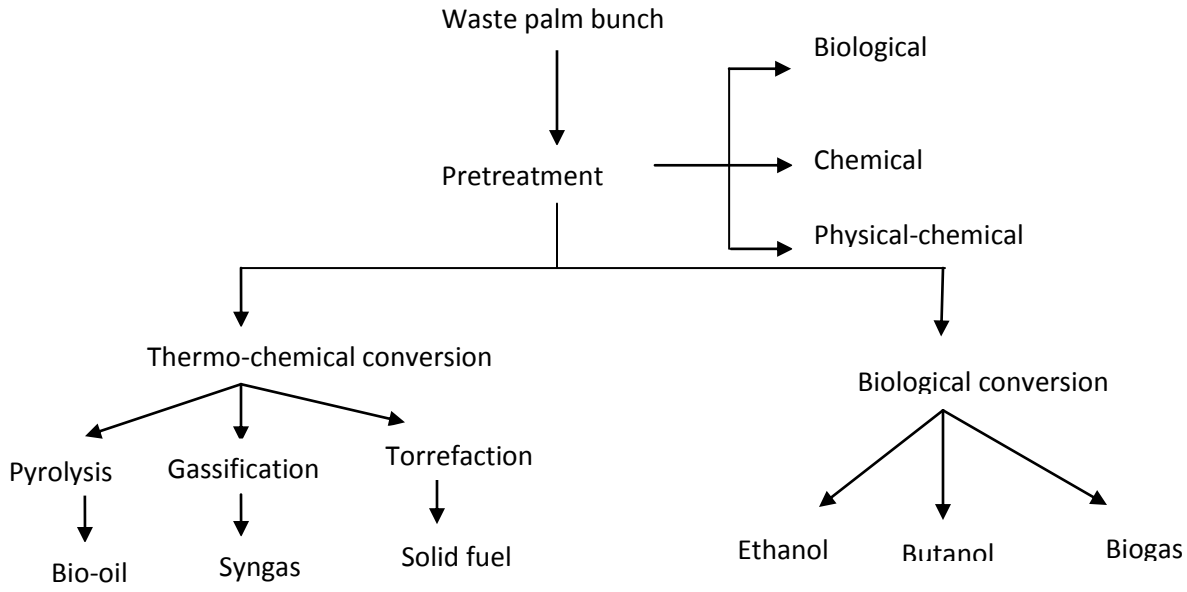

Figure 2.2: Biofuel Production from Waste Palm Bunch

Waste palm bunch is a solid residue produced in the highest amount as a by-product in palm oil processing (Gutierrez *et al*, 2009). It can be converted in useful products e.g. Nor et. al. (2012) and Abdullah et. al., (2011) derived bio-oil and diesel fuel from waste palm bunch. The liquids produced had high acid content, with a high heating value of about 50 % of conventional petroleum fuel. Waste palm bunch has a greater potency as basic raw materials used for the fermentative production because they contain 37.3 – 46.5 % cellulose, 25.3 – 33.8 % hemicelluloses and 27.6 – 32.5 %, lignin (Yanni et. al., 2012; 2008, Syafwina et. al., 2002). Lignin content varies and can be as low as 18 % excluding soluble lignin but mostly higher than other biomass like rice straw (Prassad et al 2007), barley straw (Garda et al 2006), winter rye and oilseed rape (Petersson et al 2007). The presence of high ash and silica content in rice straw makes it an inferior feedstock for bioethanol production also selection of an appropriate pretreatment technique is another major challenge in developing technology for the rice straw conversion (Parameswaran et. al., 2010). The types of main carbohydrates

in waste palm bunch are glucan, xylan, and arabinan, each is 31.0 – 35.4; 17.3 – 19.9, and 0.5 % respectively (Hayn et. al., 1993). Being abundant and outside the human food chain makes these cellulosic materials relatively inexpensive feedstocks for ethanol production and no conflict with the food supply. The compositions, physical and elemental analysis of waste palm bunch from literature are recorded in Table 2.6.

Table 2.6: Main Characteristics of Waste Palm Bunch (Abdullah et. al., 2011, Nor et. al., 2012)

Characteristics	**Literature values range**
Component/property (wt%)	-
Cellulose	38.1 - 59.7
Hemicellulose	16.8 - 22.1
Lignin	10.5 - 18.1
Physical properties analysis	-
Ash	3.02 - 7.30
Moistures	7.95 - 8.75
High heating value, HHV (MJ/kg)	19.30 - 19.35
Low heating value, LHV (MJ/kg)	17.2
Volatiles	75.7 – 83.86
Fixed carbon	10.78 - 17
Elemental analysis	-
Carbon	40.70 - 49.07
Hydrogen	5.40 - 7.33
Nitrogen	0.0 - 0.7
Oxygen	36.70 - 47.80
Sulphur	<0.1 – 0.2
Potassium,	2.0 – 2.4
K_2O	3.08 – 3.65

Figure 2.3: Oil palm and Waste Palm Bunch

Waste palm bunch (Figure 2.3) is much available; it was reported that 20 - 22 tons of waste palm bunch, 14 tons oil-rich fiber and 5 tons of shell are generated from 100 ton of fresh fruit bunch (Katamanee, 2006). Nigeria being a palm oil producing country, palm bunch waste is reasonably available in most of the states in the country, hence, it will benefit from research that will convert it to ethanol fuel. As palm oil production is not considerably seasonal, consequently, empty palm bunch is always available in the many palm oil producing areas given in the Table 2.7.

Table 2.7: Palm Oil producing Areas in Nigeria

State	Area	Palm bunch
Imo	Ohaji /Egbema, Okigwe, Mbano, Asa, Ikeduru, Ahiazu mbaise, Umudike, Avu, Umuagwo, An'ra, Okwele, Orlu, Awomama, Mgbidi.	Very abundant
Rivers	Elele, Ubima, Abua-odua, Ogoni, Etche, Ahoda. Oyoibo	Very abundant Very abundant Abundant
Abia	Okigwe, Isiukwuato, Igbere, Isiochi, Bende, Ugwunagbo, Alaye, Item, Umunochi, Ohiofia, Isialangwa N & S	Very abundant
Anambra	Aguleriotu, Nzam, Nando, Igboariam	Very abundant
Enugu	Udi, Uzo uwani, Ezeagu , Ameagu nze, Uhuokpara, Ahamufu, Ekpofu.	Very abundant
Delta	Ogwashukwu, Iselukwu, Onicha ugbo. Patani	Very abundant abundant
Akwaibom	Ibiono, Ikono, Itu, Oku iboku, Nsit ibom, Abak, Uriam. Nsit ubiom	Very abundant Very abundant abundant
Cross River	Ikot Offiong, Akamkpa. Odukpani	Very abundant Abundant
Ebonyi	Eda, Efium, Ezzagu, Ohofia agba, Ntezi, Ezzilo, Ohaozara, Obeagu, Okpoto.	Very abundant
Benue	Otukpa, Agila, Ichele.	Very abundant
Bayelsa	Ogbia, Obama, Southern ijaw, Sabagiriya Sagbama	Very abundant Very abundant abundant

2.5 Propagation and Potential Utilization of Oil Palm Biomass

Palm trees can be propagated through seeds and transplanted seedling. Seeds vary from the appearance depending on the species. Some are small birght and red while others are bigger. It is best to use vaiable fresh palm seed because they tend to sprout more readily. a vaiable palm fruit seed sinks in a bowl warm water, floated seeds lack internal organs called 'endosperm' that are necessary for reproduction. To actually sprout the seed, after two days hot water soaking, the vaiable seeds are planted in a small container of 15 x 25 cm with a very thin layer of soil or even only half buried or sown at a depth of 2.5 - 3 cm on raised beds. Palms do not readily sprout if buried deep. In nature, palm seeds are dispersed by the wind and animals and are rarely buried before they are expected to sprout. Once seed is planted, the container is wrapped in a plastic bag, and move to a very warm, very humid place. Germination takes about two to three months. To avoid root shock, young palm trees are transplanted in the main field when they have at least three or four sets of leaves while fertilizer can be applied once they start actively growing which takes about six to twelve months and about 6 – 8 years to mature.

Basically, oil palm biomass can be converted to a wide range of value added products that can be clustered into three main categories namely bio-based value added products, bio-fuel and as direct fuel for power generation i.e. bio-products, bio-fuels, and bio-power (Yusoff, 2006).

Bio-based Value Added Products: Waste palm bunch is used to produce bioplastic also known as polyhydroxyalkanoates (PHA) or polylactate (PLA). Currently there is a joint research and development in Malaysia by University Putra Malaysia, Felda Palm Industries Sdn. Bhd. and Kyushu Institute of Technology for the production of bioplastic using oil palm biomass (Siew et. al., 2008). Bioplastics have similar characteristics as petroleum-derived plastics and can be used for the production of foil, moulds, tins, cups, bottles and other packaging materials (Wikipedia 2015). However, the advantage of bioplastic is that it is 100% biodegradable and able to be recycled, composted or burned without producing toxic by-products. Besides, WPB can also be incinerated for its ash which serves as a very good fertilizer or soil conditioner. In fact, incinerating WPB to obtain its ash is currently the common practice in many palm oil mills as this can offset the increasing cost of inorganic fertilizers. Since WPB belongs to the category of fibrous crop residues or also known as

lignocellulosic residues, therefore WPB can also be converted into pulp for paper production (Wanrosli et. al., 2006). Similar to WPB, frond of the oil palm trees is also categorized as fibrous crop residues, allowing it to be converted to pulp. Oil palm fronds can also go through further processing and can be used as a roughage source for ruminants such as cattles and goats (Siew et. al., 2008). Palm fibers on the other hand can be used as fillers in thermoplastics and thermoset composites. These composites have wide applications in furniture and automobile components. Progress in this area of research finally reached to the commercialization stage when PROTON (Malaysian national carmaker) entered into agreement with PORIM (Palm Oil Research Institute of Malaysia) to develop the thermoplastic and thermoset composites and used it in PROTON car (Siew et. al., 2008). In addition, oil palm biomass or the ash derived from it can be converted into adsorbents for toxic gas and heavy metal removal.

Energy Related Products: Although oil palm biomass can be converted to various value added products, nevertheless, its potential as a source of renewable energy seems to be more promising, considering the current state of energy crisis with the price of crude petroleum hitting record high every other day (Siew et. al., 2008). Apart from that, its utilization as a source of energy will bring other environmental benefit like reduction in CO_2 emissions. It can generally be categorized into two main sections, the oil palm biomass directly be used as a fuel or initially converted to bio-fuel (intermediate product).

Directly as Fuel: Oil palm biomass such as waste palm bunch, mesocarp fiber (MF) and palm kernel shell (PKS) can be used to produce steam for processing activities and for generating electricity (Siew et. al., 2008). However, due to their characteristic, some of these fuel resources have to be pretreated before they can be burned in the boiler. Some pretreatment process that is required for the effective use of the biomass is such as using a shredding machine to reduce the size of WPB and drying to reduce the moisture content. In summary waste palm bunch as a biofuel feedstock has the following benefits:

- Abundant supply and year-round availability
- Homogenous biomass
- High cellulose, low lignin
- No logistics cost
- Outside the human food chain

2.6 Lignocellulosic Bioethanol Production

Lignocellulosic ethanol is simply ethanol produced from Lignocelluloses biomass. The importance of lignocellulosic ethanol stems from the assumed possibility of using inexpensive feedstock, avoid direct and indirect competition with human food and animal feed, and reduce environmental risks, that is, soil degradation, and water and air pollution, which are associated with first-generation biofuels (Edgard and Arnaud 2011; Parameswaran et al., 2011). In producing bioethanol fuel from lignocelluloses the following are considered; the resistance nature of biomass to breakdown, the variety of sugar which are released when the cellulose polymers are broken, the need to find or genetically engineer organisms to efficiently ferment these sugars (James & John, 2001, Ann et. al., 2000), tolerance to high temperature (reactor operates at 190 ^{0}C), acidity, cooling costs (Sugiyama *et al*, 2008). Moisture content is the main factor that affects the quality of the end product thus; an efficient dehydrating technique is to be applied. Ethanol is produced using basically one of two methods: wet milling or dry milling (Nebraska, 2011). The wet-milling operation is more elaborate and only the starch is fermented, unlike dry milling, where the entire mash is fermented. Most of the existing ethanol plants utilize a dry milling process. Ethanol that is used for fuel is denatured with a small amount (2-5 %) of some product, like gasoline, to make it unfit for human consumption. While the two main methods of producing ethanol from biomass is dry and wet milling, however, the basic process steps are pretreatment, Hydrolysis, fermentation, purificating (separating and concentrating) the ethanol produced by fermentation (Ganesan & Elango 2013, Parameswaran et al., 2011, Juliana et al. 2011, Ann et. al., 2000) as illustrated in Figure 2.4.

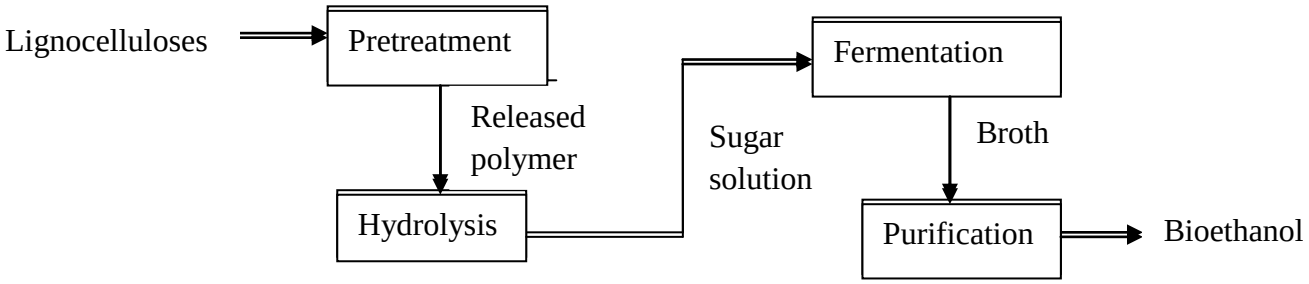

Figure 2.4: Bioethanol Production from Lignocelluloses Material

2.6.1 Drying

Drying is defined as a process of moisture removal due to simultaneous heat and mass transfer (Ertekin et al 2004). It is the removal of a solvent at temperature below its boiling point mostly from a solid material. It is a major post-harvest operation intended to prevent germination, suppress deterioration in order to retain optimum agri-produce quality (Teresita & Leila 2009; Lima et al 2002). The most important reason for the feedstock drying is substantial volume reduction and improvements in subsequent process applications. There is essential need to reduce the moisture content of the feedstock through drying before pretreatment. There are three major types of drying namely (Karbassi & Mehdizadeh 2008):

(a) Sun Drying: Sun drying is a traditional method of drying the feedstock. In fact, the major quantity of produce is being dried in the country by this method. Sun drying is the most economical method of drying grains. Agri-produce are spread on drying surfaces such as concrete pavement, mats, and plastic sheets and even on fields to dry naturally.

(b) Chemical Drying: Chemical drying method involves the spraying of a chemical solution on the agri-produce e.g. common salt solution with specific gravity of 1.1 to 1.2 on mature paddy crop. This treatment reduces the moisture content from 29% to 14.5% after four days.

(c) Mechanical Drying: Mechanical drying process means drying by ventilating natural or heated air through the agri-produce mass to evaporate the moisture from it.

The two most important considerations in selecting a drying type are: (1) drying capacity and (2) the investment necessary to get that capacity. These two items overshadow other factors such as airflow, labor requirements, operating cost, management and feed or market value of the dried feedstock (Brooker et al 1974). Sun drying is a simple and very inexpensive alternative. It is common in developing countries and when the science of drying process is not much important (Yutaka et al 2000; Jompob et al 2006). Depending on the required drying speed, many factors affect drying process, these include: moisture content, humidity, drying temperature, air velocity, and mode of heat transfer, sample surface area and sample geometry. The period of drying depends on the moistness of feedstock, drying temperature and weather condition (Sombat & Wittaya 2009; Yi-Luen 1993; Alonge & Hammed 2007). The drying time is shorter when the drying temperature is higher (i.e. sunny

days), windy and low humidity (Brooker et al 1974), which is explained by the increase in the drying rate. Hence, for optimum drying process of the feedstock; it is should be protected from humidity, spread at the direction of sun and high air velocity (IRRI, 2010b). The moisture content wet basis (MC_{WB}) is computed using the Equation 2.3 according to IRRI, (2010a,b) and Ibitoye (2005).

$$\%MC_{WB} = \frac{Initial(wet)\ Weight - Final\ Weight}{Initial(wet)\ Weight}\ X\ 100$$

$$= \frac{loss\ in\ Weight}{Weight\ of\ sample\ before\ drying} X\ 100 \qquad (2.3)$$

It is the amount of water in the feedstock as a percent of the total produce weight (Dirk & Fred 2002). The moisture content on a dry basis is the weight of water in the product per unit weight of dry solid in the product; Kongdej and Songchai (2009) also expressed it with Equations 2.4 and 2.5.

$$(a) initial\ moiture\ content\ M_i = \frac{W_i - W_d}{W_d} \qquad (2.4)$$

$$(b) final\ moiture\ content, \qquad M_f = \frac{W_f - W_d}{W_d} \qquad (2.5)$$

Where W_d, W_i and W_f are the weight of the dry sample, initial and final weight of sample respectively.

2.6.2 Pretreatment of Lignocellulosic Biomass

Pretreatment are the various means conditioning the feedstock to make it more accessible to hydrolysis and fermentation. Pretreatment could be by physical (mechanical), chemical, thermal, or biological means (Wyman 1996, Taherzadeh and Karimi 2007, Julia´n et al., 2011). It generally involves both a mechanical step to reduce the size of the biomass materials so that they can be more readily accessible to reaction with the subsequent steps and a chemical pretreatment to make the biomass more digestible. Generally, the yields of unpretreated lignocelluloses following enzymatic (and other hydrolysis) cannot be greater than 20 % of the theoretical maximum glucan conversion, even when a high level of enzyme loading or a longer reaction time is employed (Kim and Lee, 2007) whereas yield of cellulose

hydrolysis after pretreatment often exceeds 90 % of theoretical (Lynd, 1996). Therefore, the aim of the pretreatment is the removal of lignin and hemicellulose, the reduction of crystalline cellulose and the increase in the porosity of the materials. Hence, pretreatment that alters the lignocellulosic structure to provide the enzymes with greater access to cellulose is an essential step in the cellulose conversion process (Sun and Cheng, 2002). Additionally, the pretreatment should improve the formation of sugars or the ability to form them during the succeeding enzymatic hydrolysis, and avoid the formation of inhibitors for subsequent hydrolysis and fermentation processes (Oscar & Carlos 2008).

Physical pretreatment increases hydrolysis rate (Chang and Holtzapple, 2000) by reducing the technical digestion time by 23-59 %. The most efficient but also the most expensive and energy-intensive method is mechanical comminution of lignocellulose feedstock (Pereira Ramos, 2003, Ann et. al., 2000). Biomass material can be comminuted by various chipping, grinding and milling. The milling can be further detailed into hammer and ball-milling (wet, dry, and vibratory rod/ball milling) (Rivers et. al., 1987; Yoshida et al., 2008), compression milling (Ryu et. al., 1982, Tassinari et. al., 1977), pan milling (Zhang et. al, 2007), etc. Mechanical processing disrupts cellulose structure, reduces polymerization level, increases special surface of cellulose biomass when biomass is broken down to smaller particles. The energy requirements of the mechanical comminution depend on the final particle size and biomass characteristics (Oscar & Carlos 2008).

Chemical pretreatment for lignocellulosic materials employ different chemicals such as acid (HCL, H_2SO_4), alkaline (e.g. NAOH, Lime), oxidizing agents (e.g. peroxide, ozone), and other chemicals like organic solvenst, ammonia, sulfur dioxide (Taherzadeh and Karimi 2007, Farid et. al. 2010). Dilute acid pretreatment can achieve high reaction rates and significantly improve cellulose hydrolysis. One of the advantages is high xylan to xylose conversion yields, which is necessary to achieve favourable overall process economics in ethanol production lignocelluloses. The National Renewable Energy Laboratory (NREL) of the US Department of Energy preferred the dilute acid pretreatment for the design of its process alternatives in developing ethanol production technologies from biomass (Aden et al., 2002).

Acid pretreatment is carried out with sulphuric acid, hydrochloric acid, phosphoric acid or sulfur dioxide (Sun and Cheng 2002, Wyman 1996). The ratio 15:1 (w/w) of acid to the sample weight was noted to work well on WPB, rice husk and wheat straw pretreatment

(Cheng et. al., (2007). During acid pretreatment, solubilized lignin will quickly condensate and precipitate in acidic environments (Julia´n et al., 2011; Wyman 1996, Liu and Wyman, 2003). Diane et al., (1991) applied this pretreatment to some woody crops to achieve 90 % ethanol yield using S.cerevisiae in SSF. Concentrated sulphuric pretreatment system requires low energy and can be carried out at room temperature. Care must be taken that the pretreatment does not degrade the material so it can no longer be used for ethanol production. The loss of fermentable sugars and production of inhibitory compounds makes the alkaline pretreatment less attractive for the ethanol production. Nor et.al (2012) derived bio oils and diesel fuel from waste palm bunch treated with different sodium hydroxide (NaOH) concentration. After prolysis, conversions of waste palm bunch were reported to be 61 wt%, 47 wt% and 42 wt%, after pretreatment with 5 wt%, 15 wt% and 25 wt%, NaOH concentrations, respectively. Furthermore, the pretreatment was reported to have effectively improved the bio-oil quality by reducing or even eliminating undesired products. The thermal reactivity of lignocellulosic biomass depends largely on its composition (Hendriks and Zeeman, 2009), above 150 -180 ^{0}C, hemicelluloses followed by lignin, start to solubilize (Garrote et al., 1999).

Thermal pretreatments are divided into steam pretreatment/steam explosion and liquid hot water, LHW (Julia´n et al., 2011). LHW makes cellulose more accessible to hydrolytic enzymes (Zeng et. al., 2007). Steam explosion is the most widely used method due to its low cost (Hsu, 1996; Chandra, 2007, Garda et. al, 2006). Here hemicellulose hydrolysis is performed by using steam and organic acids (Weil et al, 1997). Crucial factors with regard to steam explosion include time, temperature, particle size and humidity (Ballesteros et. al., 2008; Negro et. al. 2003). Usually the temperature is between 160 and 270 ^{0}C, processing time ranges from seconds to a couple of minutes. About 90 % of the pre-treated mass is subject to further enzymatic activity, whereas relevant percentage in case of non-treated mass is only 15 % (Grous et. al., 1986). This method provides low hemicellulose yield (Wright, 1988; Excoffien et. al., 1991; Heitz et. al., 1991). Laser et. al., (2002), compared the performance of LHW and steam pretreatments of sugarcane baggase in production of ethanol by SSF. They used a 25-1 reactor, temperature 170 -230 ^{0}C, residence time 1- 46 min and 1 % to 8 % solids concentration. Both of the methods generated reactive fibers, but LHW resulted

in much better xylan recovery than steam pretreatment. It was concluded that LHW pretreatment produces results comparable with dilute acid pretreatment process.

Biological pretreatments using fungi and actinomycetes have also been tested primarily to solubilize lignin and make the cellulose more accessible to hydrolysis and fermentation (Taherzadeh and Karimi, 2008). These various pretreatment processes generally result in separating the biomass into a liquid stream composed of hemicellulose and a solid stream composed of cellulose and lignin (Ann et. al., 2000). The separated streams are then ready for hydrolysis. Piarpuza et al., (2011) used Dilute alkali pretreatment to prove Empty fruit bunches as a potential raw material for fuel ethanol production. Hector et al., (2012), reported that enzymatic saccharification autohydrolysis pretreated solids (APS) are more effective than the organosolv pretreated solids (OPS). The maximum extent of the enzymatic conversion of cellulose to glucose was 90.88 % and 64.04 %, for APS and OPS respectively, at 96 h. Alkaline pretreatment, ozonolysis, peroxide and wet oxidation pretreatments are more effective in lignin removal whereas dilute acid pretreatment is more efficient in hemicellulose solubilization (Farid et. al. 2010). Alkali pretreatment is done with NAOH, ammonia or ammonium sulfite. Dilute acid pretreatment at varied temperature and enzymatic saccharification were evaluated for conversion of wheat straw cellulose and hemicellulose to monomeric sugars by Badal et. al., (2005). The maximum yield of monomeric sugars from the wheat straw (7.83 %, w/v, DS) by dilute H_2SO_4 (0.75 %, v/v) pretreatment and enzymatic saccharification (45 ^{0}C, pH 5.0, 72 h) using cellulase, b-glucosidase, xylanase and esterase was 565 $\pm$ 10 mg/g. The yield of ethanol (per litre) from acid pretreated enzyme saccharified wheat straw (78.3 g) hydrolyzate by recombinant Escherichia coli strain FBR5 was 19$\pm$1 g. Detoxification of the acid and enzyme treated wheat straw hydrolyzate by overliming reduced the fermentation time from 118 to 39 h in the case of separate hydrolysis and fermentation (35 ^{0}C, pH 6.5), and increased the ethanol yield from 13$\pm$ 2 to 17 g/l and decreased the fermentation time from 136 to 112 h in the case of simultaneous saccharification and fermentation (35 ^{0}C, pH 6.0). The selection of pretreatment method should be compatible with the selection of hydrolysis, e.g. if acid hydrolysis is to be applied, a pretreatment with alkali may not be beneficial (Taherzadeh and Karimi 2007).

Sterilizing the WPB prior to pretreatment boosts the pretreatment benefits. Sterilization process in palm oil mill operation is the first step in the sequence of processes to extract the

oil. It is typically a batch process using steam for heating or cooking the fruits. during this process heat penetrates into the pericap of fruitlets and brings it for certain phycochemical changes such as for inactivation of lipase enzyme and for killing micro organisms that produce free fatty acid for good deoiling (Simarani et. al., 2009). It reduces lignin content and increases cellulose.

2.6.3 Hydrolysis of Lignocellulosic Biomass

Hydrolysis is the step that breaks down the cellulose and hemicellulose polymers into their basic fermentable sugars (glucose, xylose, arabinose, galactose, and mannose), (Drapcho et al., 2008). The main hydrolysis product of cellulose is glucose, whereas the hemicellulose gives rise to several pentoses and hexoses (Parameswaran et. al., 2010). Some pretreatment steps also result in some hydrolysis, especially of the hemicellulose materials. The major techniques proposed for hydrolysis include enzymatic and chemical hydrolysis usually using acid (dilute or strong) (Parameswaran et al., 2011, Ann et. al., 2000). Inorganic acids as H_2SO_4 and HCl have been preferably used for biomass pretreatment. The more hydrogen ions formed in the solution, the more rapid the hydrolysis process occurred (Mosier et. al, 2002). The breakage of hydrogen bonds in hemicellulose and cellulose fraction occures rather abruptly in response to temperature (Xiang et. al, 2003). One of the main advantages of dilute acid hydrolysis is achieving high xylan to xylose conversion yields, which is necessary to achieve favourable overall process economics in ethanol production from lignocelluloses (Sun and Cheng 2002). Xylose is of C_5 (Pentose) sugars i.e. lower order oligmers (Douglas 1981). Although concentrated acid hydrolysis results in the release of fermentable sugars, they are toxic, corrosive, generation acidic waste, require reactors that are resistant to corrosion and there is technical difficulties in recovering sugar from the acid (Julian et. al., 2011). This in turn makes the process very expensive. Dilute acid hydrolysis is the most efficient advanced technology (Cheng et. al., 2007), while enzymatic hydrolysis is viewed as the technology with the best chance of reducing the costs of producing ethanol from biomass (Parameswaran et. al., 2010). While a hydrolysis time of several days is necessary for emzymatic hydrolysis, a few minutes is enough for acid hydrolysis (Duff & Murray, 1996); also, Emzymatic hydrolysis is carried out under mild conditions (e.g. pH 4.5-5.0 and 40-50 ^{0}C), whereas acid hydrolysis requires high temperature and low PH, which results in corrosive

conditions (Parameswaran et. al., 2011). While it is possible to obtain cellulose hydrolysis of close to 100 % by emzymatic hydrolysis (Taherzadeh and Karimi 2007), it is difficult to achieve such high yield with the acid hydrolysis. Temperature influences rate of acid hydrolysis (Neureiter et al, 2002). The enzymatic hydrolysis process is represented by the simple Equation 2.6.

$$(C_6H_{10}O_5)n + n\,H_2O \xrightarrow{cellulase} nC_6H_{12}O_6 \qquad (2.6)$$

Cellulose Glucose

During acid hydrolysis, lignocellulosic materials degrad into its sugar components and other by-products according to the chemical reactions (Appriyanti 2008, Ria et. al., 2011):

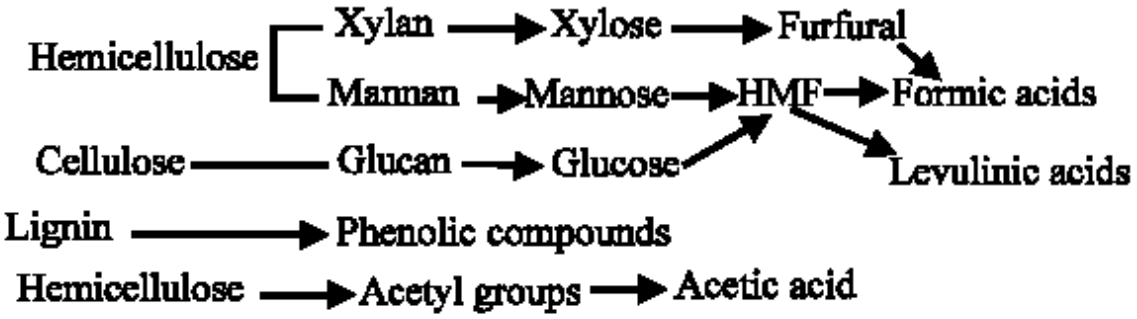

Several inhibitory compounds are formed during acid hydrolysis, whereas this problem is not so severe for emzymatic hydrolysis (Taherzadeh and Karimi 2007, wyman 1996). Though, these inhibitors can be reduce into useful material e.g. Furfural can reduce to furfuryl alcohol and furoic acid by emzyme alcohol dehydrogenase and by emzyme aldehyde dehydrogenase, respectively (Taherzadeh et. al., 1999) while HMF can be converted into its corresponding alcohol 5-hydroxymethyl-furfural alcohol (Taherzadeh et. al., 2000).

Most current designs using dilute acid involve two stages of hydrolysis. The first stage is carried out at milder conditions of temperature and pressure and maximizes the sugar yields from hemicellulose. The second stage is optimized for the conversion of cellulose into glucose. After the sugars are released, the acid solutions must be detoxified before they can be used for fermentation.

Detoxification methods can be physical, chemical or biological; these methods cannot be directly compared because they vary in the neutralization degree of the inhibitors. Several

detoxification methods like neutralization, overliming with calcium hydroxide, activated charcoal, ion exchange resins (Carvalheiro et al., 2005) and enzymatic detoxification using laccase (Chandel et al., 2007) are known for removing various inhibitory compounds from lignocellulosic hydrolysates. In the operation of neutralization, it is usual to add chemicals that neutralize the acids of the hydrolysates, forming salts. These salts have low solubility and are normally removed by filtration (Cardona et. al., 2010). The neutralization can be done using NAOH (Cheng et. al., 2007), $Ca(OH)_2$ hot water (Nuru et. al., 2014) or lime (Cardona et. al., 2010). Alkali treatment is considered one of the best detoxification methods. By this method, furaldehydes and phenolic compounds are mainly removed leading to great improvement in fermentability, especially in the case of dilute-acid hydrolyzates (Cheng et. al., 2007). Treatment with calcium hydroxide (overliming) or ammonia has shown better results than treatment with sodium or potassium hydroxide, but this difference has not been understood. However, a drawback of overliming is sugar loss due to hydroxide-catalysed degradation reactions and conversion of sugars into unfermentable compounds (Cardona et. al., (2010).

Dilute acid hydrolysis (typically 0.5 – 10 % weight) is most favoured among the chemical hydrolysis; it can be used either as a pretreatment (prehydrolysis or acid hydrolysis) preceding enzymatic hydrolysis, or as the actual method of hydrolyzing lignocelluloses to the sugars (Cheng et. al., 2007, Cardona et. al., 2010, Farid et. al., 2010). Prehydrolysis consists in the hydrolysis of the hemicellulosic fraction (which is easily hydrolyze) at moderate temperature (in the range 100 – 150 ^{0}C) (Farid et. al., 2010, Ghasem et. al. 2007). The hemicellulose been about 35 % of the total carbohydrates; the concentration of reducing sugar in the hydrolysate is relatively low due to high liquid / solid ratio during the acid hydrolysis as the cellulose and lignin fractions remain almost unaltered in the solid phase and can be further processed by increasing the temperature and time, or with enzymatic hydrolysis e.g cellulose (Cheng et al., 2008). High liquid/ solid ratio typically reduces the bioethanol yield owing to insufficient mass and heat transfer (Um and Hanley, 2008). The hydrolysate can be concentrated before fermentation by evaporation (Cardona et. al., 2010; Cheng et al., 2008). Carvalho et al., (2002) noted that increasing sugar concentration by evaporation removes small amounts of growth inhibitors such as acetic acid, furfural and HMF, besides water. The main disadvantage of such pretreatment method is the necessity of neutralization of pH for the

downstream enzymatic hydrolysis (Taherzadeh and Karimi 2007). However, to lower the cost of bioethanol distillation from WPB broth, a high initial substrate concentration is desirable (Wingren et al., 2003). Both sulfuric acid and nitric acid have been used for weak acid hydrolysis, although there is more experience with sulfuric acid. concentrated sulfuric acid (mostly at ambient) results in high yield of sugar offering advantage of not using any emzymes for saccharification, however this process has drawbacks including high acid and energy consumption, equipment corrosion and longer reaction time as well obligation for acid recovery (Farid et. al., 2010).

Enzymatic hydrolysis involves using an organism that produces enzymes that degrade cellulose into sugars e.g. cellulases and hemicellulases. Enzymes offer the advantage of producing higher yields of sugars with few degradation products. This increase of the enzymatic convertibility is probably related to the low content of lignin and hemicelluloses and the high cellulose content of the remaining solid material after delignification and/or acid pretreatment (Cardona et.al., 2010). Lignin limits the rate and extent of enzymatic hydrolysis by acting as a shield blocking enzyme accessibility, preventing the digestible parts of the substrate to be hydrolyzed, causes end-product inhibition, and reduces the rate and yield of hydrolysis (Chang and Holtzapple, 2000, Hendriks and Zeeman, 2009). In addition to lignin, cellobiose and glucose also act as strong inhibitors of cellulases (Knauf and Moniruzzaman, 2004). Most of the reports states that the optimum temperature for enzymatic hydrolysis is at 40 –50 ^{0}C, while the microorganisms with good ethanol productivity and yield do not usually tolerate this high temperature. This problem can be avoided by applying thermo-tolerant microorganisms such as Kluyveromyces marxianus, Candida lusitaniae, and Zymomonas mobilis or mixed culture of some microorganisms like Brettanomyces clausenii and Saccharomyces cerevisiae (Spindler et al., 1988). Once the cellulose and hemicellulose have been broken down into their basic sugars, it is time for fermentation. Pretreatate and hydrolysate are analysed for the content of xylose and glucose respectively, using Refractometer (Akpan et. al., 2005) or high performance liquid chromatography (Yanni et. al., 2013, Millanti et al. 2011, Chayanoot & Sairudee 2013, Nuru et. al., 2014). The extent of inhibition depends on the ratio of total enzyme to total substrate (Sun and Cheng 2002). Punnapayak and Emert (1986) studied SSF of alkali-pre-treated rice straw with Pachysolen tannophilus which resulted in ethanol yields less than 30 % of theoretical ethanol yield while

SSF of acid-pre-treated rice straw with Mucor indicus, Rhizopus oryzae, and S. cerevisiae resulted an overall yield of 40 –74 % of the maximum theoretical ethanol yield (Karimi et al., 2006). Akpan et al., (2005) reported that acid hydrolysis of maize cobs and groundnut shell at varying temperature using the optimal acid concentration of 4.5M H_2SO_4 brought about increase in glucose yield with time glucose, and a substantial amount of ethanol (which is used as a chemical feedstock) after the glucose is fermented with *Saccaharomyces cerevisiae* (baker's yeast). Farid et. al. (2010), applied acid pretreatment and enzymatic hydrolysis of wheat straw, a sugar yield of 74 – 99.6 % of maximum theoretical was achieved. Diluted acid pretreatment appears as more favourable method for industrial applications and have been studied for pretreating wide range of lignocellulosic biomass (Alvira et.al., 2010). Generally, acid and emzymatic hydrolysis can be compared as given in Table 2.8.

Table 2.8: Comparison between Dilute Acid and Enzymatic Hydrolysis (Taherzadeh and Karimi 2007).

Comparing variable	**Dilute acid hydrolysis**	**Emzymatic hydrolysis**
Mild hydrolysis condition	No	Yes
High yields of hydrolysis	No	Yes
Product inhibition during hydrolysis	No	Yes
Formation of inhibitory by-products	Yes	No
Low cost of catalyst	Yes	No
Short time of hydrolysis	Yes	No

The hydrozate can be analyzed for reducing sugar yield (glucose and xyloses) using a High performance liquid chromatography (HPLC) (Yanni et. al., 2013, Millati et al. 2011, Chayanoot & Sairudee 2013, Nuru et. al., 2014), spectrophotometer (Congcong et. al., 2013) or refractometer (Akpan et. al., 2005).

Various factors influencing the yields of the lignocellulose to the monomeric sugars and the by-products are, e.g., particle size, liquid to solid ratio, type and concentration of acid used, temperature, and reaction time, as well as the length of the macromolecules, degree of polymerization of cellulose, configuration of the cellulose chain, association of cellulose with

other protective polymeric structures within the plant cell wall such as lignin, pectin, hemicellulose, proteins, and mineral elements (Parameswaran et. al., 2010).

2.6.4 Fermentation of Lignocellulosic Biomass

Fermentation is the reduction of the hydrolysed biomass into ethanol and carbon dioxide by micro organisms. It is an energy yielding process caused by enzymes (provided by yeast) in which fuel molecules such as glucose (sugar) are broken down in the absence of oxygen. Anaerobic fermentation guarantees more alcohol and CO_2 yield. This is carried out in a tight container lid to prevent inflow of air because external air (which contains oxygen) contact with the mash promotes the formation of undesired microorganisms, e.g. film-forming or acetic bacteria, while the prepared yeast used for the fermentation of the sugar does not require any oxygen (Kriss 2004). Air can be prevented from diffusing into the container; CO_2 vented out by glycerol (Millanti et al. 2011), drops of oil (Asli et. al., 2013) or Vaseline. According to IFQC, (2004), fermentation reaction is represented by the simple Equation 2.7.

$$\underset{\text{Glucose}}{C_6H_{12}O_6} \xrightarrow{(yeast)} \underset{\text{ethanol}}{2CH_3CH_2OH} + 2CO_2 + \text{Heat} \qquad (2.7)$$

Two main fermentation approaches are micro organism and technological configuration approach. Micro organism fermentation involves the use of Fungi, bacteria or yeast, which utilize fermentable sugar as substrate for their growth and thereby converting them to ethanol, CO_2 and other metabolic end products (Mohd et. al., 2011). Ethanol-producing bacteria have a high growth rate; they have the potential to play a key role in making production of ethanol more economical. A well-known of such bacteria is Z. mobilis organism used historically in tropical areas to make alcoholic beverages from plant sap (Julia´n et al., 2011). S. cerevisiae also known as Baker's yeast is frequently used to ferment glucose (e.g. hexose not pentoses) to ethanol. It ferments hexoses abundantly present in lignocellulosic hydrolyzates, such as glucose, mannose, and galactose with high yield and productivity. S. cerevisiae has an efficient anaerobic sugar metabolism, tolerates inhibitory industrial substrates better than other microorganisms (Olsson et al., 1992). The fermentation process expressed in Figure 2.5 is started by mixing a source of sugar, water and yeast and allowing the yeast to act in an

oxygen free environment. This anaerobic environment forces the yeast to shut down the "burning" of sugar and allows them to, instead, ferment Alcohol.

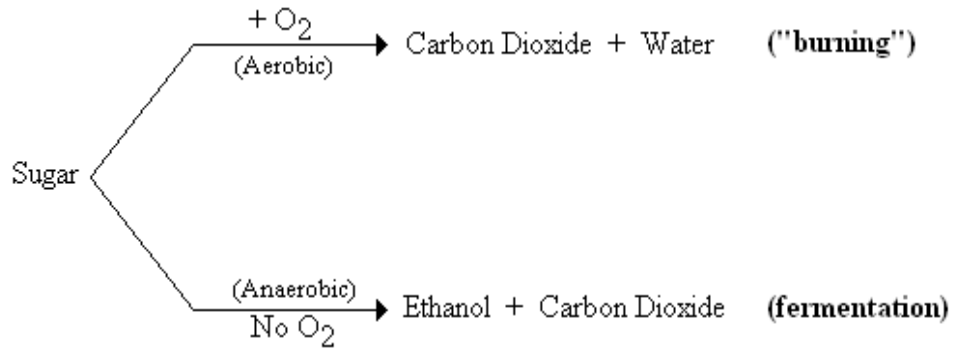

Figure 2.5: Fermentation Process

A well known ethanol producing fungus is Fusarium oxysporum which produce ethanol by simultaneous saccharification and fermentation (SSF) of cellulose. However, the conversion rate is low and significant amounts of acetic acid are produced as a byproduct. F. oxysporum produces a broad range of cellulases and xylanases (Julia´n et al., 2011). Highina et al., (2011) used *Saccharomyces cerevisiae* as a fermentative agent to study the kinetic parameters of ethanol from Molasses. reported that the maximum production of ethanol (73 gL-1) from molasses by *S. cerevisiae* can be achieved by sugar concentration of 17 %, temperature 30 ^{0}C, pH 4.5 and incubation period 72 hours. Various bacteria, yeasts and fungi have been investigated with the ethanol yield ranging from 65 % to 99 % of theoretical value. So far, the best results with respect to ethanol yield, final ethanol concentration and productivity were obtained with the native non-adapted Saccharomyses cerevisiae (Farid et. al. 2010). The best known microorganisms for ethanol production from hexoses are the yeast Sacchamyces cerevisiae and the bacterium Zymomonas mobilis (Claassen et al., 1999, Ullmann 1990, Skotnicki, 1983) offering high ethanol yields (90 – 97 % of the theoretical) and high ethanol tolerance up to ca. 10 % (w/v) in fermentation medium, has high selectivity, low accumulation of byproducts, and high fermentation rate. Yeasts have to be viable and genetically stable, but also tolerant to high temperatures during the process. The optimum temperature for most of the ethanol producing microorganism is between 30 and 37 ^{0}C (Taherzadeh and Karimi 2007). Glucose and xylose are two dominating sugars in the lignocellulosic hydrolysates; the main difficulty of using two microorganisms for the co-fermentation of these two sugars is the inability to provide optimal environmental conditions

for the two strains simultaneously (Parameswaran et. al., 2010). The result of Cheng et. al., (2007) demonstrated that inoculums concentration has no significant effect on the final ethanol concentration nonetheless; the duration of fermentation is decreased with increase of the yeast concentration. This is due to the growth of yeast been different for different concentration of inoculums described by the phenomenon called 'Diauxic growth' which is caused by a shift in metabolic pathway in the middle growth cycle (Cheng et. al., 2007). Thus, the process to consume the nutrient become shorter since the growth of yeast become dominant in higher concentration of inoculums as glucose is growth limiting factor in the medium (Cardona et. al., 2010).

Technological configuration is an integration approach to increase process efficiency through the improvement of reaction processes. Two main technological configuration employed among others are separate hydrolysis and fermentation (SHF) and simultaneous saccharification and fermentation (SSF) (Veronica et al., 2010). In SSF, the hydrolysis and fermentation are performed in a single unit while they are carried out in different units in SHF (Zheng et al., 1998). Won et. al., (2013) recorded ethanol yield of 18 % (w/w) by SSF, equivalent to 88 % of the theoretical maximum yield after achieving 85 % delignification of waste palm bunch within short reaction time using NaOH-catalyzed steam pretreatment (3 % NAOH and 160 ^{0}C, 680 sec steam pretreatment), enzymatic hydrolysis using CTec2. The sugar releaed in emzymatic hydrolysis inhibits further hydrolysis hence; SSF is usually employed to overcome this problem, in which the sugar release from the hydrolysis is directly consumed by the present microorganisms (Wyman 1996). However since fermentation and hydrolysis usually have different optimum temperatures, SHF is still favoured (Taherzadeh and Karimi 2007). Fermentation can be carried out in batch, fed-batch or continuous mode. In batch a quantity of the substrate is fermented before another, in fed-batch, some substrate starts the fermentation and more substrate is added in several times while fermentation in a steady state operates in a continuous mode. While continuous fermentation has greater reactor productivity (one fermenting for approximately 46 - 48 hours) because it is continuously operating with high yeast loads, much more care needs to be exercised to prevent contamination with bacteria, especially species of *Lactobacillus*. These bacteria allow production of organic acids that lower ethanol yields (Graves, 2006, Bayrock, 2001). The

advantages of the batch mode are; simple system that is easy to operate, less chance for contamination while the disadvantages include low efficiency and changing environment for yeast. The advantages of the continuous mode are high efficiency, easy for automation while the main disadvantage is challenge to protect from contamination. At the end of fermentation, the cellulose and hemicelluloses in the waste palm bunch must have gone through the chemical process given in Figure 2.6 by Ann et. al., (2000).

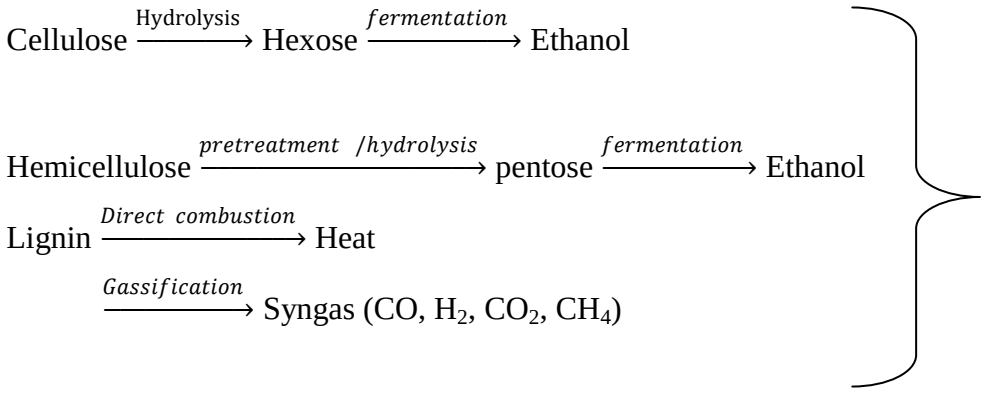

Figure 2.6: Cellulose and Hemicelluloses Degradation

Substrate concentration plays dominant role in the yield of ethanol during fermentation and distillation procedure; higher glucose concentration results to higher yield of bioethanol (Ghasem et. al., 2007). Production of bioethanol depends most on the carbon source not innoculum concentration as the carbon source from the glucose is indeed the nutrient for yeast fermentation process (Cheng et. al., 2007). Three days fermentation is a suitable time according to economics aspects (Chayanoot & Sairudee 2013, Cheng et. al., 2007).

2.6.5 Separation / Dehydration of Bioethanol Fuel

The fermentate usually contains alcohol, water and non fermentable materials from the biomass and the yeast cells. Separation Process is the technique of removing the alcohol from the fermentate. Dehydration or concentration technique is the means of removing water from ethanol to get a high concentrate (purer) product. Ethanol and water have extremely strong polar molecular interactions otherwise called hydrogen bonding, Fgure 2.5. Any molecule which has a hydrogen atom attached directly to an oxygen or nitrogen is capable of hydrogen bonding. The hydrogen bonding makes the molecules “stickier” and more heat is necessary to

separate them (Ophardt, 2003). Solutions that exhibit hydrogen bonding generally exhibit azeotropic behavior. Azeotrope is as a result of alteration or repulsion between molecules; they don't show ideal behavior according to Raoult's law. A list of common azeotropes is given in Appendix (A1). Ethanol has a hydrogen atom attached directly to oxygen and this oxygen still has exactly the same two lone pairs as in a water molecule (Ophardt, 2003).

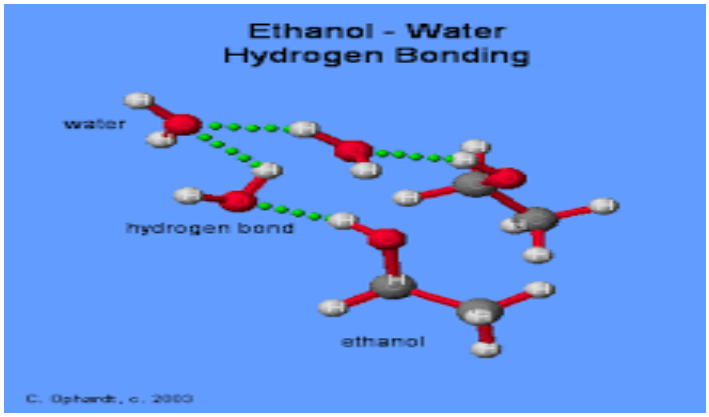

Figure 2.7: Ethanol -Water Hydrogen Bonding (Ophardt, 2003)

Breaking hydrogen bonds between ethanol molecules makes a strong stickier hydrogen bond between water and ethanol molecules. This increases with increasing ethanol concentration hence the mixture becomes difficult to separate beyond a certain concentration (Ann et. al., 2000). According to the RFA (2002), the water tolerance of blended fuels is temperature dependent, i.e. the tolerance is lower at low temperatures. A 10 % ethanol blend in petrol will tolerate approximately 0.5 % water (v/v) at temperatures of 15.5 ^{0}C or more, while the water tolerance is 0.3 % (v/v) water at approximately -12 ^{0}C. This is the main challenge facing bioethanol as bioethanol from fermentation contains water; so, major costs in the process industry are generated in the separation/dehydration step. Different dehydration techniques include vacuum fermentation, pervaporation, molecular sieve and distillation (DAF 2006, Gil et. al., 2007). The major separation technique is distillation (Wikipedia 2015a).

Distillation

Distillation is a process in which a mixture of two or more liquid is separated into its component factions of desired purity by the application and removal of heat (sudheer 2013, Smith 1995). Distillation is a thermal separation technique relying on differences in the

boiling points of the component liquids to be separated (Jungho & Hwayong 2015, Wikipedia 2015a). The motive force in all thermal separation is the drive towards thermodynamic equilibrium between the different phases (vapour liquid equilibrium, VLE) (Jugho et. al., 2015, Ohe 1991). The concentration of the lighter components will be greater in the vapour phase and conversely the concentration of the heavier components will be greater in the liquid phase, and only in the case of pure components or azeotropic mixtures will the equilibrium composition be the same in both phases (Jim 2005, Smith et. al., 2001). Boiling point and vapor pressure are the key parameters and higher vapor pressure creates a lower boiling point. Matherson (1980) noted that when alcohol/water mixture is boiled, vapours with a greater concentration of alcohol forms while liquid with a lesser concentration of alcohol remains behind. Separation of the bioethanol from water is initiated at this stage taking advantage of the low boiling point of bioethanol (78 ^{0}C) (Amornchai et al., 2008) and the positive azeotrope it forms with water (Jugho et. al., 2015, Jim, 2005). Two main type of distillation are (1) simple distillation and (2) fractional distillation. Simple distillation is separation by a single vaporization-condensation cycles (Mochamad 2011). It works particularly well on mixtures of two liquids in which the liquids have a very large boiling point difference. Fractionation is equivalent to a series of distillations, where the separation is achieved by successive distillations or repeated vaporization-condensation cycles (Kister 1992, 2008; Mochamad 2011). After a number of these recondensation/revaporization steps, the lower boiling component will be relatively free of any higher boiling components (Tham 1997, Kister 1992). Each vaporization-condensation cycle makes for an equilibrium stage, commonly known as a theoretical stage (Chen & Lin, 2001, Holland 1997). The main difference between simple and fractional distillation is presence of a fractionating column in fractional distillation instead of a straight column as in simple distillation (Kister 1992, 2008, Mochamad 2011). Biothanol is normally concentrated by distillation of its aqueous solutions, but in most cases the composition of the vapor obtained is 96 % ethanol and 4 % water (Peterson 2010, viele et. al. 2013). This azeotrope mixture of ethanol/water can not be separated further with the same technique since no further enrichment of the vapour phase occurs. This is because at this point, they behave like a pure compound and distill from the beginning to the end at a constant temperature, giving a distillate of constant composition (Smith, 1995). In most cases, azeotropic mixtures require special methods to facilitate their

separation such method utilizes a mass separating agent other than energy that causes or enhances a selective mass transfer of the azeotropic forming component (Smith, 1995; Peterson 2010). These include extractive distillation, azeotropic distillation, salt distillation, reactive distillation and pressure swing distillation (Stichimar *et al*. 1989, Leland 2005).

In pressure swing distillation; a series of columns operating at different pressures are used to separate binary azeotropes which change appreciably in composition over a moderate pressure range or where a separating agent which forms a pressure-sensitive azeotrope is added to separate a pressure-insensitive azeotrope (Peterson 2010). In salts Distillation, the added salts dissociates in the liquid mixture and alters the relative volatilities sufficiently that the separation becomes possible (Stichimar *et al*. 1989). In reactive distillation, the separating agent reacts preferentially and reversibly with one of the azeotropic constituents. The reaction product is then distilled from the non-reacting components and the reaction is reversed to recover the initial component (Stichimar *et al*. 1989). The principle of azeotropic distillation is to separate aqueous ethanol into their pure components by distillation by the addition of a third component, so called the entrainer (solvent), which forms a ternary heterogeneous azeotrope with a lower boiling point than any other binary azeotropes (Jungho & Hwayong 2015, Wikipedia 2015a, Stichimar *et al*. 1989). The formed one or more azeotropes with the other components in the mixture by the liquid separating agent, (entrainer), causes two liquid phases to exit over a wide range of compositions. This immiscibility is the key to making the distillation sequence work (Peterson 2010, Bauer and Stichlmair 1995). The liquid separating agent in homogeneous azeotropic distillation is completely miscible. Nearly pure bioethanol can be obtained as a bottom product in an azeotropic distillation column. The entainer is usually a volatile Addition such as benzene, normal pentane or cyclohexane (Gil et. al., 2007, Bauer and Stichlmair 1995). Extractive distillation adds a high boiling solvent which is exclusively familiar with a wanted component near the top of the column in a feed mixture, to favourably alter the relative volatility in order to separate the components (Stichimar *et al*. 1989, Leland 2005, Gil et. al., 2007). A desired component can be obtained in an extractive distillation column as a top product (Jungho & Hwayong 2015, Wikipedia 2015a). The entrainer is specific to the mixture in question e.g. benzene is a feasible entrainer for separating ethanol and water, but not for separating ethanol and methyl ethyl ketone- so there is no universal entrainer (Bauer and Stichlmair 1995, Smith 1995). The typical extractive

distillation entrainer has a higher boiling point than the pure components, and it does not form any azeotropes with either of the pure components (Smith 1995, Mujtaba 1999, Milani 1999). The solvent is Non-volatile addition such as ethylene glycol solvent, glycerol, acetate and inorganic salts such as: $CaCl_2$, $AlCl_3$, KNO_3, $(CuNO_3)_2 3H_2O$, $Al(NO)_3 9H_2O$, K_2CO_3 (Gil et. al., 2007, Mujtaba 1999). A second column separates the bottom in order to recycle the solvent. Extractive distillation with salts and solvents as separating agents turns up as a new possibility to obtain high purity products. This process combines the traditional extractive distillation with the "salt effect" principle. With this combined method, it is possible to solve several eventual problems of transport, dissolution, corrosion and obstruction found when only salt is used as separating agent. Compared with normal extractive distillation, the quantity of the solvent to recycle is reduced to its fourth or fifth, the number of theoretical stages required can be reduced to its third, as well as energy consumption. In addition are the following characteristics (Gil et. al., 2007):

(i) Allows continuous operation because of the high efficiency and the low waste of solvent.
(ii) A high purity product can be obtained.
(iii) The relative volatility of the ethanol-water system is increased, compared to the effect produced by each of independent agents.
(iv) Improves the solvent performance.

In the two largest producers of ethanol in the world, Brazil and United States (Poala et. al., 2010, Tan et. al., 2014) azeotropic distillation with cyclohexane, extractive distillation with ethyleneglycol and adsorption with molecular sieves are used (Poala et. al., 2010).

Pervaporation

Pervaporation is a direct separation technique without salt addition, and used as a standalone uint operation. It is a recent technology for the removal of organic from water (Peng *et al.*, 2003). Pervaporation membranes separate water at the feed side and a vapour at the permeate side, simultaneously evaporating the permeating compound (Leland 2005). A reactive distillation column in which chemical reaction and separation occur simultaneously was applied by (Amornchai et al., 2008), for the synthesis of *tert*-amyl ethyl ether (TAEE) from ethanol (EtOH) and *tert*-amyl alcohol (TAA). Pervaporation was integrated to enhance

efficiency. The performance of such a hybrid process was analyzed and the results indicated increase in the conversion of TAA and purity of TAEE produced, compared with the conventional reactive distillation. Pervaporation is seen as offering improved performance to a distillation system in three main ways (Guerreri 1992, Leland 2005):

i. The breaking of an azeotrope without needing to add a "foreign" material.

ii. Increasing the capacity for the same overall energy input.

iii. Improving the quality of both bottoms and overhead product, without any increase in energy input.

iv. Its functioning is independent of vapour-liquid equilibrium

Dehydration of solvents is the most widespread use of Distillation-Pervaporation, where the ability to break azeotropes without the introduction of a third component is of great benefit. In the petroleum industry, where the scale of operation for the potential use of Distillation-Pervaporation is the highest, several major operators have carried out pilot scale trials (Anne et. al., 2002, Haggin 1988, DOE). Exxon has done work in several European plants on treating mixtures of aromatics and aliphatic hydrocarbons; but did not proceed further with full scale industrialization owing to a too low a return on investment. Texaco did work on breaking of the dimethyl carbonate/methanol azeotrope but it too has not taken the final step into full scale production. In the processing of hydrocarbon feedstocks, there is potential for improving petrol cuts and the conversion to gas oils. Pervaporation following an upstream distillation step separates branched molecular olefins from straight chains. Branched olefins provide an improved octane number in petrol. The straight chained olefins are then further processed for improving the cetane number in gas oil (diesel). Grace Davison has developed a new high-performance post distillation pervaporation process for removing sulphur from petrol (Kujwaski 2000). Pervaporation shows considerable promise in terms of its potential in significantly reducing energy consumption in liquid separations (Guerreri 1992). This also extends to improving the quality of products from some separations but it has not yet been exploited on a big enough scale despite these benefits being apparent for at least 25 years. The drawback is clearly the lack of will to introduce the technology into the mature industries of petroleum refining and chemical processing because of cost. Up to now energy savings alone have not been enough to persuade the big players to invest (Anne et. al. 2002).

Molecular Sieve

Molecular sieves are materials composed by micro porous substances that are characterized by their excellent ability to retain on its surface defined types of chemical species e.g. Zeolite (Poala et. al., 2010, Wang & LeVan 2009). In gas processing, molecular sieving system is a common practice to remove impurities (eg. H_2O, H_2S and CO_2). These materials packed into a vessel make possible to separate ethanol from water by adsorption mechanisms at high pressure. Adsorption on molecular sieves takes advantage of the difference of molecular size of ethanol and water molecules to adsorb in a selective way water molecules and allowing ethanol separation. This technology alone reduces energy use by 10 % per litre of ethanol produced (DAF 2006). Zeolites, an aluminosilicate members of micro porous solids family, is in widespread use as molecular sieves, are suitable in aqueous and organic solvent environments (Coronas 1999, Rollma & Valyocsik 1983). Rollma and Valyocsik (1983) gave three of the common zeolites that are used as laboratory molecular seives as:

3A (pore size 3 Å): Adsorbs NH_3, H_2O.

4A (pore size 4 Å): Adsorbs H_2O, CO_2, SO_2, H_2S, C_2H_4, C_2H_6, C_3H_6, and ethanol.

5A (pore size 5 Å): Adsorbs linear hydrocarbons to *n*-C_4H_{10} and alcohols to C_4H_9OH.

3Å zeolites are frequently used in ethanol drying processes because the pore dimension is 3Å, while water molecules have 2.8Å in diameter and ethanol molecules, 4.4Å (Nomura *et al.* 2002, Wang & LeVan 2009). Thus, water molecules are adsorbed by the zeolites while ethanol passes through. The advantage of using a zeolite membrane is that it can potentially separate molecules in a continuous way. The crystalline nature of zeolites offers the opportunity to obtain membranes with a regular 3D network of micropores at the molecular scale and they are therefore able of separating mixtures of substances on the basis of differences in the molecular size and shape (Caro et. al., 2000, Rollma & Valyocsik 1983), such as isomers (Nair et. al., 2001), compounds with similar molecular weight and also azeotropic mixtures (Coronas 1999). Zeolites can withstand significantly higher temperatures (>200 ^{0}C) but are sensitivity to even weak acids. It has adsorbtion and the regeneration processes linked together into 2 columns, for ethanol drying and regeneration step respectively (Henley et. al., 2006). From the time and energy perspective, the regeneration step represents a critical process. Henley et. al., (2006) gave two major methods used for adsorbents regeneration as:

• Regeneration trough pressure variation (PSR), used for removal of weakly adsorbed molecules;

• Regeneration trough temperature variation (TSR), used for removal of strongly adsorbed molecules;

In PSR process, drying column operates almost at constant temperature; water adsorbed in the previous cycle is being desorbed by lowering operating pressure and by using a gas (N or CO_2) flow trough the adsorbent bed from the opposite direction. In TSR, lower temperatures are use in the adsorption step while the regeneration step is operated at higher temperatures. TSR process is less effective and much slower than the PSR. Ethanol can be dehydrated in either gas or liquid phase. If the gas phase is chosen then pressure swing is normally the best choice. According to Nomura *et al.* (2002) the ethanol-water separation factor of zeolite membrane is in the range of 12 – 106. The hydrophobic zeolite membranes are commercially available and expensive but, with high separation factors and flux; they are cost effective on per unit ethanol basis (Vane, 2005).

Poala et. al., (2010), investigated and compared analysis of the three main ethanol dehydration technologies, azeotropic distillation with cyclohexane, extractive distillation with ethylene glycol and adsorption with molecular sieves. They used Aspen Plus process simulator, to determine the main operating conditions taking a case base of 300 cubic meters per day of anhydrous ethanol. Additionally, a preliminary costs analysis was implemented taking into account total investment and operating costs of each technology. The results showed that extractive distillation process is the most promising technology from operating and economical points of view and there is necessity to investigate more techniques to improve the efficiency and sustainability of alcohol production.

2.7 Distillation Thermodynamics of Biothanol-Water Mixture

Ethanol and water are volatile with temperature though their volatilities differ as their individual vapor pressures differ at a given temperature. Thus, during simple distillation, the observed vapor pressure is the sum of the vapor pressure of the components i.e. bioethanol and water as shown in Equation 2.8 according to (Eastop and McGankey 1993). The observed vapor pressure increases with the increase in temperature, and the mixture boils when the observed vapor pressure is equal to the atmospheric pressure (101.3 kPa).

$$P_{observed\ \ total} = P_{observed\ \ eth.} + P_{observed\ \ water} \quad (2.8)$$

Where

$P_{observed\ \ eth.} = c_{eth.}P_{pure\ eth.}$ And $P_{observed\ \ water} = c_{water}\,P_{pure\ water}$

Where c is the mole fraction of the vapor components (i.e. ethanol and water vapor).

The initial boiling point of the mixture is normally higher than the lowest boiling component (78.8 ^{0}C for ethanol) and lower than the highest boiling component (100 ^{0}C for water). If the composition of the vapor is the same as in the mixture distillation will not take place but if enriched in the more volatile component (i.e. lowest BP component, ethanol) distillation will occur. The vapor can then be treated as an ideal gas as in Equation 2.9 before it is cooled.

$$PV = nRT \tag{2.9}$$

Where P = generated vapor pressure, V= volume that it occupies, n = number of moles of vapor, R = gas constant, T = temperature. Therefore for the generated vapor;

$$\begin{aligned} V.P_{observed\ \ total} &= n_{total}\,RT \\ &= V.P_{observed\ \ eth.} + V.P_{observed\ \ water} \\ &= n_{ethanol}\,RT + n_{water}\,RT \\ &= (n_{ethanol} + n_{water})RT \end{aligned} \tag{2.10}$$

Since the generated vapor can be treated as an ideal gas, according to Dalton's law so can each of the components. The two components are in thermal contact and are expected to be at the same temperature. The volumes of the molecules are very small compared to the total volume available thus they occupy the available volume and implies Equation 2.11.

$$\frac{P_{observed\ \ eth.}}{P_{observed\ \ water}} = \frac{n_{ethanol}}{n_{water}} \tag{2.11}$$

Since the numbers of moles of each component are equal to the weight of the component divided by its molecular weight, the ratio can be expreassed with Equation 2.12.

$$\frac{P_{obs.\ eth.}}{P_{obs.\ H_2O}} = \frac{w_{eth.}/MW_{eth.}}{w_{H_2O}/MW_{H_2O}} \tag{2.12}$$

Where $w_{eth.}$ and w_{H2O} are the weights of bioethanol and water and $MW_{eth.}$ And MW_{H2O} are their molecular weights respectively.

The amount of water required to distill all the mass of bioethanol in the mixture can be obtained with Equation 2.12 while Equation 2.11 allows the determination of the vapor composition from the observed partial pressure of the two components. This ratio at the mixture boiling point is use to establish indeed that generated vapor is enriching in ethanol and to get the composition of the vapor as soon as the mixtures begins to boil (Collier 1982). Thus as the distillation proceeds the boiler will be enrich in the less volatile component (water). This means that the composition of the mixture has changed from its initial mole ratio to a new composition which inturn introduce changes in the generated vapor composition. In other words, the composition of the vapor will also change to reflect the new composition of the boiler (Ohe 1979). The consequence is that the temperature of the boiler and distillate will slowly increase from initial value to a value approaching the boiling point and composition of the less volatile component.

2.8 Distillation Plant Analysis

The distillation unit differs with type of distillation as the process determines the setup, heat and apparatus involved. Distillation units though having same operation steps and major components differ in setup and depend on heat source, capacity and purpose. A distillation unit consists of a boiler unit, delivery pipes, condenser and a heat source.

Boiler Unit: The function of this unit is to heat the feed to the boiling point of its constituents respectively. It comprises of the boiler shell and fuel combustion chamber, which may be internally or externally incorporated to the boiler. The boiler is normally a cylindrical container close at both ends of a defined capacity normally made of steel or alloyed steel. The boiler shell is never loaded to the brim; a considerable space must be left to accommodate piping and the resulting vapor from distillation process (Boiling & Suarez 2001). Also, a considerable part of boiler surface (heating surface) should be expose to the fire or hot gases from the fire. Combustion chamber is the space generally below the boiler shell meant for burning fuel to liberate heat energy that increase the broth temperature to boiling point. It consists of the grate and the furnace; grate is a platform upon which fuel is burnt while

furnace is the space above the grate and below boiler shell, in which the fuel is actually burnt (Khurmi & Gupta 2006).

Condenser as a Heat Exchanger

A heat exchanger is an equipment use to transfer heat from a hotter fluid to a colder fluid. Heat is energy in transit under the driving force of a temperature difference, and flows in the direction of lower temperature. The shell and tube HE is mostly used for distillation recovery process. The condenser shell together with the delivery tube that is nested in, and run parallel to it forms a shell and tube HE (Colburn 1951). The transfer of heat in a condenser is by conduction following Fourier Law given in Equation 2.13, which states that heat is diffused at a rate directly proportional to the product of area 'A' and temperature gradient dT/dx (Holman 1990).

$$Q = \pm KA\left(\frac{dT}{dx}\right) \qquad (2.13)$$

The factor of proportionality 'K' known as the thermal conductivity is a property of the material conducting the heat. K is a function of temperature particularly for liquids and gases. The signs indicate the direction of the temperature gradient.

A condenser consists of a coolant jacket and delivery pipes. Coolant jacket is connected to the coolant retention reservoir. The function of this unit is to extract heat from the vapor flowing through the pipe thereby cooling the vapor causing it to reliquify and drips into a receiving flask (Collier 1982). The coolant circulates through the jacket by means of natural convection or force convection using a pump. The condenser position follows the piping inclination and must be unlagged to enhance cooling. Delivery pipes direct the movement of ethanol vapor from the boiler and via the coolant jacket to the collection point. Shell and tube HE provides a comparatively large ratio of heat transfer area to volume and weight. It can be constructed with a very large heat transfer surface in a relatively small volume. Considering Equation 2.14, it would be possible to choose a large HE with a small dT/dx or a smaller one with a large temperature difference for a particular dT/dx (Frank and David 2002). The shell and tube HE may consist of seven basic elements which are (1) bonnet or header (water box), (2) tube sheet (3) shell (4) tubes (5) nozzles (6) baffles or support plates and flanges. Due to stringent space limitations imposed on distillation HE and for ease of maintenance and cleaning, fluid inlet and outlet piping connection can be arranged to permit access to the tubes and tube sheets without dismantling the attached piping. The shell of HE is usually cylindrical

with/without flanges attached to each end. The tube bundle is attached to the floating head and can be pulled through if the head is moveable relative to the shell. The flanges or tie rods separate the tubes and hold the baffles in position. The baffle also separates and holds the tubes in position, and controls the direction of flow of the shell side fluid. This is done by placing the baffles to a particular arrangement relative to the type of flow required. Hence, the shell fluid flow pattern is a function of the baffle geometry (colburn 1951). In the shell, turbulence and friction are induced by using baffles to improve heat transfer characteristics. Considering the direction of flow of the two fluids relative to each other, there is two types of flow in a HE which are co-current flow and counter current flow (Yunus and Afshin 2015). The tube sheet may be a single pass, two pass or four pass etc depending on how many flow directions taken by the tube side fluid. A single pass means that the tube side fluid flows in only one direction. The two and four pass would have the tube side fluid inlet and outlet connections at the same end. In these exchangers, there is the flow of the media that supply or remove heat as well as the product to be treated. Number of pipes and its arrangement play an important role for an optimum condensation. Thus condenser inclination relative to the boiler should ensure slow vapor velocity to ensure complete condensation (Yunus and Afshin 2015). Parameters considered are available space, required length of pipe, its shape (e.g. Spiral, coiled, gilled and straight), pipe spacing and shell volume. Figure 2.8 illustrates two pattern of flow in a single pass shell and tube heat exchanger.

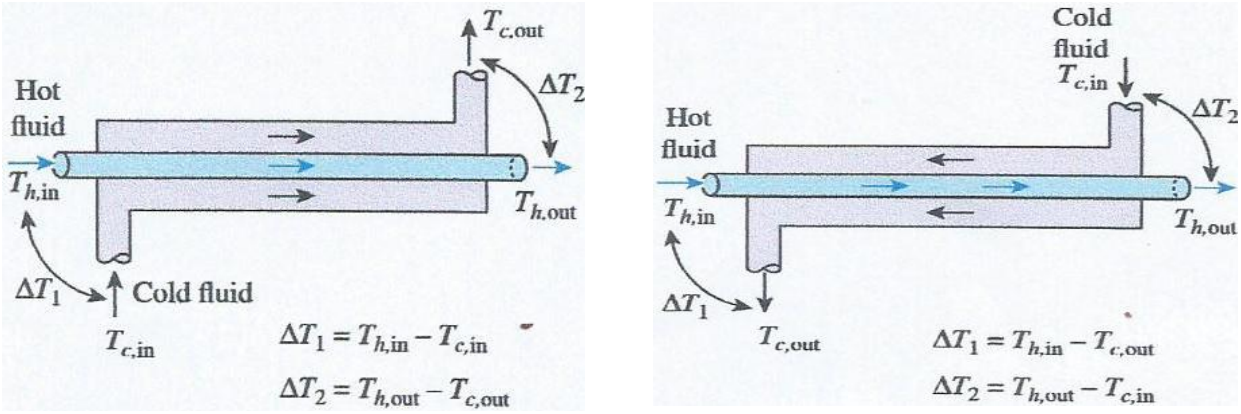

Parallel Flow Heat Exchanger **Counter-Current Flow Heat Exchanger**

Figure 2.8: Flows in Single Pass Shell and Tube Heat Exchanger

A first-stage consideration in the design process of a HE is the allocation of fluids to either shell or tubes and, in principle either stream can be in either tube or shell. By and large, the corrosive fluid is passed through the tubes to reduce the costs of expensive alloys and clad components (Collier 1982; Yunus and Afshin 2015). Similarly, fluid with the greatest fouling tendency is usually pass through the tubes where cleaning is easier, it also gives better control over the design fluid velocity and the higher available velocity in the tube reduce fouling (Collier 1982). Streams with higher pressure are best handled in the tube side, because high pressure tubes are cheaper than a high pressure shell also only the tube and the tube side fittings need be designed to withstand the high pressure as the shell may be made of lighter weight metal. If both streams are at high pressure, a heavy shell will be required and other considerations will detects which fluid goes to the tube. In any case, high shell pressure puts a premium on the design of long, small diameter exchangers (Frank and David 2002). However, where no phase change occurs, for the same pressure drop, higher heat transfer will be obtained on the tube side than the shell side. Therefore, fluid with lowest allowable pressure drop should be allocated to the tube side. The heating fluid is best put in the shell while cooling fluid goes to the tubes, for sufficient heat transfer per time, but where the HE is a cooler, the heating fluid is put in the tubes while cooling fluid goes to the shell e.g. HE for production of distilled water (. Allocating the fluid with the lowest flow rate to the shell side normally gives the economical design (Yunus and Afshin 2015). The fluid having inherently low heat transfer coefficient (such as low pressure gases or viscous liquids) is preferentially put on the shell side so that extended surface may be used to reduce the total cost of the exchanger. In summary, factors considered in allocating fluids to either shell or tube side are: corrosion, pressure drop, operating pressure, viscosity, fouling, fluid temperatures, fluid flow rates and low heat transfer coefficient. The condenser that is mostly used for distillation is called the "Liebig Condenser". It has a single pipe nested in and runs through a coolant jacket. The heating fluid is put in the pipe while the cooling fluid goes to the shell. As a cooler HE, running the coolant as the lowest flow rate fluid gives the most economical design.

Storage Tanks

Three kinds of storage tanks are needed in this system: water tank, wash tank, and product storage tank. Tank construction is not important to the process performance but is a substantial cost in the construction of the facility and the layout of the pipe network.

(a) Wash Tank Storage Capacity: The wash tanks must be able to accommodate the quantity of feed or fermentate depending on the operational conditions of the facility. The feed tanks should have flat base to enhance sediment of any lingering particulates which remained after filtration (Yuelei et. al, 2012).

(b) Water Storage Tank Capacity: The water storage tanks should be able to accommodate at least two operation of the system. Only about two operating capacity is required because the water can be recycled.

(c) Product Storage Tank Capacity: This also called recovery container needs to accommodate the bioethanol produced. It is good practice to use the expected operating capacity, of full system loading to determine the storage requirements. The ethanol storage tanks require a special design to enable quick fluid extraction as well as easy filling. The most common tank suitable for this purpose has a conical bottom with a release valve located at the vertex (Yuelei et. al, 2012). The bottom valve would be used to distribute the ethanol to an appropriate transportation vessel.

2.8.1 Fouling

Fouling is the presence of water or unpleasant deposit, in this case mainly due to decay. In practice after a period of operation the heat transfer surface becomes coated with various deposits (layers of materials of low heat conduction) present in the flow system. These deposits may be as silt or sediments from fluids carrying suspended solids or scale from crystallization or similar processes, or film from polymerization in the fluid HE. Fouling reduces performance by increasing thermal resistance. Also, the transfer surface may become corrode as a result of the interaction between the fluids and the material used for construction of the HE. Thus, the performance of HE depends on the heat transfer surfaces been clean and corrosion free (Yunus and Afshin 2015). Fouling, if present by any means constitute a heat transfer resistance r_o and/or $r_{i,}$ to the detriment of the overall heat transfer coefficient, U_o. Recognition of this effect takes the form of a 'fouling factor' R_f, also known as fouling resistance. Fouling factor is a multiplier less than unity applied to the overall coefficient for new, clean equipment to provide some reasonable operating period before the apparatus becomes incapable of handling the specified heat load, and had to be shut down and cleaned (Kay and Perkins 1972). It is the inverse of the filament

transfer coefficient of the fouling substance expressed as resistances. Therefore, the overall heat transfer U_f with fouling is related to the clean overall heat transfer coefficient U_c, in Equation 2.14 by (Yunus and Afshin 2015).

$$R_f = \frac{1}{U_c} + R_i + R_o \qquad (2.14)$$

Fouling like vapor blanketing has other adverse effect than loss of heat transfer capabilities, especially when it occurs on the coolant side of high temperature equipment. In this case, tube over heat and failure may be a hazard. Beyond this porous or spongy deposit may act as concentration cells for corrosive agents, which, in combination with a higher corrosion rate at elevated temperature, may lead to tube failure. Finally, since pressure loss increases inversely as the fifth power of the diameter for flow inside tubes, fouling deposits there have a severe effect (Yunus and Afshin 2015).

2.8.2 Cleaning and Maintenance of Distillation Devices

New boiler or boiler not used for a period of time regardless of the design should be flushed by boiling several times before operating. For this purpose it should be filled up to the rim with water. After closing the water is distilled without cooler. The steam exiting the cooler is passed into a drain or led into the ambient air using a tube. After daily operation the boiler should be cleaned in general. Very dirty stills as they are encountered after distillation need to be brushed out thoroughly using suitable cleaning detergents (e.g. 1 kg sodium carbonate or per filling of the still) (Kriss 2004). The delivery pipe is best cleaned with a sponge or brush. This sponge or brush is connected to a rope and led through the tube several times. The higher allowable velocity in the tube reduces fouling. Tube coolers are to be cleaned in the same manner whereas the coil coolers which are difficult to clean should be closed at the bottom and filled with a hot sodium carbonate solution and left for 1 hour. A thorough rinsing with cold water is required in any case. The rinse water ought to be checked for remains of basic material using indicator paper (Kriss 2004). For the cleaning of the outer parts, a 10 % citric acid solution has proven successful for cupper boiler. This solution is best applied to the parts still warm and flushed thoroughly with cold water after a short period of contact. Weakly alkaline or synthetic means are often sufficient to clean the exterior of high-grade steel parts (Kriss

2004). Water spots can be removed with a little vinegar. It is important not to clean high-grade steel with abrasive materials (steel brushes, steel wool). It is important to neutralize the slops after the distillation directly in the boiler using slaked lime or sodium hydroxide (mixing can be done through direct steam injection) (Kriss 2004). The remains (Slop) of the mash after distillation or distillers grain is commonly use as fodder (animal feed). The reactor should be lightly brushed after operation to remove slag or clinkers caused by melted and agglomerated ashes to prevent chocking of air channeling in subsequent operation. Remedies for fouling problems include the following:

i. To ignore its effect, but this is impossible as it will give wrong design data.
ii. To eliminate the fouling agent from the stream, but this is not often practicable on process streams since fluid itself is sometimes the fouling agent through coking or polymerizing reactions.
iii. Introduction of recirculating streams, such as boiler water, jacket water, cooling tower water, controls fouling.
iv. To minimize fouling, fluid flow should be of high velocity, and eddy flow region should be avoided.
v. Wide tube pitch, suitable tube array and a floating head system facilitate frequent cleaning of the HE's inner component, thereby checking fouling.

2.8.3 Environmental Effect

Consideration is mostly on air pollution. The air quality impacts of burning biomass for boiler heat depend on what fuel biomass is replacing, how it is burned, quality of the fuel and to an extent where it is burned. Biomass fired boilers has a positive impact on air quality as they contribute to reduce CO_2 emissions. However, biomass combustion can also increase other pollutant emissions. The typical pollutants related to biomass combustion are: nitrogen oxides (NO and NO_2, represented as NOx), sulphur dioxide (SO_2), particulate matter (PM), carbon monoxide (CO) and carbon dioxide (CO_2) (Jonsson & Hillring 2006). PM is a major pollutant of interest when considering biofuels (Holt et. al., 2006, Obernberger et. al., 2006). These pollutants can be grouped as (Thomas 2003):

- Unburnt pollutants: CO, PAHs (Polycyclic Aromatic Hydrocarbons), H_2, HCN, NH_3, N_2O, tar, soot and CxHy

- Complete combustion pollutants: NOx and CO_2
- Ash and contaminants: ash particles, SO_2, HCl, and heavy metals

The addition of air pollution control devices to boiler furnace may allow emissions to remain below acceptable limits even with a change in fuel which would have otherwise caused these limits to be exceeded. Operating costs for existing air pollution control equipment should be considered when calculating fuel associated costs. Equipments designed to reduce particulate matter emissions include the following:

(i) **Cyclones** separate particles from a gas stream by forcing flow to spiral through a tube. Centrifugal force causes the particles to move outward and collide with the tube wall. Particles then fall to the tube bottom where they are collected for disposal. Remaining clean gas flow travels upward through the center of the tube (Cooper & Alley 2002).

(ii) **Fabric Filters** (also called baghouses in large installations) are also used to control PM emissions. In these devices gas flows through a fabric filter which entrains solid particles. Reusable filters are cleaned by shaking or reversing the direction of airflow (Cooper & Alley 2002).

(iii) **Electrostatic Precipitators,** here flow gas past high voltage electrodes so that PM becomes electrically charged. Particles are then drawn to charged plates. Plates are periodically cleaned by shaking or by impact from rapping hammers (Cooper & Alley 2002).

(iv) **Wet Scrubbers** are also used to control PM emissions. This technology uses water droplets to intercept PM in exhaust flows. Water is then separated from the gas stream, usually by gravity, and treated before reuse or discharge (Cooper & Alley 2002).

Equipments designed to reduce particulate matter emissions include the following:

(i) **Incinerators** (also called thermal oxidizers or afterburners) operate with the addition of extra fuel to transform VOC's to products of complete combustion. Similar reactions may also be achieved using a catalytic converter instead of an afterburner.

(ii) **Gas Adsorption Technology** is used to control VOC emission as well. Gas particles adhere to solid porous materials such as activiated carbon. This material is usually packed in a bed which can be introduced to low pressure steam for reactivation when it becomes saturated with VOC's (Cooper & Alley 2002). Gas absorption occurs when

a gas is dissolved in a liquid. This technology is also called washing or scrubbing and can be used to control PM, VOC, NOx, or SOx emissions.

(iii) **Combustion Parameters -** NOx emissions are often effectively controlled through combustion parameters, such as excess air ratio (Moran & Shapiro 2000, Thomas 2003), good burner and chimney design, where the combustion is fulfilled completely, reducing the formation of unburnt compounds. When this is not practical NOx may be controlled with the use of catalysts which convert NO and NO_2 to pure nitrogen, which is a normal component of air. Adsorption techniques and wet scrubbing may also be effective in NOx control (Cooper & Alley 2002).

2.9 Heat Energy Source Considerations

Depending on the availability and cost, different fuels can be used for heating such as fossil fuels: kerosene, diesel, LPG; electricity; or biomass: firewood, charcoal, pellets etc. Fossil fuels have been the conventional sources of fuel for heat energy. The use of LPG as source of fuel is common both in industries and homes, urban and rural areas, particularly in places where its supply is readily accessible. However, because of the continued increase in the price of oil in the world market, the price of LPG fuel has gone up tremendously and is continuously increasing at a fast rate. With this problem, research centers and institutions are challenged to develop a technology for heating that will utilize alternative sources other than LPG. Considering solar energy as a heat source (e.g. solar drying or solar assisted drying) evaluated intensively by many projects and institutions (Kongdej & Songchai 2009, PATB 2010, Sombat & Wittaya 2009); it can be concluded that solar energy as a heat source for this distillation will not be technically feasible, thus, it is not a good prospect for commercial purpose. The potential of other biomass as alternative fuel source to replace LPG is a promising option (Hassan et. al., 2011). Biomass or electricity is often used because of their availability, ease of handling and simplicity of design. Biomass combustion equipment is often simpler and cheaper than equipment for other technologies (Sheng and Azevedo 2005). According to Joseph et. al., (2011), about 70 % of the total national energy consumption is accounted for by biomass in either direct or processed form, a trend that has continued for the last decade. Traditionally, energy in the form of firewood, pellets, twigs and charcoal has been the major source of renewable energy for many developing countries (Emerhi, 2011).

Charcoal could be used as a heat source for bioethanol distillation because of its low price and ease of procurement in agricultural countries like Nigeria.

2.9.1 Charcoal as a Heat Source

Charcoal is the product of simultaneous physical-chemical processes (pyrolysis and carbonization) of biomass which changes the biomass into pyrolytic gases and a solid fuel charcoal. The pyrolysis perspective focuses on the chemical breakdowns in the range from about 200 – 500 ^{0}C that result in the liberation of pyrolytic gases while carbonization focuses on the chemical build-ups of the carbon atoms into solid structures at temperatures, generally above 300 ^{0}C. Gas composition data of wood and charcoal is shown in Appendix A2 (FAO 1986). Charcoal varies in sizes sometimes depending on the producing wood and production process adopted. Medium to big size is better to use in attaining longer combustion. Bailey and Blankenhorn (1984) described the desirable criteria for quality wood charcoal as having low moisture content, relatively easy to cut, easy to handle, easy to ignite and burn with high calorific value, producing very little or no smoke without toxic fumes and neither spits nor sparks. They retain grain of the wood; has jet black color with shining luster; it is sonorous with metallic ring and does not soil the finger. These criteria are found in many tropical wood and other woody species. Moisture is an adulterant which lowers the heating value of the charcoal. Thus, quality specifications for charcoal usually limit the moisture content to around 5 - 15 % of its gross weight. The physical properties are thermal conductivity and specific heat, and structural properties, particle size, density and porosity (Grønli, 1996). Determining the thermal conductivity of charcoal is challenging due to its dependency on feedstock and pyrolysis condition (Ijagbemi et al 2014). Grønli (1996) reported specific heat of charcoal at room temperature ranging from 0.67 - 1.35 kJ/kgK. Koyuncu and Pinar (2007) reported 19.3 MJ/kg highest heating value, 4.1 % moisture content and 46 % thermal efficiency in a simple heating stove. Charcoal's physical properties influence the output of the furnace whereas chemical properties are more related to the quantity needed. A comparative combustion characteristic of charcoal and other biomass is shown in Appendix A3. According to Baldwin (1987), ultimate analysis of charcoal by mass is given in Table 2.9 while other properties of charcoal from different wood species are given in Table 2.10.

Table 2.9: The Ultimate Analysis of Charcoal (Baldwin 1987)

Element	Carbon	Hydrogen	Nitrogen	Oxygen	Sulphur	Ash
% mass	82.0	3.1	0.2	11.3	0.0	3.4

Table 2.10: Properties of Charcoal from Different Wood Species (Ijagbemi et al 2014)

Charcoal property	**Wood feedstock**				
	Afara specie	**obeche**	**iroko**	**oak**	**mahogany**
Density,g/cm^3	0.453 ± 0.038	0.620 ± 0.046	0.5567 ± 0.042	0.5300 ± 0.035	0.4567 ± 0.032
HV kJkg−1	$3.3236 \times 10^4 \pm$ 171.932	$3.3038 \times 10^4 \pm$ 169.604	$3.2149 \times 10^4 \pm$ 248.974	$3.2956 \times 10^4 \pm$ 430.128	$3.2230 \times 10^4 \pm$ 337.054
MC %	2.110 ± 0.661	2.663 ± 0.448	3.820 ± 0.931	4.823 ± 0.954	3.733 ± 1.106
Volatile matter %	7.833 ± 1.155	11.00 ± 0.5000	7.833 ± 1.607	7.167 ± 2.082	5.000 ± 0.866
Fixed carbon %	89.167 ± 1.258	85.500 ± 0.500	86.000 ± 0.866	89.000 ± 2.291	89.000 ± 0.500
Ash %	3.000 ± 0.500	3.500 ± 0.500	6.167 ± 0.764	3.833 ± 1.258	6.000 ± 1.000

Ash Content: Ash is the noncombustible component of the biomass. It is a measure of the mineral content of the original sample (Onwuka 2005). The higher the amount of ash in a fuel, the lower is the calorific value of the fuel. Ash impurities consist of silica, iron, alumina, and other incombustible matter. The Ash content varies from about 0.5 % to more than 5 % depending on the species of wood used to produce the charcoal (Nakorn et. al. 2010, FAO 1985), Koyuncu and Pinar (2007) reported 5.9 %. Good quality lump charcoal typically has an ash content of about 3 % (FAO 1985). The amount of ash is determined by heating a dry sample of biomass in a crucible in a furnace which is kept at 500 ^{0}C to 900 ^{0}C for sometimes to burn off moisture and organic materials completely. Sample is taken out of the furnace and the residue remaining in the crucible is ash. Measure the weight of the ash (M_s). Percentage ash content is then obtained with Equation 2.15.

$$a = \frac{\text{weight of ash}}{\text{weight of orignal sample}}\ x\ 100 \qquad (2.15)$$

Volatile Matter: volatile matter of biomass is that component of the carbon present in the biomass, which, when heated, converts to the vapor. It is gases released when heated. It is a function of the carbon to hydrogen ratio. The volatile matter can vary from a high of 40 % or more down to 5 % or less (Nakorn et. al. 2010). High volatile charcoal is easy to ignite but may burn with a smoke flame. Low volatile charcoal is difficult to light and burns very cleanly. High volatile matter charcoal is less friable than ordinary hard burned low volatile charcoal and so produces fewer fines during transport and handling. It is also more hygroscopic and thus has higher natural moisture content (FAO 1985). The amount of volatile matter is determined by heating a dried ground sample of biomass with an initial mass M_i in a closed crucible in an oven with a temperature of 600 ^{0}C for six minutes followed by heating the sample in an oven with the temperature of 900 ^{0}C for another six minutes before its weight (M_f) is measured FAO (1985). Volatile matter is then calculated with Equation 2.16.

$$V = \frac{M_i - M_f}{M_i}\ x\ 100 \qquad (2.16)$$

Fixed Carbon: The amount of fixed carbon is determined from mass balance expression in Equation 2.17 according to FAO (1985).

$$c = 100 - (M + a + V) \qquad (2.17)$$

Fixed carbon is the solid fuel left after the volatile matter is driven off, but not just carbon. The fixed carbon content of charcoal ranges from 50 % - 95 % (FAO 1985), thus charcoal consists mainly of carbon.

Calorific Value: the calorific value of a fuel is defined as the amount of heat evolved when a unit weight of fuel is completely burned and the combustion products such as CO_2 and H_2O are cooled of 298 ^{0}K. The calorific value of any given species of biomass is dependent on the moisture content and its density. It is determined by a bomb calorimeter. A sample of air dried biomass with a known mass is burnt in an atmosphere of oxygen in a stainless steel high pressure vessel known as a bomb. The bomb is placed in a calorimeter which is highly polished outer vessel containing a known amount of water with a known temperature. The combustion products CO_2 and H_2O are allowed to cool to the standard temperature. The resulting heat of combustion is measured from the accurate measurement of the rise in the

temperature of water in the calorimeter, the calorimeter itself and the bomb. The calorific value so estimated is the gross calorific value.

2.9.2 Charcoal Combustion

Charcoal has high carbon content. Efficient and complete combustion is a prerequisite of utilizing charcoal as an environmentally desirable fuel. In addition to a high rate of energy utilization, the combustion process should therefore ensure the complete destruction of the charcoal and avoid the formation of environmentally undesirable compounds. In order for combustion to continue; an adequate mixture of fuel and oxygen (air) in a controlled ratio should be ensured, the fuel already ignited in the boiler furnace should transfer some of its heat to the feed in order to ensure a continuous combustion process. It is important to understand that gases burn like flames while solid particles glow, thus during the production of charcoal from wood combustion of wood, approximately 80 % of the energy is released in the form of gas (producer gas) and the remaining part should be from the charcoal. During mixing of the fuel and air, it is important to achieve good contact between the oxygen of the air and the combustible constituents of the charcoal. The better the contact is the faster and more complete is the combustion and this calls for attention in the charcoal size. Firing technology for solid fuels is thus difficult and more complicated than the firing technology in a natural gas or oil-fired heating system. In order for combustion to occur, the charcoal fuel must pass through three stages, which are (1) Drying, (2) Gasification and combustion and burnout. When charcoal is heated, water begins evaporating from the surface. Hence two things occur: Gasification occurs at the surface, and the temperature deeper inside it will increase resulting in evaporation of moisture from the interior of the charcoal. As the water evaporates and is passed away, the area that is pyrolysed spreads. At this point, charcoal reacts with oxygen of the air at a glowing red heat to form colorless carbon monoxide and methane gas. The gas thus produced is ignited above the fuel, burns with a blue flame with more oxygen from the air to produce carbon dioxide gas and transfers heat to the ongoing evaporation and pyrolysis. The combustion process is continuous. Due to the heat liberated by both of these reactions, the charcoal reaches a glowing red, the gasified charcoal then glows, as shown in Figure 2.9 below and radiates heat energy, transformed by oxygen until only ash is left and the hot carbon dioxide gas leaves the combustion zone, hopefully giving up by

convection most of its heat by direct physical contact with the boiler. The gas temperature falls as it transfers heat and it passes off into the surrounding through the exhaust pipe. The larger the charcoal particle is, the longer is the combustion process but moderate size ensures good contact between fuel and air, quickly dries, give off gases and burn, resulting in a high combustion intensity. The size of the fuel, therefore, is of great importance to the speed of combustion. Wood gasifiers operate on wood blocks and woodchips ranging from 80 x 40 x 40 mm to 10 x 5 x 5 mm while Charcoal reactors are generally fuelled by charcoal lumps ranging between 10 x 10 x 10 mm and 30 x 30 x 30 mm - 60 x 60 x 60 mm (Turare 2008, Wusana et. al., 2014).

The moisture content in fuel reduces the energy content expressed by the calorific value, since part of the energy will be used for evaporation of the water (FAO 1985). Therefore, dry charcoal has a high calorific value, and the heat from the combustion should be drawn away from the combustion chamber in order to prevent overheating and consequent damage to material while wet charcoal has a low calorific value per kg total weight, and the combustion chamber should be insulated so as to avoid reduction in boiler efficiency and enable a continuous combustion process. Moisture content above 55 - 60 % of the total weight will make it very difficult to maintain the combustion process unless the evaporating gases are needed for direct combustion purposes (FAO 1985).

Figure 2.9: Natural Charcoal and Burning Charcoal

In order to completely burn charcoal, Baldwin (1987) reported stoichiometric air requirement of 9.98 kg, ET, (2016) reported 8.4 m^3 per kg of charcoal. Charcoal has high Stoichiometric

weight air-fuel ratio due to its low oxygen content. The amount of airflow for gasification per unit mass of fuel wood is about 0.3 to 0.5 of the stoichiometric air requirement of the fuel (Ojolo et. al., 2012). Thus, burning it using 30 to 40 % of the stoichiometric air or an equivalence ratio of 0.3 to 0.4 only of the air needed for combustion will rather gasify the charcoal, which produces a flammable, bluish gas (Belonio 2005). Mcdougall (1991), Eastop and McConkey (1993) expressed reaction of burning charcoal in Equation 2.18:

Combustion $C + O_2 = CO_2 + heat$ → complete combustion

Water Gas $C + H_2O = CO + H_2$

Water Shift Reaction $CO + H_2O = CO_2 + H_2$ ↓ gasification

Boudouard Reaction $C + CO_2 = 2CO$

Methane Reaction $C + 2H_2 = CH_4$ (2.18)

An efficient combustion requires sufficient: (1) High temperature (2) Excess oxygen (3) Combustion time and (4) Mixture. This ensures a low emission of CO, HC, polyaromatic HC (PAH), and unburned carbon in the slag. Unfortunately, (1) to (2) is also directly related to the formation of NOx. The technology applied should therefore be a so-called "low-NOx" technology, i.e., a technology applying methods resulting in a reduced NOx emission. In addition to CO_2 and H_2O, the flue gas will contain air (O_2, N_2 and Ar) and a low amount of undesirable reaction products, such as CO, hydrocarbons, PAH, NOx etc. When wood, residues or energy crops are converted into energy, they produce about as much CO_2 as they had previously fixed during their growth (UK Bioenergy Strategy, 2012). Koyuncu and Pinar (2007) reported 2095 mg/MJ CO, 0mg/MJ SO_2 and 2.62 mg/MJ NO_x in a space heating stove. Other advantages of Charcoal furnace are as follows: 1) oxygen can spread throughout the furnace therefore the combustion can occur completely, 2) its combustion can be non flame, clean, relatively odourless and smoke-free compared to wood or coal, 3) SO_2 is not greatly emitted as it is essentially a zero to low sulphur fuel. Wood contain about 70 – 80 % volatiles (in % dry matter) which means that the component of wood will give up 70 – 80 % of its weight in the form of gases, while the remaining part will be turned into charcoal. This is one reason why a sack of charcoal seems light compared to the visual volume. The charcoal has

more or less kept the original volume of the green wood, but has lost 80 % of its weight. Generally, high volatiles content requires the combustion air to be introduced above the fuel bed (secondary air), where the gases are burnt, and not under the fuel bed (primary air). In practice charcoal is the only biomass fuel that does not need special attention on volatile matter, having less than 3 – 30 % (Ojolo et. al., 2012, FAO 1985). A special characteristic of ash is its heat conservation property. For heating systems using a grate, the ash content is important in order to protect the grate against heat from the flames, also ash layer under the grate helps in drying fresh charcoal for oncoming combustion.

2.10 Distillation Considerations

Main 'Performance Criteria' of a distillation unit are energy efficiency; time to distill; and capacity relative to yield. Boiler capacity depends on the maximum quantity of feed it is required to handle which determines its sizing for a particular geometry. In setting up a distillation unit the following parameters are considered:

2.10.1 Fluid Properties

The design of a distiller considers certain properties of the involved fluids which in this work are water and bioethanol, the boiler's feed. Water and ethanol fluid properties are given in Appendix A4 while properties of the feed and its proportioned components are determined from the preliminary experiment. The mixture should gently bubble and vaporize.

2.10.2 Distillation Energetic

This refers to the amount of heat that needs to be supplied by the combustion chamber i.e heat of vaporization. The energy required to vaporize ethanol from the broth is dependent upon its boiling temperature and moisture content (Brooker et al 1974). The amount of energy needed can be calculated from the psychometric chart or from energy balance equations. First, the temperature of the substrate is to be raised from its initial temperature to the boiling temperature of bioethanol by heat energy Q_1, obtained from Equation 2.19, and then bioethanol is changed to vapor at boiling phase by heat energy Q_2, determined with Equation 2.20.

$$Q_1 = MC\Delta\theta \qquad (2.19)$$

And

$$Q_2 = ML \quad (2.20)$$

M = Mass of fermented feedstock (kg), C = Specific heat capacity of fermented stock (J/g^{0}C), Δθ = Change in temperature (^{0}C) and L = the latent heat of vaporization (J/g).

According to Eke (1991), needed vaporizing or distillation energy, Q_n (kJ) can be calculated with Equations 2.21 and 2.22.

$$Q_n = W c_p (T_2 - T_1) + m_e h_{fg} \quad (2.21)$$

$$Q_n = MC\Delta\theta + ML \quad (2.22)$$

Where w: mass of broth to be dried (kg). c_p: Specific heat of the broth to be dried (kJ/kg^{0}C). m_e is the mass of produced ethanol (kg/h). h_{fg} is specifc latent heat of evaporation of bioethanol at its boiling point (kJ/kg^{0}C).. h_{fg} is chosen at its boiling point because highest energy to convert bioethanol to vapor is achieve at that point (Li et al 2010; Iguaz & Vı´rseda 2007). T_1 and T_2 are the initial temperature of mash and boiling point of bioethanol respectively. The temperature of mash 'T_1' at the entrance of the boiler must be controlled within the range between the azeotrope point of wash and boiling point of pure water *(*Yuelei et. al 2012). Latent heat of evaporation is equal to the increased internal energy of the vapor phase compared with the liquid phase, plus the work done against ambient pressure. It can be calculated from Equation 2.23 or deduced from property tables.

$$h_{fg} = \Delta U_{vapor} + \rho\Delta V \quad (2.23)$$

According to Mohammed and Abul (2009) and Brooker et al (1974), the rate of energy required for evaporation is given as Equation 2.24.

$$\dot{q} = m_e \, x \, h_{fg} \quad (2.24)$$

Where $\dot{q}$ is the rate of heat transfer.

Deducing from Khurmi & Gupta (2006), Q_n can be calculated with Equation 2.25

$$Q_n = m_e (h_2 - h_1) \quad (2.25)$$

Where h_1 is the enthalpy of ethanol in the broth at distillation time, t (0), h_2 is the ethanol enthalpy at its boiling point, $(h_2 - h_1)$ is heat required to evaporate 1kg of ethanol.

Heat Input: Distillation rate is controlled by the heat input. This is the amount of heat energy available in the fuel fed into the combustion chamber for distillation process. It is the combustion chamber or reactor input and can be calculated with Equation 2.26 due to Belonio (2005).

$$Q_f = WFU \times HVF \quad (2.26)$$

WhereQ_f: heat energy input (kJ), WFU: weight of fuel used (kg) and HVF: heating value of fuel (kJ/kg). Normally Q_f may differ from Q_n as it also accounts for heat loss in the boiler unit. As deduced from Tharaja et al (2001), Q_f and boiler power rating p_f can be determined from Equation 2.27 and 2.28 respectively.

$$Q_f = Q_n / e_{ff} \quad (2.27)$$

$$p_f = \frac{Q_f}{3600\,(\text{sec})} \quad (2.28)$$

Furnace Efficiency: Furnace or calorific efficiency is related to the useful heat generated and the calorific value of 1kg of fired sampled materials. It is Sensible heat in boiler unit per kg of fuel fired x 100 % (Rajviv *et al*., 1980). Up to 70 % of the energy originally present in the wood may be lost in charcoal production process. The available energy and heat conversion efficiency for some heat source materials are given in Table 2.11.

Table 2.11: Available Energy and Heat Conversion Efficiency for some Fuel Materials

Fuel	**Available energy, AE**	**Conversion efficiency, E_{ff}**
Wood	3,355(Kcal/kg)	
Wood charcoal	5,893(Kcal/kg)	
Rice husk	3000Kcal/kg	
Kerosene	11,000(Kcal/kg)	3.66(%)
Electricity	3,414 – 3, 412 Btu/kWh	95 (%)
Gasoline	142,000 – 137,000Btu/gal; 11,528(Kcal/kg)	60 (%)
Diesel	10,917(Kcal/kg)	
LPG	96,000 – 91, 500 Btu/gal; 11,767(Kcal/kg)	85 (%)
Natural gas	100,000 Btu/Therm; 1000 Btu/ft^3	95 (%)

(Source: Dirk & Fred 2002, Belonio 2005).

2.10.3 Estimation of Fuel Requirements

Fuel consumption is the quantity of fuel to be fed into the furnace in order to provide the amount of energy needed for the operation. The fuel requirement is determined base on the calorific value per unit mass of fuel. It is achieved by solving the heat balance in the furnace as in Equation 2.29 according to Belonio (2005).

WFU = Q_f / HVF (2.29)

The fuel consumption rate is the amount of fuel consumed per hour. It has been frequently determined by investigators (Viboon Thepent 2010, Dirk & Fred 2002, Rathore et al 2009) with Equation 2.30.

$$\text{FCR} = \frac{\text{Q}_\text{n}}{\text{HVf x } e_{ff}} = \frac{\text{quantity of charcoal (kg)}}{\text{operating time (hr)}} \quad (2.30)$$

Where: FCR - fuel consumption rate, kg/hr, Q_n - heat energy needed, KJ/hr

HVF - heating value of fuel, KJ/kg, e_{ff} – boiler calorific efficiency, %.

2.10.4 Amount of Air Needed for Complete Combustion

The rate of flow of air needed to completely burn the charcoal is very important in determining the nature, size of the fan or of the blower if need be. It is determined using the rate of consumption of fuel (FCR), stoichiometric air of fuel (SA), density and the recommended equivalent ratio ε for gasifying the solid fuel e.g. ε for wood is 0.25 – 0.5 (Okpolo et. al., 2012, Reed 1981). This implies that charcoal will have low ε value since its carbon content is lesser compared to wood. Belonio (2005) expressed the amount of air needed for the gasification with Equation 2.31.

$$AFR = \frac{\varepsilon \; x \; FCR \; x \; SA}{\rho_a} \quad (2.31)$$

Where

$$\varepsilon = \frac{Actual \, \frac{air}{biomass} \; ratio}{Stoichiometric \, \frac{air}{biomass} \; ratio} \quad (2.32)$$

Thus for complete combustion

$$AFR = \frac{FCR\ x\ SA}{\rho_a} \qquad (2.33)$$

Axtell (2002) expressed AFR as volumetric flow rate of the drying air with Equation 2.34.

$$AFR_v = m_a\ x\ v_s \qquad (2.34)$$

Where AFR_v is volumetric flow rate of air in m^3/s; v_s is specific volume of air in m^3/kg.

According to Adzimah & Seckley (2009), mass flow rate of hot air is obtained with Equation 2.35 derived by equating work done by reactor to work done on air.

$$m_a = \frac{P_{Tn}}{C_{air}\,\Delta\theta_{air}} = AFR\ x\ air\ density \qquad (2.35)$$

Where: P_{Tn} - work done by reactor in watts, m_a - mass flow rate, C_{air} – specific heat of heat, $\Delta\theta_{air}$ – change in air temperature i.e. 30 ^{0}C to 99.74 ^{0}C, AFR - air flow rate, m^3/hr, ε – recommended equivalence ratio, 0.25 to 0.5, ρ_a - Air density, SA - stoichiometric air of charcoal.

2.10.5 Time to Consume Fuel

This refers to the total time required to completely consume the charcoal inside the furnace. This includes the time to ignite the fuel and the time to generate gas, plus the time to completely burn all the fuel in the reactor (Singh 2008). The mass of charcoal and its consumption rate (FCR) are the factors used in determining the total time to consume the charcoal in the reactor. The time can be computed using Equation 2.36 according to Belonio (2005).

$$T = \frac{m_f}{FCR} \qquad (2.36)$$

Where T - Time required to consume the charcoal; m_f – charcoal mass, kg

2.10.6 Combustion Zone Rate (CZR)

This is the time required for the combustion zone to move down the reactor and is computed with Equation 2.37 according to Ojolo et. al., (2012).

$$CZR = \frac{reactor\ length\ (m)}{operating\ time\ (h)} \qquad (2.37)$$

2.10.7 Reactor Diameter

Reactor diameter is the diameter of the cylinder in which charcoal is burned. It is usually a function of the amount of fuel consumed per unit time (FCR) and the specific gasification rate (SGR) of the fuel material, which is in the range of 100 to 250 kg/m^{2}h for fuel wood (Ojolo et. al., 2012, Wikipedia 2010). The reactor diameter can be computed using Equation 2.38 according to Belonio (2005).

$$D = \left(\frac{1.27\ FCR}{SGR}\right)^{0.5} \qquad (2.38)$$

Where: D - Diameter of reactor, m, FCR - fuel consumption rate, kg/hr,

SGR - specific gasification rate of fuel, kg/m^2-hr and is calculated with Equation 2.39 according to Ojolo et. al., (2012).

$$SGR = \frac{\text{weight}\ of\ fuel\ used(kg)}{reactor\ area\ x\ operating\ time} \qquad (2.39)$$

Gasification is the production of combustible (synthetic) gases CO, H_2, CO_2, H_2O and CH_4, (commonly called smoke) from carbon containing feedstock by the application of heat with limited air under intense pressure (Babu 2005). SGR is the biomass consumption rate (m_f) per unit cross sectional area (A).

2.10.8 Furnace Height

This refers to the total distance from the top to the bottom end of a vertical reactor or the length of a horizontal reactor (combustion chamber). It determines how long the distiller would be operated in one loading of fuel (Belonio 2005). Basically, it is a function of a number of variables such as the required time to operate the system (T), required feedstock holding capacity, the specific gasification rate (SGR), and the density of charcoal (ρ_{rh}). It can be computed with Equation 2.40 according to Singh (2008).

$$H = \frac{SGR\ x\ T}{\rho_{ch}} \qquad (2.40)$$

Where: H = height or Length of the reactor, (m), T = Time required to consume charcoal (h), SGR = specific gasification rate of charcoal, kg/m^{2}h, ρ_{ch}- charcoal density, (kg/m^3).

Usually, the combustion zone moves down the entire height of the reactor at a speed of 1 to 2 cm/min. The higher the reactor, however, the more pressure draft is needed to overcome the resistance exerted by the fan or by the blower.

2.10.9 Furnace Volume / Cross Sectional Area

Inferring from the volume equations, the volume of a reactor defines the quantity of heat that can be released in the combustion chamber. This refers to the total space available in the reactor to accommodate the fuel. Somchart et al (2010) expressed it with Equation 2.41.

$$V_r = B\,HVF/Q_{fr} \tag{2.41}$$

Where B: feed rate of charcoal, kg/h. HVF: high heating value of charcoal, kJ/kg.

Q_{fr}: Design parameter for charcoal, KJ/h.m^3.

A cylindrical reactor V_r is also expressed with Equation 2.42 and 2.43.

$$V_r = \pi r^2 h \tag{2.42}$$

$$V_r = \frac{FCR\ x\ Time}{fuel\ density} \tag{2.43}$$

Uniform combustion can be achieved when the reactor is designed in circular rather than in square or in rectangular cross-section. Wider cross-sectional area reactor gives stronger power output. According to Rathore et al (2009), the Cross sectional area (CSA) of the reactor can be computed using Equation 2.44 and 2.45.

$$CSA = \frac{FCR}{SGR} \tag{2.44}$$

$$s = 2\pi r(h\ + r) \tag{2.45}$$

Where r and h are radius and height respectively

2.10.10 Superficial Air Velocity

This refers to the speed of the air flow in the fuel bed. The velocity of air in the charcoal bed will cause channel formation, which affects combustion. Similarly, the thicker the layer of fuel in the reactor, the greater is the resistance required for the air to pass through the fuel

column. The diameter of the reactor (D) and the airflow rate (AFR) determine the superficial velocity of air in the combustor. According to Belonio (2005) and Srinivasa et. al., (2016), superficial gas velocity is computed with Equation 2.46.

$$Vs = \frac{4\ AFR}{\pi(D)^2} \qquad (2.46)$$

Where: Vs - Superficial gas velocity, m/s, AFR - air flow rate, m^3/hr, D - Diameter of reactor, m.

From Belonio (2005), total pressure draft of charcoal can be obtained with Equation 2.47.

$$Pd = H\ x\ \Delta p \qquad (2.47)$$

Where Pd is the total pressure draft of charcoal, H is Reactor height and Δp is the corresponding pressure draft of charcoal in centimeter of water per meter depth of fuel at the calculated superficial gas velocities.

2.10.11 Resistance of Fuel Material to Airflow

For biomass solid fuel, the thicker the layer of fuel material in a reactor, the greater is the resistance required for air to pass through the fuel column. In the fuel column, resistance of fuel material to airflow refers to the amount of resistance exerted by the fuel inside the reactor during combustion (Singh 2008). This is important in determining whether a fan or a blower is needed for the reactor. The thickness of the fuel column (Tf) and the specific resistance (Sr) of charcoal, will give enough information for the total resistance needed for the fan or the blower. According to Belonio (2005), resistance of fuel (Rf) is computed with Equation 2.48.

Rf = Tf x Sr (2.48)

Where, Rf and Sr are measured in cm of H_2O and cm of water/m of fuel respectively.

2.10.12 Exhaust Pipe

Fresh air (oxygen) enters the fuel bed by natural or mechanical (forced) means; difference of pressure (draught) above and below the fire grate causes the gases of combustion to exhaust from the combustion chamber. The chimney ensures a natural draught which objectives are to provide an adequate supply of air for charcoal combustion, exhaust the gases of combustion from combustion chamber, and discharge these gases to the atmosphere through the chimney

(Holaman 1990). The height of the chimney 'H" is calculated from this driving pressure difference as given in Equation 2.49 – 2.52 according to Khurmi and Gupta (2006)

$$h_{draug\ ht} = 353H\left(\frac{1}{T_{atm}} - \frac{m+1}{mT_{fl}}\right) mm\ of\ water \quad (2.49)$$

This implies that

$$H = \left[\frac{p_{draug\ ht}}{353\left(\frac{1}{T_{atm}} - \frac{m+1}{mT_{fl}}\right)}\right] \quad (2.50)$$

Where H= height of chimney above charcoal grate, T_{atm} = temperature of air outside the chimney, T_{fl} = temperature of flue gas inside the chimney, m = mass of air actually used in kg/kg of fuel. (m + 1) = mass of flue gases in kg/kg of fuel.

Height of hot gas column producing the draught and velocity of flue gases through the chimney is given in Equations 2.52 and 2.53 respectively.

$$H^{'} = H\left(\frac{m}{m+1} \times \frac{T_{fl}}{T_{atm}}\right) - 1 \quad (2.51)$$

$$V_{flue} = \sqrt{2g}H^{'} = 4.43\sqrt{H\left(\frac{m}{m+1} \times \frac{T_{fl}}{T_{atm}}\right) - 1} \quad (2.52)$$

Actual draught is always less than the theoretical draught (static draught) due to the (1) effect of frictional resistance offered to the passage of air through the fire bars fire flues and chimney, (2) temperature of flue gases inside the chimney diminishes for every metre of its height. The chimney has maximum discharge when the flue gas temperature is slightly more than the atmospheric temperature as given in Equation 2.53.

$$T_{fl} = 2\left(\frac{m+1}{m}\right)T_{atm} \quad (2.53)$$

Height of hot gas column producing the draught is equal to the height of the chimney thus:

$$H^{'}_{max.discharge} = H \quad (2.54)$$

Draught pressure in mm of water at chimney maximum discharge is given in Equation 2.55.

$$h_{draug\ ht.max} = \frac{176.5H}{T_{atm}} \quad (2.55)$$

2.10.13 Blower / Fan

The fan or blower is use to create the necessary airflow (Dirk & Fred 2002), that is needed for the fuel combustion. They are available in AC or DC. The fan to be used should be capable enough to overcome the pressure exerted by the charcoal in the fuel bed and, subsequently, by the char, ash. A high- pressure fan is usually ideal for down-draft type reactor. Using blowers can overcome pressure in long reactors or those with thicker fuel column. However, the noise produced by its impeller can be destructive to the users. Depending on the required airflow rate and the needed pressure creation, either axial-flow or centrifugal fans are used (Dirk & Fred 2002). An overview of axial flow and centrifugal fans are shown in Table 2.12. Generally axial-flow fan operates at 2915 rpm at 50 Hz while centrifugal operates at 1460 at 50Hz (Dirk & Fred 2002). The axial-flow fan, as the name implies, moves air parallel to its axis and at right angles to the field of rotation of the blades. The energy used in creating pressure in centrifugal fan is produced by centrifugal action. The air enters the centrifugal fan parallel to the shaft, moves radially through the blades and is discharged tangentially from a scroll housing surrounding the impeller (Brooker et al 1974). Oliver & Williams (2010) and Adzimah & Seckley (2009) expressed fan power requirement with Equation 2.56.

$$P_{Fan} = \frac{air\ flow\ rate\ x\ pressure\ drop}{6320\ x\ fan\ efficiency} \quad (2.56)$$

According to Brooker et al (1974) mechanical and static efficiencies of the fan performance can be obtained with Equation 2.57 and 2.58 respectively.

$$\text{mechanical efficiency (ME)} = \frac{\text{cfm x total pressure}}{6356\ \text{x BHP}} \quad (2.57)$$

$$\text{static efficiency (SE)} = \text{ME x } \frac{\text{static pressure}}{\text{total pressure}} = \frac{\text{cfm x static pressure}}{6356\ \text{x BHP}} \quad (2.58)$$

BHP is the power delivered to fan shaft.

Table 2.12: Overview on Axial Flow and Centrifugal Fans

Fan type	Axial flow	Centrifugal, forwards curved	Centrifugal, backwards curved
	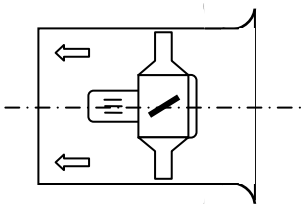	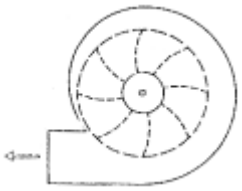	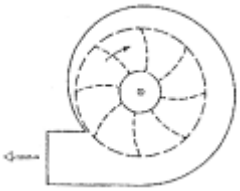
Cost	Cheap	more expensive	most expensive
Characteristics	non-overloading	overloading	Non-overloading
Pressure creation	10-15 cm water	0-15 cm water	0-30 cm water
Unstable region of operation	At high pressure	None	None
Construction	Sturdy	Light	Sturdy
Noise level	High	Low	Medium
Typical use	Aeration, recirculation batch dryer, batch dryer		In-store dryers

(Source: IRRI 2010; Brooker et al 1974)

Non-overloading characteristics means that regardless of changes in the system characteristics e.g. if the outlet of the fan is blocked, the electric motor driving the fan will still be within normal overload tolerance (IRRI 2010). Below the efficient range of output, the fan experiences a 'dip' and is said to be unstable and tends to ''hunt'' between two air flows that give the same (static) pressure (Brooker et al 1974). The efficiencies of the axial-flow, forward-curved and backward- curved centrifugal fans are 55-75%, 30-50% and 50-65% respectively (Brooker et al 1974). Axial fan has no belt to adjust or to wear out unlike others.

2.10.14 Power Required for Furnace Fan

The power of a fan (or air power) required doing internal work on the air or gas to deliver its certain volume is given in Equation 2.59 according to Khurmi and Gupta (2006).

$$P(watts) = \frac{\rho v}{60.\,\eta_f} \qquad (2.59)$$

Where volume of air 'v' in (m^3/min) flowing through fan is given by Equation 2.60.

$$v = \frac{0.773\,.m.M.T_{atm}}{273} = \frac{m\,.M.T_{atm}}{353} \qquad (2.60)$$

Where M = mass of fuel in kg/min. Also mass of flue gases '$mass_{flue}$' in (kg/min) handled by induced draught fan is given in Equation 2.61 while Equation 2.62 is for forced draught fan.

$$mass_{flue} = M(m+1) \qquad (2.61)$$

$$P(watts) = \frac{\rho.m.M.T_{atm}}{60.\eta_f.353} = \frac{9.81.h_{draug\ ht}.m.M.T_{atm}}{60.\eta_f.353} = \frac{h_{draug\ ht}.m.M.T_{atm}}{60.\eta_f.36} \qquad (2.62)$$

Where ρ = draught pressure in N/m^2 = 9.81 x $h_{draught}$, η_f = induced draught fan efficiency.

$$P(watts) = \frac{h_{draug\ ht}.m.M.T_{fl}}{60.\eta_f.36} \qquad (2.63)$$

Forced draught differs from induced draught as given in the Table 2.13.

Table 2.13: Comparison between Forced Draught and Induced Draught

Force draught	**Induced draught**
Fan is placed before the charcoal grate	Fan is placed after the charcoal grate
Furnace pressure is above atmospheric pressure	Furnace pressure is below atmospheric pressure
Forces air into the combustion chamber	Sucks hot gases from the combustion chamber, and forces them into the chimney
Requires less power as the fan has to handle cold air only. Moreover, volume of air handled is less because of low temperature of the cold air	Requires more power as the fan has to handle hot air and flue gases. volume of air and gases is more due to high temperature of the air and gases
Flow of air is more uniform	Flow of air is less uniform
As the leakages are outward, therefore there is a serious danger of blow out when the fire doors are opened and the fan is working	As the leakages are inward, therefore there is no danger of blow out but if the fire doors are opened and the fan is working there will be a heavy air infiltration

Condenser

In designing a condenser which is a heat exchanger, the process conditions must be specified e.g. heat transfer rate, stream composition, fluid flow rate and temperature conditions must be specified. The required physical properties of the fluids over the temperature and pressure ranges of interest must be specified which include density, viscosity and thermal conductivity.

2.10.15 Coolant Quantity

The quantity or volume of water needed to cool ethanol vapor in the condenser determines the volume of the water tank (reservoir). The volume of water can be calculated by equating the quantity of heat energy lost by ethanol vapor to the heat energy gained by water (Khurmi and Gupta, 2006; Biodiesel, 2009), as expressed in Equation 2.64.

$$M_w C_w(\theta_{exit} - \theta_{30}) = M_{eth}\ x\ L_{c.eth} \quad (2.64)$$

Where, M_w = mass of water (kg), C_w = specific heat capacity of water, θ_{exit} = the highest desired temperature water should get to, θ_{30} = inlet temperature of water, M_{eth} = mass of ethanol (kg) and $L_{c.eth}$ = latent heat of condensation of bioethanol. Enthalpy of condensation (heat of condensation) is by definition equal to the enthalpy of vaporization but assigned negative as heat is release by the substance i.e. '$-L_{v.eth}$'.

2.10.16 Fluids Flow Properties

The fluids mass flow rate, volumetric flow rate and velocity are calculated with Equations 2.65, 2.66 and 2.67 respectively.

$$mass\ flowrate = \frac{mass\ (kg)}{operation\ period\ (s)} \quad (2.65)$$

$$Volumetric\ flowrate = \frac{mass\ flowrate\ (kg/s)}{density\ (kg/m^3)} \quad (2.66)$$

$$V = \frac{volumetric\ flowrate}{tube\ CSA} \quad (2.67)$$

Their Reynold's number is calculated with Equation 2.68.

$$R_e = \frac{\rho V D}{\mu} \quad (2.68)$$

Where, ρ, μ and Vare density, dynamic viscosity and velocity of the vapor or liquid phase. This differs at the bioethanol tube because of phase change. Thus, inlet and outlet condition of the bioethanol tube gives Reynold's number of bioethanol vapor and liquid respectively.

2.10.17 Heat Transfer in Condenser

Design aims to calculate overall heat transfer that is less than the assumed or prescribed heat dissipated by the distillation plant. As correlated by engineers, heat transfer data depend on the Nusselt number which is a function of Reynolds number Re, and Prandtl number Pr as given in Equation 2.69.

$$Nu = CRe^{m}Pr^{n} \tag{2.69}$$

Where

$$Pr = \frac{C_p \mu}{\delta} \tag{2.70}$$

Where C, m and n are constants determined from experimental data. μ is dynamic viscosity, δ is thermal diffusivity, C_p is specific heat. C is 0.027 for viscous liquids, 0.023 for non viscous liquids and 0.02 for gases.

The heat transfer coefficient is one of the most important quantities in heat transfer; it must be computed for both the hot and cold fluid streams and depends on the flow type (laminar or turbulence) and nature of velocity (high or low). The Nusselt number relates to the heat transfer coefficient by Equation 2.71.

$$Nu = \frac{hD}{K} \tag{2.71}$$

Where h, D and K are heat transfer coefficient, diameter and conductivity respectively.

Tube-side Heat Transfer Coefficient: Condensation took place in the small copper tube. Calculation of the condensation heat transfer coefficient h_t, takes note of the different fluid phases, flow type and velocity. For a laminar with low velocity, the condensation heat transfer coefficient is calculated according to Chato (1962) and considering inclination angle with Equation 2.72.

$$h_t = 0.555\left[\frac{g\rho_l(\rho_l - \rho_v)K_l^3}{\mu_l(T_{sat} - T_s)D}\ h_{fg}^*\right]^{1/4}(Sin\ \theta)^{1/4} \quad (2.72)$$

Where

$$h_{fg}^* = L_{eth} + \frac{3}{8}C_{pl}(T_{sat} - T_s) \quad (2.73)$$

Where T_{sat} and $T_{s,}$ are saturated temperature of ethanol and tube surface temperature. L_{eth} and ρ_v are properties of saturated ethanol whileρ_l, μ_l, K_l and C_{pl} are bioethanol properties at film temperature T_f which is (T_{sat} + T_s) / 2. h_{fg}^* is the modified latent heat of vaporization according to Rohsenow (1956).

Shell-side Heat Transfer Coefficient: coolant flows in the shell and heat transfer does not involve a phase change. The flow pattern in the shell which depends on the presence of baffles affects the Nusselt number. The flow in the main stream of fluid for a segmented shell will be a mixture of cross flow between baffles, coupled with axial (parallel) flow in the baffle windows. For a developed internal laminar flow, the Nu is constant value (Kay and Perkins, 1972, Yunus and Afshin 2015). The values depend on the hydraulic diameter and ranges from 3.66 to 4.364 or 4.86 which are for convective uniform surface temperature and convective uniform heat flux respectively, for a circular annular tube. Nu of at the shell side is that corresponding to the ratio of OD of the tube to the ID of the shell, read from Appendix A5. Yunus and Afshin (2015) gave shell side heat transfer coefficient as Equation 2.74.

$$h_s = \frac{(N_u)_{read}\ .K}{D_h} \quad (2.74)$$

Overall Heat Transfer Coefficient: In a HE, heat is first transferred from the hot fluid to the wall by convection, through the wall by conduction, and from the wall to the cold fluid again by convection. The thermal resistance network associated with this heat transfer process involves two convection and a conduction resistances. The overall heat transfer coefficient is the reciprocal of the overall resistance to heat transfer (Holman 1990). It is a convenient means of expressing the capability of transferring heat through tube. For a negligible tube thickness, Yunus and Afshin (2015) gave overall heat transfer coefficient 'U' as Equation 2.75.

$$\frac{1}{U} = \frac{1}{h_t} + \frac{1}{h_s} + R_{ft} + R_{fs} \quad (2.75)$$

R_{ft} and R_{fs} are tube and shell side fouling factor, which here is due to alcohol and water respectively. Fouling factor is the thermal resistance due to fouling for a unit surface area. According to Tubular Exchange Manufacturers Association, fouling factor for alcohol, and water below 50 ^{0}C are 0.0001 m^2.K/W. The total thermal resistance of the condenser is then given as Equation 2.76.

$$R = \frac{1}{UA_t} \quad (276)$$

2.10.18 Log Mean Temperature Difference

The temperature difference varies from location to location within the exchanger, and consequently does the rate of heat transfer. Thus, calculations are based on the average temperature difference across the tube over the entire tube length. The closer the temperature approach (i.e. difference between outlet temperature of one stream and inlet temperature of the other stream), the larger will be the heat transfer area required for a given duty. The optimum will depend on the application and can only be determined by making an economic analysis of alternative design (Seider and Tate 1936). LMTD for counter current is given in Equation 2.77.

$$LMTD_{cc} = \frac{[T_{h1} - T_{c2}] - [T_{h2} - T_{c1}]}{ln\left[\frac{T_{h1} - T_{c2}}{T_{h2} - T_{c1}}\right]} = \Delta T_{lm} \quad (2.77)$$

Where, T_{h1} and T_{h2} are the inlet and outlet temperature of the hot fluid respectively. And T_{c1} and T_{c2} are the inlet and outlet temperature of the cold fluid respectively. LMTD can equally be expressed as in Equation 2.78.

$$LMTD = \frac{Q}{U.A_t.F} \quad (2.78)$$

Where, Q is the rate of heat transfer, A_t is the total heat transfer surface area, F is the correction factor. The correction factor depends on the geometry of the heat exchanger, the inlet and outlet temperatures of the hot and cold fluid streams. The correction factor is less

than unity for a cross-flow and multi pass shell and tube heat exchanger i.e. $F \leq 1$. The limiting value of F = 1 corresponds to the counter-flow heat exchanger. Thus, the correction factor F for a heat exchanger is a measure of deviation of the ΔT_{lm} from the corresponding values for the counter-flow case (Yunus and Afshin 2015). Equation 2.79 is the basic analytical tool employed to establish the thermal design of a HE. The factors considered are:

1) The overall heat transfer coefficient is constant along the flow path.
2) The flow rate and specific heat of both shell and tube stream are constants.
3) The heat transfer surface is uniformly distributed along the flow paths.
4) There is no internal leakage or bypassing of fluid around the tube bundle.
5) There is no transfer of heat between the HE and its surrounding.

2.10.19 Condensation Tube Properties

The delivery tube must be a good conductor and non corrosive material e.g. copper.

Total heat transfer surface area: this is the total surface area through which heat is transferred from the hot fluid to the cold fluid and is calculated with Equation 2.79.

$$A_t = \frac{Q}{U.LMTD.F} \tag{2.79}$$

Condensation Tube Length: This can be obtained from Equation 2.80.

$$L_{tube} = \frac{A_t}{\pi D} \tag{2.80}$$

2.10.20 Pressure Drop

In many applications, the pressure drop available to drive the fluids through the exchanger will be set by the process conditions. When the designer is free to select the pressure drop, an economic analysis is to be made to determine the exchanger design which gives the lowest operating costs taking into consideration capital and pumping costs (Seider and Tate 1936). Also, it is necessary to ensure that stresses greater than the design value do not occur.

Tube-side Pressure Drop: the total pressure loss in the tube is the sum of the hydrostatic, momentum and frictional pressure losses. Thus

$$\Delta P_{total} = \Delta P_{static} + \Delta P_{momentum} + \Delta P_{friction} \tag{2.81}$$

Hydrostatic is a function of the fluid density and play role when there is difference in elevation for the inlet end to the outlet end of a pipe. Frictional loss is resistance to fluid movement due to interaction of the fluid with the pipe wall; it depends on fluid properties and flow conditions within the pipe. Momentum loss is always minimal and negligible in most application. Applying homogenous model for two phase pressure drop; Collier (1982) gave static pressure loss for inclined pipe as in Equation 2.82.

$$\Delta P_{static} = \rho_H . g . H \sin\theta \tag{2.82}$$

Where homogenous density, ρ_H is given as:

$$\rho_H = \rho_l(1 - \in_H) + \rho_G \in_H \tag{2.83}$$

ρ_l and ρ_G are liquid and vapor phase density respectively. ϵ_H is the homogenous void fraction or simply void fraction calculated with Equation 2.84.

$$\in_H = \frac{1}{1 + \left(\frac{U_G}{U_l}\left(\frac{1-x}{x}\right)\right)\frac{\rho_G}{\rho_l}} \tag{2.84}$$

x is the vapor quality while velocity ratio U_G/U_l is '1' for a homogenous flow.

$$\Delta P_{friction} = \frac{2 f_\varphi . L . \dot{m}_{total}^2}{d_i . \rho_H} \tag{2.85}$$

L and d_i are length and internal diameter of the pipe. According to Blasius equation, the frictional factor for a laminar flow is expressed as in Equation 2.86.

$$f_\varphi = \frac{0.079}{R_e^{0.25}} \tag{2.86}$$

The Reynold's number in the tube is given by Equation (2.87).

$$R_e = \frac{\dot{m}_{total} . d_i}{\mu_{tp}} \tag{2.87}$$

The mass velocity, ṁ is calculated by dividing the mass flow rate by the tube CSA while the quality average viscosity is calculated with Equation 2.88.

$$\mu_{tp} = x\mu_G + (1-x)\mu_l \quad (2.88)$$

The momentum pressure drop reflects the change in K.E of the flow. Applying separate flow model which considers the two phase to be artificially separated into two streams flowing in its own pipe. Then, momentum pressure drop depends on the inlet and outlet vapor qualities and void fraction and is calculated with Equation 2.89.

$$\Delta P_{mom} = \dot{m}_{total}^2 \left[\left(\frac{(1-x)^2}{\rho_l(1-\epsilon_H)} + \frac{x^2}{\rho_G \epsilon_H} \right)_{out} - \left(\frac{(1-x)^2}{\rho_l(1-\epsilon_H)} + \frac{x^2}{\rho_G \epsilon_H} \right)_{in} \right] \quad (2.89)$$

Shell-side Pressure Drop: the shell-side pressure drop includes the pressure loss from the shell inlet and outlet nozzle. Yunus and Afshin (2015) expressed it with Equation 2.90.

$$\Delta P = \frac{32\mu L V_{avg}}{D_h^2} \quad (2.90)$$

According to Yunus and Afshin (2015), the head loss and pressure loss are calculated with Equations 2.91 and 2.92 respectively.

$$h_L = \frac{f L V_w^2}{2 g D_h} \quad (2.91)$$

$$\Delta P_L = \rho\, g [h_L - L\, sin\theta] \quad (2.92)$$

Where Frictional factor 'f' for laminar flow is

$$f = \frac{64}{R_e} \quad (2.93)$$

2.10.21 Pump Capacity

If pump is used to circulate the coolant, pump capacity p, is determined base on the volume of water to be circulated from the retention reservoir to the condenser, total head of circulation and the demand flow rate. Total head or head loss is the additional height the fluid needs to be raised by a pump in order to overcome the frictional losses in the shell (Frank 2012).

Shell Side Pumping Power: The pump capacity 'p' is given by Frank (2012) and Khurmi (2005) as Equation 2.94.

$$\dot{W}_{pump} = \dot{V} \Delta P_L = \dot{V} \rho\, g\, H = \dot{m}\, g\, H \quad (2.94)$$

Where

$$H = h + h_f \tag{2.95}$$

Where H is total head, h is height of the Column above pumping level and h_f is frictional loss.

2.11 Machine Effectiveness

Condenser Efficiency: According to Khurmi and Gupta (2006), the efficiency of the condenser can be calculated with Equation 2.96.

$$\eta_{cond} = \frac{(T_o - T_i)_{coolant}}{T_{cond} - T_i} \tag{2.96}$$

Where T_o, T_i are outlet and inlet temperature of the coolant. T_{cond} is condenser temperature corresponding to its pressure which is equal to T_{atm} if operating at atmospheric condition.

Capacity Ratio: is the ratio of the product of mass flow rate and specific heat of end flow. It is always the ratio of the smaller value to the larger value. Thus, if M_nC_{pn} is for the hot fluid, M_cC_{pc} for cold fluid and $M_nC_{pn} > M_cC_{pc}$, capacity ratio c, is Equation 2.97 and vice versa (Yunus and Afshin 2015).

$$c = \frac{M_c C_{pc}}{M_n C_{pn}} \tag{2.97}$$

Heat Exchanger Effectiveness: This is the ratio of the energy actually transferred, to the maximum theoretically possible. The maximum possible heat transfer will result if one fluid undergoes a temperature change equal to the maximum temperature difference available. For instance if the hot fluid is greater than the cold fluid, then the effectiveness is:

$$\varepsilon = \frac{M_c C_{pc}(t_2 - t_1)}{M_n C_{pn}(T_1 - t_1)} \tag{2.98}$$

The rate of distillation should not be too rapid, if not, the heat applied to the boiler must be decreased. With too rapid a rate, the measured boiling point is likely to be inaccurate and the purity of the distilled liquid will be compromised. The first material that distills before the temperature stabilizes is called the forerun. The forerun will contain any low boiling

impurities and is usually discarded after checking its purity. The material collected after the temperature stabilizes is the purified substance. Usually the temperature stabilizes slightly below the literature value for the boiling point and then slowly creeps up. As a safety precaution, distillations are never carried out to dryness. The residual liquid plus the liquid from the take-up volume is the price one pays for purity.

Boiler / Distiller Efficiency: this is the thermal efficiency of the boiler. It is the ratio of heat actually used in producing the fuel to the heat liberated in the furnace (Khurmi and Gupta, 2006) expressed as Equation 2.99.

$$\eta_{th} = \frac{heat\ used\ to\ produce\ fuel}{heat\ liberated\ in\ furnance}$$

$$= \frac{m_{eth}(h_2 - h_1)}{WFU\ x\ HVF} = \frac{D_c(h_2 - h_1)}{HVF} \qquad (2.99)$$

Boiler efficiency can also be related to the quantity of vapor produced, as in Equation 2.100.

$$\eta_{vap} = \frac{vapor\ produced}{expected\ vapor\ qty} \qquad (2.100)$$

Where $(h_2 - h_1)$ is heat required to evaporate 1kg of bioethanol. Thermal efficiency has been shown to depend more on equipment than fuel selection (Kristensen & Kristensen 2004; González et al. 2004; Turn et al. 2006). Inefficiencies include incomplete combustion as well as heat losses.

Distiller Capacity: this is the power of the constructed distillation unit; it is the amount of bioethanol evaporated or bioethanol fuel (condensate) produced in kg expressed in (kg/h), or (kg/kg) of fuel burnt given in Equation 2.101 and 2.102 respectively.

$$D_c = \frac{fuel\ produced, m_{eth}}{time} \qquad (2.101)$$

$$D_c = \frac{m_{eth}}{WFU} \qquad (2.102)$$

2.12 Product Yield

Yields of reaction are calculated to get the percentage yield which is an indication of the efficiency of the reaction. The closer the actual yield is to the theoretical yield, the closer the percentage yield will be to 100 %, and the more efficient the reaction.

Hydrolysis Yield: According to Tangka et. al., (2011), total sugar yield after hydrolysis can be calculated with Equation 2.103.

$$\text{sugar yeild (L/kg)} = \frac{Q_{sc}\,(\text{L})}{m_{rm}\,(\text{kg})} \qquad (2.103)$$

Where Q_{sc} is the quantity of sugar got after hydrolysis and m_{rm} is the mass of feedstock.

Hydrolysis comprises of glucose and xylose yield. The glucose yield from cellulose can be calculated by dividing the glucose produced by the initial cellulose used based on the Equation 2.104 according to Isroi et. al., (2012).

$$\text{glucose yield (\%)} = \frac{glucose\ \ (g)}{initial\ \ cellulose\ \ (g)\times 1.1111} \times 100 \qquad (2.104)$$

Where glucose (g) is the amount of glucose in the liquid after hydrolysis and initial cellulose (g) is the amount of cellulose in the substrates before hydrolysis. Cellulose can be 100 % weight due to glucan. Ratio of molecular weight of glucose / glucan is same as that of mannose / mannan which is 180 / 162 (Jie et. al., 2012). Theoretically, 1 g cellulose yields 1.1111 g of glucose (Mingjia et. al., 2010, Isroi et. al., 2012).

Xylose yield from hemicelluloses can be calculated by dividing the xylose produced by the initial hemicelluloses used based on Equation 2.105 according to Jie et. al., (2012).

$$\text{xylose yield (\%)} = \frac{xylose\ \ (g)}{initial\ \ hemicellulose\ \ (g) \times 0.7 \times\ 1.1364} \times 100 \qquad (2.105)$$

Where xylose (g) is the amount of xylose in the liquid after hydrolysis and initial hemicelluloses (g) is the amount of hemicelluloses in the substrates before hydrolysis. Hemicelluloses' has about 70 % weight due to xylan presence. Ratio of molecular weight of xylose / xylan is 150 / 132 (Jie et. al., 2012). Theoretically, 1 g hemicelluloses yields 0.7955 g of xylose (Mingjia et. al., 2010, Isroi et. al., 2012).

Fermentation Yield: this is measured in litres of absolute alcohol in broth (beer) per ton of sugar in feedstock. According to sugar news (Saturday, 23 July, 2016: distillery yield), there are four commonly used measures of bioethanol yield; fermentation yield, fermentation efficiency, alcohol recovery and overall conversion efficiency. These are expressed below.

$$\text{Fermentation yield } (l) = \frac{vol.of\ broth\ (l)\ x\ alcohol\ content\ of\ broth\ (v/v)}{mass\ of\ feedstock\ (ton)\ x\ fermentable\ sugar\ content\ of\ feedstock\ (m/m)} \quad (2.106)$$

Fermentation yield which is actual bioethanol yield after fermentation can also be base on mass of feedstock used, sugar utilized, volume of broth or fermentation time as expressed with Equation 2.107 – 2.110 by Tangka et. al., (2011), Mohd et. al., (2011) and Nurul et al (2014).

$$bioethanol\ \ yeild\ (kg/kg) = \frac{Q_{f.be}}{m_{rm}\ (kg)} \quad (2.107)$$

$$bioethanol\ yeild\ (g/L) = \frac{Q_{f.be}\ (g)}{brot\ h\ (l)} \quad (2.108)$$

$$bioethanol\ yeild\ (g/g) = \frac{Q_{f.be}\ (g/l)}{initial\ \ glucose\ (g/l)} \quad (2.109)$$

$$bioethanol\ productivity = \frac{Q_{f.be}\ (g/l)}{fermentation\ \ \ time\ ,\Delta t} \quad (2.110)$$

Where $Q_{f.be}$ bioethanol produced in broth, Q_{sc} is sugar yield after hydrolysis.

Theoretical yield is the expected yield if 100% of the reactant (xylose, cellulose or glucose) completely turns into the product (glucose or bioethanol). Efficient reaction means maximum product formation. Considering Equation 2.111 and 2.112 of xylose and glucose fermentation to bioethanol given by IFQC, (2004) and Cheng et. al., (2007) respectively.

$$C_5H_{10}O_5 \xrightarrow{(yeast)} \frac{5}{3}CH_3CH_2OH + \frac{5}{3}CO_2 + \text{Heat} \quad (2.111)$$

$$C_6H_{12}O_6 \xrightarrow{(yeast)} 2CH_3CH_2OH + 2CO_2 + \text{Heat} \quad (2.112)$$

This implies that 1mol of xylose yeids 1.67 mol of ethanol or 150.13g/mol of xylose yield 1.67 (46.08) g/mol of ethanol. Also, 1 mol of glucose yields 2 mol of ethanol or 180.18 g/mol

of glucose yield 2(46.08) g/mol of ethanol. Theoretically, 1g glucose and xylose yields 0.511g of ethanol (Mingjia et. al., 2010, Yanni et. al., 2013, Christos et. al., 1996, Isroi et. al., 2012). Also, 100 kg sugar (glucose, fructose) will yield approximately 51kg or 64.5 liters alcohol (Stephen et. al., 2013). In practice, however, this number is actually not achieved, because fermentation equation is just a simplified description of the actual processes. For these reasons a yield less than 64.5 liters of pure alcohol per 100 kg glucose or fructose is generally realized in practice (Stephen et. al., 2013, Christos et. al., 1996). Fermentation theoretical bioethanol yield (%) is calculated according to Tangka et. al., (2011) and Nurul et al (2014) with Equation 2.113.

$$Theoritical\ \ ethanol\ yeild\ (g) = \frac{actual\ mass\ of\ \ glucose\ (g)}{glucose\ mass\ per\ mol\ (g/mol)}\ x\ 2(ethanol\ mass\ per\ mole) \qquad (2.113)$$

Fermentation Efficiency: this is an expression of how much alcohol was actually produced in broth relative to the amount that could be theoretically produced. It is calculated by Tangka et. al., (2011), Nurul et al (2014) and Mingjia et. al., (2010) with Equation 2.114

$$percentage\ \ yeild\ (\%) = \frac{actual\ ethanol\ yeild\ (g)}{theoritical\ \ ethanol\ yeild\ (g)}\ x\ 100 \qquad (2.114)$$

Sugar news (23 July 2016) expressed it as Equation (2.115).

$$\text{fermentation efficiency } (\%) = \frac{\text{fermentation yield } x\ 0.794}{0.5111kg\ x\ \ (100/1000)} \qquad (2.115)$$

The factor 0.794 corresponds to the specific gravity of absolute alcohol while 0.511 kg is best explained as follows: if 1 kg of sugar is completely fermented using 100 % efficient yeast, 511.1 g of alcohol and 488.9 g of CO_2 (i.e 1000 – 511.1) would result (Sugar news (2016).

Distillation Yield: This is alcohol recovery also called evaporation and distillation efficiency**.** It is a measure of how much alcohol was finally produced relative to the amount that was in the broth. It shows the amount of losses in the evaporation and distillation sections combined Sugar news (23 July 2016). Distillation yield can be base on mass of feedstock used, sugar

utilized and distillation time according to Tangka et. al., (2011) and Nurul et al (2014) as in Equation 2.116 - 2.117

$$bioethanol\ fuel\ yeild\ (l/kg) = \frac{Q_{be}\,(l)}{m_{rm}\,(kg)} \quad (2.116)$$

$$bioethanol\ fuel\ yeild\ (l/min) = \frac{Q_{be}\,(l)}{time\ ,\Delta t} \quad (2.117)$$

$$bioethanol\ productivity = \frac{Q_{be}\,(l/min)}{feed\ \ volume\ \ (l)} \quad (2.118)$$

Where Q_{be} bioethanol fuel produced in liters, m_{rm} is mass of raw material.
Distillation efficiency is expressed in Equation 2.120 by Sugar news (2016).

$$\text{distillation efficiency} = \frac{\text{Vol. of feints as litres absolute alcohol}}{\text{Vol. of beer as litres absolute alcohol}}\ x\ 100$$

$$= \frac{vol.of\ distillate}{bioethanol\ content\ in\ feed\ (L)}\ x100\% \quad (2.19)$$

Overall Conversion Efficiency: this is a measure of how much alcohol is finally produced relative to the amount that could be theoretically produced. It is calculated with Equation 2.120) according to Sugar news (23 July 2016).

$$\text{overall conversion efficiency} = (\text{ferm. eff.})\ (\text{alcohol recovery})\ \text{x}\ 100 \quad (2.120)$$

2.13 Factors Limiting Bioethanol Yield

The factors limiting ethanol yield include:

1. Less than theoretical yield is caused by sugar consumption by the yeast, incomplete fermentation, the formation of fermentation side products (e.g. fusel alcohols), and alcohol loss in the distillation process (Kris 2004). During fermentation most of the yeast cells used suffer from various stresses, including environmental stress such as glucose concentration, nutrient deficiency, temperature, rate of agitation and pH (Mohd et. al., 2011).

2. pH of the hydrolysate: the pH of the substrate must be within acceptable limits of fermenter (enzymes) otherwise it will destroy the enzymes or reduce ethanol that can be fermented (Liu & Shen 2008).

3. Temperature: temperature can affect the yeast development, ethanol yield, and type of fermentation by-products, yeast sensitivity in relation to alcohol concentration, growth and fermentation rate (Sener et. al., 2007; Torija et. al., 2003). An acceptable limit of substrate is between 30 – 45 ^{0}C for optimum yield.

4. Hydrolysate Concentration: the amount of substrate to be fermented is proportional to the ethanol that can be fermented from it, if all other condition is maintained.

2.14 By-products in Bioethanol from Lignocellulosic Materials

In addition to bioethanol and water the fermentate contains a number of other materials that can be classified into microbial biomass, fusel oil, volatile components, lignin and stillage. Fusel oil is use to produce pharmaceutical grade of ethanol not for fuel ethanol. Stillage, also termed distillery waste water, distillery pot ale, distillery slop, distillery spent wash, dunder, mosto, vinasse, and thin stillage is an aqueous byproduct (Ann et. al, 2000). The main by product is lignin though lesser in quantity and quality in the solid residue than in feedstock and the applied processes. Hence, part of the lignin must have been solubilized (e.g. during acid pretreatment, acid hydrolysis} or degraded by enzyme (in enzymatic process). The formation of the biomass of the fermenting microorganisms' byproduct is unavoidable. Hence, filtration, recirculation of produced cell mass, immobilization, encapsulation and sedimentation are possible methods for separation of cells from the media. The remaining waste water after distillation contains none or low volatile fractions of materials, its component greatly on the feedstock type. It generally contains non fermentable sugars, traces of bioethanol, metabolites e.g. glycerol produced during fermentation, inhibitors produced during hydrolysis, waxes, fats, and mineral salts. All these by products are much more in enzymatic than acid hydrolysis. Preliminary analysis of ethanol production waste water characteristics and treatment revealed a consensus toward anaerobic digestion as an economically viable and sustainable byproduct recovery scheme (Ann et. al, 2000)

2.15 Related Studies on Bioethanol Production Techniques from Waste Palm Bunch

Yani et. al. (2012), set up a pilot scale unit for development and testing of a process for ethanol production based on enzymatic saccharification. The Testing process included pretreatment of 50 kg ground waste palm bunch using alkali NaOH 10 % w/w (250L), at temperatures 140-145 ^{0}C for 30 minutes; saccharification using modified cellulase enzyme

50-52 ^{0}C, pH 4.8-5.5 and fermentation of WPB was carried out in the 350 L of fermentor tank using local strains *Saccharomyces cerevisiae* Mk, at at 32 ^{0}C and pH 6-5 for 48 h their study achieved 69 % bioethanol yield.

Ria et. al., (2011) carried out two stage of hydrolysis of waste palm bunch with dilute sulphuric acid (0.2, 0.8 %) at 170 – 230 ^{0}C with a holding time of 5 and 15 min. The maximum yield of xylose was 135.94 gkg^{-1} of raw material, obtained at 0.8 % acid, 190 ^{0}C and 5 min. The maximum yield of glucose was 62.70 gkg^{-1} of raw material, obtained at 0.8 % acid, 210 ^{0}C and 5 min. Hydrolyzate from the first stage was fermented by *mucor inicus* while that from the second stage was fermented by *saccharomyces cerevisae*. The corresponding bioethanol yields were 0.45 and 0.46 g bioethanol g^{-1}sugar consumed.

Richana et. al., (2015) reported 540 – 655 ml of 90 % bioethanol yield from pilot plant scale of 3.82 - 4.63 kg waste palm bunch after mixing and soaking of the raw material in 1 % NaOH solution reducing up to 90.3 % lignin. According to them sequential pretreatment hydrolysis in sodium hydroxide solution, steaming in autoclave for 15 minutes, and subsequently the addition of xylanase and cellulase pH 6 and incubation for 6 days showed the best process in which 19.34 – 20.56 % sugars was released. Fermentation took 2 days using *S.cerevisae*.

Yanni et. Al., (2008) reported Alkali pretreatment of waste palm bunch using NaOH 1 N with varied temperatures 30 and 60 ^{0}C and reaction times 30, 60, 90, 120 and 150 minutes. The pretreated substrate was subjected to an enzymatic saccharification using meicelase (10, 20 and 40 FPU/g substrate) at 40 ^{0}C, pH 4.5, 100 rpm for conversion of cellulose and hemicellulose into monomeric sugars. The results showed optimum pretreatment condition was NaOH 1 N at 30 ^{0}C and 90 minutes with optimum loss of lignin and hemicellulose as 45.8 % and 35.6 % respectively; while saccharification of waste palm bunch pretreated by NaOH 1 N (at 30 ^{0}C and 90 minutes) for 45 hours and pH 4.5 resulted in optimum glucose and xylose concentration of 19.95 mg/ml and 25.24 mg/ml respectively.

Ghasem et. al., (2007) investigated the effect of four different process variables such as effect of pretreatment (0.5 – 1 M NaOH solution), solid size, HCl concentration, solid percentage and temperature in a single stage of acid (HCl) hydrolysis process of waste palm bunch,

carried out under moderate temperature (45 ^{0}C) and ambient pressure. They found that the smaller the particles the more surfaces for acid-solid contact and reduced reaction time; high acid concentration improved the reaction rate and sugar yield. Sugar yield was found to be dependent on acid concentration and temperature. For a reaction time of 40 minutes, 5 % waste palm bunch solid with 15, 20, 25 and 30 % of HCl, lignocelluloses fibers conversion of 36, 60, 65 and 80 % were achieved, respectively. The sugar concentration in acid hydrolysis of the pretreated fibers with 0.5 M sodium hydroxide solution resulted in 35 % more sugar.

Gil et. al., (2007) reported the simulation and analysis of an extractive distillation process for azeotropic ethanol dehydration with ethylene glycol and calcium chloride mixture as entrainer. Their work was developed with Aspen Plus® simulator version 11.1. The calculation of the activity coefficients employed to describe vapor liquid equilibrium of ethanol – water – ethylene glycol – calcium chloride system was done with the NRTL-E equation and validated with experimental data. Two dehydration process columns were used: the main extractive column and the recovery column. A substantial reduction in the energy consumption, compared with the conventional processes, was predicted by using ethylene glycol and calcium chloride as entrainer.

Zetty et. al., (2014) studied the properties of waste palm bunch directly treated with steam without size reduction and acid/alkali treatments. They varied the temperature and time of pretreatment and found that there was no significant difference in the production of glucose and xylose after Cellic CTec2 enzymatic hydrolysis; furthermore, pretreatment neither changed in the moisture content nor the pH values in waste palm bunch; however, a small reduction in pH was observed due to the generation of acetic acid, formic acid and levulinic acid. Thus, pretreatment of the samples yields higher cellulose and lesser lignin content.

Jinlan et. al., (2014) applied sulfite pretreatment to overcome the recalcitrance of lignocelluloses (SPORL) in waste palm bunch for bioethanol production. The SPORL facilitated delignification through lignin sulfonation and dissolution of xylan to result in a highly digestible substrate. The pretreated whole slurry was enzymatically saccharified at a solids loading of 18 % using a relatively low cellulase loading of 15 FPU/g glucan and simultaneously fermented without detoxification using Saccharomyces cerevisiae of YRH400. An ethanol yield of 217 L/tonne waste palm bunch was achieved at titer of 32 g/L.

Compared with literature studies, SPORL produced high ethanol yield and titer with much lower cellulase loading without detoxification.

2.16 Potential Risk of Energy Palm Cultivation

Potential Risks Associated with Land Use Changes: Changes in existing land uses can create conflict and economic hardship if not managed properly because property title regulation and enforcement in Nigeria are sensitive, so it is difficult for communities not to have a legal title to their property. Inappropriate land use change can also attract conflict and criticism and long-term environmental damage; e.g., an area of existing forest of ecological or cultural significance could be cleared to make way for energy palm cultivation. This is not a problem for farmer landowners who decide to shift existing land use; however, there is a risk that the benefits from energy palm may tempt these farmers to plant palm trees on land where food crops are growing, thus competing with food crops (Phillips et al., 2011).

Potential Risks pertaining to Fuel Quality and Sustainability: If fuel quality is not maintained there could be a net cost to the country from the introduction of biofuel due to engine damage by low-quality fuel. If this were to occur, the sustainability of the industry and the livelihoods of farmers and businessmen involved would be threatened. Therefore, it is important that appropriate fuel standards and testing are established and enforced.

Potential Risks relating to the Government's Tax Revenues: Diesel fuel and gasoline are currently subject to tariff rates of around 100 % in Nigeria. If biofuel is introduced successfully, the government's tax revenue could be reduced as biofuel would replace taxable fossil fuel. However, this scenario is unlikely because

(i) the total energy demand, including fossil fuels, is projected to grow strongly in the medium term and this would likely more than compensate for any small reduction in fossil fuel consumption;

(ii) a significant proportion of petrol consumed in Nigeria is exported across the borders, and therefore does not contribute to the government's tax revenue;

(iii) Any potential reduction in direct tax revenue from reduced fossil fuel sales should be compensated by increased tax revenue from other parts of the economy that would be stimulated by the new income generated from the biofuel industry.

Notwithstanding the risks outlined, there are many potential benefits to the development and use of palm bunch for bioethanol fuel.

2.17 Palm Bunch Base Bioethanol Fuel Production Opportunities

Globally to improve environmental health, efforts are formalized in the Kyoto Protocol – an international, legally binding commitment by countries to lower their GHG emission levels to an agreed level by 2012 (Kyoto protocol 1997) thereby encouraging bioethanol production. Both developed and developing countries are in need of bioethanol (Ruth, 2008). Nigeria in her response to minimize carbon emission is investing in bioethanol technology in partnership with Brazil (Tan et. al., 2014). Nigeria's commitment to bioethanol development under the Kyoto Treaty has put an upward pressure on agricultural prices in the past decade (Antoni 2003) which main solution is utilizing cellulosic waste as feedstock (Raneses et.al., 1998). The primary market for bioethanol is as a petrol additive for octane enhancement. Motor fuel is oxygenated to help control vehicle emissions. ASTM defined oxygenates as an oxygen-containing, ash less organic compound, such as an alcohol or ether, which may be used as a fuel or fuel supplement. The two most common oxygenates are ethanol and methyl tertiary butyl ether (MTBE) (Nebraska, 2011, IFQC, 2004). MTBE was rather used in reformulated petrol blends to meet fuel oxygen requirements. It was later banned to date because of its carcinogen potential. Bioethanol can perfectly replace MTBE in reformulated petrol providing the oxygenate standard or as ETBE (CNN News 2001, WEM 2006). Though similar emission benefits could be achieved without the addition of oxygenates all this call for increase in production of bioethanol. There are other potential transportation fuel uses that could increase bioethanol demand. The use of petrol-ethanol blends e.g. E-85 (85 % ethanol / 15 % gasoline) in flexible fuel vehicles (FFVs) has received the most attention and auto manufacturers are gearing up to produce even larger volumes (Bourne, 2007, Kojima & Johnson 2005). While increase production of bioethanol is dependent on the ability of auto manufacturers to increase FFVs Ethanol fueling infrastructure, general support for domestically produced fuels is encouraging. All three major US auto manufacturers produce FFVs (Wikipedia, 20a, Karl et. al., 2005). In most cases, drivers are completely unaware that they are operating a FFV and should be encourage on the usage (Nissan 2005). Table 2.14 presents a list of vehicle make and models that are capable of E85 operations (Nebraska, 2011, Kristina et. al. 2008).

Table 2.14: E85 Compatible Vehicles (Nebraska, 2011, Wikipedia, 2012a).

All 1999 and 2000 Ford 3.0-L Ranger pick ups
Ford: Focus, C-Max, S-max, Mondeo, Galaxy
All 1999 and 2000 Mazda 3.0-L B-3000 pick ups
Volvo: S40, V50 and C30, S80, V70
Peugot: 307 Bioflex. Volkswagen: Golf 1.6
Audi: A3, A4. Seat: Leon and Altea,
Renault: Megane. Citroen: C4 and C5
Renault: Megane. Skoda: Oktavia Flexifuel
All 2000 GM 2.2-L S-10 pickups. Saab: 9-5, 9-3
All 2000 and 2001 GMC 2.2-L Sonoma pick ups
All 1998, 1999, 2000 and 2001 Chrysler 3.3-L mini vans
All 1998, 1999, 2000 and 2001 Dodge 3.3-L mini vans
All 1998, 1999, 2000 and 2001 Plymouth 3.3-L mini vans
Selected 1995-2001 Ford 3.0-L Taurus sedans
All 2002 GM Suburban 5.3-L SUVs
All 2002 GM Tahoe 5.3-L SUVs
All 2002 GMC Yukon 5.3-L SUVs

The demand for bioethanol could increase by 20 % per year provided vehicles were operated 50 % of the time on bioethanol. To achieve these volumes, bioethanol would need to be priced competitively with petrol on a gallon equivalent basis (James & John, 2001, Nissan 2005, Hossein et. al., 2006). Encouraging Nigerians to purchase these alternative fuel vehicles will present a sizable market potential for bioethanol sales, Stations to dispense E85 fuel will be built which in turn provides job opportunity. Another possible market for bioethanol is blending it with diesel to produce Oxydiesel fuel (CNN, 2001). Oxydiesel contains about 10 - 15 % bioethanol and is being marketed as a way to capture fuel emission benefits in unmodified diesel engines. The fuel has been demonstrated in a number of fleets both in Europe and U.S. but is still in the early commercialization stage. The market potential for this fuel is large. The transportation sector alone consumes over a million gallons of diesel annually. Diesel operators are extremely sensitive to fuel price, and Oxydiesel is expected to

be cheap. If federal government under renewable fuels requirements campaign would require that 0.3 % of all motor fuels use in the country be renewable fuels such as ethanol or biodiesel, gradually increasing a gallon of bioethanol derived from cellulosic feedstocks would count as a gallon of renewable fuel, in an effort to create greater development of this resource (Hossein et. al., 2006). Farmers and cooperatives that implement processes to add value to crops, towards promoting bioethanol production should be encouraged through Value-Added Agriculture incentives (Antoni 2003, Nissan 2005, Ruth 2008, Luyna et. al., 2009). Historically, food and energy economies have been largely separate, but now with increase feed base bioethanol distilleries, they are merging. If food value of grain is less than fuel value, market will move the grain into the energy economy. Thus as the price of oil rises, the price of grain follows upward. World Bank reports that for each 1 % rice in food prices, caloric intake among the poor drops 0.5 %. Millions of those living on the lower rungs of global economic ladder which are barely hanging on, will lose their grip and begin to fall down (Inderwildi 2008). So, production of bioethanol from waste palm bunch saves the food chain and the environment.

The developing of a palm bunch based bioethanol production would have an obvious economic impact on the nation. The raw material is locally available in reasonable number of states in Nigeria. Locating conversion facilities in the most palm oil producing area of these states will as well reduce the net production cost. There will be positive economic relationship in form of flows of goods and services to producers, among producers, and finally to consumers. The "direct effects are the changes in the industries (ethanol) to which a final demand change could be made. Indirect effects are the changes in inter-industry purchases as they respond to the new demand of the directly affected industries. Induced effects typically reflect changes in spending from households as income increases or decreases due to the changes in production". Finally, bioethanol market is completely dependent on government tax support, incentive bills and to a lesser degree, air quality policies (USDA 2007, Kojima & Johnson 2005). A lignocellulosic based bioethanol production will also remain dependent on these incentives for the near future, but offers the potential for a stand-alone industry as it matures. The widespread role of lignocellulose bioethanol should be campaigned as other feedstock is cost competitive with human feed. The International Energy Agency presents two scenarios in its World Energy Outlook, and discussions of these two scenarios show how

policies affect the global energy market, energy security and energy-related climate change concerns. The Outlook contains two energy scenarios: a reference or baseline scenario, which depicts how global energy markets would evolve in the absence of new government policies; and an alternative policy scenario which depicts global energy markets as impacted by additional government interventions and policies (IEA 2006). This calls for rapid adoption of policies that are favourable to biofuels and other renewable sources in Nigeria. A legal regime favourable to development of biofuels must also be created following the path of Brazil. In summary benefits of manufacturing bioethanol fuel from waste palm bunch is:

- Less dependence on crude oil and foreign (refined) oil
- Lower energy cost
- Improve combustion efficiency which improves fuel economy
- Abundant feedstock for a renewable fuel.
- Reduces GHG emissions; air pollution as it burns efficiently reducing unburn carbons.
- Increase octane rating at low cost as an alternative to harmful fuel additives.
- Helping emerge a new market.
- Job and business opportunities.
- Expands market opportunity in agricultural field thus enhancing rural economic development.

It is obvious that the benefit cuts across economic and rural development, poverty reduction, potential for community energy cooperative, energy security, health and safety, renewability, good climate and environmental impact. The main environmental impacts of energy crop cultivation for biofuel production relate to (i) areas brought into production, (ii) change in crops cultivated for biofuel, (iii) changes in the use of chemical inputs and (iv) prevention of the abandonment of agricultural land.

2.18 Nigeria Effort in Biofuel Realization in the Country

Nigeria presently has a policy on bio-fuels entitled Nigerian Biofuel Policy and Incentives (2007) approved and gazetted by the Federal Executive Council on June 20th, 2007. The Nigeria National Petroleum Corporation was given the mandate to create an environment for the take-off of a domestic ethanol fuel industry. The framework of the policy and the incentives is meant to create an enabling environment that is expected to sensitize and

catalyze the development of the country‘s biofuels industry (Dayo 2008). The biofuel programme constitutes a major and unique attempt to integrate the agricultural sector of the economy with the downstream petroleum sector, while fostering the use of other renewable energy sources. To make the project a realizable objective; the federal government through the Nigeria National Petroleum Corporation, (NNPC) created the Renewable Energy Division (RED), to champion the implementation of the programme. The NNPC, by mandate of the former President, Olusegun Obasanjo, inaugurated the Renewable Energy Division in August, 2005, and charged it with the responsibility of developing the biofuel industry in Nigeria (Nigeria Tribune 16/09/2008). RED shall provide a consistent, steady supply of alternative fuel to the utmost satisfaction of customers and continuously seek to improve the quality of its management systems. The implementation plan includes initial market seeding (E10), a bio-fuel production programme (PPP) to achieve 100 % domestic production by 2020, a complete biofuel uptake arrangement, and joint-venture distilleries. This is anchored on agricultural productivity and competitiveness. The policy is intended to create market demand for biofuel products. Already, US$4 billion has been committed to a sugar-cane sourced ethanol project in the northern states of Jigawa and Benue while cassava-sourced bioethanol projects are earmarked for the southern Anambra and Ondo states (Azih 2007). For the purposes of implementing the provisions of the Policy, a Biofuels Energy Commission was proposed. The Biofuels Energy Commission is charged with responsibility for implementing the strategies for biofuels in the country. It shall specifically exercise the following responsibilities:

1. Register all biofuel plants / projects in the country.
2. Issue license to biofuel operators for production of bioethanol or/and biodiesel. 3. Formulate and recommend fiscal, financial and other incentive policies for the biofuel industry, as well as protection measures if required.
4. Periodically, review and assess the economic, technical, environmental and social impact of the use of biofuels, and determine changes in policies required when necessary.
5. Monitor the supply and utilization of bio-fuels and biofuel blends and recommend appropriate measures to the Department of Petroleum Resources in case of shortages in the supply of biofuels or feedstock.

6. Review and adjust the minimum mandated biofuel blends as it deems appropriate.
7. Determine and put in place industry stabilization mechanisms.
8. Designate and oversee the activities of the investment bank appointed to manage the Biofuel Industry Equity Fund.
9. Establish and support the biofuels Research Agency to be established under the biofuels Programme.
10. Monitor intra-industry commerce, in particular relationships between out growers and biofuel producers. Present quarterly reports and briefings on the status of the biofuel industry to the National Assembly.
11. Present quarterly reports and briefings on the status of the biofuel industry to the National Assembly.
12. Disseminate and share information with investors and other interested members of the public.
13. Liaise with the Energy Commission of Nigeria in the formulation, revision and implementation of the National Energy Policy.
14. Liaise with the National Sugar Development Council as may be required.
15. Liaise with government ministries, agencies, parastatals, research institutes.

A research agency to be known as the Biofuels Research Agency shall be established to act as the central coordination body for biofuel research in the country. Provisions for incentives in the biofuel industries have also been made. For instance, there exist provisions for application for waivers granting Pioneer Status for an initial 10-year period with the possibility of additional 5 years extension since biofuel is not listed as one of the companies benefiting from such under the Industrial Development (Income Tax Relief) Act. The Policy explores the various provisions of the tax laws (LFN 2004) in Nigeria in order to create a wide range of incentives to the biofuels market. It, therefore, becomes necessary for the amendment of the tax laws in the country to bring them in consonance with the intent and purpose of the policy.

The policy stresses a collaborative efforts with local research institutes in feasibility studies namely, International Institute of Tropical Agriculture (IITA), National Cereal Research Institute (NCRI), National Root Crops Research Institute (NRCRI), Nigerian Institute for Oil Palm Research Council (NIFOR), Forestry Research Institute Nigeria (FRIN), Nigerian Stored Products Research Institute (NSPRI), Institute for Agricultural Research and Exten-

sion Services (IARES), Agricultural Research Council of Nigeria (ARCN), National Biotechnology Development Agency (NABDA), SHEDA Science and Technology Complex (SHESTCO) Federal Soil Conservation School (FSCS), National Centre for Agricultural Mechanization (NCAM), National Agricultural Seeds Council (NASC), Nigerian Automotive Council, Raw Materials Research and Development Council (RMRDC) and Federal Institute of Industrial Research Oshodi (FIIRO) and other relevant agencies. There is also collaboration with Government agencies and parastatals in biofuels policy development. The Biofuels Research Agency shall collaborate with the Ministry of Agriculture and Ministry of Science and Technology to provide direction for research in crop production, industry technology and processes pertaining to the production of biofuels.

In conclusion, the present Nigerian government needs to formulate policies that have legislative support, as in Brazil. There is need for a new legal framework that will enable the process of complementing traditional sources of energy with renewable energies like biofuel. The lack of enabling legislation in the Nigeria energy sector has retarded the implementation of clean energy policies. Technical information on biofuels has also been hindered. Besides, there have been logistics bottlenecks. Moreover, the government has not encouraged the research and development required to enable the use of biofuels and other renewable sources of energy to achieve full efficiency and sustainability. Multi-sectoral coordination and support is equally lacking. In addition, no effort has been made toward the development of local expertise and institutional procedures to facilitate project finance and provision of appropriate fiscal and economic incentives, hence the call for enabling legislation that will fill these regulatory gaps in the energy sector. There is a need for a public-private partnership in the development of bio-fuels in the country. The proposed partnership should optimize benefits amongst parties, either public or private, by allocating responsibilities to the party that is best positioned to control the activity that will produce a desired result. Clear and transparent legislation to develop the industry is critical and must be put in place.

2.19 Internal Combustion Engine

Internal Combustion Engine (ICE) is any type of heat machine that obtains mechanical energy directly from the expenditure of the chemical energy of fuel burned in a combustion chamber that is an integral part of the engine (Khurmi & Gupta 2006, Pulkrabek 1997). The engine block comprises of the crankshaft, combustion chambers in which are cylinders, cylinders head, pistons, connecting rod. Fuel is stored in a tank until it is needed, then delivered to the combustion chamber by the engine fuel system. IC engine is powered by the combusting of a precise mixture of liquefied fuel and air to convert its chemical energy to thermal energy. This thermal energy raises the temperature and pressure of the gases within the engine and the high-pressure gas then expands against the mechanical mechanisms of the engine. This expansion is converted by the mechanical linkages of the engine to a rotating crankshaft, which is the output of the engine. The crankshaft, in turn, is connected to a transmission and/or power train to transmit the rotating mechanical energy to the desired final use. For engines this will often be the propulsion of a vehicle (i.e., automobile, truck, locomotive, marine vessel, or airplane). Other applications include stationary engines to drive generators or pumps, and portable engines for things like chain saws and lawn mowers. The pistons' motion rotates the crankshaft at speeds ranging from about 600 to thousands of revolutions per minute (rpm), depending on how much fuel is delivered to the cylinders. Due to high thermal efficiency and power density, IC engines are widely used for transportation and stationary power source (Ashish & Deshmukh 2012, Hiregoudar et. al., 2014 a&b).

2.19.1 IC Engine in Automobile

In power generation, the crankshaft rotation in the presence of a magnetic flux creates electric flow. In automobile ICE, the turning of the ignition key operates a switch that sends electricity from a battery to a starter motor. The starter motor turns a disk known as a flywheel, which in turn causes the engine's crankshaft to revolve. The rotating crankshaft causes pistons, which are solid cylinders that fit snugly inside the engine's hollow cylinders, to move down drawing fuel / air into combustion chamber. After combustion, mechanical energy through the connecting rod is transferred to the crankshaft which now rotates via the up-and-down motion of the pistons, permitting the starter motor to disengage from the flywheel. The rotating crankshaft through connected transmission gears (gearbox) pass the energy along to a driveshaft (propelling shaft). The driveshaft transfers the energy via a differential gear to the axles. The differential gear divides the force equally between the axles,

causing the axles to rotate but permitting them to follow paths of different lengths at different speeds as when turning a corner or traversing on uneven road. The axle's rotation keeps turning the drive wheels which in turn cause the idle wheels to turn. On a straight road the wheels rotate at the same speed while when turning a corner the outside wheel has farther to go and will turn faster than the inner wheel if unrestrained. By using gears of different sizes, a transmission alters the rotational speed and torque of the engine passed along to the driveshaft. Higher gears permit the car to travel faster, while low gears provide more power for starting a car from a standstill and for climbing hills. The combustion, electrical, lubricating, and cooling systems need to work together to make the engine run smoothly and deliver power efficiently to the vehicle.

2.19.2 IC Engine History

Early development of modern internal combustion engines occurred in the latter half of the 1800s and coincided with the development of the automobile. History records earlier examples of crude internal combustion engines and self-propelled road vehicles dating back as far as the 1600s (Pulkrabek 1997). Major development of the modern steam engine and, consequently, the railroad locomotive occurred in the latter half of the 1700s and early 1800s. By the 1820s and 1830s, railroads were present in several countries around the world. In 1859, the discovery of crude oil in Pennsylvania finally made available the development of reliable fuels which could be used in these newly developed engines. Fuels like whale oil, coal gas, mineral oils, coal, and gun powder which were available before then were less than ideal for engine use and development. It still took many years before products of the petroleum industry evolved from the first crude oil to gasoline, the automobile fuel of the 20th century. However, improved hydrocarbon products began to appear as early as the 1860s and gasoline, lubricating oils, and the internal combustion engine evolved together. Up to this time, the lack of good, consistent fuels is a major drawback in engine development. The second technological invention that stimulated the development of the internal combustion engine was the pneumatic rubber tire, which was first marketed by John B. Dunlop in 1888 (Woehrle 1995). This invention made the automobile much more practical and desirable and thus generated a large market for propulsion systems, including the internal combustion engine. Electricity and steam engines competed with internal combustion engine as the basic means of propulsion in automobile but faded from the automobile picture in early 20th

century; electricity because of the limited range it provided, and steam because of the long start-up time needed. Thus, the 20th century is the period of the internal combustion engine and the automobile powered by the internal combustion engine. In the 1880s the internal combustion engine first appeared in automobiles (Givens L. 1992). By 1892, Rudolf Diesel (1858 - 1913) had perfected his compression ignition engine into basically the same diesel engine known today. The lack of good, consistent fuels which is a major drawback in engine development upto date is calling for biofuels e.g bioethanol, biodiesel etc that can be obtained from renewable low cost energy sources.

Classification of IC Engines

Most internal combustion engines are reciprocating engines having pistons that reciprocate back and forth in cylinders internally within the engine. Internal combustion engine is broadly divided into two based on the ignition system namely: (a) spark ignition engine (SIE) and (b) compression ignition engine (CIE) (Khurmi & Gupta 2006). Though the mode of operation of Spark ignition engine contrasts with the compression ignition engine their steps of operation are the same. Others ICE include rocket engines, jet engines, and firearms. Considering the fuel used, compression ignition engine is called diesel engine while spark ignition engine is petrol or gasoline engine, though it can be run on other fuels like methanol, ethanol, bioethanol, compressed natural gas (CNG), autogas (LPG) and hydrogen etc.

2.19.3 Spark Ignition Engine

Spark ignition engine are internal combustion engine where the combustion process of the air-fuel mixture is ignited by a spark from a spark plug. The ignition system supplies high-voltage current from the battery to spark plugs that project into the combustion chambers, an electric arc between two electrodes at the bottom of the spark plug ignites the fuel vapor in the chamber. The fuel system is either the carburetor or injection systems. Carburetor controls the mixture of gas and air that travels to the engine. It mixes fuel with air at the head of a pipe, called the intake manifold, leading to the combustion chamber. A vacuum created by the downward move of pistons draws air through the carburetor, the airflow transforms drops of fuel into a fine mist, or vapor. The intake manifold delivers the fuel vapor (fuel-air mixture) to the combustion chamber. In fuel injection system, injectors through its nozzles spray carefully calibrated bursts of fuel mist into the combustion chambers, where it is mixed with

air. In the combustion chamber, pistons compress the fuel vapor inside the cylinders; at the end of the compression an electric current flows through a spark plug to ignite the compressed fuel vapor. The fuel mixture combusts, creating hot expanding gases that push the pistons down, and cause the crankshaft to rotate. Since the exact quantity of fuel needed is injected into the cylinders, fuel injection is more precise, easier to adjust, and more consistent than a carburetor, delivering better efficiency, gas mileage, engine responsiveness, and pollution control. Fuel injection systems vary widely, but most are operated or managed electronically. Here, electronic sensors respond to varying engine speeds and driving conditions by changing the ratio of fuel to air. All new cars produced today are equipped with fuel injection systems instead of carburetors. Engine output can be increased by fitting air compressing equipments e.g. superchargers are compressors powered by the crankshaft while turbochargers are turbine powered compressors run by pressurized exhaust gas (Mařík et. al., 2014). Superchargers and turbochargers increase the pressure to increase the density of the air to increase engine power. By increasing the air and fuel flow to the engine, these features produce greater horsepower. In order to reduce the heat loss to the engine, cooling water jacket through the surfaces exposed to the heat transfer such as cylinder head, liner, pistons crown and piston rings, Ananda and Saravanan (2010) applied thermal barrier coatings (TBCs) to the combustion chamber and cylinder liner to act as low heat rejection engine.

2.19.4 Compression Ignition Engine

In CI engine, the piston compresses air instead of fuel inside the cylinders, with greater force than a petrol engine does, producing temperatures hot enough to ignite the fuel on contact without needing any external spark (Pulkrabek 1997). The combustion as in SIE causes the crankshaft to rotate. When fuel is injected into the turbulent compressed air, it does not ignite immediately. There is a time period called the ignition delay, during which the fuel heats up, vaporizes, mixes with air, and undergoes chemical precombustion reactions that produce the radicals necessary for spontaneous ignition (Pulkrabek 1997, Stone 1992). After sufficient time has elapsed, ignition will occur spontaneously at multiple locations. Ignition occurs in regions of fuel-air mixture that have fuel-air ratios close to the stoichiometric ratio. Combustion proceeds very rapidly due to the backlog of prepared or nearly prepared fuel-air mixtures formed during the ignition delay period. The rapidly rising temperatures and pressure in the cylinder accelerate the combustion in an uncontrolled manner until the backlog

is depleted. This portion of the combustion process is usually called premixed combustion. The remainder of the fuel in the spray core is still too rich to burn, so combustion slows down and is controlled by the rate at which the air is entrained and a combustible mixture formed. This portion of the combustion process is called mixing controlled or diffusion burning (Pulkrabek 1997). Thus, while chemical kinetics dominates the ignition delay, the high temperatures and pressures of the post-ignition gases promote very fast reaction rates that make fuel-air mixing the rate determining process. Power from compression and expansion stroke is called gross power while power from exhaust and intake strokes is called pump power. Force due to gas pressure on the moving piston generates the work in an IC engine cycle, is expressed as Equation 2.121 (Pulkrabek 199, Moran and Shapiro 1995, Stone 1992).

$$W = \int F dx = \int p A_p dx = \int p dV \qquad (2.121)$$

Where p = pressure in combustion chamber, A_p = area against which the pressure acts (i.e. piston face), x = distance the piston moves, dV= differential volume displaced by the piston.

2.19.5 Losses in IC Engine

Only a fraction of the chemical energy of the fuel is converted into mechanical energy by ICE operation. The "loss work" can be attributed to the following (Pulkrabek 1997, Moran and Shapiro 1995, Stone 1992):

i. Fuel properties
ii. Heat transfer: this involves the heat lost of the hot burned gases which occur during combustion and expansion. Heat transfer also occurs between the cylinder wall and the working fluid.
iii. Mass loss: a fraction of the high pressure unburned gases flows from the combustion chamber into the crankcase (blowby) thus the cylinder pressure drops and the output work decreases. This mass loss is about 1 % of the charge.
iv. Incomplete combustion: the exhaust gases usually contain unburned particles. (H_2, CO, CH) carrying a fraction of the fuel's chemical energy. Approximately 5 % in SIE and 1-2 % in CIE.
v. Limited combustion speed: in ideal SI engine the combustion time is zero i.e. the combustion speed is infinitive. Practically, the combustion process requires certain

time therefore ignition starts before the TC and complete after the TC, thus the peak pressure will be less than that of the perfect cycle and extracted work will be less, too.

vi. Exhaust blow down loss: since the blow down process takes time the exhaust valve must be opened before the BC thus the expansion stroke will be incomplete and work will be lost.

vii. Pumping work: the friction of the streaming gases and the aerodynamic loses during intake causes pressure drop in the cylinder before compression and sequentially lower peak pressure and less work. Blow down process of exhaust gases requires work, too. The pumping loss is most superior in quantity governed (SI) engines at part load.

viii. Friction: the most significant source of this loss is the friction between the piston skirt, rings and the cylinder (about 60 - 80 % of the total frictional work). It is usually higher in diesel engines because of the stronger piston rings. Other sources of frictional losses are crankshaft, camshaft, valve mechanism and gears, etc.

Several methods for achieving low heat rejection (LHR) to the coolant are using ceramic coatings on piston, liner and cylinder head and creating air gap in the piston and other components with low thermal conductivity materials like superni (nckel alloy), cast iron and mild steel (Nurali et. al., 2011, Ananda & Saravanan 2010).

2.19.6 Internal Combustion Engine Fuel Requirements

Fuel combustion is the process that occurs when a hydrocarbon fuel burn in the presence of air compressed to a high temperature, in the combustion chamber of an engine. Compression ignition engine requires fuel of high auto-ignition ability while spark ignition engine requires fuels of high compressibility without auto igniting but waits for the timed plug spark ignition. Hence, the ignition delay, a period during which the fuel heats up before combustion occurs, is very important in defining a fuel as CI engine or SI engine fuel. CI engine where auto ignition is needed requires fuel of low ignition delay while SI engine requires fuel of high ignition delay which is a mark of high compression tolerance. The laboratory test that is used to measure this tendency (ignition delay/compressibility) is the cetane and octane number test respectively (ASTM). Generally, IC engine fuel must fulfill the following (sudheer 2013, Gaurav et. al. 2013):

(i) The fuel must ignite in the engine.

(ii) Good fire safety.

(iii) High or low ignition temperature for SI and CI engine respectively.

(iv) The fuel must release energy when it burns.

(v) The fuel must provide a large amount of energy per gallon.

(vi) The fuel must not limit the operability of the engine at low temperatures.

(vii) The fuel must not contribute to corrosion.

(viii) The fuel must not contain sediment that could plug orifices or cause wear.

(ix) The fuel should not cause excessive pollution.

(x) The fuel properties should not deviate from the design specifications.

(xi) The fuel should be intrinsically safe..

Fuels suitable for fast chemical reaction have to be used in IC engines such as Hydrocarbons in liquid form, Alcohols (methanol, ethanol), LPG (propane and butane), Natural gas (methane), diesel and Hydrogen (Antoni 2003). The categories of additives use to improve fuel quality include oxygenates, ethers, emulsifiers, antioxidants (stabilizers), antiknock agents, fuel dyes, metal deactivators, corrosion inhibitors and some that can't be categorized (RFA 2002, Sreenivasulu et. al., 2013, Tan et. al., 2014).

(i) Oxygenates are fuels infused with oxygen. They are used to reduce the CO emissions from fuel combustion. Oxygenates can be based on either alcohol or ethers.

(ii) Antioxidants are used as a stabilizer in fuel to prevent oxidation.

(iii) Metal deactivators are fuel and lubricant additives that are used to stabilize the fuel. It works by deactivating metal ions to inhibit the formation of gummy residues.

(iv) Corrosion inhibitors slow down metal corrosion. A good corrosion inhibitor will give 95 % inhibition in certain circumstances.

(v) Emulsifiers are use increase lubrication and miscibility to avoid phase separation.

(vi) Co-solvents are use to improve miscibility to avoid phase separation.

Examples of these additives are given in Appendix A6.

2.20 Engine Fuel Properties

Refiners must meet fuel standards set by the American Society for Testing and Materials (ASTM), the Environmental Protection Agency (EPA), state regulatory agencies and their own company standards. In Nigeria the state regulatory agencies include Standards Organization of Nigeria (SON), Department of Petroleum Resources (DPR), and any other competent government agency (NNPC 2005). Fuel properties include physical state, fuel material (feedstock), fuel stability, chemical structure, fuel inflammability expressed by cetane number, anti-knock resistance expressed by pump octane number, flash point, auto-ignition temperature, calorific value, lower and higher energy content, viscosity, volatility, gasoline gallon equivalent, distillation curve, fuel composition: ash and sulphur content etc., freezing point, specific gravity, surface tension, maintenance issues, energy security impacts, materials compatibility etc. Fuel properties are measured by the ASTM standards. Fuel properties especially chemical compositions determine the performance and emission characteristics of the engine (Ashish & Deshmukh 2012).

2.20.1 Viscosity and Material Compatibility

Viscosity is a measure of a fluid's internal resistance to flow or fluid's friction i.e. dynamic viscosity, (η) (Abdullah et. al., 2011). The greater the viscosity, the less readily the liquid flows. Viscosity affects fuel flow and amount atomized e.g. on pumping and injecting (viele et. al. 2014). If fuel viscosity is high, the injection pump will be unable to supply sufficient fuel to fill the pumping chamber, causing poor atomization and a loss in power (Van et. al., 2004). Lower viscosity causes smaller diameter of the droplets in the spray. Below certain limits, low viscosity increases the leaks in the fuel system. The viscosity of a fuel is a strong function of temperature with the viscosity decreasing as the temperature increases. It varies inversely with Temperature – must be given at certain Temperature values, usually given at 20 – 40 ^{0}C. Also, viscosity of fuels is important for the estimation of its lubrication, optimum storage, handling, and operational conditions. The kinematic viscosity (ν) of a fuel is its resistance to flow under gravity (Van et. al., 2004) and related to the dynamic viscosity through the density (ρ) with Equation 2.122.

$$\nu = \frac{\eta}{\rho} \qquad (2.122)$$

Fuel has to be compatible with the engine materials to avoid corrosion and damage .e.g. ethanol is known to dissolve or damage certain materials, and can cause enhanced corrosion of metals, especially bare aluminums. In such case materials of high ethanol tolerance are recommended.

2.20.2 Volatility and Vapor Pressure

Volatility is the major determinant of the tendency of a fuel to potentially produce explosive vapors. It is fuel's tendency to change into vapor. If volatility is too high and too much vapor is formed, it could cause a decrease of fuel flow resulting in vapor lock, loss of power, rough running or stalling, decreased fuel canister (Chevron 2004). If volatility is too low, symptoms could include: poor cold start, poor warm up performance, poor cool weather driveability, unequal fuel distribution, or increased deposits in the crankcase, combustion chamber, and spark plug. During cold start, high volatility ensures that sufficient fuel actually vaporized during the compression stroke for there to be a flammable mixture for the spark plug to ignite.

Vapor pressure provides an indication of how a fuel will perform under different weather conditions. It determines whether a fuel will cause vapor lock at high ambient temperature or at high altitude, or will provide easy starting at low ambient temperature. Vapor pressure is a measure of "front end" volatility, and a fuel with extremely high vapor pressure may cause problems with hot start ability, hot drivability and vapor lock protection (Karl et. al., 2005, Chevron 2004). Vapor lock in engine is the reduction in fuel flow as a result of vapor formation, typically caused by high temperatures, while the vehicle is being driven (Chevron 2002). Vapor lock may be increased with carburetor. Vapor Lock Index (VLI) of a fuel is the ratio of the volume of vapor formed at atmospheric pressure to the volume of fuel tested in ASTM D2533 (RFA, 2002). RFA, (2002) expressed VLI with Equation 2.123 base on the vapor pressure (VP) in kPa and percent evaporated fuel at 70 ^{0}C.

$$VLI = 10\,(VP) + 7(E\ 70\ ℃.) \qquad (2.123)$$

A fuel vapor pressure specification within the recommended vapor pressure limits ensures a product of suitable volatility performance. Allowable RVP for petrol is 0.7 bar in summer and 0.9 bar in winter (at 37.8 ^{0}C). The chemical compound in petrol that contributes most to the RVP is butane (Karl et. al., 2005). A vapor pressure test to determine volatility is referred to

as a Reid Vapor Pressure (RVP) test and is recorded in pounds per square inch (psi). The method involves filling fuel into a metal chamber which is connected to an air chamber and that is connected to a pressure gauge. The apparatus is then immersed in water bath at 37.8 ^{0}C and is shaken until constant P is obtained i.e. Reid VP. The constant P is the total vapor pressure of the solution. For liquid-liquid solutions where both components are volatile e.g. petrol-ethanol blend, Jones and Dugan (1998) expressed this in Equation 2.124.

$$P_{\text{total}} = P_{\text{gas}} + P_{\text{eth}} = X_{\text{gas}} P^0_{\text{gas}} + X_{\text{eth}} P^0_{eth} \; ; \; X_{\text{gas}} + X_{\text{eth}} = 1 \qquad (2.124)$$

P_{total} is total v. pressure of the blend, χ_{gas} and χ_{eth} are the mole fractions of petrol and ethanol, and P^0_{gas} and P^0_{eth} are thier pressures of the "pure" solutions respectively.

2.20.3 Cetane Rating / Flash point

Cetane rating or cetane number, CN is an indicator of the combustion speed of a fuel and its readiness to self-ignite when exposed to the high temperatures and pressure in the diesel engine combustion chamber. In a CI engine, higher cetane fuels will have shorter ignition delay even in cold starting than lower cetane fuels (Van et.al., 2004, Josef laurin 2006). Cetane number is measured by comparing the "ignition delay time" of the sample fuel with a mixture of cetane ($C_{16}H_{34}$) and alphamethyl naptane ($C_{10}H_7\ CH_3$). The cetane percentage in the mixture gives the CN of the sample fuel. CN of the reference fuel cetane is arbitraryly set at 100, and of alphamethyl naptane at 0. Cetane number can be obtained from the self ignition temperature equation 2.125 according to (Chevronon, 2005).

$$T_{self\ ignition}\ (℃) = 310 - 0.75\ x\ CN \qquad (2.125)$$

An easier and practical method to obtain CN is by calculating the Diesel Index, Equation 2.126, as increasing the DI increases the tendancy to ignite according to (Chevronon, 2005).

$$DI = \frac{anilin\ \ point\ (°F) \text{x API (at } 60°F)}{100} \qquad (2.126)$$

API is obtained by heating equal amounts of annilin and diesel fuel; while cooling down, the temperature at which the annilin separates from the mixture is the AP.

Fuel flash point is the lowest temperature at which a combustible mixture with air can be formed above the liquid fuel (Van et. al., 2004). It is the lowest temperature of a sample at

which the fuel vapor starts to ignite when in contact with a flame (ignition source) (Pulkrabek 1997). It is dependent on both the lean flammability limit of the fuel as well as the vapor pressure of the fuel constituents. The flash point is determined by the Marcusson method; by heating a sample of the fuel in a stirred container and passing a flame over the surface of the liquid (Van et. al., 2004). If the temperature is at or above the flash point, the vapor will ignite and an easily detectable flash can be observed (ASTM). For gasoline it is 25 ^{0}C, diesel fuel 35 ^{0}C and heavy diesel 65 ^{0}C. Flash point is the minimum temperature at which a compressed fuel will ignite while auto-ignition point is the temperature at which a compressed fuel will have self ignition.

2.20.4 Octane Number

Octane rating or octane number is a standard measure of the performance of an engine or aviation fuel. It is not an indicator of the energy content of the fuel but a measure of the fuel's tendency to burn in controlled manner, rather than exploding in an uncontrolled manner (Dahiru et. al. 2014). The higher the octane number, the more compression the fuel can withstand before igniting. Compression ignition engine do not compress the fuel but only air and then inject the fuel into the air heated up by compression while spark ignition engine rely on ignition of fuel and air compressed together as mixture without ignition, which is then ignited at the end of the compression stroke using spark plug. Therefore, high compressibility of the fuel matters mainly for SIE. Hence, fuels with a higher octane rating are use in high performance spark ignition engine that requires higher compression ratio while fuels with lower octane numbers but higher cetane numbers are ideal for compression ignition engines (Dahiru et. al. 2014). When gasoline with lower octane number is heated or compressed too much, it will explode when triggered or even self ignite before the ignition system sparks causing much higher pressure than engine components are designed for which in turns causes a knocking or pinging sound. Premature ignition causes engine knock: a sharp sound of detonation occurring outside the domain of flame front (Dahiru et. al. 2014). Octane number of a fuel corresponds to its activation energy, so higher octane number means large amount of energy is required to induce the ignition for combustion. Thus, higher octane fuels are more likely to sustain controlled combustion at higher compression and resist auto-ignition or detonation. Higher compression ratio sweeps more areas under the Otto-cycle curve, which means for a given amount of fuel more energy is released. So, higher compression ratio

corresponds to higher power, better thermodynamic efficiency and greater the tendency for knock to occur. But higher octane number fuel can sustain greater rise in temperature during compression stroke of an IC engine as it can resist auto-ignition. So, a higher power can be extracted from the Otto-Cycle. During the compression stroke, if the air-fuel mixture reaches a temperature higher than ignition temperature of the fuel, auto ignition occurs. If it happened before the top dead end of the piston is reached, the rapidly expanding burned gas mixture will oppose the piston movement and thus will destroy the mechanical efficiency and damage cylinder wall due to explosion.

The octane rating of a fuel is measured in a test engine and is defined by comparison with the mixture of iso-octane and n-heptane that would have the same anti-knocking capacity as the fuel under test (Dahiru et. al. 2014). Iso-octane has octane rating of 100 whereas n-heptane has 0 octane rating hence, the percentage by volume of the iso-octane in the mixture is the octane number of the fuel e.g. petrol with the same knocking characteristics (detonation resistance properties) as a mixture of 90 % iso-octane and 10 % n-heptane would have an octane rating of 90. Where the octane number is raised by blending in bioethanol, energy content per volume is reduced. Other petrol addictives 'octane booster' are MTBE, ETBE, isooctane, isoheptanol, toluene and lead alkyls: as tetraethyllead (TEL; $(C_2H_5)_4$ Pb) and tetramethyl lead (TML) (Ananda & Saravanann 2010, Antoni 2003, Dahiru et. al. 2014), addition of about 0.8 g lead per liter, provides a gain of about 10 ON in petrol. These additives are designed to improve fuel quality as they raise ON, control surface ignition, reduce spark plug fouling, resist gum formation, prevent rust, reduce carburetor icing, remove carburetor or injection system deposits, minimize deposits in intake system, prevent valve sticking. ON can be increased by antiknock agents - at less expense than modifying HC composition by refinery process. Test engine for determining Octane values, was developed by Cooperative Fuel Research Committee (CFR). It is a single cylinder, variable CR engine. The most common type of octane rating measured worldwide is RON, MON, AKI and RdON. RON correlates with low speed, mild driving conditions while MON relates to high speed, high severity conditions. Two different test conditions specify the Research Octane Number (RON) and the Motor Octane Number (MON).

(i) Research octane number (RON): this is determined by running the fuel in a test engine with a variable compression ratio under controlled conditions and comparing results with those for mixtures of isooctane and nheptane.

(ii) Motor octane number (MON): this is determined at 900 rpm engine speed instead of 600 rpm for RON. MON is done in test engine with a preheated fuel mixture, higher engine speed and variable ignition timing to further stress the fuel knock resistance.

Anti knock index (AKI): also called posted octane number (PON) is the average of RON and MON. According to ASTM, AKI is calculated with Equation 2.127.

$$\text{Antiknock Index} = \frac{(\text{RON} + \text{MON})}{2} \qquad (2.127)$$

This difference of MON from RON of a fuel is its sensitivity. Thus for fuels of same RON, high sensitivity fuel has lower MON. ASTM expressed fuel sensitivity with Equation 2.128.

$$\text{Fuel sensitivity} = (\text{RON} - \text{MON}) \qquad (2.128)$$

(iii) Observed road octane number (RdON): this is determined by testing fuel on real world cylinder engines normally at wide open throttle. It can be done with cars on the road or with chassis dynamometers with environmental controls to improve consistency. Generally, the octane rating of the fuel pump is either the minimum RON, minimum MON or the AKI.

For paraffin fuel, Octane Number changes linearly (for paraffinic fuels) For non paraffinic fuels, ON relation is not linear TEL is added to it to increase the ON above 100 or n-heptane is added to the sample to reduce ON below 100, then nonlinear extrapolation is applied. Different blends of fuel though having the same average octane number can affect engines differently, depending on the octane requirement of that particular engine, and explains why engines can perform differently with a change of fuel. Factors affecting the octane number requirement include Compression ratio, Barometric pressure/altitude, Ignition timing, Temperature, Air/fuel ratio, Humidity, Combustion temperature (intake manifold heat, inlet air temperature, coolant temperature), Exhaust gas re-circulation rate, Combustion chamber deposits and Combustion chamber design.

Engines that operate at a high compression and required fuels of higher octane are designed for high performance. The common misunderstanding here is that efficiency and output power can be increase when we burn fuel at higher octane rate than its design specification by engine manufacturer (Dahiru et. al. 2014). The fact is that energy density of the burnt fuel play the key role in determining the output power of an engine. The same densities are obtained for fuel of different octane rating. Increasing the fuel octane rating will not increase the content of oxygen or hydrocarbon in the fuel and as such the output power of the engine will remain the same. There will be decreases in efficiency and the power output of an engine when fuel is burnt at lesser octane rating than that of which the engine is design for (Dahiru et. al. 2014). Knocking can cause severe engine damage so, in computer controlled engines, engine management system have a knock sensor e.g. (piezoelectric microphone) to detect knocking and automatically alter ignition timing to reduce the knock to an acceptable level.

2.20.5 Fuel Calorific Value and Freezing Point

This is the energy content of a fuel, it is characterized by the amount of heat released when the fuel starting at ambient conditions is burned and the products are cooled to ambient conditions (Van et. al., 2004). Specific heating value, is a measure of the energy content of the fuel per unit mass (kJ/kg or kcal/kg) gaseous fuels specific heating value is given in terms of energy content per unit volume (kJ/liter or kJ/m^3, $kcal/m^3$). Heating value of the combustible air-fuel mixture is a decisive factor for engine performance. It is the enthalpy of combustion (or the heat of combustion) since the combustion process produces water and energy but will be different depending on whether the water is liquid or vapor. If the water in the exhaust products is assumed to be liquid, the heat extracted will be the higher heating value or the gross heating value. If it is considered to be vapor, then the heat extracted is the lower heating value or the net heating value. Since engines do not have the ability to condense water in the exhaust, the lower heating value is the most commonly used measure of fuel energy content (Van et. al., 2004). The energy content of the fuel depends on the refinery in which it was produced, the time of year, and the fuel feedstock. Beyond these differences, the heating value will depend on the composition of the fuel. The air-fuel ratio and exhaust gas temperature (EGT) play important role.

Freezing point is the least temperature at which the fuel form precipitate, it can lead to clogged filter. Freezing can be prevented by either removing precipitate from the fuel or

adding flow improvers (additives). Anti freezing properties are determined by its filterability. For gasoline freezing point is –65 ^{0}C and for diesel fuel –10 ^{0}C. This normally occurs during cold weather. For SI engines to start, A/F ratio must be within the ignitable range, ie in general must be between 7:1 and 20:1 by weight. When the engine is cold (cold starting), it is difficult to ignite lean mixtures, because fuel may not vaporize sufficiently - under these conditions the mixture is richened to bring it to ignitable range. This is done by increasing the injection time or by the use of a choke with carbureted engines.

2.20.6 Specific Gravity, Surface Tension and Fuel Stability

The differences between fuels relate mostly to the density (American Petroleum Institute, API). More dense fuels and aromatic fuels provide greater energy per gallon and since fuel is sold volumetrically, the higher the density, the greater the potential energy. The specific gravity is a relative measure of the density of a substance. It is defined as the ratio of the density of the substance, ρ, to a reference density, expressed in Equation 2.129.

$$G = \frac{\rho}{\rho_{ref}} \tag{2.129}$$

The most common reference density used in the measurement of specific gravity is the density of water at 4 ^{0}C, which corresponds to a reference density of 1 g/cc. Thus, specific gravity [kg/m^3] is the measurement of the ratio of the weight of a given volume of fuel to the weight of the same volume of water, both at 20 ^{0}C and 101.325 kPa. A hydrometer is use to measure specific gravity.

Surface tension is a parameter which affects the formation of fuel droplets in sprays. The lower the value of surface tension the smaller the fuel droplet diameter becomes. It is directly proportional to fluid densities which differs with fluids and affects the fluidity. For diesel fuel and gasoline are 0.023 – 0.032 N/m and 0.019 – 0.023 N/m respectively.

A fuel is considered unstable when it undergoes chemical changes that produce undesirable consequences such as deposits, acidity, or a bad smell (Van et. al., 2004). Thermal stability addresses fuel changes that occur due to elevated temperature. These changes may occur at conditions encountered in modern fuel injection systems as fuel is re-circulated through the

engine cylinder head and back to the fuel tank. Oxidative stability refers to the tendency of fuels to react with oxygen at temperatures near ambient. These reactions are much slower than those that would occur at combustion temperatures, and they produce varnish deposits and sediments. Storage stability is also a frequently used term and refers to the stability of the fuel while it is in long-term storage. Storage stability might also involve issues of water contamination and microbial growth. The stability of a fuel is base on its Viscosity Index which measures the relative change in viscosity with time (Abdullah, 2011), expressed with Equation 2.130.

$$VI = \frac{(\mu_f - \mu_i)}{\mu_i} \qquad (2.130)$$

Where, μ_i is the initial viscosity, the viscosity of the fresh fuel and μ_f is the final viscosity after a specified period of storage. A lower VI number indicates greater stability of the liquid. A VI of zero would be a completely stable liquid.

2.20.7 Distillation Profile and Drivability

Distillation or volatility characteristics of liquid fuels and solvents have an important effect on their safety and performances. They are critically important for both automotive and aviation fuels, affecting starting, warm-up, and tendency to vapor lock at high operating temperature or at high altitude, or both. The boiling range gives information on the composition, the properties, and the behavior of the fuel during storage and use. The presence of high boiling point components in fuels can significantly affect the degree of formation of solid combustion deposits. The distillation curve is determined by relating the fraction of a fuel sample that is removing by heating a fuel sample to progressively higher temperatures at atmospheric pressure (Van et. al., 2004). It is a result of the plot of temperature against a corresponding evaporated fuel (%). Typically, the curve is characterized by the initial point, the temperature at which the first drop of liquid leaves the condenser, the temperatures at each 10% of the liquid, and the end point. Distillation rate is controlled by the heat input.

Drivability index (DI), is the quality of being drivable, of being easy or pleasant to drive. In other words DI of a fuel gives insight on how it response to the drivers demand and driving comfort. Cold start is to attempt to start a vehicle when the engine is cold relative to its normal operating temperature. This results to (1) higher compression stroke as lack of heat

makes ignition or difficult. (2) Oil becomes more viscous and difficult to circulate. (3) Air becomes denser and cooler affecting A/F and thus flammability. These problems can be solved with automatic adjustment of fuel pump to pump more fuel and using a fuel of good drivability. Drivability index is based on the relationship between the distillation temperature of the fuel and the cold start and warming up parameters of the vehicle. According to Renewable Fuels Association (2010) and Chevron (2009), DI can be calculated with Equation 2.131 and 2.132.

$$DI\ (℃) = 1.5T_{10} + 3.0T_{50} + 1.0T_{90} + 1.33(ethanol\ \%) \quad (2.131)$$

$$DI\ (℉) = 1.5T_{10} + 3.0T_{50} + 1.0T_{90} + 2.4(ethanol\ \%) \quad (2.132)$$

Where, T is distillation point temperature at 10 ml, 50 ml and 90 ml respectively.

DI varies with gasoline grade and season. Lower values of DI generally result in better cold-start and warm-up performance, but once good drivability is achieved, there is no benefit to further lowering the DI.

2.20.8 Fuel Purity, Ash, Sulphur and Benzene Content

Fuel purity is how free a fuel is from water, other contaminations and impurities. Petrol-ethanol blends or similar hydrocarbons have a limited solvency for water. Water has mostly negative effect on fuels, which include cold starting, shift in calibration output, drivability, fuel energy content reduction and thus adversely affects fuel economy and power. Consequently, free water is undesirable because it can freeze and cause problems. Petrol-ethanol blend fuel containing water will separate into a lower alcohol-rich aqueous phase and an upper hydrocarbon phase if cooled to about 7 ^{0}C of which normal SI engines will not run on the aqueous phase material, such a separation is likely to cause serious operating problems (ASTM, 2011). Dissolved water is usually unavoidable during manufacture. Because ethanol is hygroscopic and easily picks up water from ambient air and the distribution system, the water content of the denatured fuel ethanol must be limited when blended with gasoline to reduce the risk of phase separation (IFQC, 2004). The phase separation of gasoline-ethanol blends is affected by the total water content of the mixture. This includes the water content from the ethanol and gasoline hydrocarbons blended at the rack, water adsorbed from the

atmosphere, and transportation and storage infrastructure for the blended fuel. A centrifuge or water content distillation is use to measure quantity of water present in a fuel.

Ash consists of the residual alkali catalyst and other ash-forming compounds left when the fuel is heated to a sufficiently high temperature that combustible material burns and leaves as CO_2 and H_2O. Ash primarily consists of inorganic compounds and their oxides which can be abrasive and contribute to engine wear, injector or carburetor deposits or fuel system fouling.

Sulphur is a corrosive element that can corrode fuel lines, carburetor and injection pump, so, it is required to be very low. It unites with oxygen to form sulphur dioxide, which in presence of water at low temperature, forms sulphurous acid. It has low ignition temperature, promote knock in SI engines, limited to approx 250 ppm (50 ppm is aimed for low pollutant emitting vehicles). Benzene maximum allowable concentration is specified because it is highly toxic material, the level is 5 %. For leaded and unleaded petrol max lead content is specified, lead causes pollution and destroys catalytic converters in the exhaust system. Manganese is used for antiknock in petrol, maximum amount is specified, 0.00025 to 0.03 gMn/L.

Acidity of a fuel is primarily an indicator of the presence of degradation products e.g. free radicals and can be elevated if a fuel is not properly manufactured or has undergone oxidative degradation. The acidity of combustion gases in combination with the lubricating ability of lube oil will significantly increase the wear rate (DOE). According to information from the National Ethanol Vehicle Coalition, Ford no longer require the use of synthetic oil for the lubrication of engines designed to be fuelled with E85. Other car manufacturers like Chrysler may still require special oil for their FFVs (National Ethanol Vehicle Coalition, 2004, DOE).

Acid strength, as measured by pHe, is a good predictor of the corrosion potential of ethanol fuels. It is preferable to total acidity because total acidity does not measure acid strength; overestimates the contribution of weak acids, such as carbonic acid; and may underestimate corrosion potential of low concentrations of strong acids, such as sulfuric acid (ASTM 2010).

2.21 Engine Performance Characteristics

Performance of an engine reveals its power output, economy, durability and emission. Hence, performance of an engine can be access based on the following operating parameter: engine Speed, fuel consumption (FC), torque, brake power (BP), compression ratio, brake specific

fuel consumption (BSFC), brake thermal efficiency (BTE), brake specific energy consumption (BSEC), Brake Mean Effective Pressure (BMEP)**,** heat balance, exhaust gas temperature, volumetric efficiency. These parameters are measured at different loads of fuels and fuel blends.

Engine Speed: engine speed, n is the number of revolution per second. The effect of speed is allied to the design of the combustion chamber and varies with individual engines. If combustion is sped up then, (i) the engine speed is increased and therefore power output is higher, and (ii) the chain reactions that lead to knock are reduced (Stone 1992). Delay may be reduced or increased. Ethanol blends tend to increase engine speed (Tangka et. al., 2011). The average combustion chamber speed is a function of engine speed in a typical SI engine (Pulkrabek 1997).

Delivery Ratio: this is calculated with the Equation 2.133

$$\lambda = \frac{m_a}{V_s.\rho_{atm}.N.i} = \frac{T_{atm}}{T_{atm} + \Delta T_{intake}} = \frac{P_{atm} + \Delta P_{intake}}{P_{atm}} \quad (2.133)$$

$\rho_{atm}, P_{atm}, T_{atm}$ are ambient density, pressure and temperature, and $\Delta T_{intake}, \Delta P_{intake}$ are temperature and pressure change through intake. m_a, is mass flow rate of air (kg/s). And:

$$\rho_{atm} = \frac{P_{atm}\ x\ 10000}{273.15 + T_{atm}}\ x\ \frac{M}{R_u} \quad (2.134)$$

M is molar mass of air (29.4 kg/kmol), R_u is the universal gas constant.

Excess Air Factor: SI engines are quantity governed by opening and closing of throttle valve which regulates the mass of charge to the cylinder. Excess air factor is practically determined by running the engine with the air-to-fuel ratio as the only variable. This is carried out at a constant speed, constant throttle opening and a constant ignition setting. Excess air factor is obtained from Equation 2.135.

$$\lambda_m = \frac{m_a}{B.\infty} \quad (2.135)$$

Where ∞ is stoichiomeetric air-fuel ratio**.**

Compression Ratioε : Increase in compression ratio increases brake thermal efficiency (Ashish & Deshmukh 2012). Compression depends on the provision of better quality of fuel and combustion chamber design to avoid the self ignition or preignition causes knocking.

However higher compression ratio makes petrol engines using low octane-rated fuel prone to engine knocking by building up the cylinder pressure, thereby reducing tremendously the efficiency or even damaging the engine (Norhisam et. al., 2011). CFR (Cooperative Fuel Research Committee) engine is used to measure the compression ratio at which ignition starts. CR is gradually increased while the engine is driven by an electric motor - a curve of CN against critical CR is obtained. The piston sweeps through a volume that is called the displacement volume, V_d, the minimum volume occurs when the piston is in its uppermost position (TDC). This minimum volume is called the clearance volume, V_c. The maximum volume is the sum of these two. The ratio of the maximum volume to the clearance volume is called the compression ratio (Pulkrabek 1997) and calculated with Equation 2.136.

$$\varepsilon = \frac{\text{max .volume}}{\text{min .volume}} = \frac{V}{V_c} = \frac{V_d + V_c}{V_c} \qquad (2.136)$$

Volumetric Efficiency: This is the mass of air equal to the density of atmospheric air times the displacement volume of the cylinder per each cycle **(**Nyachaka et al 2013). It is use as an overall measure of the effectiveness of a four stroke cycle engine and its intake and exhaust system as an air pumping device. It is usually higher in CIE than in SIE. According to Nyachaka et. al., (2013), volumetric efficiency is calculated with equation 2.137.

$$VE = \frac{(V_a + V_f)}{V_s} \qquad (2.137)$$

Where V_a is Volume of air, V_f is Volume of fuel, V_s is total swept or displacement volume. And

$$V_f = \frac{\text{Volume of Sample}}{\text{Rate of consumption}} \qquad (2.138)$$

$$V_s = aLN(n_{cyl}) \qquad (2.139)$$

$$V_a = \frac{M_a R T_a}{P_{atm}} \qquad (2.140)$$

$$M_a = 0.866 \sqrt{\frac{P_{atm}\ x\ h}{T_a}} \qquad (2.141)$$

Where a is cylinder bore, L is the stroke, N is engine revolution, n is number of cylinder, M_a is mass of air, R is gas constant, h is Manometer reading in (in) = H sin θ. And T_a is air or ambient Temperature.

Volumetric efficiency improves more with pure fuels than with fuel blends (Nurali et. al., 2011). But Ashish & Deshmukh (2012) reported increase in octane number and volumetric efficiency with increase in percentage of ethanol in LPG blend. This is due to evaporative cooling of the charge in the cooling manifold and during the intake stroke (Antoni 2001).

Torque / Brake Power: Both torque and power is functions of engine speed. Torque is a good indicator of an engine ability to do work, defined as force acting at a moment distance while brake power is the actual work output of an engine or the actual work available at the crank shaft (Nyachaka et al 2013). Torque increases as engine speed increases to a maximum and then decreases with further speed increase. Torque decreases because the engine is unable to ingest a full charge of air at higher speeds. Torque and brake power are usually measured by a dynamometer. Both curves show maximum values but they occur at different speeds. Torque is obtained by reading off a net load W (N) at known radius R (m) from the axis of rotation (Sudheer 2013; Pulkrabek 1997) and calculated with Equation 2.142.

$$\text{Torque}\,(Nm) = W.R \qquad (2.142)$$

Brake Power output of an engine is largely a function of the amount of heat that can be released in the combustion chamber which is determined by the amount of the air available and the properties of fuel (Antoni 2003). Brake refers to a device used to load an engine and hold it at a desired rpm. In a generator end, Gaurav et. al. (2013) gave brake power as Equation 2.143.

$$\text{Brake Power}\,(\text{kW}) = \frac{2\pi NT\ (\text{kW})}{10^3} = \boldsymbol{\frac{P_b lan}{10^3}} \qquad (2.143)$$

Power is the measure of an engine's horsepower before the loss in power caused by the friction, gearbox, alternator, water pump, and other auxiliary components like power steering pump, muffled exhaust system, etc (Pulkrabek 1997), expressed in Equation 2.143. It is the power at the crankshaft expressed in Equation 2.144 according to Ganesan & Elango (2013) and Pulkrabek (1997) respectively

$$\text{Brake Power (kW)} = \frac{2\ x\ 3.14\ x\ \text{N}\ x\ \text{T}}{60\ \text{x}\ 1000} \qquad (2.144)$$

Where T is engine torque, *N* is engine revolution, IHP is indicated power and FP is friction power.

Indicated Power: indicated here implies that it is the power from the combustion chamber produced by the fuel. It is the rate of work done by the gas on the piston evaluated from the indicator diagram obtained from the engine. Indicated power increases with speed, while brake power increases to a maximum and then decreases at higher speeds (Gaurav et. al. 2013, Ananda & Saravanan 2010). This is because friction losses increase with speed and become the dominant factor at very high speeds (Ashish & Deshmukh 2012). The indicated (IHP) and brake power (BP) becomes similar as the engine speed increases.

Friction Power: this is the power required to overcome the frictional resistance of the engine parts. Therefore, frictional power comprises that fraction of indicated power not available at the crankshaft i.e. other but brake power. Here, friction is classified as a loss in form of power; it presents problems to the engine by reducing the power output and hence its efficiency. The frictional forces in a piston are more or less the same for the intake, compression, and exhaust stroke. During the compression stroke the pressure and forces are greater so the frictional forces increase. According to Pulkrabek (1997), piston contributes as much as 50 % of the total friction to the engine while piston rings contribute about 20 %. Also, friction increases at high engine speeds. At speeds greater than 15 m/s the danger of having structural failure increases (Pulkrabek 1997).

Brake Mean Effective Pressure (BMEP)**:** This is the mean effective pressure which would have developed power equivalent to the brake power if the engine were frictionless (Nyachaka et al 2013). It is defined as the average pressure the engine can exert on the piston through one complete operating cycle, in other words it is the work output per engine cycle. It is the average pressure of the gas in the fuel mixture inside the engine cylinder based on net power. BMEP is independent of the RPM and size of the engine. If n is the number of revolutions per second i.e. engine speed, and N the number of revolutions per cycle, the number of cycles per second is just their ratio (W), and expressed by Gaurav et. al. (2013) and Nyachaka et. al. (2013) in Equation 2.145.

$$BMEP \quad = \frac{2\,.\,\pi\,.N\,.\,T\,x\,1000}{L\,x\,a\,x\,n} \quad = \frac{2\,.\,\pi\,.N\,.\,T\,x\,1000}{L\,.\,a\,.\left(\frac{N\,.\,n_{cyl}}{i\,.\,60}\right)} \tag{2.145}$$

Where i = 1 for 2-stroke and i = 2 for 4-stroke engine.

While the indicated mean effective pressure (IMEP) is measure with a planimeter or calculated with Equation 2.146.

$$IMEP = \frac{net\ area\ of\ indicator\ \ diagram}{lengt\ h\ of\ \ diagram}\ x\ spring\ constant \tag{2.146}$$

Mechanical Efficiency: Part of the indicated work per cycle is used to expel exhaust gases, induct fresh air, and also overcome the friction of the bearings, pistons, and other mechanical parts of the engine. The mechanical efficiency is the measure of the ability of the engine to overcome the frictional power loss (Gaurav et. al. 2013) expressed in Equation 2.147.

$$Mechanical\ efficiency\ \eta_m = \frac{\text{work output}}{\text{work input}} = \frac{BMEP}{IMEP} = \frac{\text{BP}}{\text{IP}} \tag{2.147}$$

According to Pulkrabek (1997), work input or heat input is expressed in Equation 2.148.

$$Q_{in} = Specific\ Fuel\ Consumption\ x\ BP\ x\ \frac{LHV}{3600} = m_f LCV \tag{2.148}$$

Brake Thermal Efficiency: Brake Thermal Efficiency (BTE) is the ratio of the power output of the engine to the rate of heat energy liberated by the fuel consumed during the combustion as indicated by the lower calorific value (LHV) of the fuel (Ganesan & Elango 2013). It is the ratio of the thermal energy in the fuel to the energy delivered by the engine at the crankshaft (Gaurav et. al. 2013). BTE is obtained with Equation 2.149 according to Ganesan and Elango (2013) and Van et. al., (2004).

$$BTE = \frac{3600}{fuel\ mass\ rate\ x\ LCV}\ x\ BP = \frac{BHP}{B.\mathrm{H}_t} \tag{2.149}$$

There is some ambiguity in the definition of the thermal efficiency based on whether the higher or lower heating value should be used (Van et. al., 2004). Furnace efficiencies tend to be based on the higher heating value. Natural gas is sold on the basis of higher heating value. However, for engines, the normal procedure is to use the lower heating value since the engine

does not condense the water vapor in the exhaust gases (Van et. al., 2004, Eknath et. al., 2011). BTE greatly depends on the manner in which the energy is converted as the efficiency is normalized respect to the fuel heating value. The actual heating value of a fuel depends on its refining, time of year, feedstock and its composition.

Fuel Consumption, FC: This is often expressed as fuel combustion rate. Fuel combustion rate is necessary in order to determine the effect of product fuel and the various blends on mileage. FC according to Ganesan and Elango (2013) and Tangka et. al., (2011) can be calculated using Equation 2.150.

$$\mathrm{FC(kg/h)} = \frac{\text{fuel consumption}}{\text{time (sec)}} \text{ x } \frac{3600}{1000} \text{ x fuel specific gravity} \qquad (2.150)$$

Brake Specific Fuel Consumption (BSFC): BSFC is the parameter most often used by engine manufacturers to characterize fuel economy. It is the fuel flow rate per unit of power output in an hour or engine stroke; a measure of the efficiency of the engine in using the fuel supplied to produce work (Gaurav et. al. 2013). Hence, it is desirable to obtain a lower value of BSFC meaning that the engine used less fuel to produce the same amount of work. (Ashish & Deshmukh 2012, Ibrahim 2011). The BSFC measures how much fuel may be required to do a certain quantity of work but does not contain information about the amount of energy that may be available from the fuel, so it cannot be used to make comparisons between engines burning different fuels. BSFC increases with biofuels blends than with pure fuels due to lower energy value in biofuels which engines respond to the load by increasing the fuel flow (Hiregoudar et. al., 2014 a&b). BSFC can be calculated with Equation 2.151 according to Yanuandri et. al. (2014) and Gaurav et. al. (2013).

$$\mathrm{BSFC\ (kg/kW-h)} = \frac{fuel\ consumed\ \ rate\ (kg/h)}{Brake\ \ power} \qquad (2.151)$$

The testing of IC engines consists of running the engine at different loads and speeds and taking sufficient measurements for the performance criteria to be calculated. It can be carried out at a constant throttle setting (in SIE) or at constant speed setting. If the throttle area is the maximum then the test is called wide open throttle (WOT) test. The most frequent engine test is that which gives the power speed and torque speed characteristics.

2.22 Bioethanol as Engine Fuel

It has been reported that bioethanol achieves higher energy efficiency in an internal combustion engine than its fossil alternative, both as a blend and as a pure fuel. For instance, The Brazilian auto industry association, ANFAVEA, claims that cars running on an E22 achieves 5.5 % fuel efficiency over pure petrol and that pure ethanol cars achieve 30 % improvements on average. Though bioethanol has a very low cetane number, it has high qualities and also works well in a compression-ignition engine in the presence of ignition improver additive. These are partly because bioethanol has certain superiority as engine fuel as explicitly explained below.

(a) Bioethanol and Safety Handling

Bioethanol is biodegradable, less detrimental to ground water unlike diesel and petrol. There is no increased risk associated with bioethanol compared with petrol fuel when it comes to fire and safety aspects. Bioethanol has a lower vapor pressure than petrol at low temperatures but vapor pressure of their fuel blends increases so is their volatility. For example, E85 is more flammable than petrol at 0 ^{0}C but at higher, normal, temperatures E85 is less flammable because of the higher auto ignition temperature of 454 ^{0}C. The high auto-ignition of ethanol makes the storage and transportation issues less important (Ashish & Deshmukh 2012). However, certain risks with bioethanol are different from petrol. Combustible vapors can occur in closed spaces (e.g. fuel tank in vehicles and at filling stations) at higher ambient temperatures, and in a broader temperature interval than for pure petrol fuels. This may cause problems with hot start ability, hot drivability and vapor lock protection (Chevron 2004). Consequently, the pistol valve on refilling pumps for bioethanol and its blends should not be equipped with lock-up mechanism so that vapor can leave t he pistol without building up static electricity. Department of Energy advised that skin and vapor contact with E85 should be avoided and ethanol-resistant gloves should be used. There are several benefits associated with bioethanol compared with petrol, such as, slower fire propagation and less violent fires that are easier to control than petrol fires. There is visual difference of the smoke and flame characteristics of the two fuels. Unlike ethanol pure petrol produces black smoke and visible flame color. But increasing ethanol concentrations in their blends produces less black smoke and decreases the visible flame color. Extinguishing agents include water, alcohol foam, CO_2 or dry chemical for ethanol while that of petrol are alcohol foam, CO_2 or dry chemical

(Chevron 2004). Under fire conditions in ethanol-petrol blend, when foam or water has been flowed on the burning product, petrol burns off first leaving the less volatile ethanol/water solution which may have no visible flame or smoke. Sometimes a slight orange flame may be visible. Rescue Services Agencies show concern that ethanol can adversely affect the foam used by fire fighters, although ethanol-resistant foam is available.

(b) **Bioethanol and Fuel Blending**

Fuel ethanol is that used in blends with petrol (Ashish & Deshmukh 2012), diesel, and in dedicated 100 % ethanol fuelled vehicles (Gaurav and Nitin, 2014, Eknath et. al., 2011, Seshaiah, 2010, Amit Pal et. al., 2004). Blending these fuels together alters the physical and chemical characteristics of the original fuels as well as reducing the lubricating ability of the lubricating oil (Karl et. al., 2005). The higher the concentrations of ethanol, the more the fuel has polar solvent-type characteristics with corresponding effects on conducting fire suppression operations (Chevron, 2004). Previously no single engine manufacturer approves more than 10 % ethanol in diesel (Shyam et. al., 2012, Karl et. al., 2005), but Environmental Protection Agency (EPA), USA, came out with legal mandate for 15 % ethanol in diesel. However, researches are improving towards more percentage ethanol even in diesel. Petrol blended with ethanol is particularly promising since it is more readily incorporated into the existing fuel combustion system (Tan et. al., 2014). Thus, bioethanol cars have only one fuel tank, which can be filled with either ethanol blends or petrol. The amount of bioethanol in the fuel is detected by a sensor that analyses the content of the fuel tank. The information is sent to the engine and the fuel injection system is adjusted according to the data. A major drawback of diesel-ethanol (DE) blends in CI engines is the limited solubility of ethanol in diesel fuel; so, phase separation and water tolerance are vital problems (Pang et. al., 2006, Lapuerta et. al., 2007). Al-Hassan et. al., (2012) experimental report on phase stability revealed that the DE blends is not stable and separated after 2, 5, 24 and 80 hours, for 20 %, 15 %, 10 % and 5 % ethanol concentration, respectively; and 1, 3 and 9 days for 20 %, 15 %, 10 % ethanol concentration respectively in diesel-biodiesel-ethanol blends (DBE); the blend of DBE5 was of the best stability with very little separation. Their result may suggest that presence of biomass base biodiesel improved miscibility in DBE resulting to longer separation time. Phase separation in DE blend can be prevented by adding an emulsifier that

acts to suspend small droplets of ethanol within the diesel fuel, or by adding a co-solvent that acts as a bridging agent through molecular compatibility and bonding to produce a homogeneous blend (De-Menezes et. al., 2006, Shi et. al., 2005, Lapuerta et. al., 2007) e.g. haxanol (Ganesan & Elango 2013), n-butanol, 1-octylamino-3octyloxy-2propanol and N-octyl nitramine (Sreenivasulu et. al., 2013). Phase separation can also occur in petrol-ethanol blends as water makes them immiscible; this problem can be overcome by using semi – polar co-solvents (solubility improvers) such as isopropanol (Ananda & Saravanan 2010). The higher the concentrations of ethanol, the more the fuel has polar solvent-type characteristics with corresponding effects on conducting fire suppression operations (Chevron, 2004). More sophisticated blending technologies are Ratio blending, Sidestream blending and Wildstream blending (Karl et. al., 2005).

(c) Bioethanol and Cold start properties

Bioethanol cars can have cold start problems when the temperature goes below -15 ^{0}C, hydrocarbons emissions increases in cold weather, because its miscibility with other fuels becomes low (Ghobanian et. al., 2008, Karl et. al., 2005) so, from 5 ^{0}C use of engine pre-heater is recommended. In the absence of engine heater pure bioethanol fuel, E100, is mostly used in warmer climates or where cold start problems are not a factor. Ether can also reduce cold starting. Rong et. al., (2011) reported that in petrol-ethanol blend for best cold-start emissions, the ethanol content is to be at least 20 % but no greater than 30 %. High blend bioethanol can be used in adapted vehicles (FFVs) with petrol engines and diesel engines (Rutz and Janssen, 2008). The inflammability and lubricating capacity can be adjusted almost perfectly by the use of suitable additives 4 to 12 % to increase CN so that bioethanol can be used for diesel engines without any interference with the engine design (Al-Hassan et. al., 2012). Blend E85 in adapted petrol engines mitigates against cold start problems as well as blend ED95 in adapted diesel engines with 5 % ignition improver (Kristina et. al., 2008).

(d) Bioethanol and Engine Materials Compatibility

Most operating problems with bioethanol fuelled vehicles have been traced to contaminated fuel and corrosion. Consequently, choosing the right materials for fuel storage and dispensing systems and following proper fuel handling procedures are crucial for successfully operating bioethanol fuelled vehicles. The problems of corrosion are eliminated in dedicated ethanol

vehicles and FFVs by using unplated steel, stainless steel, black iron and bronze, which have all shown acceptable resistance to ethanol corrosion (Rutz and Janssen, 2008). Non-metallic materials successfully used with E75 and E85 include thermoset reinforced fiberglass, thermo plastic piping, neoprene rubber, polypropylene, nitrile, Viton and Teflon materials. Materials that can be used with only petrol are old-time lacquered cork carburetor floats, the antique zinc-based "pot metal" castings for fuel pumps and carburetors, and Lexan or Plexiglas if there is warm vapor contact (ASTM, 2010). Materials that can be used with both ethanol and petrol fuels include neoprene rubber (any color), steel, aluminum, most polypropylene-type plastics, and both Lexan and Plexi glass if limited to liquid contact. The corrosives of ethanol to aluminum and steel is not serious as long as the ethanol is dry, however, Aluminum should be protected by a surface coating. Those that cannot be used with either petrol or ethanol are natural rubber, butyl rubber, and polystyrene plastics, because both fuels dissolve these materials. The technology for storing and dispensing petrol can be applied to alcohols and alcohol blend fuels because they are liquid fuels at ambient pressures and temperatures (Josef laurin 2006). Infact, as a rule of thumb, "anything good for petrol is good for ethanol" is a pretty good guide, as long as Lexan or Plexiglas are not involved, and no truly antique parts are used (i.e. zinc-based pot metal castings and the lacquered cork float.

(e) Bioethanol and Driving Range

Bioethanol fuel contains approximately 35 % less energy compared to petrol. This means that the consumption of bioethanol is higher than petrol and thus the driving range is shorter. A bioethanol car that uses 0.7 L petrol/10 km needs 1.0 L E85/10 km. Therefore, present bioethanol cars are equipped with larger fuel tank in order to operate over the same distances as pure diesel or pure petrol cars. However, bioethanol fuel has a higher octane number and can be used with a higher compression ratio, resulting in higher energy efficiency (Dhanapal et. al., 2010, Ibrahim 2011). This means that engines optimized for bioethanol can be more energy efficient than engines that are currently optimized for petrol (Wallner et. al., 2009). As bioethanol has a higher octane number than petrol, it offers increased torque and higher power, especially when used in combination with turbo-technology (Rakopoulos et. al., 2008, Mařík et. al., 2014). Additional cost includes the engine heater which is standard equipment.

(f) Bioethanol and Regulated Emmision

Two types of emissions are released from vehicles i.e. exhaust and evaporative emissions. Bioethanol has a positive effect on vehicle emissions (Wallner et. al., 2009). Exhaust carbon monoxide (CO), methane (CH_4) and nitrogen oxide (NO_X) have been reported to be minimal with bioethanol fuels compared to conventional fuels (Ashish & Deshmukh 2012, Ozer et. al., 2004, Lin & Huang 2003, Kristina et. al. 2008, Rakopoulos et. al., 2008). E10 is widely documented to achieve a 25 % or greater reduction in CO, NO_x and most toxic hydrocarbons (HCs) such as benzene (Rong et. al., 2011, Mustafa et. al., 2009, Dhanapal et. al., 2010, Rutz and Janssen, 2008, IFQC 2004). Increasing ethanol quantity in the blend further lowers the resulting emissions (Ashish & Deshmukh 2012, Rutz and Janssen, 2008, Van et. al., 2004). Huseyin et. al., (2006) reported maximum decrease in HC emission using E60 in SI engine. Hassan et. al., (2005) and He et. al., (2003), results on a bioethanol adapted diesel engine with catalytic converter and exhaust gas recirculation system (EGR for NOX reduction) showed that bioethanol fuel emits less particulate matter (PM). Pure ethanol has less emissions resulting from evaporation due to its fewer highly volatile components than petrol. However, when added to petrol, the vapor pressure of the blend is increased thereby increasing evaporative emissions (Rutz and Janssen, 2008). This is because in its pure form, ethanol molecules are polar and bond to each other via the hydroxyl (OH) groups. These forces of attraction prevent the molecules from leaving the liquid (Ophardt, 2003) but in the presence of hydrocarbons, this bonding does not take place for the first 2 – 3 vol% of ethanol added to petrol. Thereafter, increased addition of ethanol will not further boost the vapor pressure. However, using a petrol base-stock for ethanol blending that initially has a lower vapor pressure negates this effect.

However, emissions of acetaldehyde, formaldehyde and peroxyacetyl nitrate (PAN) may increase in petrol-ethanol blends. Despite fuel, the quantity of pollutants released also depends upon how well the vehicle's emission control system captures and burns emissions, and how well the engine is designed and "tuned" for using fuel ethanol (IFQC 2004).

(g) Bioethanol and Car Retrofitting

The maximum ethanol content of the fuel mixture, which can be used in the non-modified engines, differs with the car's model (AVL 2008). In response to the few shortcomings of

bioethanol as engine fuel, convectional engines can be retrofitted (modified) to operate on bioethanol fuels efficiently i.e bioethanol compatible engines. In Sweden, it is legal to retrofit petrol cars to bioethanol cars since mid-2008, after which it is to be certified at the Swedish Motor Vehicle Inspection Company. The car has to meet the emission standard it did prior to the retrofit. When a car is retrofitted, the fuel injectors are changed and the engine control plan has to be calibrated for the new fuel. These modifications include replacing the gaskets, filters, metallic and rubber based materials in fuel management system to bioethanol compatible substitutes, advancing of engine timing, resetting the engine calibration system, resetting injection timing, larger injector holes, provision of airtight conduit lines, raising cylinder compression ratio, fuel pump with larger flow capacity, roughening of the piston head to improve pre-combustion fuel homogenization and inserting sensor in the exhaust manifold (Tangka et. al., 2011, AVL 2008, DOE, Poala et. al., 2010, Tan et. al., 2014, Van et. al., 2004). At present, it is not possible to retrofit diesel engines to enable bioethanol propulsion. The fuel used consists of bioethanol and an ignition improver. Neat bioethanol has a low cetane number and therefore the ignition improver is required, together with increased compression ratio in the engine.

Considering the ease at which ethanol fuel forms combustible vapors in closed space, ethanol fuel tank is equipped with pressure vacuum relief filler cups for maximum safety. Considering the low calorific value of ethanol and reduced energy density in blends, fuel tank has to be 1.7 times and 1.5 times bigger in volume than that for pure diesel and pure petrol respectively so as to obtain the same range of travel from a vehicle (Josef laurin 2006). Fuel consumption increases by about 30 % as the energy content per liter of ethanol is lower than that of petrol (Tangka et. al., 2011, Antoni 2003). It has been reported that ethanol fuel has a "gasoline gallon equivalency" (GGE) value of 1.5 US gallons (5.7 L), which means 1.5 gallons of ethanol produce the energy of one gallon of gasoline. That is, loss of fuel economy is experienced with ethanol. In practice, there is only a 5 % to 12 % decline in fuel mileage per liter of E85, though this is offset by the fact that the FFV is about 7 % more powerful than a pure petrol engine, and the energy is utilized much more effectively (Van et. al., 2004, Tangka et. al., 2011, Tan et. al., 2014,). Also, increased oxygen content in blends of petrol-bioethanol makes fuel leaner thereby causing unstable engine idling; hence the necessity for increasing fuel supply to the engine (Rong Horng et. al., 2011, Antoni 2003, Siddegowda &

Venkatesh 2013). World Wide Fuel Charter (WWFC) reported 3.5 % oxygen content level for petrol-ethanol blends as too high (WWFC 2002, RFA 2002). Consequently, engine management system is modified to prepare air-fuel mixture so that it would close to stoichiometric ratio of 14.7:1; the system may be close loop control principle (Antoni 2003). The close loop control principle has a sensor that detects the amount of bioethanol in the fuel and signals the engine control unit which then adjusts the fuel injection system according to the data (Chevron 2004). The adjustment increases duration of injection to increase the fuel supply (Alvydas et. al., 2003, AVL 2008). As addition of ethanol to petrol results to maximum pressure reduction and increase in flame speed, the spark timing of the blends has to be optimized (Dhanapal et. al., 2010, Pulkrabek 1997). Also ferrous picrate can be use to improve combustion and increase mileage (Sreenivasulu et. al., 2013, Tangka et. al., 2011). One of the benefits of an FFV is that this vehicle operates with equal efficiency on petrol, ethanol and petrol-ethanol blend, and needs only a single fuel tank.

(g) Bioethanol and Maintenance Needs

Bioethanol cars need more frequent service than conventional fuel cars. Manufacturers recommend service every 10,000 km or once a year, compared to every 20,000 km or once a year for new petrol cars. The reason is that engine oil and the oil filter have to be changed more often in a bioethanol car, as the bioethanol fuel is not lubricating the engine as much as conventional fuel does; the oil gets worn out faster (Scott 2013, Norhisam et. al., 2011, NREL 2002). The main service needs are change of motor oil and oil filter. Change of fuel injectors is required much frequently, as pollutants formed in the engine can get stuck in the fuel injector, making the injection pressure fall (Siddegowda & Venkatesh 2013).

2.23 Related Studies on Bioethanol Fuel in ICE

Bioethanol has unavoidable anti fuel characteristics like moisture, lower calorific value and a higher flash point (Tangka et. al., 2011). The question has been the effects of the various blends, from which feedstock and what is the best suitable mixture for fuel purposes (Antoni 2003). In response to this, suitability of bioethanol fuel from different raw materials in ICE is currently a major research goal. Some related studies also towards solving this quest are highlighted below.

(Tangka et. al., 2011) evaluated the physicochemical and operational properties of various petrol-bioethanol blends. Bioethanol was obtained from maize (*Zea mays*), sugar cane (*Saccharum* L), raffia (R*affia vinefera*) wine, and palm wine and then purified using a rotavapor. The vapour pressure, octane number, flash point, specific gravity, and energy density of various compositions of the blends were evaluated. Sugar cane gave the highest yield of alcohol 97.99 g/kg of produce while the lowest amount of alcohol of 10.5 ml/kg was obtained from palm wine. Engine power decreased from 0.4 kW with 100 % petrol to 0.108 kW with a petrol-ethanol ratio of 1: 10. The octane number increased from 93 at E10 to 106 at E90. The energy density decreased from 33.18 MJ/l at E10 to 23.6 MJ/l at E90.

Altun and Hakan (2009), investigated the effect of unleaded petrol and unleaded petrol blended with 5 % and 10 % of ethanol or methanol on the performance and exhaust emissions of a SI engine. The engine tests were performed at 1000, 4000 anad 5000rpm at 3/4 throttle opening positions. The results showed that BSFC increased while BTE, CO emissions and HC decreased with methanol- petrol and ethanol-petrol blends. It was found that 10 % ethanol or methanol in petrol works well in the existing design of engine and operation parameters.

Mustafa et. al., (2009) investigated the effect of petrol-ethanol blends on engine performance and exhaust emission in SI engine. They used unleaded petrol (E0) and the petrol–ethanol blends (E50 and E85) on a single cylinder four-stroke SI engine at 10:1 and 11:1 compression ratios. Engine speed was changed from 1500 to 5000 rpm at wide open throttle. Their results showed that ethanol–petrol blends allow increasing compression ratio without knock occurrence. Blends increased the torque, power and fuel consumption and reduced CO, NO_x and HC emissions but CO_2 increased. In addition Al-Hassan (2003) reported increase in volumetric and brake thermal efficiencies but decrease in BSFC and equivalence air/fuel ratio; E20 has best results at all engine speeds. Huseyin et. al., (2006) reported that with increasing compression ratio up to 11:1, engine torque increased with E0 fuel at 2000 rpm speed and at higher compression ratios the torque output did not change noticeably. At 13:1 compression ratio compared with 8:1, the highest increment was obtained for E40 and E60. At 11:1 compared with 8:1, BSFC of E0 fuel reached minimum value and decreased about 10 %, after this compression ratio the BSFC increased.

Amit Pal et. al. (2004) operated a Kirloskar, four strokes, 7.35 kW, twin cylinder, DI diesel engine in dual fuel mode (with substitution of up to 75 % diesel with CNG). They reported significant reduction in smoke, 10 – 15 % increase in power, 10 – 15 % reduction in fuel consumption and 20 – 40 % saving in fuel cost considering low cost of CNG. There was about 33 % reduction in engine noise which may prolong the engine life significantly and the consequent sound levels of giant diesel engine reduced to that of a similarly sized petrol engine. Kass et al. (2001) tested the torque output from the same model engine with DE10 and DE10. They reported an approximate 8 % engine power reduction for both blends. Hansen et al. (2003) studied the Cummins engine performance with DE15 and found that power decreases by about 7 – 10 % while BTE increases by about 2 – 3 % at rated speed.

Seshaiah (2010) tested the variable compression ratio SI engine with pure petrol, LPG (Isobutene), and E10, E15, E25 and E30. Also, petrol mixed with kerosene at 15 %, 25 % and 35 % by volume without any engine modifications was tested for CO and CO_2 emissions. Brake thermal and volumetric efficiency variation with brake load was compared. It was observed that LPG is a promising fuel at all loads and gave lesser CO emission than other fuels tested. Among the petrol-ethanol blends, E10 is better at all loads and compression ratios, without any loss in efficiency or need of engine modification.

Jitendra et. al., (2013), tested a four cylinder, four stroke, varying rpm, petrol (MPFI) engine on blends containing E5, E10, E15 and E20; performance characteristics, and exhaust emissions were evaluated. Results showed that there is a reduction in exhaust gases, such as HC, O_2, CO, CO_2 and increase in BTE on blending. They concluded that E10 is most effective and so can be utilized in SI engines with little or no engine modification

Norhisam et. al., (2011) studied the effect of an optimized blend ratio of biofuel such as ethanol, butanol and methanol, with petrol on engine performance improvement and thereby on the electrical generator output. The results showed improved brake specific fuel consumption and increase electrical power output with the blends. With load resistance of 15 and E10 Ω, the engine performance was increased up to 6 % while 20 % butanol–petrol increased the performance up to 8 % compared to the use of E0.

Rakopoulos et al. (2008) studied the effects of diesel-ethanol blends, with 5 % and 10 % (v/v) on the performance and emissions of a turbocharged DI diesel engine. Results showed that increasing ethanol quantity in the blend increased the BSFC and decreased the BTE. Huang et al. (2009) investigation using DE10, DE20, DE25 and DE30 blend fuels showed that the brake thermal efficiencies decreased with increasing amount of ethanol in the blends. Ibrahim (2011) and Ananda & Saravanan (2010) reported that BSFC and BTE increases with the increment of the percentage of ethanol in petrol blend compared to petrol fuel.

Shyam et. al., (2012) investigated the physical stability of bioethanol-biodiesel blends and bioethanol-biodiesel-biobutanol blends using Jatropha oil methyl esters and enerdiesel emulsifier as additives. DI engine performance was studied base on fuel consumption, thermal efficiency, exhaust gas temperature and emissions (CO, NOx, HC and smoke) using E5, E10 bioethanol-biodiesel and E15B15, B20E20 bioethanol-biodiesel-biobutanol blends compared to pure diesel. The results showed that the blends are physically and thermally stable up to 17 days at room temperature. The physicochemical properties of all blends show good resemblance with that of diesel except the flash point; E5 has maximum BTE and minimum BSFC at higher loads. E10 has best overall emission characteristics.

Siddegowda & Venkatesh (2013) studied performance and emission characteristics of MPFI engine with petrol-ethanol blends at the designed Vehicle speed of 60 km/h and engine speed of 2500 rpm. Emission parameters like UBHC, CO, CO_2, and NO_X were measured using gas BOSCH analyzer. They reported reduction in heat loss and increase in power with increase in load thereby resulting to increase in BTE. E20 gave higher efficiency than the petrol for all load condition while the efficiency for E10 and E30 are slightly lower than the petrol. CO and HC emission decreases notably as a result of the leaning effect caused by the ethanol addition but CO_2 emission increases because of the improved combustion.

Gaurav and Nitin (2014) studied the performance of two stroke single cylinder SI engine with ratio of E10, E20 and E30. BTE and BSFC were determined at various loads on engine. BTE and BSFC of blends showed comparable performance with that of pure petrol. BTE increased for a particular percentage of alcohol blends. Performance decreases after a particular fixed percentage of blending. E10 showed least BSFC and better engine performance.

Eknath et. al., (2011) used a Single Cylinder diesel engines connected to a rope break dynamometer, to test for DE5 to DE20 on three different compression ratios adjusted by moving the cylinder head. At engine load of 2.138 kW (at 57 %), BTE of pure diesel and DE was almost same. BTE for kerosene was low compared to diesel and DE. DE20 has a very good efficiency compared with diesel, and kerosene blend. DE20 has higher volumetric efficiency compared to diesel, and kerosene blend. Exhaust gas temperature for DE showed no substantial increase compared to diesel. DE20 blend has better engine performance than with pure diesel.

Al-Hassan et. al., (2012) studied the effects of diesel-biodiesel-ethanol blends (DBE) on a CI engine. Ethanol proportion was varied. The engine was operated with DBE having 5, 10, 15 and 20 % ethanol with fixed 10 % biodiesel on a volume basis, as well as on diesel fuel alone at constant load and at engine speed ranges from 800 to 1600 rpm for each run. Results indicated that the equivalence air-fuel ratio and the BSFC for the blends are higher than that of pure diesel and increases with the increase of ethanol concentration. DBE with 5 % ethanol has brake power close to that of diesel and decreases with higher ethanol concentrations. BTE increased with fuel blends of 5 and 10 % ethanol and decreases with a higher ethanol concentration. In conclusion, the blends containing 5 and 10 % ethanol concentration are the most suited for CI engines due to its acceptable engine performance and fuels solubility. Their result is line with Gaurav et. al. (2013).

Yanuandri et. al. (2014) studied the engine performance and exhaust emission of bioethanol derived from WPB and blended with petrol for E10, E20 and E25. Four strokes, four cylinders Honda/L15A SI engine operated at 1500 – 4500 rev/min with 85 % throttle position was used in the study. E10 gave the highest torque at 3000 to 4500 rpm with its brake power greater than that of E0. E10 and E20 resulted to greater BSFC than pure petrol at low speed of 1500 to 3500 rpm this is in line with finding of Ashish and Deshmukh (2012). Emissions of CO and HC decreased as speed increased.

MacLean and Lave (2003), and Hsieh et al, (2002) reported that power and torque does not decrease when petrol-ethanol blends are used, in spite of its smaller lower heating value compared to E0. They reported increased RON, heat of vaporization and autoignition temperature with higher ethanol concentration in blends. Vapor Pressure is higher for ethanol compared to petrol, but in blends, their value was influenced by petrol quality, i.e how much butane it has and what are the T50 and T90 distillation temperatures (Orbital 2002).

Combustion in general is improved with petrol-ethanol blend compared to E0. Another way to see this is to look at emissions CO decrease 10 – 40 % (Orbital, 2002, Li et al, 2005, Al-Baghdadi, 2000) and HC decrease and 5 – 20 % (Niven 2005, Hammel-Smith et al, 2002, Morris and Brondum, 2000), as ethanol concentration in blend increases. Oppose to that are the trend for NOx increasing 1 – 18 % (Schifter et al, 2001, Apace, 1998, Mayote et al, 1994), and aldehyde emissions increasing 5 – 200 % (Health 2003).

2.24 Summary

General conclusions arrived from the above literature review are that ethanol can be produced abundantly and economically from various organic materials and it will be an attractive alternative fuel for IC engines. The steps of producing bioethanol include pretreatment, hydrolysis, fermentation and separation process. Moisture content is the main factor that affects the quality of the end product thus; an efficient dehydrating technique is necessary. The key dehydrating technique, distillation yields 96 % pure ethanol and 4 % water, hence for higher purity ethanol a series of distillation or a hybrid of distillation with another efficient technique need to be employed. Acid pretreatment, acid or enzymatic hydrolysis and fermentation with s.cerevisae or bacterium Zymomonas mobilis increases ethanol yield. Inhibitory substances are generated as a result of the hydrolysis of the extractive components, organic and sugar acids esterified to hemicellulose (acetic, formic, glucuronic, galacturonic), and solubilized phenolic derivatives. In the same way, inhibitors are produced from the degradation products of soluble sugars (furfural, HMF) and lignin (cinnamaldehyde, p-hydroxybenzaldehyde, syringaldehyde), and as a consequence of corrosion (metal ions) (Lynd, 1996). Bioethanol can be used either as a pure fuel, gasoline blend, LPG blend or diesel blend. Gasoline-ethanol blends including ethanol at low proportions can be used without any modifications in the engine but pure ethanol usage requires major modifications to the engine design and fuel system. Fuel modification technique is employed in the form of fuel additives e.g. oxygenates, emulsifiers or co-solvent (solubility improvers) to the blend that enhances the fuel properties. Oxygenated blends gave a better anti-knock performance during low speed acceleration than hydrocarbon fuels of the same octane range. Consequently, the use of ethanol-fuel blends with fuel additives in the IC engines is more practical than using ethanol alone. However, bioethanol has unavoidable anti fuel characteristics like moisture, lower calorific value and a higher flash point. The question has been what are the effects of the various blends on these characteristics and what is the best suitable mixture for fuel purposes? The answers from previous and on-going studies would help energy stakeholders in mapping out the choice of strategies towards energy self sufficiency using bioethanol. Based on this, the present experimental study has been focused on efficiently producing bioethanol from lignocellulosic waste palm bunch that is abundant in Nigeria, and analyzing its performance in IC engine.

CHAPTER THREE
MATERIALS AND METHODS

3.1 Material

3.1.1 Sample Collection

The raw material for this study which is waste palm bunch was collected in August 17th 2016 from Siat Nigeria Limited a subsidiary of Risopalm located at Ubima Local Government Area of Rivers State, Nigeria. The collected waste palm bunch is already shredded, cleaned and sterilized, in the course of operation of the palm mill unlike those from local palm mills. Waste palm bunch less than two weeks from the harvested date were used for the study, this is to minimize the effect of post harvest history and biochemical degradation. Picture of the collected feedstock is shown in Plate 3.1.

(a) Waste palm bunch **(b) Collected Compressed Shredded Waste Palm Bunch**

Plate 3.1 Raw material

3.1.2 Required Materials Provision

The materials required in the course of this project include some chemicals for preparing reagents shown in Plate 3.2 and apparatus among others. These include H_2SO_4 for hydrolysis, NaOH for nuetralization, distilled water, phenol and phloroglucinol for colour reagents, D-xylose and D-glucose for standard solutions, yeast for fermentation. Apparatus include Weighing machine, sieve cloth, thermometer, spectrophotometer, Oven dryer, Stirring rod, pH meter, water bath, calibrated containers, pressure gauge, laboratory and constructed distiller. All the reagents and standard used in this work were of analytical grade; the chemicals used were supplied by Jucenco Enterprises, at Njiribako Street Owerri. The

prepared reagents include Sulphuric acid solution, sodium hydroxide solution, D-xylose solution, D-glucose solution, phloroglucinol solution, chromic acid solution and phenol solution for the analysis. Precaution is taken always adding acid to water and not vice versa to avoid splash that can lead to injury.

Plate 3.2: Prepared Reagents

3.2 Sample Preparation

The compressed shredded feedstock collected was prepared for bioethanol fuel production by drying, mechanical comminute, dilute acid pretreatment and hydrolysis, the product is then fermented and dehydrated to pure sample fuel as explained below. The methods used in this work for the various determinations of samples are the standard methods.

3.2.1 Drying

Freshly sterilized empty fruit bunches typically have a water content of 60 % on a wet basis (Abdullah et. al. 2011), the water content reduces during compression and shredding. Thus, the obtained sterilized feedstock was oven dried at 60 ^{0}C for 3hrs in a 7.756 kW FRA Series of Southstar Industriel Four Oven Dryer shown in Plate 3.3, until it is dry. Total of 10 bags of shredded WPB was dried.

Plate 3.3: Feedstock Oven Drying

3.2.2 Physical Pretreatment

Particle size reduction was required to reduce cellulose crystallinity, provide enough surface area, increase sugar concentration, and allow fast hydrolysis and fermentation (Ghasem et. al., 2007). Hence, the dried sample undergoes mechanical commute being pulverized and ground to fine particles using fibre grinding machine powered by 220 V / 13.8 A, 1460 rpm / 3 HP ATLAS exclusive electric motor, fixing the right blade for the respective step as shown in Plate 3.4 and Plate 3.5 respectively. The blades are made of mild steel but of different carbon content. The ground WPB was screened with a Filterwel Test Sieve to obtain 850 microns WPB powder (ASTM 20) shown in Plate 3.6. Also, the sterilization operation is efficient in increasing sugar concentration as it acts as auto hydrolysis in the regular pretreatment methods, depolymerising cellulose, hemicelluloses and lignin in WPB (Simarani et. al., 2009). Though, it could reduce the hemicellulose content, and more critically, by collapsing the structure of the glucan, it increased recalcitrance (Jinlan et. al., 2014). The by-product can be used as solid fuel or pellets for heating. The ground feedstock was stored in a closed plastic container at room temperature until used for hydrolysis as was also done by Yanni et. al., (2013).

(a) Machine for Physical Treatment

(b) English Blade for 1st Grinding

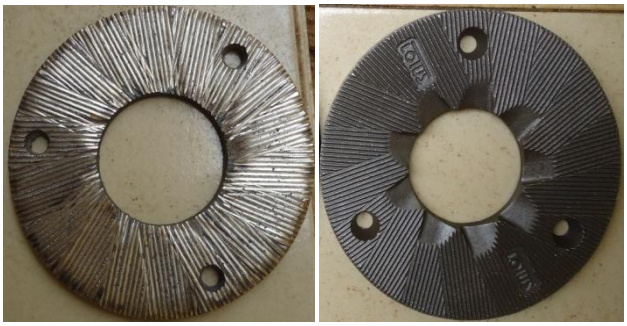

(c) Local and English Blade for 2nd Grinding

Plate 3.4: Machine and Blades for Physical Treatment

Plate 3.5: Blade Changing

(a) Ground Feedstock **(b) By-Product**

Plate 3.6: Feedstock after Physical Pretreatment

3.2.3 Feedstock Characterization

The ground feedstock was characterized for its lignocellulosic compositions (hemicelluloses, cellulose, lignin, moisture content) following the method of Nurul et. al., (2014). The chemical compositions of pulverised WPB were analysed according to ASTM 1104-56 and ASTM D1103-60 method for holocellulose and α-cellulose, respectively. For the gravimetric method of lignin determination, 3 g of sample was weighed into a 100 ml Erlenmeyer flask and stirred for 2 h in 60 ml of cold 72 % (v/v) H_2SO_4 solution. The mixture was transferred into a 500 ml beaker and boiled for 4 h in 600 ml distilled water bath under continuous stirring; and filtered using glass microfiber filter grade GF/B (Whatman) in porcelain crucible. The residue retained was washed with hot water until it was acid free and allowed to dry at 105 ^{0}C for 2 h and weighed.

The holocellulose - a composite of cellulose and hemicellulose - was extracted from WPB using acidified sodium chlorite method. Approximately 12.0 g of sample was mixed with 480 ml distilled water and treated with 1.5 ml acetic acid and 4.5 g sodium chlorite at 70 – 80 ^{0}C for 4 h under continuous stirring. The mixture was then washed with hot water, filtered and dried at 105 ^{0}C for 24 h. Determination of holocellulose was carried out using dry weight method. A total of 6.0 g of dried holocellulose obtained was further dissolved in 120 ml of 17.5 % (v/v) NaOH solution and stirred for 30 min. A total of 30 ml of NaOH solution was added into the mixture and allowed to mix to separate hemicellulose from the holocellulose and leaving α-cellulose. The insoluble α-cellulose was filtered and washed separately with 8.3 % (v/v) NaOH solution followed by 10 % (v/v) acetic acid. The α-cellulose was finally washed with hot water to a neutral pH and dried overnight at 80 ^{0}C.

The ash content % on dry basis was determined by the AOAC (1980) method. Triplicates of 2.0 g ground WPB were weighed $W_{2,}$ into three dried porcelain crucibles of weight $W_{1.}$ The samples were charred on a heat mantle (Plate 3.7) to drive off smoke and prevent flaming in the furnace. The charred samples were then transferred into a muffle furnace (Plate 3.8) set at 550 ^{0}C for 3 h to ensure proper ashing. They were then cooled in a desiccator and finally weighed $W_{3.}$ The average percentage ash was calculated with Equation 3.1.

$$Ash, mass\ \% = \frac{w_3 - w_1}{w_2} \tag{3.1}$$

Plate 3.7: Sample Char on Heat Mantle.

Plate 3.8: Sample Ashing in Muffle Furnace

3.2.4 Dilute Acid Hydrolysis

Considering its effectiveness compared to HCL, nitric acid and phosphoric acid according to previous researches, dilute H_2SO_4 acid was used to hydrolyze the sample (Farid et. al., 2010, Millanti et al., 2011, Nurul et. al. 2014, Akpan et. al., 2005, Kumar et. al., 2009), on a single stage hydrolysis (Saha et. al., 2005), under a controlled temperature using a 550 W, 200 V/50 Hz regulated digital oven shown in Plate 3.9 which serves an autoclave.

Plate 3.9: DHG – 9023A Model Digital Oven (B.Bran Scientific & Instrument Company England)

The oven has a temperature range of ambient +5 – 250 ^{0}C with +/-1 ^{0}C fluctuation. A single stage hydrolysis was carried out instead of 2-stage hydrolysis done by Millati et al. (2011) who reported low yield. The ratio of sample to acid solution was controlled at 1:10 (w/v) (Fitriani & Anwar 2013, Mingjia et. al. 2010, Nurul et. al. 2014). Preliminary experiment was done with 3 multiplicates of each acid concentration with 10 % (w/v) solid loading for various holding time. The parameters examined were: sugar yield per holding time of 15, 30, 45, 60 minutes, with 0.8, 1 and 1.2 % acid concentration (acid % of water volume) at 160, 180 and 200 ^{0}C. For the preliminary; 200 g of the ground WPB weighed on a 4 W electronic 'Adventurer Pro AV313C model' Ohaus digital weight scale, of weight range 310 g+/- 0.001 g, was mixed with 2000 ml of distilled water and H_2SO_4 at different concentrations in a cylindrical vessels made of a corrosion resistant alloy (e.g. high steel alloy). The mixture was stirred very well for homogeneity, and then hydrolyzed in a regulated digital oven to ensure constant heat supply. The time of the reaction starts when the reactor (oven) reaches the set reaction temperature thereby serving as an autoclave. The autoclaving is believed to modify the physical structure of lignin (Ghansem et. al., 2007). The acid hydrolyzed slurry was allowed to cool to room temperature in an ice bath to stop the reaction, neutralized with 2M NAOH standard solution in 1dm^3 water (Cheng et. al., 2007, Farid et. al., 2010, Nuru et. al., 2014) to a neutral 4.8 pH. The pH was measured using a 3510 model Jenway pH meter. The filtrate was then analyzed for reducing sugar (glucose and xyloses) using a spectrophotometer (Congcong et. al., 2013) as explained below. Six optimum yields were adopted for fermentation.

Spectrophotometer

A 220 V, 340 ~ 950 nm wavelength range spectrophotometer shown in Plate 3.10 was used for this research. It has +/-2.5 nm and +/-1 %T (cuvette) wavelength and photometry accuracy respectively. To achieve best performance, it is allowed a warm up period of 20 minutes.

Plate 3.10: Globe CS-100 Model Spectrophotometer

The "0 %T" knob was adjusted to set to "0.0" display. After warming up, T/A switch was set to T position while "100 %" knob adjusted to set "100" digital display. Then T/A switch was set to A position and Abs. zero knob adjusted to "0.0" digital display. The scale was rechecked to ensure digital display of "0.0" in A scale and "100" in T scale. If not Abs. zero knob was adjusted to ensure this. Wavelength selective knob was adjusted to select 488 and 540 standard wavelength for glucose and xylose respectively (Caputi et. al., 1968). The solution to be tested was then inserted into the test tube well in the sample room, paying attention to the tube direction. The tube was firmly clipped in the spring clip to avoid data error caused by wrong direction. Sample absorbance was then determined by using T/Abs. selective switch. Since each blank solution has different absorbency background, the energy difference of each single wavelength testing data have to be normalized, so the absorbency of blank solution in testing wavelength was adjusted to zero. The solution poured into the cuvette was higher than 6 cm in order to exceed the testing light passing through the tube. All the C_5 and C_6 sugars exhibit the same general behavior as xylose and glucose, respectively, although there may be some deviation in the details.

3.2.5 Glucose Determination

Glucose determination was carried out using the Phenol Sulphuric method (Duboise et. al., 1956; Congcong et. al., 2013). Glucose standard solutions shown in Plate 3.11 are prepared by dissolving 1.25 g of Glucose in 250 ml distilled water. Aliquots were taken from this solution to obtain 1.0, 2.0, 4.0, 8.0 and 10 ppm. 1 ml of 5 % phenol followed by 5 ml concentrated sulphuric acid was added before reading the standard solutions.

Plate 3.11: Glucose Standard and Sample Solutions

5 % phenol solution was prepared by dissolving 5 g of phenol in 95 g of distilled water making 100 g of solution, and a 5 % by mass solution. To determine glucose, 1 ml of the hydrolyzate is mixed with 1ml of 5% phenol solution. The mixture is mixed well with 5 ml conc. sulphuric acid to form the sample solution. Sample solutions were allowed for 30min to cool and glucose then measured at absorbance 488 nm. The spectrophotometer was standardized by adjusting it to zero absorbance with a reagent blank containing 1 ml of distilled water and 1 ml of 5% phenol followed by 5ml conc. sulphuric acid, before reading. Dilution with same quantity of water was carried out on the samples for readability. Absorbance at 488nm is converted to glucose concentration from a standard curve formed with laboratory grade glucose standard solution,

3.2.6 Xylose Determination

Xylose determination was carried out using colour reagent method (Miller, 1959; Congcong et. al., 2013). It is based on the following reaction mechanism: in the solution of HCL, phloroglucinol gives colour reaction with sugars or their degradation products, for different sugar ratios showing maximum absorbance at 554nm wavelength for xylose (Hu et. al., 2008; Browning 1967). The colour reagent consists of 0.5g Phloroglucinol, 100ml of acetic acid and 10ml of conc. HCL. This reagent is stable for 4 days at room temperature if protected from sunlight. Xylose standard

solutions are prepared by dissolving 2.5 g D-xylose in saturated solution of benzoic acid to make 0.7, 1.0, 1.3, 2.6 and 3.9 mmol/L concentrations. 2 g of benzoic acid was dissolved in 200 ml hot water to get saturated solution of benzoic acid. To determine Xylose, 5 ml Phloroglucinol colour reagent was added to 5 ml of xylose or sample solution in a test tube, and then heated for 4 minutes at 100 ^{0}C in a TT - 420 Model Techmel & Techmel USA Water Bath shown in Plate 3.12, then cool to room temperature in water. Blank solutions containing 5 ml water and phloroglucinol reagent (5 ml) were prepared by heated and cooled along with the solutions. The spectrophotometer was standardized by adjusting to zero absorbance with the reagent blank before reading the standard and sample solution (Plate 3.13), absorbances. Xylose concentration is obtained from a standard curve formed with the xylose standard solution.

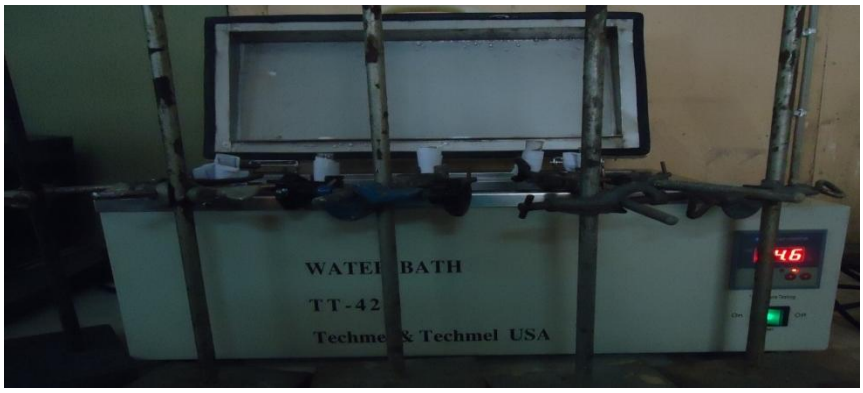

Plate 3.12: Xylose Standard Solutions in a Water Bath

a 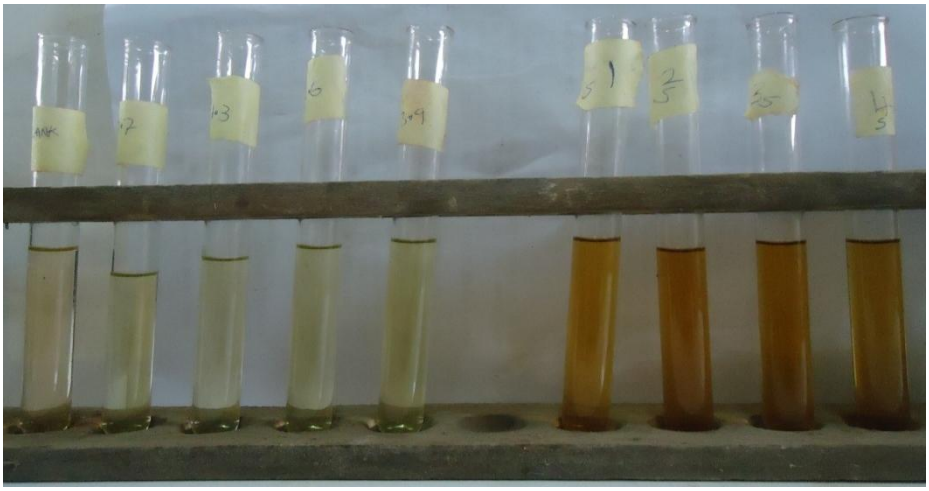 b

Plat 3.13: Xylose Standard[a] and Sample[b] Solutions

3.2.7 Fermentation

A catalyst has to be introduced to enhance the conversion of sugar into alcohol and CO_2. Previous researches have proved S.cereviciae to be hexose assimilating and even better yield in xylose fermentation than xylose assimilating yeasts. Also, considering the reports of Chayanoot & Sairudee (2013) and Cheng et. al., (2007) of higher ethanol yield, the hydrozate was fermented with S.sereviciae as a catalyst. The yeast was cultured as explained below before introducing it to the fermentation process.

Inoculums Preparation: S.serevicis in Plate 3.14 was isolated from palm wine using Saboured Dextrose Agar (SBA). This was done by inoculating 0.1 ml aliquote of 10^{-2} dilution of freshly tapped palm wine and incubating the already inoculated plates at 27 ^{0}C for 24 h. At the end of the inoculation period, the isolated yeast was characterized by using morphological characteristics and Lactophenol cotton blue staining technique. Thereafter, a loopful of the identified yeast was subcultured into 60ml of nutrient broth contained in a test tube and incubated at 27 ^{0}C for 24 h.

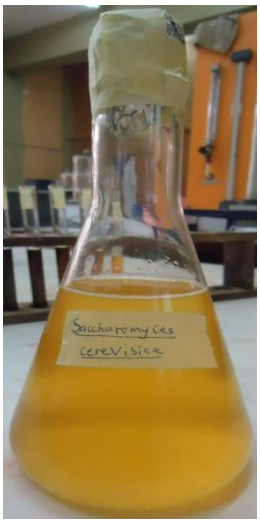

Plate 3.14: S. Serevicies Innoculum

Fermentation process: six optimum hydrolysates were fermented at room temperature and pH condition of about 4.8 for optimum salinity for yeast growth (Liu and Chen 2008). 100 ml of the prepared yeast innoculum was asceptrically inoculated unto the optimum hydrolysates from the palm bunch samples 200 g each in a 12 L fermenter sealed with Vaseline and nylon to avoid air diffusion into it but CO_2 exit, as shown in Plate 3.15 below. They were then covered with sack bag to screen off sunlight as shown in Plate 3.16.

Plate 3.15: Samples Fermentation

Plate 3.16: Samples Fermentation Screened from Sunlight

Aliquote were collected after 24 h interval for sugars consumption and bioethanol yield, analysed using spectrophotometer (Caputi et. al., 1968; Congcong et. al., 2013) as explained below. The fermentation process was stopped once bioethanol yield starts declining, with 0.5ml HCL. Bioethanol yield with time was examined.

3.2.8 Bioethanol Determination

Total bioethanol concentration in the filtrate medium was estimated by Chromic acid method and measuring absorbance at 584 nm wavelength using a spectrophotometer (Caputi et. al., 1968). The chromic acid reagent was prepared by dissolving 34 g of potassium dichromate in 500 ml of distilled water. 325 ml of concentrated H_2SO_4 was added and the volume was makeup to 1000 ml. Bioethanol was estimated calorimetrically as described by Caputi et. al., (1968): the volume of 1ml of sample in a test tube is made up to 5 ml with distilled water, 5 ml of the chromic acid is then added, after which the test tube was incubated in a water bath at 60 ^{0}C for 20 minutes. The absorbance was determined in a spectrophotometer at 584 nm and converted to bioethanol concentration from a standard curve for standard solution of absolute ethanol (Plate 3.17).

Plate 3.17: Ethanol Standard

3.2.9 Preliminary Dehydration

Distilling the whole slurry will definitely affect clear separation of the fermented portion of the feed and invariably affect the final yield (Rosentrater, 2006). Thus, the feed was separated from the slurry by filtering. The initial temperature which is mostly within room temperature (28 – 30 ^{0}C) and volume of feed was noted. Laboratory distillation of the 3 optimum fermentate was carried out to obtain and confirm bioethanol presence in the WPB, Plate 3.18.

Plate 3.18: Preliminary Distillation Setup

The distillation flask, column and distillation head make up the part of the simple distillation apparatus where the feed components were volatilized and separated. The rest of the apparatus serves to condense the hot vapor back to a liquid as it flows out the side-arm of the distillation head into the water-cooled condenser. The distillation flask was charged with the feed and a couple of boiling chips. The feed in the flask was heated to bioethanol boiling point of 78^0C to cause distillation. Condensed bioethanol flows down the condenser into a measuring cylinder. As the bioethanol is removed, the feed was depleted of the lower boiling point component.

As two distillers cannot be compared except when operating at the same condition and capacity, the obtained distillate is only to further confirm the presence of bioethanol fuel from the used WPB, and does not affect the proposed distiller design. However, better refined bioethanol fuel is expected from the research distiller. In conclusion, a total of 18 runs for hydrolysis, 6 runs for fermentation and 3 runs for distillation were carried out at the preliminary stage. These production steps was studied and the optimum conditions adopted for main experiment in obtaining (1) optimum quantity yield (2) feed batch capacity for distiller construction and (3) to determine the distiller energetic, for establishing a production rig. Photographs of some physical measurements carried out during the experiment are given in Plate 3.19.

Sample, Phenol and NAOH Mass Measurement (OHAUS weight Scale, USA)

Reagents Volume Measurements **pH Reading (Jenway pH meter Bibby Scientific LTD. UK)**

Plate 3.19: Physical Measurements

3.2.10 Distiller Fabrication

The study proposes fabricating a distiller for the distillation process. Based on the prelimnary results, the main experiment was to be carried out with 2500 g WPB, hydrolysed for 30 min with 1.2 % H_2SO_4 in 25000 ml distilled water to obtain 20 L fermentate after 3days fermentation period with 1250 ml innoculum, which is the proposed distiller batch capacity. Distiller feed was separated from the slurry by thorough filtering, thus, feed is considered to contain only bioethanol and water. Quantity of component other than water is negligible considering water quantity present in the feed. All these were considered in determining the distiller energetics.

The distillation process needs sufficient heat energy to vaporize the bioethanol produced. The designed system requires; high energy inputs to take care of heat losses and not too high to exceed ethanol heat of vaporization, and proper heat control measures to minimize heat loss from the boiler to the condenser. The following were considered in the design:

1. Thermal and physical properties of ethanol; e.g. specific heat, latent heat, thermal conductivity etc.
2. Thermal and physical properties of feed and its constituents.
3. Quantity of feed and bioethanol content to be distilled.
4. Heat energy requirement
5. Fuel type and the required quantity.
6. Properties of fuel and conditions for complete combustion.

These parameters were used in the sizing and material selection of the different components of the distilling unit. In coming up with the desired design, charcoal was selected as the fuel. The basic principles of gasification and combustion of charcoal, economics of manufacturing and operating the unit were utilized. Other considerations included ease of loading fuel into and removing ash out of the combustion chamber; structural stability, air flow and channeling. The construction technique must be known to the local farmers or craftsmen and materials must be locally and easily available. The boiler should be batch unit and can be operated by one person.

3.2.11 Distiller Calculations

The distillation unit is a fixed setup, of 20 L feed loading capacity operated with charcoal. It consists of a combustion unit, boiler unit, condenser unit and the condensate collection point. The condenser is inclined to the boiler unit at angle 45^0 to ensure slow vapor velocity and achieve complete condensation. Operation period of T_d - 60 minutes and 75 % distiller caloric efficiency were adopted. The thermal and engineering properties of the feed, heat source and distillate were established from various sources as follows: the specific heat capacity of ethanol is 2.47 kJ/kgK at density of 794 kg/m^3, the latent heat of vaporization is 855 kJ/kg and the boiling temperature is 78.5 ^{0}C (Bromberg et. al., 2006; Thermal fluidpedia atom feed, 2016).

Properties of charcoal depend on its wood specie. Charcoal sold in Owerri market (ekenuwa market) is a mixture from different wood species of which Acacia Congo (Ugba wood) though expensive is always among being common in Imo State. Among Acacia species, Acacia Congo has the highest heating value followed by other wood species e.g. Obeche, Oak, Alfara, Mahogany and Iroko. Since these are reduced in the mixture, the heating value of the Charcoal obtained from the Owerri market is often below the individual heating value of any of the mentioned wood species. Thus, for this research the heating value of the obtained Charcoal is classified within the range for that of Acacia species residue given by Tarig and Osman (2012) as 17,386 – 19,309 kJ/kg with density range of 226.3 – 728 kg/m^3. ET (2016) recorded stoichiometric air of 8.4m^3 air per kg charcoal while 9.98 kg/kg was given by (Baldwin 1987). Ojolo et. al., (2012) and Reed (1981) gave its equivalence ratio 'e' of 0.25 considering its low carbon content compared to wood, specific gasification rate (SGR) ranges from 78 – 86 kg/m^2-h (Ojolo et. al., 2012). In the design, the following were considered for charcoal: 19,309 kJ/kg HVF, 80 kg/m^2-h SGR, 230 kg/m^3 density and 10 kg/kg SA.

Based on the preliminary experiment, 200 g ground sample hydrolysed with 1.2 % H_2SO_4, at 160 ^{0}C for 30 minutes which resulted to 1.6 L of feed fermentate, made the highest sugar conversion yielding 51.22 g bioethanol in 72 h. Hence, this sample was used to carry out the main experiment in the production rig. Prevailing ambient temperature (T_{amb}) was simulated to be 30 ^{0}C while other parameters were calculated below.

1. Destiller Feed Properties

From preliminary experiment, 1 L feed yields 32 g bioethanol. Thus, design feed batch (20 L) will contain 640.3 g bioethanol and will be generated from 2500 g ground feedstock. Total mole

of feed and liquid mole fraction of its components was calculated. Vapor pressure of the components was calculated with Antoine Constants as given in Equation 3.2 while Equation 3.3 gives their vapor mole fraction (Eastop and McConkey, 1993).

$$Log_{10} P_{(mmHg\ )} = A - \frac{B}{C + T} \tag{3.2}$$

$$Vapor\ mole\ fraction = \frac{(liquid\ mol\ fraction)(vapor\ pressure)}{(atm\ pressure)} \tag{3.3}$$

Where A, B, C are constants corresponding to temperature and adopted from Appendix A4.
Feed bubble point was calculated iteratively at atmospheric pressure to be 99.6 ^{0}C. The bubble point of the binary feed is the temperature (at a given pressure) at which the first bubble of vapor is formed when heated i.e. the point at which the first drop of a liquid mixture begins to vaporize (Kister 1992, Perry 1997). The latent and specific heat of the feed is calculated at its bubble point with Equation 3.4 and 3.5 respectively (Jones and Dugan1998).

$$L_{feed} = (L_{eth}.x_{eth}) + (L_w x_w) \tag{3.4}$$

$$C_{feed} = (C_{eth}.x_{eth}) + (C_w x_w) \tag{3.5}$$

Where, x, L and C are liquid mole fraction, latent and specific heat at 99.6 ^{0}C respectively. L and C of water and ethanol were determined from Appendix A4.

***2.* Energy / Fuel**

(a) The heat energy Q_1, required to raise the temperature of the feed from initial temperature to its bubble point; heat energy Q_2, needed to change ethanol to vapor at feed bubble point; Energy needed for distillation Q_n and furnace heat energy input Q_f were calculated using Equation 2.22, 2.23, 2.25 and 2.29 respectively. Water and ethanol thermal physical properties are given in Appendix A4.

(b) The quantity of charcoal required M_f, charcoal consumption rate *FCR* were calculated using Equation 2.32 and 2.33 respectively.

3. Boiler Unit

Boiler is incorporated with a thermometer and pressure gauge for temperature and pressure reading. The boiler tank is the feed holding space where pressure is built in response to increasing temperature due to heat supply from the reactor.

(a) The boiler shell is an alloyed steel cylindrical vessel of 20 L feed load batch capacity and oriented vertically. The boiler forms a continuous column with the reactor, thus have same shape and diameter.

(b) Boiler volume V_b is double of the feed volume, i.e.

$$V_b = 2 \text{ x } 20 \text{ L} = 40\text{L} = 0.04 \text{ m}^3$$

The boiler was never loaded full; ¼ to 1/2 of boiler volume clearance is recommended above the surface of the feed to accommodate generated vapor (Bolling & Suarez 2001).

(c) Boiler height H_b is determined from Equations 3.6.

$$H_b = \frac{V_b}{2\pi r^2} \qquad (3.6)$$

Where, 'r' is the boiler radius, and πr^2 is the heating surface area of the boiler. The height of the boiler is moderate for quick even heat distribution in the entire content.

4. Furnace or Reactor

The reactor consists of the combustion chamber and ash chamber. Complete combustion is considered in the reactor design.

(a) Diameter, Height, volume and CSA of the combustion chamber were calculated using Equation 2.41, 2.43, 2.45 and 2.47 respectively. To ensure complete combustion, air cavity of 5.69 cm diameter is introduced to the combustion chamber which increases its calculated diameter with 5.69. Also 12 cm is added to the calculated height, for feeding charcoal into the reactor.

(b) Combustion chamber has a false floor made of mesh (grate) 0.25in diameter air holes.

(c) Ash collection chamber of 32 cm height is incorporated to the combustion chamber, and carries the fan casing.

(d) The ash chamber has 18 cm clearance from the production rig floor. Thus, the working height of the column is 150 cm. The reactor was not insulated as a means of controlling the temperature, avoiding burning and explosion as charcoal mixture can't be ascertained clearly.

Flue gas produced from the reactor is released to the atmosphere through a chimney at the reactor top base.

5. Air

(a) Airflow rate, *AFR* in the furnance was calculated using Equation 2.36. Properties of air are obtained from Appendix B1.

(b) Superficial velocity *Vs* in fuel bed was calculated using Equation 2.49.

(c) Specific pressure draft of charcoal Δp was derived from expression for total pressure draft given in Equation 2.50.

Considering the work of Bello et. al., (2010, 2015), BBRG (2008), Joseph and Oliver (2016), Wusana et. al., (2014), Klavina et. al., (2014); the pressure drop of charcoal >6.7 mm particle size is within the range of 30 – 36 Pa for AFR of 0.103 – 115 m/s having a specific air resistance of the range 83 – 102.4 Pa/m. A total pressure drop of 30 Pa was considered for this research design.

(d) Fan power appropriate for the furnace was calculated using Equation 2.62.

Natural convection of air instead of a blower, for complete combustion was utilized to reduce cost. Hence, in order to meet the furnace requirement i.e supplying the air flow rate while overcoming fuel pressure drop; it is constructed with a perforated column (air cavity) attached to its perforated false floor, fan chamber is rather vented and aligned with natural air current in the production rig. The perforated column and false floor also helps to remove ash.

6. Condenser

In order to extract a higher proportion of heat from the hot fluid, the condenser is designed for counter current fluid flow. It is related to many factors such as coolant flow rate and the pipe characteristics, etc. (Yuelei et. al 2012). The condenser is cylindrical and inclined at angle 45^0 to the boiler column at 46cm boiler height.

(a) Condenser Tubing: The distillation tube is ½" Nominal 'D' copper tube with 0.02005 m OD, 0.01905 m ID and negligible thickness. It has a CSA of $2.8506 \times 10^{-4}\ m^2$.

(i) Velocity of bioethanol vapor in the tube V_t and its Reynold's number at the tube inlet were obtained from Equation 2.70 and 2.71 respectively and found to be laminar with low velocity.

(ii) Condenseation heat transfer coefficient was calculated with Equation 2.75.

(iii) The log mean temperature difference for the counter current flow HE is calculated with Equation 2.80. Coolant inlet temperature is 25 ^{0}C and is required to flow out at 40 ^{0}C.

(b) Condenser Shell: The condenser shell is cylindrical mild steel material of 15 cm diameter, 3 mm thickness and CSA of 0.01482 m^2. The difference of shell internal diameter and tube outside diameter gives the hydraulic or annular diameter of the shell (i.e. $ID_{shell} - OD_{tube}$).

(i) Quantity of water coolant was obtained from Equation 2.67. Coolant is to exit at 40 ^{0}C. Drum as a reservoir was used to hold coolant and is connected to the shell with hoses.

(ii) Velocity of water in the shell V_s and its Reynold's number are obtained from Equations 2.70 and 2.71 respectively and found to be laminar with low velocity. A centrifugal Pump of 0.5 HP was used to circulate coolant. Rate of water flow into shell jacket is slower than the flow rate of ethanol vapor in the delivery tube for effective distillation.

(iii) Shell-side heat transfer coefficient was calculated with Equation 2.77.

Summary of calculated parameters is given in Table 3.1 – 3.5.

Table 3.1: Feed Parameters at Initial Condition

Parameter	Quantity	unit	Equation
Volume of feed at full load	20	L	-
WPB per batch	2500	g	Preliminary
Feed initial temperature	30	^{0}C	Thermometer
Feed bubble point	99.6	^{0}C	3.2 & 3.3
Mole fraction of bioethanol in liquid 'x' at 30 ^{0}C	0.013	Mol/mol	-
Mole fraction of bioethanol vapor in 'y' at 99.74 ^{0}C	0.987	Mol/mol	3.3
Latent heat of feed L_f	2187.28	kJ/kg	3.4
Specific heat capacity of feed C_f	4.1808	kJ/kg.K	3.5
Specific heat capacity of ethanol C_{eth}	2.485	kJ/kg.K	Appendix
Specific heat capacity of water C_{water}	4.1485	kJ/kg.K	Appendix
Latent heat of ethanol L_{eth}	927.66	kJ/kg	Appendix
Latent heat of water L_{water}	2203.87	kJ/kg	Appendix
Molar solution of ethanol	58.68	ml	Literature

Table 3.2: Calculated Energy Parameters

Parameter	Quantity	Unit	Equation
Heat energy required to bubble feed Q_1	5768.64	kJ	2.20
Heat energy needed to vaporize bioethanol, Q_2	24159.13	kJ	2.21
Operation time	60	min	2.37
Design efficiency	75	%	-
Required heat energy for distillation Q_n	6.71	kW	2.23
Furnace heat input, Q_f	32212	kJ/h	2.27
Power rating of furnace P_f	8.95	kW	2.29
Total furnace heat input, $Q_{tf.}$ (5% loss insulator	7.16	kW	
charcoal HFV	19309	kJ/kg	Literature
Charcoal SGR	80	$Kg/h.m^2$	Literature
Charcoal Density	230	kg/m^3	Literature
Quantity of charcoal required	1.67	kg	2.30
Fuel consumption rate FCR	4.64×10^{-4}	kg/s	2.31

Table 3.3: Calculated Boiler Unit Parameters

Parameter	Quantity	Unit	Equation
Reactor Diameter, D_r	16.31	cm	2.39
Reactor air cavity Diameter	5.69	cm	-
Reactor height, H	35	cm	2.41
Fuel feeding space height	12	cm	-
Reactor total volume, V_r	0.02	m^3	2.43
Reactor total surface area	4217	cm^2	2.45
Boiler Diameter	22	cm	Same as reactor
Boiler Volume, V_b	40	L	3.6
Boiler Height, H_B	53	cm	3.7
Heat surface area A_{bs}	380.133	cm^2	πr^2
Ash chamber height, H_A	32	cm	-
Ash chamber Diameter	22	cm	Same in boiler
Reactor airflow rate, AFR	8	cfm	2.34
Superficial air velocity in reactor, V_s	14	cfm/ft^2	2.47
Total pressure draft of charcoal p_d	30	Pa	2.48
Reactor fan power	1.3	HP	2.60
Mass flow rate of hot air, $\dot{m}$	0.102	kg/s	2.36

Table 3.4: Calculated Condenser Fluids Properties

Parameter	Quantity		Unit
	Bioethanol	coolant	
bulk temperature		32.5	^{o}C
Film temperature	62.3		^{o}C
Inlet density	3.3704	990.61	kg/m^3
Inlet viscosity	1.0628×10^{-5}	6042.25×10^{-7}	kg/m.s
Film density	859		kg/m^3
Film viscosity	0.568875×10^{-3}		kg/m.s
Film specific heat	2.81		kJ/kg.K
Film thermal conductivity	0.17061		W/m.K
Density at bulk temperature			kg/m^3
Viscosity at bulk temperature			kg/m.s
specific heat at bulk temperature		4.183	kJ/kg.K

Table 3.5: Calculated Condenser Parameters

Parameter	Quantity	Unit	Equation
Condenser type	Counter current	-	-
Tube / Shell construction material	Cu / mild steel	-	-
Tube / Shell internal diameter	0.0191 / 0.15	m	
Annular internal diameter	0.13	m	$ID_{shell} - OD_{tube}$
Tube-side fluid	Bioethanol	-	-
Shell-side fluid	water	-	-
Tube inlet Temperature	99.6	^{0}C	iterative
Shell inlet / outlet Temperature	25 / 40	^{0}C	chosen
Mass flow rate of ethanol vapor, $\dot{m}_E$	0.64	kg/h	2.66
Volumetric flow rate of ethanol vapor, $\dot{V}_E$	5.28×10^{-5}	m^3/s	2.67
Velocity of ethanol vapor, V_E	0.185224	m/s	2.68
Reynold's number of ethanol vapor,	1118.499	-	2.69
Tube-side heat transfer coefficient, h_{cond}	847.67	W/m^2K	2.73
LMTD	67	^{0}C	2.78
Mass of coolant	10.264	kg	2.65
Mass flow rate of coolant, $\dot{m}_C$	0.00285	kg/s	2.66
Volumetric flow rate of coolant, $\dot{V}_C$	2.877×10^{-6}	m^3/s	2.67
Velocity of coolant, V_C	2.1632×10^{-4}	m/s	2.68
Reynold's number of coolant	46	-	2.69
Shell-side heat transfer coefficient, h_{shell}	51.89	W/m^2K	2.75
Total fouling factor	0.0002	-	2.77
Overall heat transfer coefficient, U	48.42	W/m^2K	2.76
Total heat transfer surface area	0.0551	m^2	2.80
Length of condenser tube, L	88	cm	2.81
Thermal resistance of HE	0.4	W/K	2.77

Plate 20 presents the Pictorial View of the Distiller while drawings of its different views are presented in Appendix K.

Plate 20: Pictorial View of the Distiller

3.2.12 Material Selection for Dryer Components

Material selection was based on strength/fatigue resistance, wear resistance, corrosion resistance, cost, workability and appearance. Appropriate selection of the best materials was ensured to enable the best quality of the distiller and bioethanol quality, and to meet design standards. Some properties of metal materials are given in Appendix B2. Considering the entire desired properties alloy steel was used for the coolant jacket and boiler unit. The shells have considerable thickness i.e. corrosion allowance.

Corrosion and Wear Resistance: Corrosion generally dictates the choice of material of construction, rather than exchanged design. The shells are normally difficult to clean and are always in contact with fluid; therefore they are designed with a high corrosion resistance material of which mild steel is the best. These materials contain sufficient amount of chromium. Copper serves well for the tube as it has optimal resistance to acids (Kriss 2004). A plastic hose is used for coolant input and output lines, but prevented to come in contact with the vapor or product take off path. A good rule of thumb in distilling is that NO plastics (or other synthetics) should have ANY contact with high proof ethanol or ethanol vapor (Yuelei et al 2012). Plastic is basically fine at the low alcohol end (e.g. broth), but should be avoided where it will encounter strong alcohol (such as anywhere within the boiler vapor), or to store high proof bioethanol product. So, plastic containers were confidently used for hydrolysis and fermentation process, because of their advantages with respect to high corrosion resistance, cleaning, maintenance, and sealing (Kriss 2004) while glass is preferable for the collection and storage.

Thermal Conductivity: Heat transfer occurs on the tube surface; such surface needs to have a high heat tolerance. This implies that the higher the conductivity of the tube material the higher the efficiency of the HE. As a result, copper, which has high thermal conductivity and takes a long time to corrode, becomes the best material for the tubes (Kriss 2004).

Strength / Fatigue Resistance: To ensure strength resistance, mild steel with the appropriate carbon content is required. High carbons alloy steel was chosen, which has between 0.3 - 0.8% carbons, possesses high fatigue and toughness as well as enough hardness, strength and wears resistance. It is also less susceptible to carbon transfer i.e. less degradation. Degradation, as used here, refers to the loss of desirable physical properties such as strength without actual loss of material. This can be caused by corrosion embrittlement, mass transfer of alloy constituents, and fatigue, all affecting the metallurgical structure of components. Thickness of the alloy sheet, copper and other structures was chosen for safety and durability (Baqui et al 1997).

Cost: To achieve the economic goal of low cost in the material selection, the boiler unit and condenser shell were made of mild steel sheet 8mm. Although, cost of copper is high, it will be cheaper in the long run because being corrosion resistant; cost of its maintenance is low. Though

copper or high grade steel (e.g. stainless steel) is best, alloyed steel was used for boiler to save cost. Using this for the boiler will not impact the end product but the boiler may corrode with time.

Although thermal engineering and economics are important considerations in the designing of this type of equipment, the choice of type, dimensions and conditions of operations is primarily determined by the process requirement. Thus, optimization is much more different because the quality of the product has to be considered in the evaluation of the process. Copper affects the quality of distillates positively; it has inert property which can limit reaction with vaporized bioethanol. Copper material for distillate vapor produce cleaner distillates compared to such as is made of high-grade steel or glass since copper forms non-volatile products with volatile sulfur combinations arising during the fermentation which then remain in the slops (Kriss 2004). A well-known example of such a quality-reducing sulfur combination is hydrogen sulfide. The distiller was fabricated according to the design specifications and installed at the production rig located at Mechanical Engineering Department of Federal University of Technology Owerri, Imo state, Nigeria. The fabrication steps involved selection and/or cutting of metal sheets into desired sizes, and arc welding joints where necessary to ensure toughness and strength. Parts were welded perfectly with firm joints to avoid vapor loss. Pipe settings were carried out with utmost carefulness. HE was subjected to hydrostatic pressure test. Hand pump was used to fill in the condenser shell with water and by pressurizing to set pressure of the exchanger, say 4 or 6 bars. The pressure was observed for 20 – 30 minutes to ascertain if there is leakage on the tube. Once there is no leakage, the exchanger is boxed-up and made ready for use. Any leakage was then solved. Dye penetration test was done on welded edges. No leakages were observed confirming that there were no holes and cracks.

3.2.13 Insulation

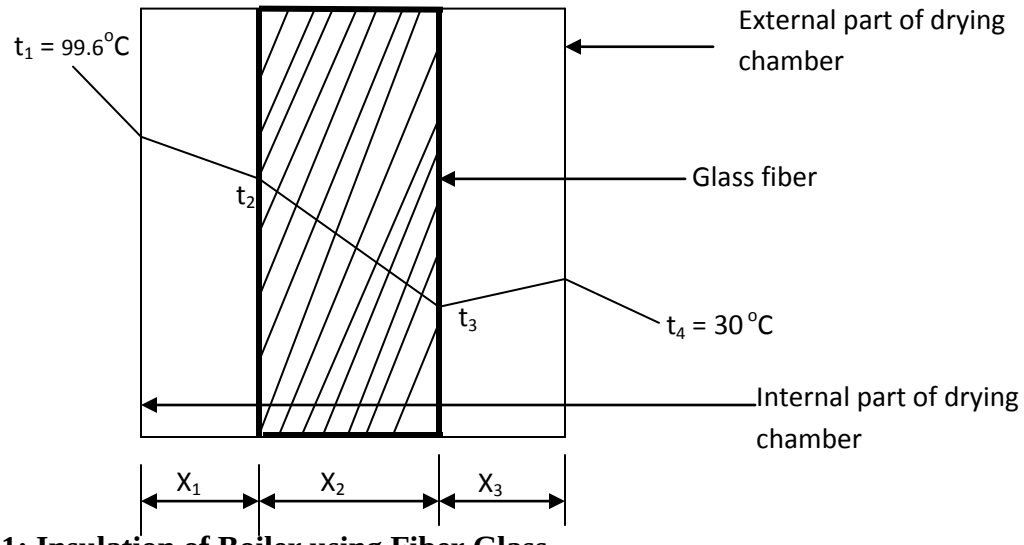

Figure 3.1: Insulation of Boiler using Fiber Glass

Different materials were available for insulation but considering the expected temperature range, availability and cost of insulating material, fiber glass was chosen for installation (Figure 3.1). Considering 5 % loss of the quantity of heat produced per sec, through the walls of the reactor; i.e. 5 % of 8.95 kW which is 447.5 W. Thickness of the fiber glass was calculated from the quantity of heat lost per unit area (q), using Equation (3.7) due to Adzimah & Seckley (2009).

$$\text{Quantity of heat lost per unit area (q)} = \left.\begin{aligned} &\lambda_1/X_1(t_1 - t_2) \\ &= \lambda_2/X_2(t_2 - t_3) \\ &= \lambda_3/X_3(t_3 - t_4) \\ &= U(t_1 - t_4) \end{aligned}\right\} \quad (3.7)$$

Where:

λ_1 and λ_3 are conductivity coefficient of mild steel = 46 W/m^{0}C

λ_2 is conductivity coefficient of fiber glass = 0.045 W/m^{0}C

X_1, X_3 and X_2 are the respective thicknesses of mild steel and fiber glass.

$X_1 = X_3 =$ 0.8 mm i. e. 0.0008 m

3.2.14 Principle of Operation

The fabricated distiller follows the principle of producing heat in complete combustion with stoichiometric air requirement of 10 kg/kg of charcoal just enough to convert the fuel to ash. The fuel is stationary, fed at and ignited from the top of the reactor using Kerosene as ignition source.

Air intake is at the bottom while gas leaves at the top. Sufficient air necessary to burn the fuel was supplied by natural air current. The fuel reached stable ignition which improved to complete combustion. The reactor is the inverted down draft (IDD) or Top Lit Updraft (T-LUD) type (Appendix B3) fired with charcoal of moderate lump. Fuel combustion zone moved down the reactor in a batch mode as a result of the conversion of the biomass and the removal of ashes. The more air was introduced to the fuel from the bottom, the faster was the downward movement. As the combustion zone moved downward, burnt fuel is left inside the reactor in the form of ash. Heat was generated upwards, as illustrated in Figure 3.2 and was directly transferred to the boiler by conduction and radiation where it acts as the vaporization heat once the temperature reaches the boiling point of bioethanol.

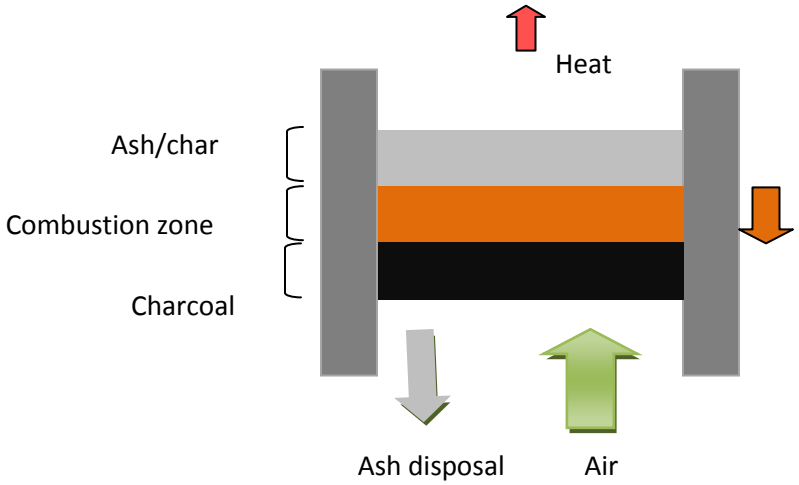

Figure 3.2: Inverted Down Draft Type Combustion

At that point bioethanol vaporized above the broth and flowed via the delivery tube across the entire condenser length into the collection container. It condensed within the length of the condenser as it exchanged heat with the circulating coolant, and was thus collected as a pure liquid fuel. This type of direct heated device is often referred to as an alambic style (Kriss 2004). The direct heating allows a fast control of the distillation process. A disadvantage for distillation equipment with direct heating is that thick (i.e. viscous) mashes tend to burn due to the very high surface temperature. Distillates made from such mashes often have a burnt-bitter taste (Furfural formation) which is hardly removable (Kriss 2004). It is advised to be cautious with older distillation stills because they may burn out (i.e. burn through) such that explosions may occur. Thus, direct heated distillation devices should only be used for distillation conversions of raw

distillates. An additional feature of this system is that the high temperature boiler surface actually catalyses a series of chemical reactions that contribute to the distillate qualities (Kriss 2004). Considering all these, precautions were taken to avoid the difficulty of burning of mixture by neglecting the insulation. Updraft reactor was chosen because of its advantages which include (FAO 1985); (1) ease of operation (2) high charcoal burnout (3) high equipment efficiency (4) possibility of operating with fuel varieties (5) high heat transfer. Its main disadvantage is channeling difficulty which can lead to oxygen breakthrough and consequence explosion; this was checked by appropriate air current and channel column.

The condenser fluid flow is counter current. The working general principle is to allow two fluids with different temperatures into the HE, each through a different inlet. The higher temperature fluid (bioethanol vapor) otherwise called the heating fluid flows through the tubes while the lower temperature fluid (coolant: water) flows via the next inlet across the condenser shell. As these fluids flow through the HE, heat is transferred from the heating fluid in the parallel pipes to the cooling fluid in the shell through the pipe walls. There is temperatures change as they flow, and consequently the temperature difference is continuously changing.

3.2.15 Experimentation

The distiller after its design and fabrication was used to distill bioethanol from WPB fermentate. Four different experiments were carried out: (1) monitored feed production (2) verification of distiller performance (3) bioethanol / blends characterization to determine their fuel properties, and (4) engine performance investigation on the fuel samples.

(1) Monitored Feed Production

The feed production step involves physical pretreatment, chemical hydrolysis, and fermentation. A preliminary test was carried out at different hydrolysis temperatures (160 ^{0}C, 180 ^{0}C, 200 ^{0}C), acid concentrations (0.8 %, 1.0 %, 1.2 %) and residential times (15 min, 30 min, 45 min, 60 min), and at different fermentation period (1 – 5 days) at room temperature using S.cerevisea cultured from palm wine. In the preliminary test, 200 g ground WPB was subjected to the above conditions to determine the optimum preparation condition to produce the distiller feed. The optimum preparation condition was based on high sugar yield from hydrolysis and consequent high bioethanol yield from fermentation. Based on the preliminary test result, 2.5 kg of ground WPB was prepared to obtain 20 L batch boiler feed as follows:

Pretreatment: shredded WPB was oven dried and ground to obtain 2.5 kg WPB powder of 850 microns size.

Hydrolysis: the WPB powder was subjected to optimum hydrolysis condition of 160 ^{o}C for 30 minutes using 1.2 % H_2SO_4 acid concentration. The obtained sieved hydrolysate was cooled to room temperature and neutralized to 4.8pH with 2M NAOH.

Fermentation: the neutralized hydrolysate was fermenetated with 1250 ml S.cerevisea cultured from palm wine, at room temperature for 3 days. The obtained broth was sieved to separate the feed from the slurry.

(2) Verification of Distiller Performance

The prepared feed was distilled in 20 L batches using the fabricated distiller. Feed at about 27 - 29 ^{0}C was loaded into the boiler with the reactor charged to full capacity of 1.67 kg of locally sourced charcoal. Before turning the water flow on, the hoses were checked to ensure that connections were carefully secured and will not pop off. The water flow was adjusted so there was a slow, constant flow of cold water to the condenser. The coolant initial temperature and flow rate were noted. The fuel was fired. Ambient air at average temperature of 30 ^{0}C and 40 % relative humidity was naturally aspirated into the reactor supplying air, ensuring complete combustion and distribution of hot air while the temperature of the mixture gradually increases. Heat was transferred from the reactor to the boiler content mainly by direct conduction. The separation operation continued till the last drop of distillate. The extent of fuel consumption was noted, changes in temperature and pressure were noted from reading of a thermometer and pressure gauge fixed to the boiler column. A container was used to collect condensed drops of bioethanol and the total volume of distillate per time was read on a graduated scale. Parameters such as time taken to heat the feed to the bioethanol bubble point, volume of distillate per time at 5 min interval, amount of fuel used, distillate temperature, were recorded for performance analysis. Actual boiler calorific efficiency was determined using Equation 3.8 (Milind 2009; Rajviv *et al*., 1980).

$$e_{ff\ actual} = (Q_n / M_{act.char}\ x\ HVF)\ x\ 100 \qquad (3.8)$$

According to Thanit et al (2010) and Somchart et al (2010):

$$e_{ff\ actual} = (H_s / H_a)\ x\ 100 \qquad (3.9)$$

And

$$H_s = \Delta H \; x \; (M_a / V_a) \qquad (3.10)$$

$$H_a = \left(M_f \; x \; HVF\right)/3600 \qquad (3.11)$$

H_s and H_a are the supplied and available heat, (kJ/kg) respectively. ΔH is the enthalpy change between ambient and exit air, (kJ/kg). M_a is the airflow rate m^3/s. V_a is the specific volume of exit air, m^3/kg. M_f is the charcoal feeding rate, (kg/h) while HVF is the heating value of fuel (kJ/kg). The distillate an azeotrope of water and bioethanol was dried in a rotavapour to improve the bioethanol purity. However, in Brazil, hydrated bioethanol has been used as a fuel with good results (Kojima & Johnson 2005).

3.2.16 Characterisation of Sample Fuels

The extracted bioethanol was then characterized for other (1) elemental characteristics and (2) fuel properties. Different fuel blends were formulated using the produced bioethanol and petrol by varying their proportion in the mixture. These blends were also characterized to determine their conformity with the ASTM D 4814 standard specification for automotive SI engine fuel.

(1) Elemental Analysis of Produced Sample Fuel

Elemental analysis of the produced bioethanol fuel was carried out following the ASTM standard test procedures in order to determine the produced bioethanol's conformity with the ASTM D4806 standard specification for denatured fuel biothanol blendable with petrol for use as automotive SI engine fuel. The elemental properties analyzed include ash content, water content, acidity and pH, purity and the measured raw data are reported in Table 4.4.

(i) Determination of Bioethanol Content

The bioethanol content otherwise purity of the fuel was determined according to ASTM D 5501. A representative aliquot of the fuel bioethanol sample is introduced into a gas chromatograph equipped with a polydimethylsiloxane bonded phase capillary column. Helium carrier gas transports the vaporized aliquot through the column where the components are separated by the chromatographic process. Components are sensed by a flame ionization detector as they elute from the column. The detector signal is processed by an electronic data acquisition system. The bioethanol component is identified by comparing its retention time to the ones identified by analyzing standards under identical conditions. The concentrations of all components are determined in mass percent area by normalization of the peak areas.

(ii) Determination of pH

The pH of the fuel was determined at room temperature using a pH meter according to ASTM D 6423. The pH meter was turned on and allowed to warm up. The pH meter was calibrated in a water-base pH7 buffer and water-base pH4 buffer. After each, it was rinsed with distilled water and blotted to remove excess water. The electrode returned to the pH7.00 buffer. A 100 mL beaker was rinsed with the sampled fuel. 50 mL of fuel was placed in the beaker and stirred. The glass electrode was inserted into the sample and pH was measured at 30 s. The electrode was then withdrawn, rinsed and rehydrated by soaking for at least 20 s in the water-based pH 7 buffers until the reading falls below 7.05. It was then recalibrated to pH7 to prepare it for the next reading. Average of triplicate readings was taken. Reslts are reported in Table 4.4.

(iii) Determination of Water Content

Water content of the fuel was determined according to ASTM D95. The produced bioethanol was subjected to water content distillation using a Dean and Star distillation unit as seen in Plate 3.21. Here 100 ml of the bioethanol was mixed with 100 ml of aromatic mixture (80 % toluene and 20 % xylene) and subjected to heat for 2 h from boiling point. The trap solution was observed for separation and changes in the presence of methyl red dye. Methyl red dye was used because it dissolves in PMS but dissolves not in water. Reslts are reported in Table 4.4.

Plate 3.21: Water Content Distillation

(iv) Determination of Ash Content

The ash content of the fuel was determined according to ASTM D482. Crucible made of porcelain, of 120 mL capacity was heated at 700 ^{0}C for a minimum of 10 min. It was cooled to room temperature in a suitable container, and weighed as W_1. The sample of 5 g quantity (W_2) was poured into the crucible, ignited and allowed to burn until only ash and carbon remains. The carbonaceous residue is reduced to ash by heating in a muffle furnace at 700 ^{0}C, cooled and weighed W_3. The average percentage ash was calculated with Equation 3.1 and reported in Table 4.4.

(v) Determination of Acidity

The acidity of the fuel was determined according to ASTM D974. 10 ml quantity of the fuel was weighed into a 500 ml Erlenmeyer flask. 100 mL of the titration solvent and 0.5 mL of the indicator solution were added to it. The indicator was premixed with the titration solvent before adding to the fuel. The mixture was swirled without stoppering, until the sample was entirely dissolved by the solvent. It then assumes a yellow-orange color. Without delay, titration was carried out at room temperature (< 30 ^{0}C). This was done by adding 0.1 *M* KOH solution in increments and mix to disperse the KOH. It was shook vigorously near the end point, reducing the increment size drop wise. This continued until end point was reached, and held for a minimum of 15 s after the addition of the last increment. The acid number was calculated by comparing to that of a blank as given in Equation 3.12. Acid number of the blank was determined by performing a blank titration on 100 mL of the titration solvent and 0.5 mL of the indicator solution, adding 0.1 mL of the 0.1 *M* KOH solution. Data is reported in Table 4.4.

$$\text{Acid number, mg of KOH /g} = \frac{[(A-B)M\ x\ 56.1]}{W} \qquad (3.12)$$

Where: A = KOH solution required for titration of the sample mL, B = KOH solution required for titration of the blank, mL, M = molarity of the KOH solution, and W = sample used, g.

(2) Characterisation of the Formulated Fuel Blends

The produced sample fuel and its blend with petrol was charcterised according to ASTM standard procedures for gasoline, bioethanol, and gasoline-oxygenated fuels at NNPC Port Harcourt Refining Company Limited, Elesa-Eleme, Port Harcourt Rivers State. This is to determine its fuel properties and suitability in spark ignition engine. Certified petrol (99.9 % pure, NNPC) was used in the study; the blends E0, E10, E20, E30, E40, E50, E60 and E100

formulated in 0:100, 10:90, 20:80, 30:70, 40:60, 50:50, 60:40 and 100:0 volume percentage of bioethanol/petrol respectively were prepared and shown in Plate 3.22. Phase separation was checked at 27 ^{0}C for 24 h was not seen. Fuel properties analyzed are kinematic viscosity, flash point, density, octane number, calorific value and Vapor pressure; and the measured raw data are reported in Table 4.5.

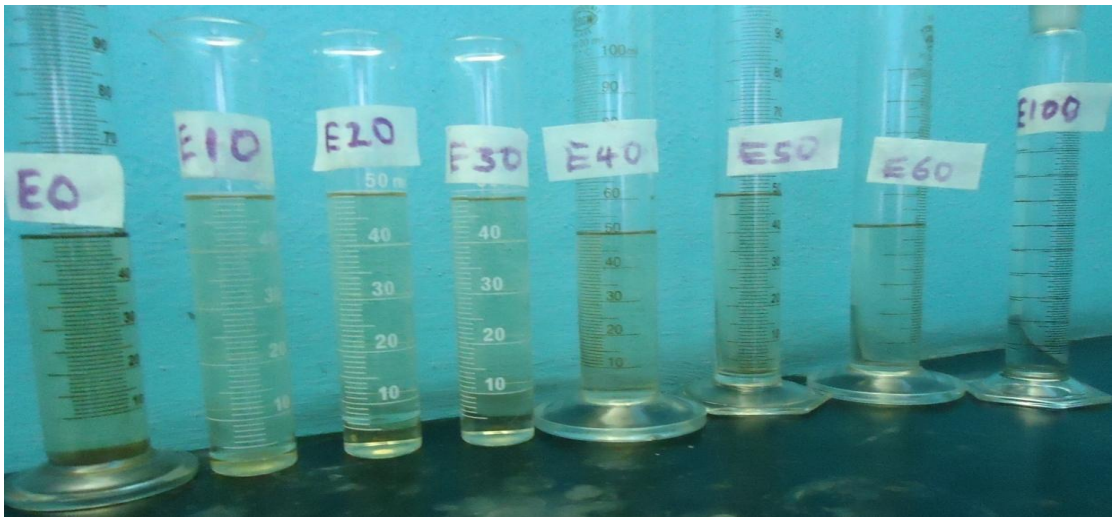

Plate 3.22: Sample Fuels

(i) Determination of Density

Density of the fuel was determined using the weight per volume method (Tangka et. al., 2011). 20 ml of the fuel was pipetted into a dried cleaned container of known mass 'a' and placed on a weigh balance to determine total mass of container and fuel 'b'. Taken the volume of the sample to be X, density of the sample is then determined with Equation 3.13 and reported in Table 4.5.

$$\text{Density} = \frac{(b-a)}{X} \qquad (3.13)$$

Where b = mass of fuel + container, a = mass of container.

(ii) Determination of Viscosity

This was carried out based on ASTM D 445 using capillary viscometers shown in Plate 3.23 at a fixed temperature of 40 ^{0}C following the method of Abdullah et. al., (2011). The viscosity was measured by determining the time taken for a fixed volume of the fuel sample (about 4 ml) to flow under gravity between two marked points. The kinematic viscosity 'V' in centipoises is

then product of the measured flow time‘t’ in seconds and the viscometer constant ‘C’ as expressed in Equation 3.15 and reported in Table 4.5.

$$V = Ct \qquad (3.15)$$

C is not affected by the temperature.

Plate 3.23: Capillary Viscometers

Plate 3.24: Pensky-Martens Closed Cup Tester

Plate 3.25: Ignition Source

(iii) Determination of Flash point

Flash point of the sample fuels was determined by ASTM D 93 method, using the Pensky-Martens closed cup tester shown in Plate 3.24. A sample of the fuel was heated in a brass test cup of specified dimensions filled to the inside mark and fuel was stirred at specified rate of about 90 – 120 rpm. An ignition source in Plate 3.25 was directed into the test cup at regular intervals with simultaneous interruption of the stirring, until a flash is detected. Once the temperature is at or above the flash point, the vapor will ignite and at much higher temperature steady flame will be observed as the produced vapor is sufficient to maintain a continuous flame (fire point) (Babgy et al., 1987). Data is reported in Table 4.5.

(vii) Determination of Vapor Pressure

Vapor pressure of the blends was obtained using ASTM D4953 with an auto vapor pressure tester shown in Plate 3.26. The experimental set up is similar to the one described by Kar et al. (2009). It involves filling chilled fuel into a metal liquid chamber connected to an air chamber that is connected to a pressure gauge at 37.8 ^{0}C. The apparatus is then immersed in water bath at 37.8 ^{0}C and is auto-shaken until constant Reid vapor Pressure is displayed and is reported in Table 4.5.

Plate 3.26: Auto Vapor Pressure Tester

Plate 3.27: Auto Ignition Point Tester

(vii) Determination of Auto Ignition Point Tester

The auto ignition point was measured according to the procedure described in ASTM E659 using the Auto Ignition Point Tester shown in Plate 3.27. Data are reported in Table 4.5.

(iv) Determination of Calorific Value

Calorific value of the fuel samples was measured using a bomb calorimeter in Plate 3.28 base on ASTM D240. A known amount of fuel was placed in a crucible. The crucible was then placed over a ring and a fine magnesium wire touching the fuel sample is stretched across the electrodes. The lid was tightly screwed and the bomb was filled with oxygen up to 25 atmosphere pressure. The initial temperature was recorded. The electrodes were then connected to a 6 V battery and the circuit was completed. As soon as the circuit was completed and the current is switched on, the fuel in the crucible burns with evolution of heat. Heat liberated by

burning of the fuel increases the temperature of water and the maximum temperature attained was recorded and are reported in Table 4.5.

Plate 3.28: Bomb Calorimeter

(vi) Determination of Octane Number

The octane rating of the fuels was measured based on ASTM D 2699 in a Comparative Fuel Research Engine (C- 48386 model) with at least 1000 ml of the sample to ensure it is within range (0.7 – 1.7) in the carburetor sight glass fuel level. The engine is of 1-stroke, 1-cylinder shown in Plate 3.29 it has four carburetors and operates on a fuel at a time. The engine consists of four carburetors, a detonation pick up, a dial indicator or micrometer, a detonator meter and a knock meter. Two carburetors are for primary fuels blend (iso-octane and n-heptane), one for sample fuel and one sample fuels that need temperature conditioning before combustion (samples of lower or higher temperature than required in the combustion chamber). Thus one of the carburetors has accessories for heating or cooling fuel to the required temperature needed for combustion. The detonation pick up is threaded to the cylinder; it has a magnetrostritive transducer (sensor) exposed to combustion chamber pressure and sends same as voltage signal proportional to the rate of pressure change, to the detonation meter. The detonation meter which is amplifier/signal conditioning equipment accepts, amplifies and then sends it to a knock meter. The knock meter, a 0 – 100 strip chart recorder displays the signal as the knock intensity. The dial indicator displays the cylinder height with respect to the piston. The octane number was determined using the bracketing procedure (ASTM 2699); here, the knock meter reading was bracketed at constant compression ratio between knock meter readings for two reference blends, and the sample rating was calculated by interpolation. Cylinder height was adjusted thereby varying the compression ratio, by a screw attached to each of the carburetor while reading was

taken at knock meter display of '50' to ensure a reliable result. This reading was then compared with the ASTM guide table for the corresponding octane number at the standard knock intensity for the specific fuel. Thus octane number is defined by comparison with the mixture of iso-octane and n-heptane that would have the same anti-knocking capacity as the fuel under test (Dahiru et. al. 2014). In other words, it is the percent of iso-octane in the iso-octane-normal heptane mixture which has the same knocking resistance with the test sample. Data is listed in Table 4.5.

Plate 3.29: Comparative Fuel Research Engine (C- 48386 model)

(vii) Determination of Volatility

100 ml of each fuel samples was distilled to observe its volatility. The distillation was performed According to ASTM D 93 in a batch atmospheric distillation apparatus HDA 620 model (Plate 3.30) at ambient pressure under conditions that are designed to provide approximately one theoretical plate fractionation. Systematic observations of temperature readings and volumes of condensate were made. The initial boiling point, IBP, end boiling point, EP and total distillate TD were determined anad listed in Table 4.5. The product fuel characteristics are compared with that from other biomass feedstocks in Table 4.6.

Plate 3.30: A**tmospheric Distillation Apparatus**

3.2.17 Engine Performance Test

Engine run test was carried out to determine the effect of the produced bioethanol blends on SI engine performance, relative to the conventional fuel 'petrol'. Standard petrol used was obtained from NNPC Port Harcourt Refining Company Limited, Elesa, Eleme, Port Harcourt Rivers State. Engine tests were carried out at (i) constant load under full, ¾ and ½ engine load, and (ii) constant engine speed of 2500 rpm, 3000 rpm and 3500 rpm conditions respectively considering 0 kg, 1 kg, 2 kg, 3 kg, 4 kg and 5 kg external load with E0, E10, E20 and E30 fuel samples. These speeds are chosen because they are within ¾ and full load speeds range under which the performance of internal combustion engine is peak.

Engine Description and Operation

A small IMEX petrol engine attached to a friction rope brake dynamometer, and rigidly fixed to engine bed by bolts and nuts was used for the engine run test. The engine dynamometer assembly is shown in Plate 3.31 while its specification is given in Table 3.7.

Plate 3.31: Single Cylinder IMEX Petrol Engine and Speed Tachometer

Table 3.6: Engine Specification

Parameter	**Basic Data**
Type/Model	IMEX/G200
Cylinder	Single cylinder, 4 stroke
Bore/Stroke	68 mm / 45 mm
Compression Ratio	8.5 : 1
Area of cylinder	$0.00363m^2$
Engine Capacity / Weight	196cc / 155.71N
Fuel Tank Capacity / Cooling System	3.6L / Air
Starter	Recoil Hand Operated
Rack Diameter	144 mm

The friction rope brake dynamometer is attached to the engine flywheel; a belt runs over the flywheel, one end connected to the spring balance and another end to the load plate. The engine is loaded by applying force on the load plate and the resulting reading of the spring balance was taken as the external load on the engine. Then each load was use to determine the corresponding torque. The frictional torque due to the rope is equal to the torque transmitted by the engine. Engine was checked for lubrication and fuel supply. Fuel tank was attached with a graduated burette. The valve at the bottom of the tank was closed when fuel consumption was measured so that fuel was consumed only from the burette. Time taken to consume "X" amount of fuel was

recorded and fuel consumption rate calculated. The engine setup has accessories for obtaining the parameters being investigated at various data points throughout the tested speed range.

The engine was started and left to warm up for 10 minutes. A constant engine load was achieved by setting the throttle to a particular position of its range while constant speed was achieved by adjusting the throttle till the tachometer reading of the engine speed (flywheel speed) was at the required constant speed. The engine was calibrated using only petrol. The various fuel samples shown in Plate 3.32 were then used to run the engine.

Plate 3.32: Fuel Samples for Engine Run

Before filling in a new load of fuel, sufficient time was allowed for the engine to consume the leftover fuel from the previous experimental run. For the stabilization of measuring parameters at each load setting and at the start of each test, time period of 20 and 5 sec was allowed respectively. The readings obtained during calibration were taken as standard values so that the readings obtained using other fuel samples were compared to these. These tests were carried out at 0 kg, 1 kg, 2 kg, 3 kg, 4 kg and 5 kg spring balance readings. The readings obtained for the engine performance are on the following parameters: load, fuel consumption, torque (T), the values of brake power output (BP), fuel consumption rate (FCR), brake specific fuel consumption (BSFC), frictional power (FP), brake thermal efficiency (BTE), mechanical efficiency (ME) and brake mean effective pressure (BMEP) were computed using torque output and the maximum engine speed read applying standard equations as explained below.

Determination of Power Outputs

a) Fuel power (Fuel-$_P$) was calculated with Equation 3.16 according to Pulkrabek (1997).

$$Fuel\ Power\ (kW) = m_f\ .\text{LCV} \qquad (3.16)$$

Where, m_f is mass of fuel in kg/s and LCV is its lower heating value.

b) Torque was calculated with Equation 2.142.

c) Brake power was calculated with Equation 2.144

Determination of Fuel Utilization

a) Fuel consumption rate (FCR) was calculated with Equation 2.150.

b) Brake specific fuel consumption (BSFC) was calculated with Equation 2.151.

Determination of Pressures in Engine

a) Brake mean effective pressure was calculated with Equation 2.145.

Determination of Engine Efficiencies

a) Brake thermal efficiency (BTE) was calculated with Equation 2.149.

CHAPTER FOUR

RESULTS AND DISCUSSION

4.1 Results

4.1.1 Raw Material Characterization Result

Table 4.1: Raw Material Properties before Hydrolysis

Chemical compositions	Percentage (wt %, dry basis)
Holocellulose	74.33
α-cellulose	57.44
Hemicellulose	16.89
Lignin	15.87
Ash	5.57

4.1.2 Glucose, Xylose and Bioethanol Standard Analysis Results

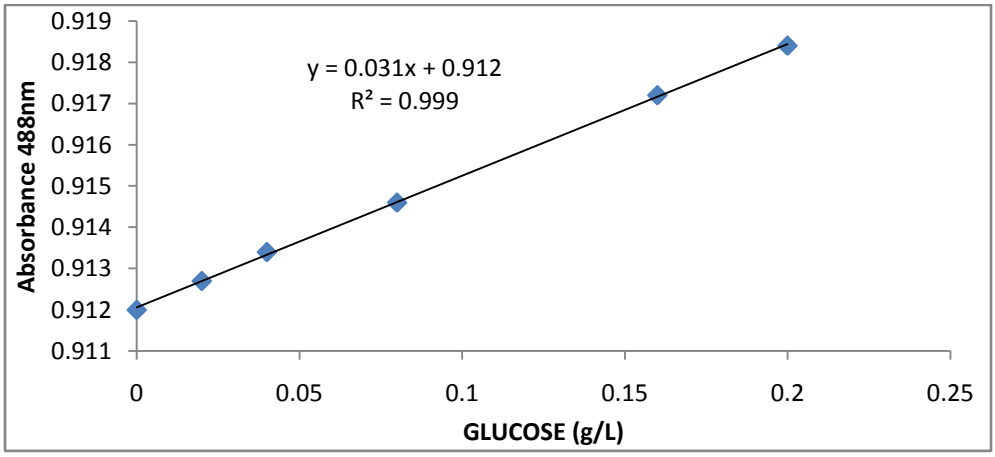

Figure 4.1: Absorbance of Glucose Standard Solution

Figure 4.1 shows that increase in glucose concentration increases absorbance at 488 nm wavelength. It provided Equation 4.1 for the calculation of glucose concentration at 488 nm.

$$glucose\ concentration\ (g/L) = \frac{(A - 0.912)}{0.031} \qquad (4.1)$$

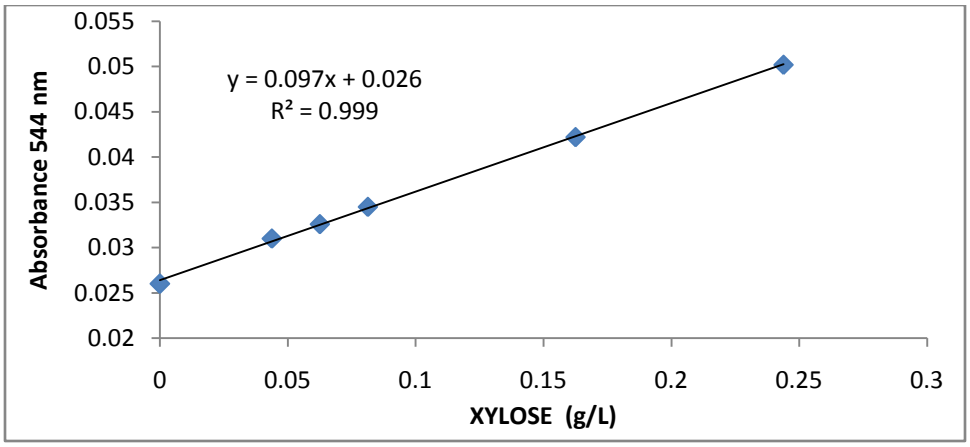

Figure 4.2: Absorbance of Xylose Standard Solution

Figure 4.2 shows that increase in xylose concentration increases absorbance at 554nm wavelength. It provided Equation 4.2 for the calculation of xylose concentration at 554 nm.

$$\text{xylose } concentration\ (g/L) = \frac{(A - 0.026)}{0.097} \qquad (4.2)$$

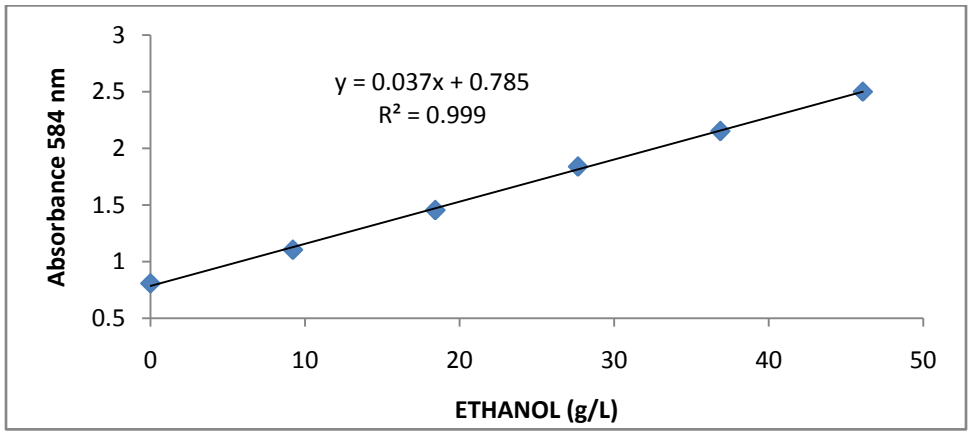

Figure 4.3: Absorbance of Ethanol Standard Solution

Figure 4.3 shows that increase in bioethanol concentration increases absorbance at 584 nm wavelength. It provided Equation 4.3 for the calculation of bioethanol concentration at 584 nm wavelength.

$$\text{bioethanol } concentration\ (g/0.05\ L) = \frac{(A - 0.785)}{0.037} \qquad (4.3)$$

Base on the condition subjected to, the samples were labeled as $An_{1\text{-}3.m1\text{-}4}$, B $An_{1\text{-}3.m1\text{-}4}$ or C $An_{1\text{-}3.m1\text{-}4}$, where A, B, C are concentration 0.8, 1.0 and 1.2 % respectively, n_{1-3} for temperature 160, 180 and 200 ^{0}C respectively, and m_{1-4} for time intervals.

4.1.3 Preliminary Hydrolysis Result

Table 4.2: Observed pH of Hydrolyzates before Neutralization

Temp. (°C)	Time (min)	Acid conc 0.8 (%, v/v)		Acid conc 1.0 (%, v/v)		Acid conc 1.2 (%, v/v)	
		Sample	pH	Sample	pH	Sample	pH
160	15	A_{11}	1.59	B_{11}	1.49	C_{11}	1.58
	30	A_{12}	1.76	B_{12}	1.54	C_{12}	1.39
	45	A_{13}	1.80	B_{13}	1.61	C_{13}	1.57
	60	A_{14}	1.85	B_{14}	1.77	C_{14}	1.69
180	15	A_{21}	1.72	B_{21}	1.27	C_{21}	1.66
	30	A_{22}	2.02	B_{22}	1.38	C_{22}	1.70
	45	A_{23}	2.16	B_{23}	1.42	C_{23}	2.05
	60	A_{24}	2.3	B_{24}	1.58	C_{24}	2.51
200	15	A_{31}	1.81	B_{31}	1.56	C_{31}	1.58
	30	A_{32}	2.2	B_{32}	1.88	C_{32}	1.60
	45	A_{33}	2.29	B_{33}	2.12	C_{33}	1.63
	60	A_{34}	3.24	B_{34}	2.48	C_{34}	2.20

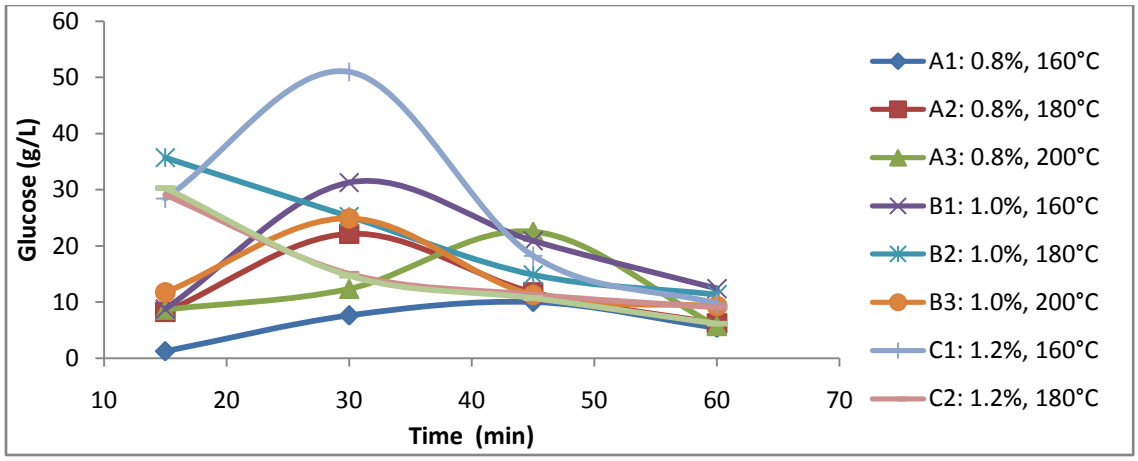

Figure 4.4: Glucose Yield from Hydrolysis

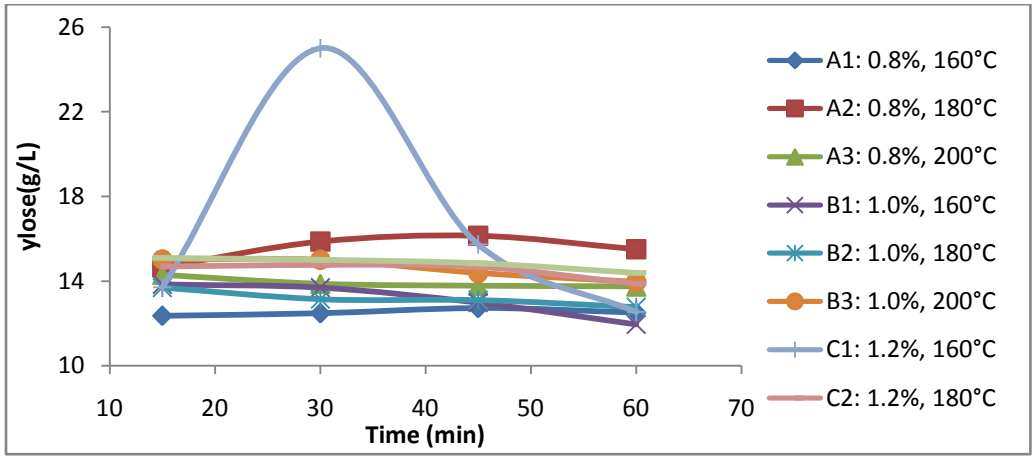

Figure 4.5: Xylose Yield from Hydrolysis

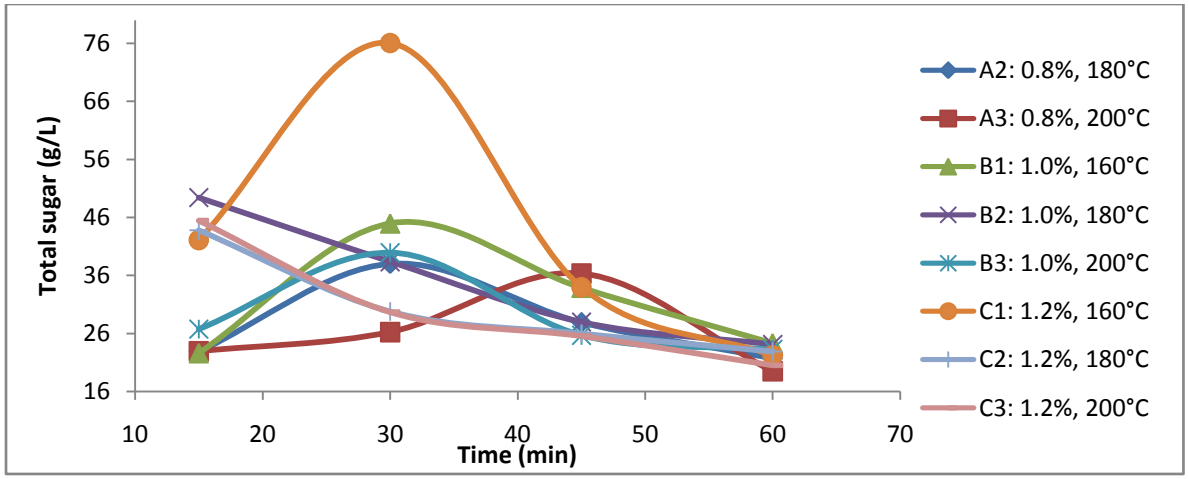

Figure 4.6: Total Sugar Yield with Time from WPB Hydrolysis

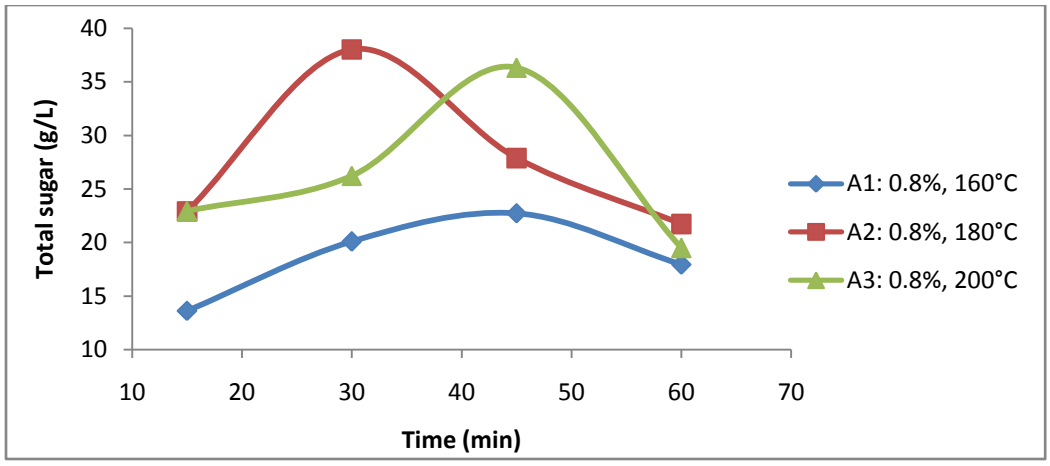

Figure 4.7: Effect of Temperature on Total Sugar Yield at 0.8 % Acid Concentration

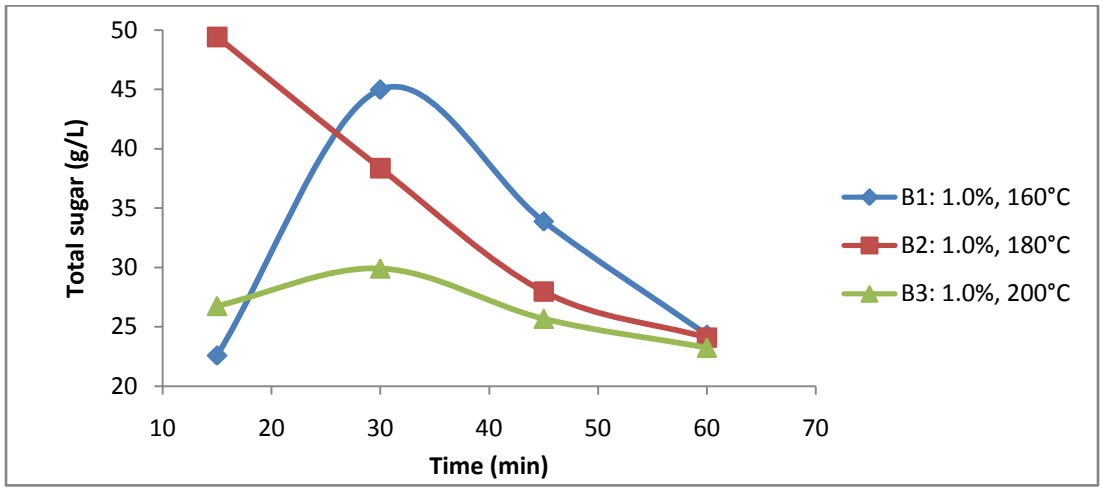

Figure 4.8: Effect of Temperature on Total Sugar Yield at 1.0 % Acid Concentration

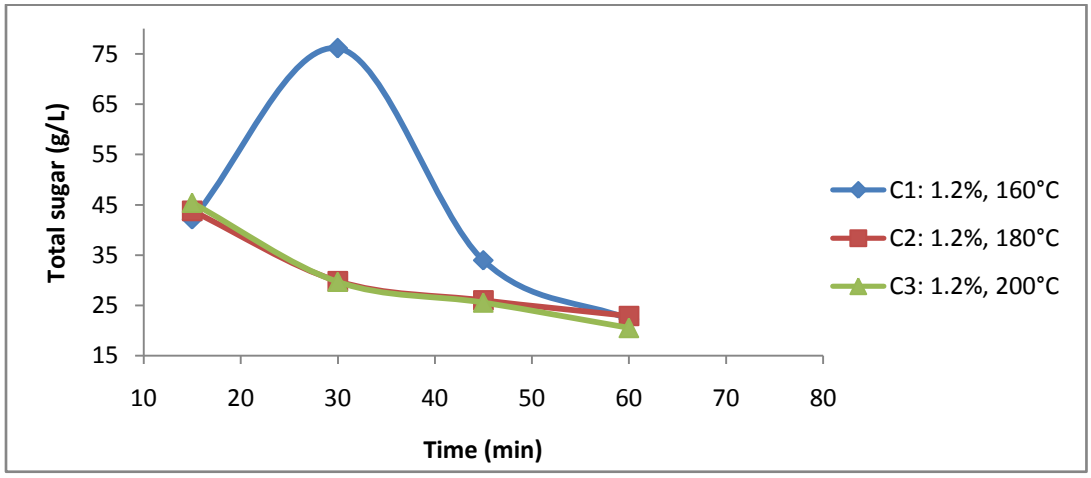

Figure 4.9: Effect of Temperature on Total Sugar Yield at 1.2 % Acid Concentration

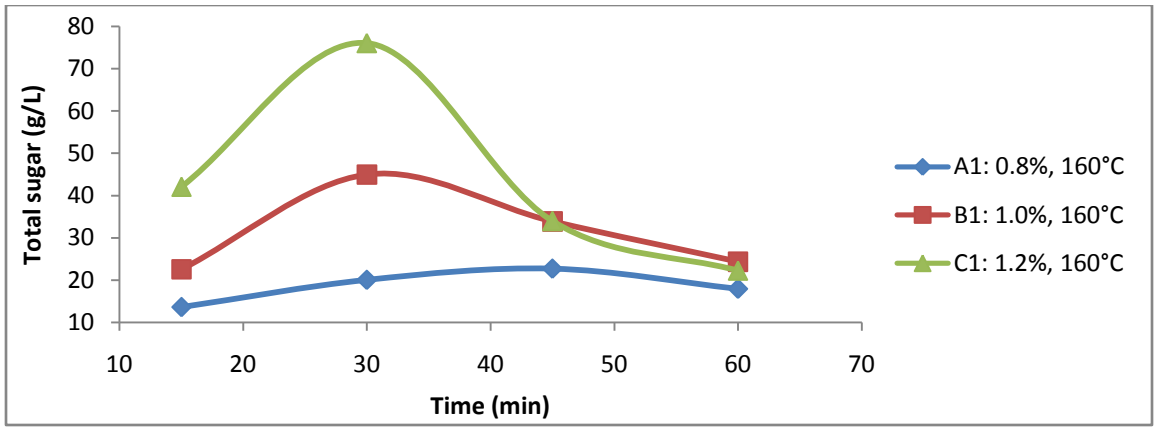

Figure 4.10: Effect of Concentration on Total Sugar Yield at 160 ^{0}C

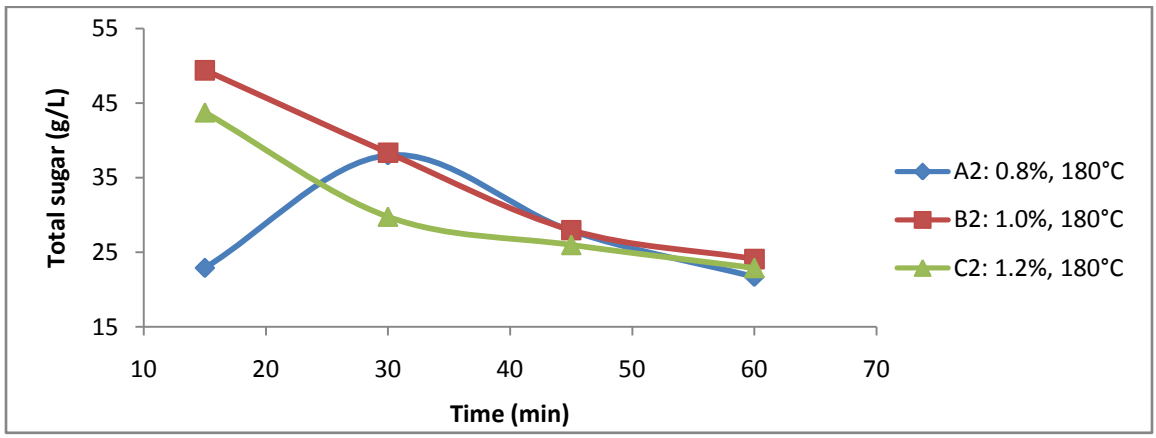

Figure 4.11: Effect of Concentration on Total Sugar Yield at 180 ^{0}C

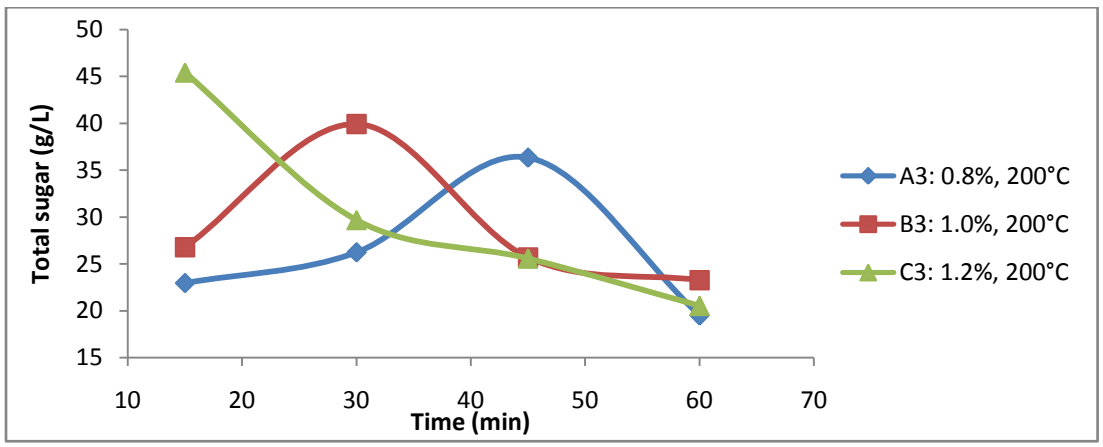

Figure 4.12: Effect of Concentration on Total Sugar Yield at 200 ^{0}C

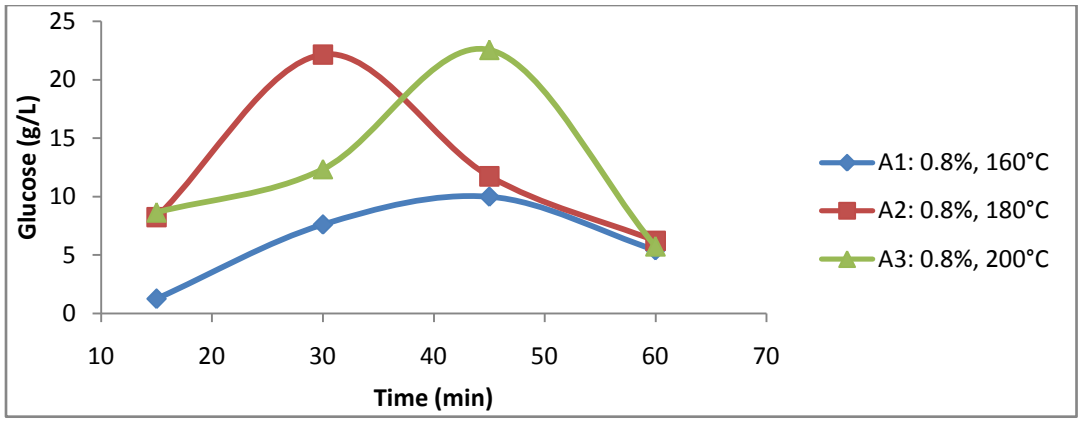

Figure 4.13: Effect of Temperature on Glucose Yield at 0.8 % Acid Concentration

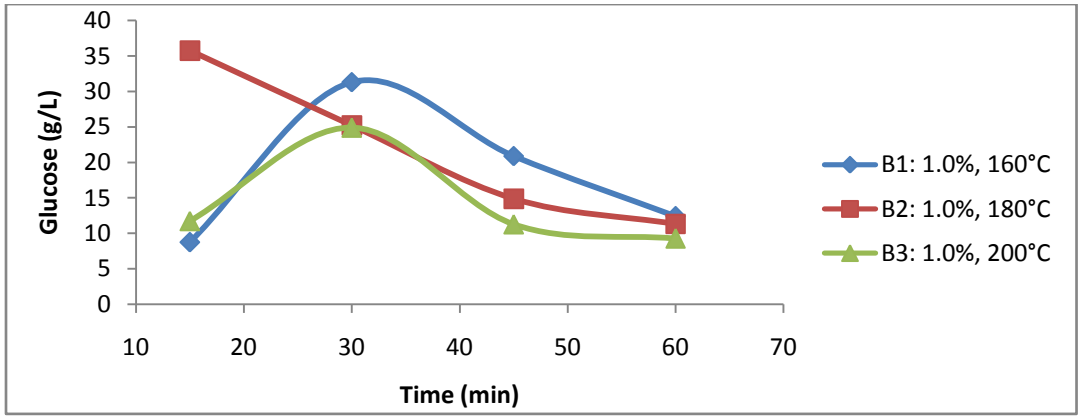

Figure 4.14: Effect of Temperature on Glucose Yield at 1.0 % Acid Concentration

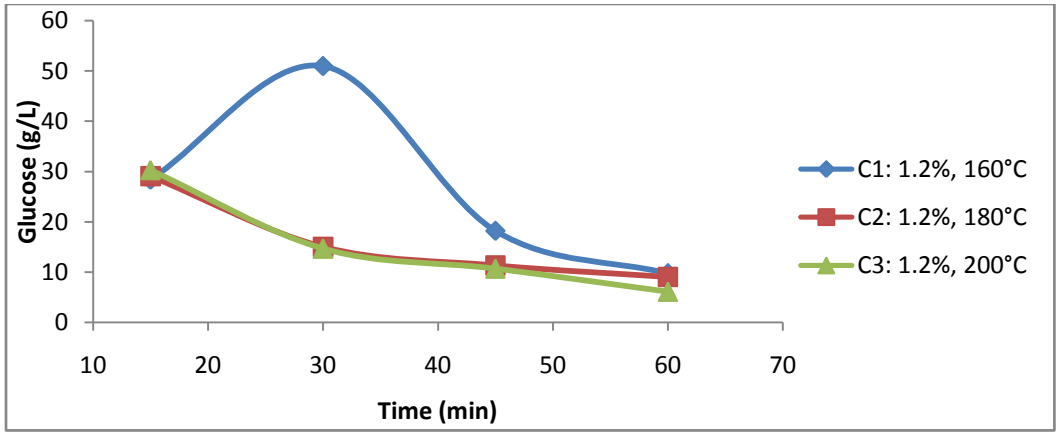

Figure 4.15: Effect of Temperature on Glucose Yield at 1.2 % Acid Concentration

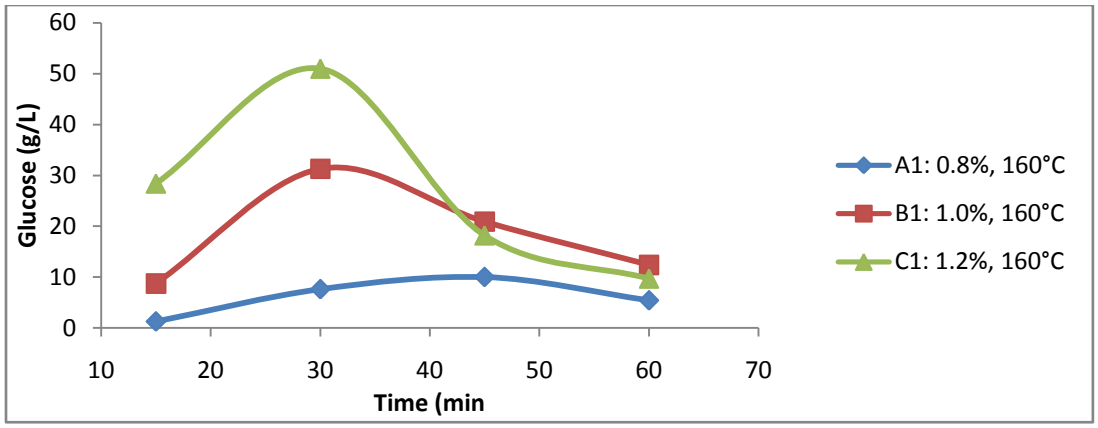

Figure 4.16: Effect of Acid Concentration on Glucose Yield at 160 ^{0}C

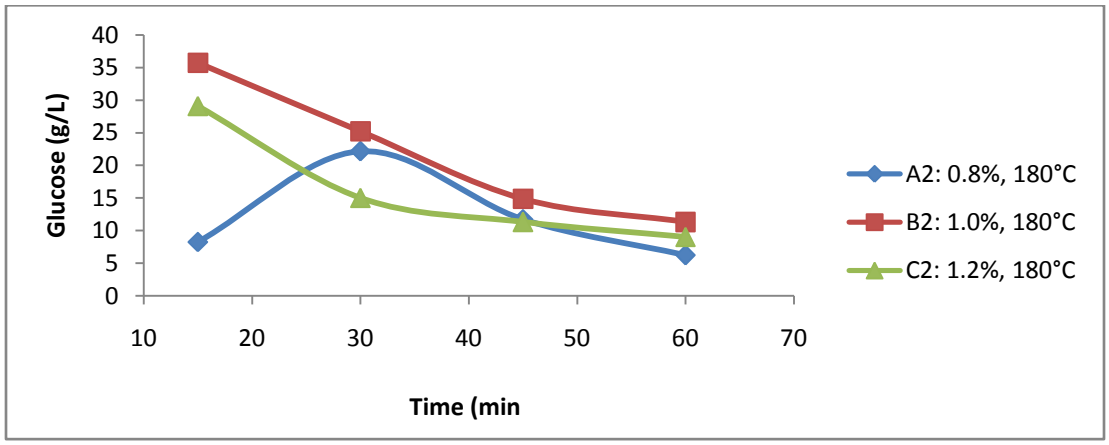

Figure 4.17: Effect of Acid Concentration on Glucose Yield at 180 ^{0}C

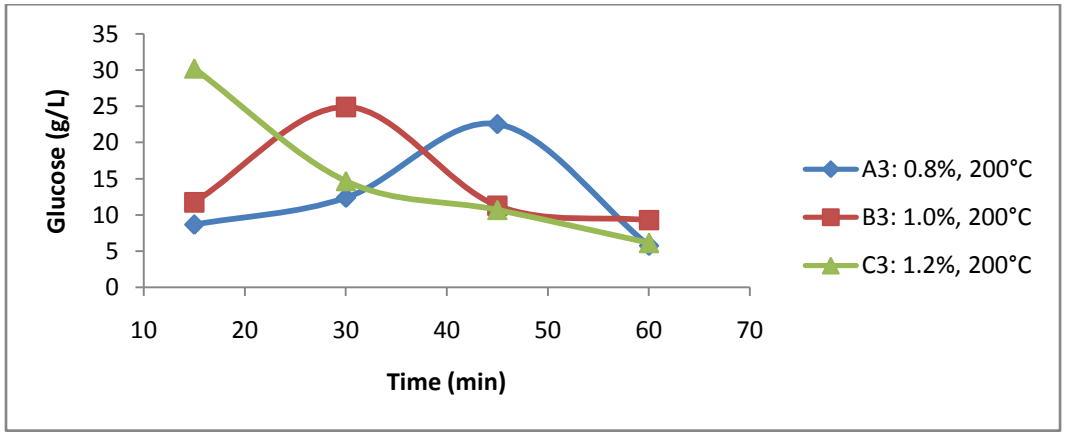

Figure 4.18: Effect of Acid Concentration on Glucose Yield at 200 ^{0}C

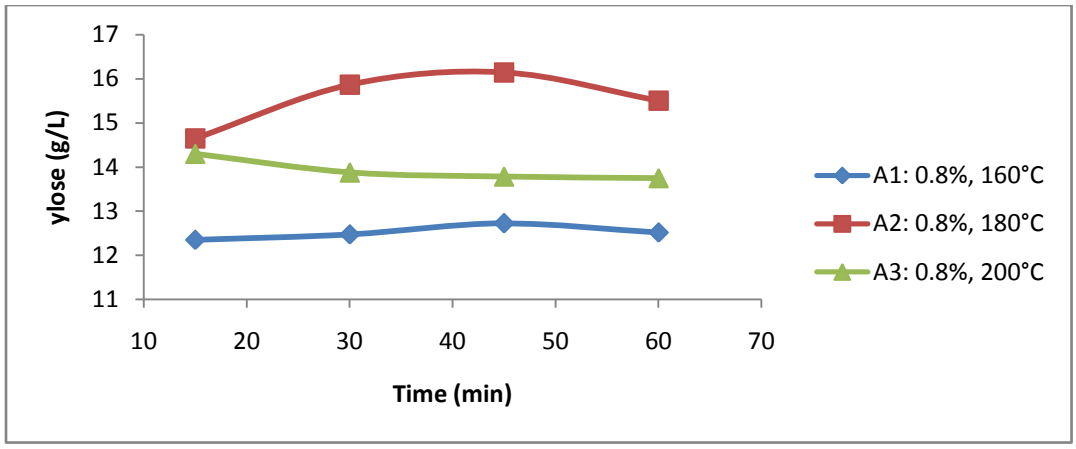

Figure 4.19: Effect of Temperature on Xylose Yield at 0.8 % Acid Concentration

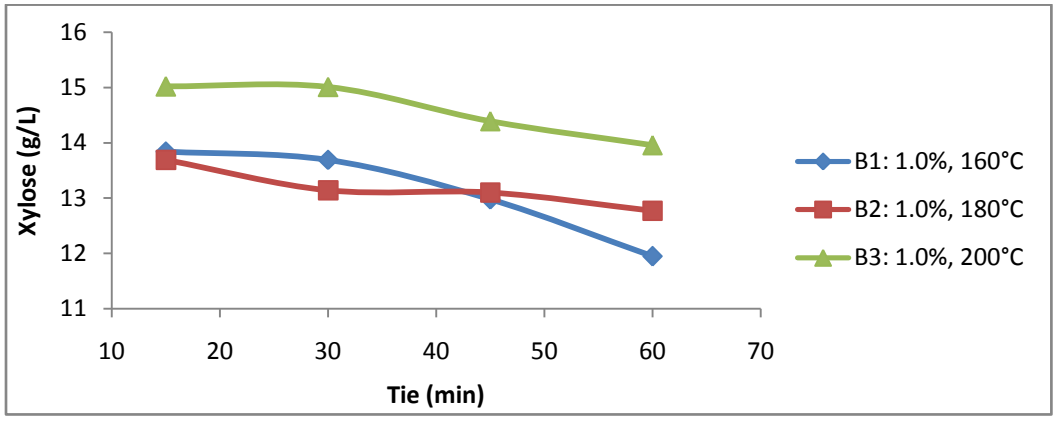

Figure 4.20: Effect of Temperature on Xylose Yield at 1.0 % Acid Concentration

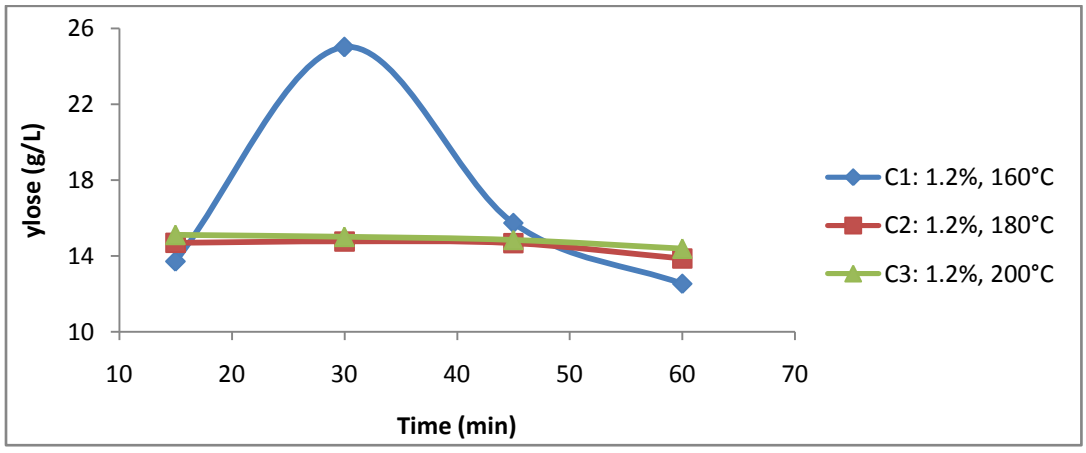

Figure 4.21: Effect of Temperature on Xylose Yield at 1.2 % Acid Concentration

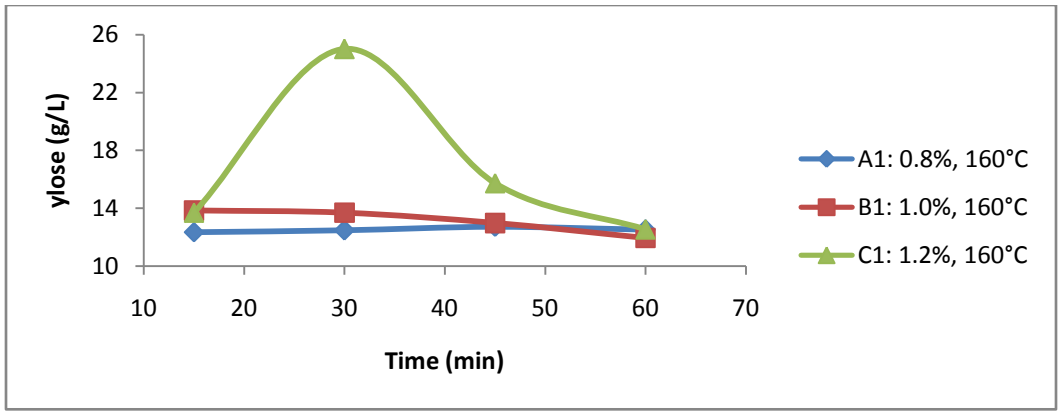

Figure 4.22: Effect of Acid Concentration on Xylose Yield at 160 ^{0}C

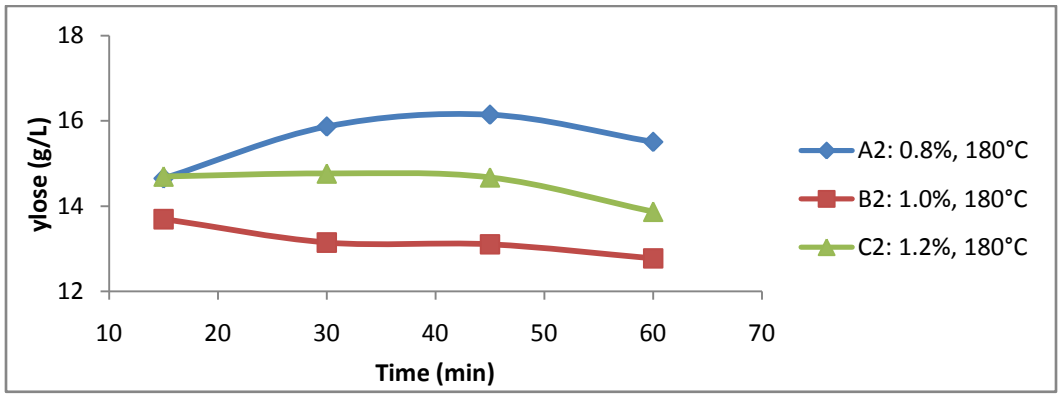

Figure 4.23: Effect of Acid Concentration on Xylose Yield at 180 ^{0}C

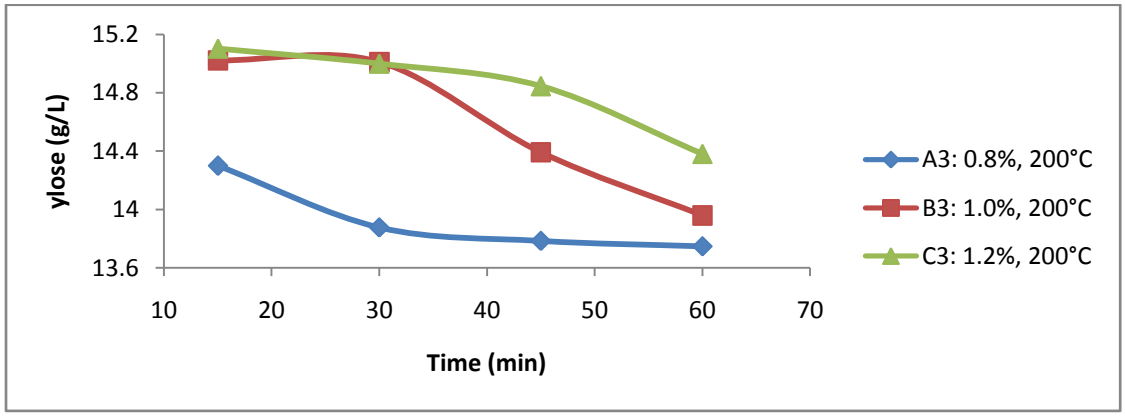

Figure 4.24: Effect of Acid Concentration on Xylose Yield at 200 ^{0}C

4.1.4 Preliminary Fermentation Result

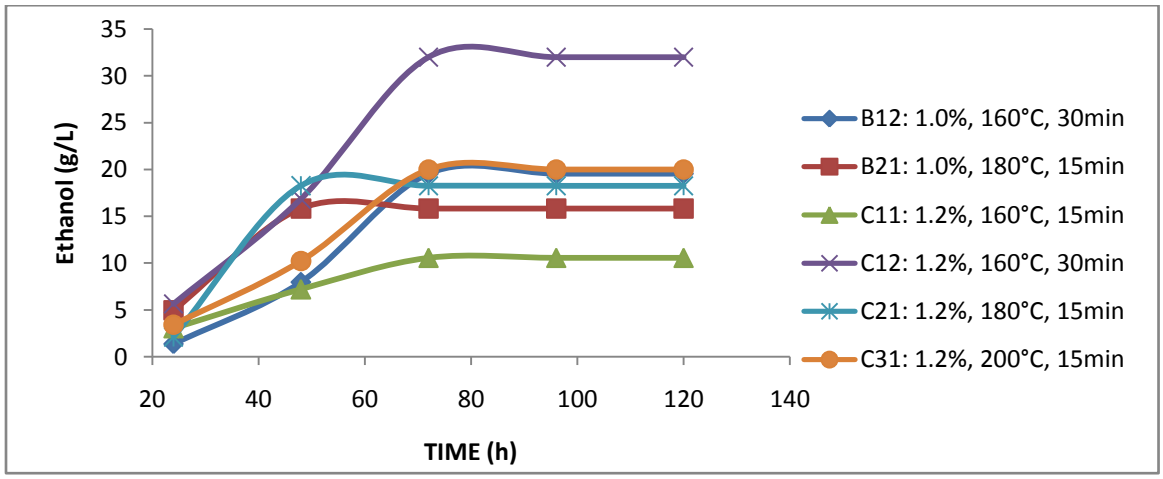

Figure 4.25: Bioethanol Yield from Fermentation

4.1.5 Distiller Operation Result

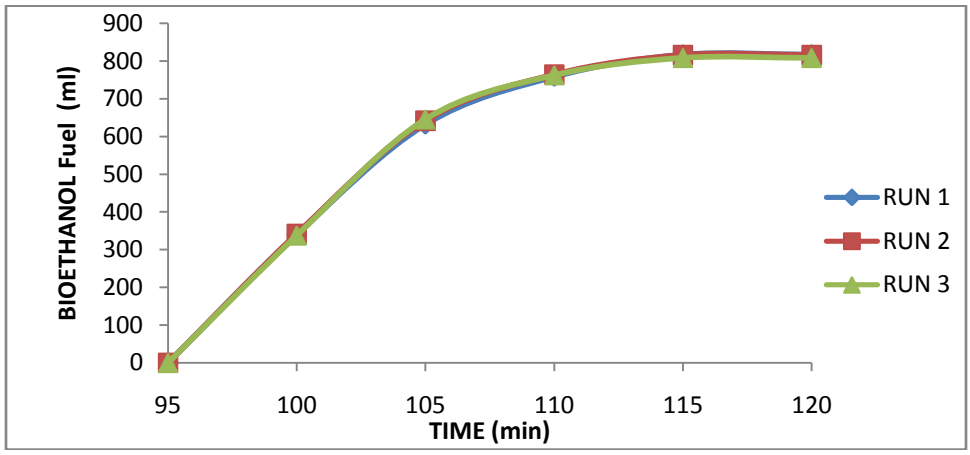

Figure 4.26: Bioethanol Yield from Distillation

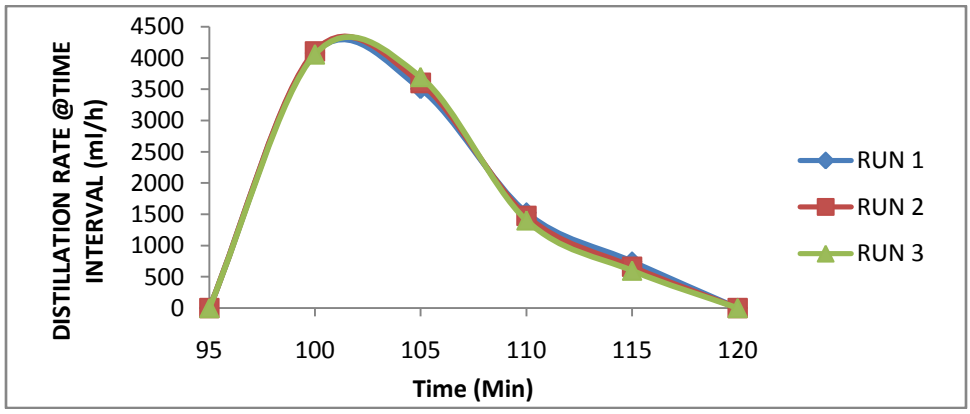

Figure 4.27: Distillation Rate at Time Intervals with Time

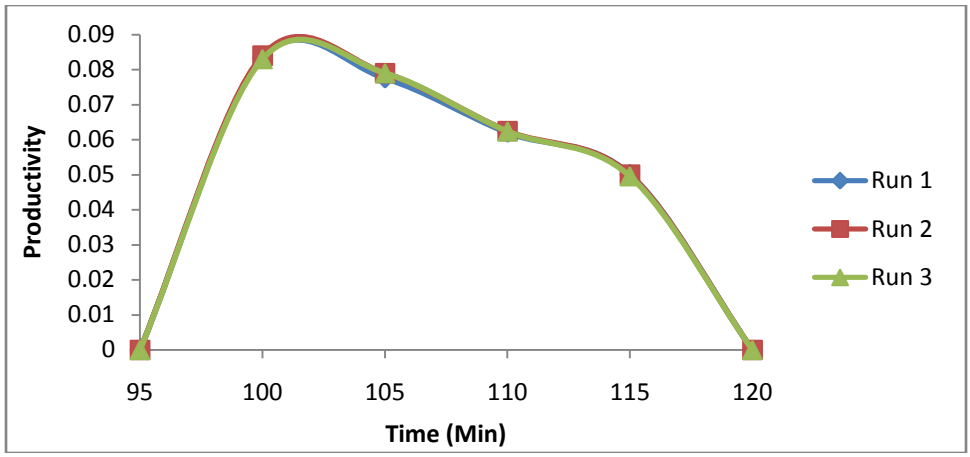

Figure 4.28: Distillation Productivity with Time

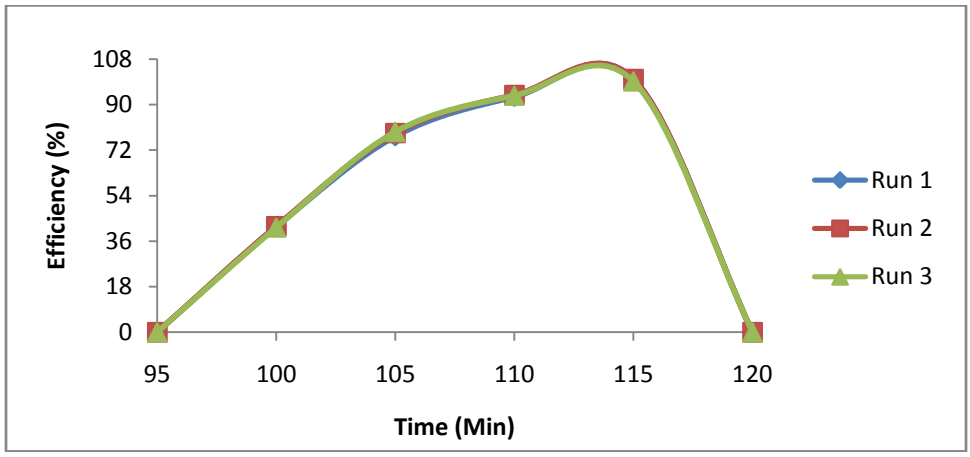

Figure 4.29: Distillation Efficiency with Time

4.1.6 Distiller Performance Data

Table 4.3: Distiller Performance Data

Parameter	**Calculated**	**Actual**
Loading capacity	Full load/ h	Full load
fuel Weight (kg)	1.67	2.2
Fuel start-up time (min)	-	4 - 7
Bubble point (^{0}C)	99.6	95
Bubble point / Total operating time (min)	60 / -	95 / 115
Fuel consumption rate (kg/h)	1.67	1.83
Specific gasification rate (kg/h-m^2)	80	87.372
Combustion zone velocity (cm/min)	0.583	0.3043
Reactor Power input (kW)	8.95	12.2
Combustion efficiency (%)	75	55
Bioethanol yield (ml)	815.67	817
Distillation Temperature (^{0}C)	99.6	96 - 98
Vapor pressure (bar)	3.2	2.81 – 3.01
Feed inlet / Distillate outlet temp. (^{0}C)	27 / 27	27 / 28.3

4.1.7 Fuels Characterization Result

Table 4.4: **Elemental Analysis of the Product Fuel**

Parameters	**E100**	**ASTM Range**	**ASTM Method**
Purity %	97.68		D 5501
Ash content %	0.03	0.05	D 482
H_2O content (% vol)	0.42	1.0 (% vol) or 1.26 mass %	D 95
Acidity	5.05 mg/ L	0.007 % mass or 56 mg/L (max)	D 974
pH	6.61	6.5 – 9.0	D 6423

Table 4.5: Fuel Properties of the Sample Fuels

Parameters	Sample Fuel								ASTM Method
	E0	E10	E20	E30	E40	E50	E60	E100	
Density @ 15 ^{0}C (kg/m^3)	744.73	747.65	752.7	759.93	768.89	777.64	782.5	791.13	D 4052
viscosity @ 40, ^{0}C	0.6097	0.6508	0.7132	0.9636	0.9951	1.3835	1.3592	1.6692	D 445
RON	89.2	91.8	93.4	95	96.5	98.8	100	124	D2699
RVP (kPa)	48.1	53.0	42.1	42.4	44.0	41.7	36.8	13.043	D4953
Flash pt, ^{0}C	-69	-38	-27	-18	-13.2	-8.7	-4.8	12.8	D93
Distillation Temp. range, ^{0}C	44 - 205	46 - 206	45 - 200	48 - 202	52 - 196	47 - 102	55 - 182	79 - 101	D86
Auto-ignition, ^{0}C	245	253	266	271	285	298	329	358	D
Calorific value (MJ/kg)	43.62	41.81	40.22	38.54	37.03	35.36	33.73	29.16	D240
Drivability Index, ^{0}C	723.84	704.51	588.56	615.31	622.68	539.69	532.57	589.51	D4814

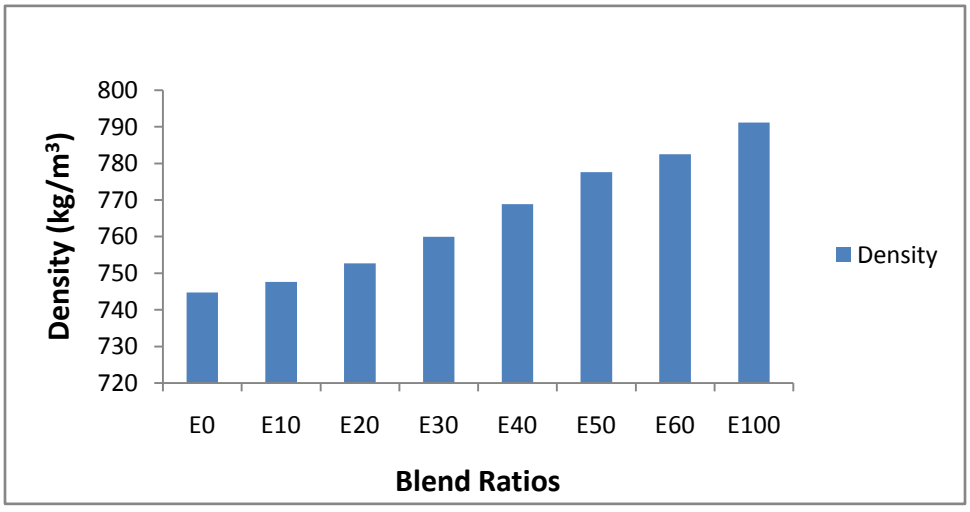

Figure 4.30: Effects of Blend Ratios on Density at 15 ^{0}C

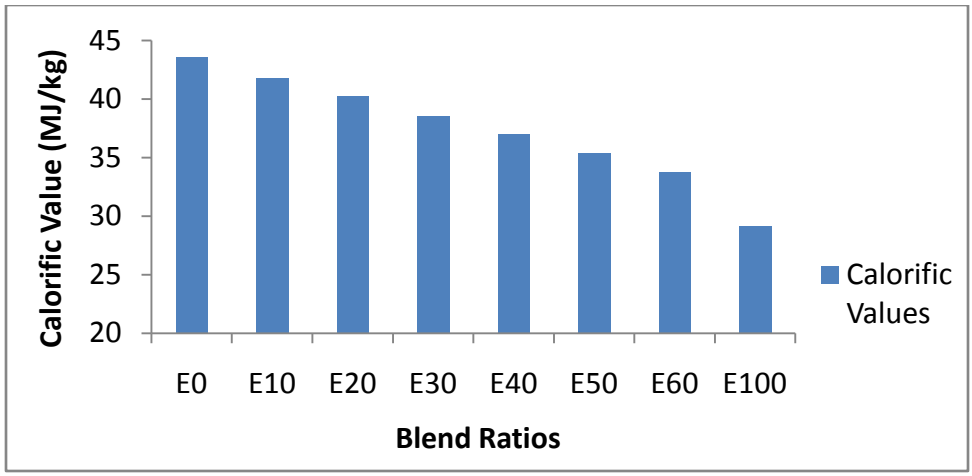

Figure 4.31: Effects of Blend Ratios on Calorific Value

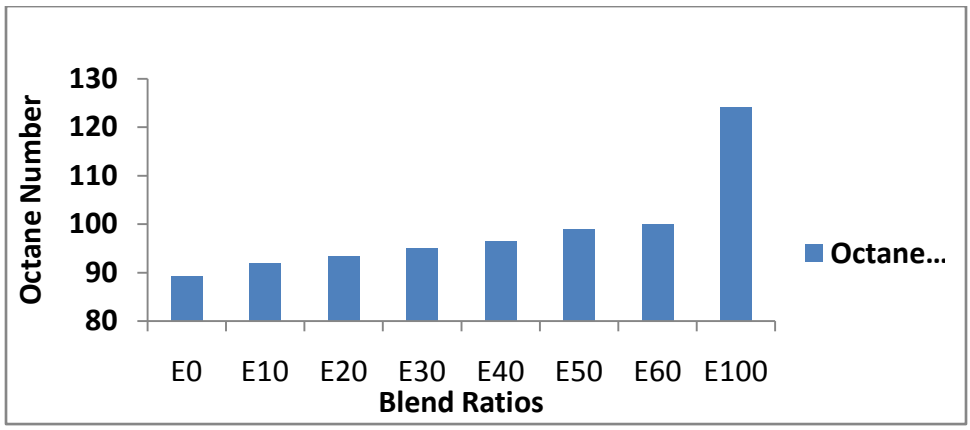

Figure 4.32: Effect of Blend Ratios on Octane Number

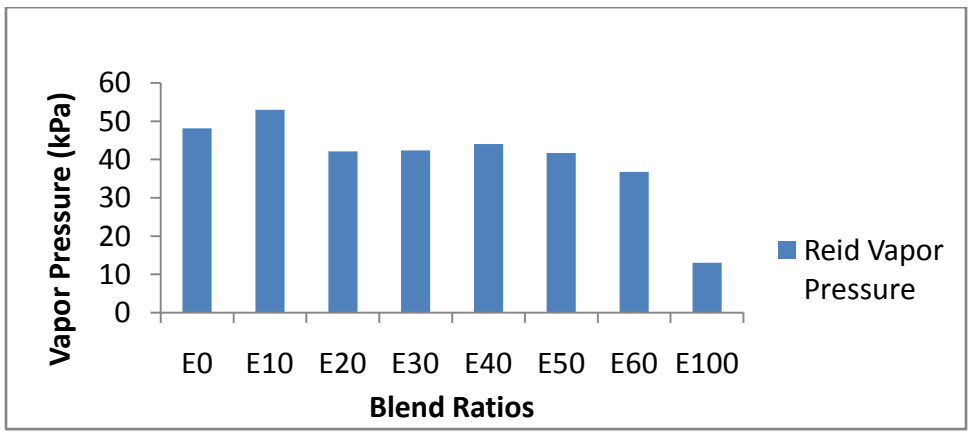

Figure 4.33: Effect of Blend Ratios on Vapor Pressure

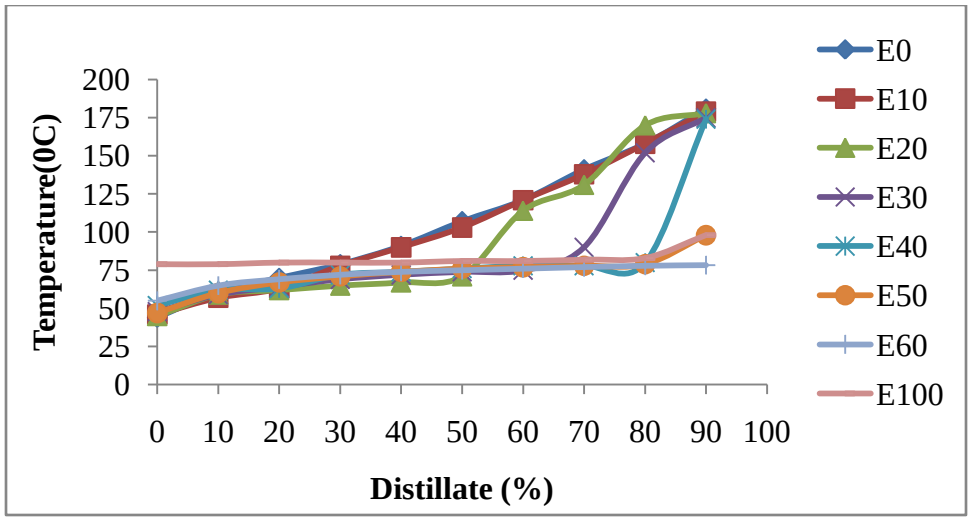

Figure 4.34: Effect of Blend Ratios on Distillation Profile

Table 4.6: Comparison of Fuel Properties

Property	ASTM Method	Potato waste (Talal et.al., 2012)	Sugar cane / palmwine / raffia trunk (Nwufor et. al., 2014)	Maize / raffia wine / palmwine (Tangka et. al., 2011)	Reported
Density	D 4052	785 kg/m^3	789 kg/m^3	789 kg/m^3	767
Viscosity (cSt)	D 88	1.1			1.6692
Auto ignition			638K, 336.7 ^{0}C	365 ^{0}C	328 ^{0}C
Heating value	D 240	27000 kJ/kg	29.78 (MJ/kg)	23.5 (MJ/L)	29.16 (MJ/kg)
RON	D 2699	108.6	114	129	124
Flash point	D 93	14 ^{0}C	12.5 ^{0}C	12.5 ^{0}C	12.5 ^{0}C
Vapor pressure	D 323	48 kPa	9.5 kPa	9 kPa	13.043 kPa
Distillation	D 86		55 - 68		79 - 101 ^{0}C

4.1.8 Engine Performance Result

a. Constant Engine Loads Results

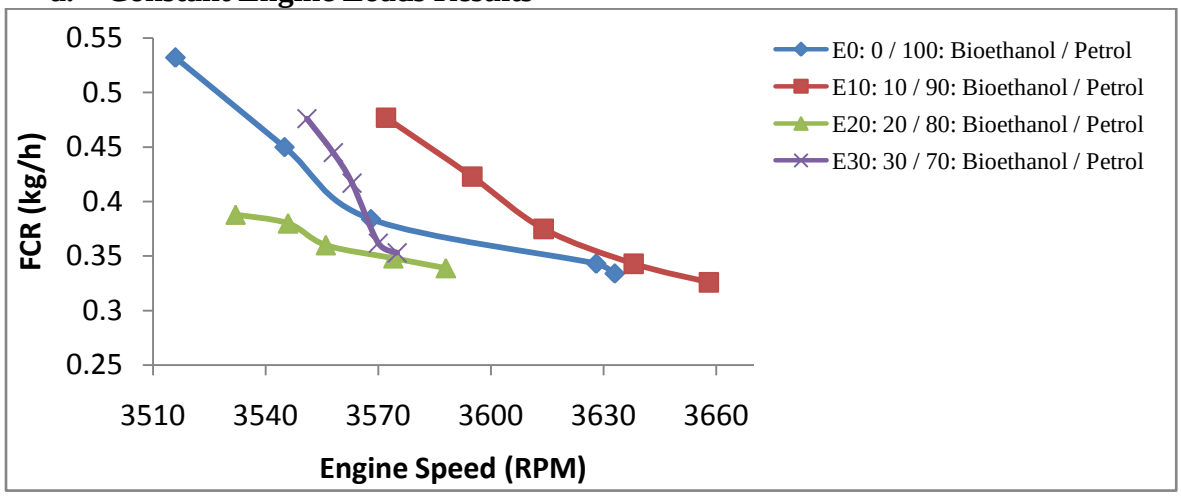

Figure 4.35: Effect of Blends on Fuel Consumption under Full-Load Conditions

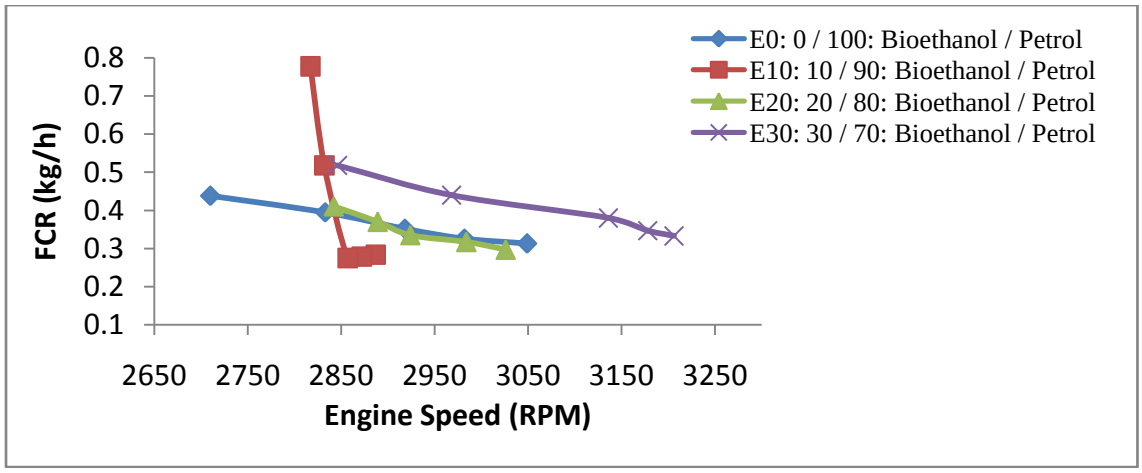

Figure 4.36: Effect of Blends on Fuel Consumption under ¾-Load Conditions

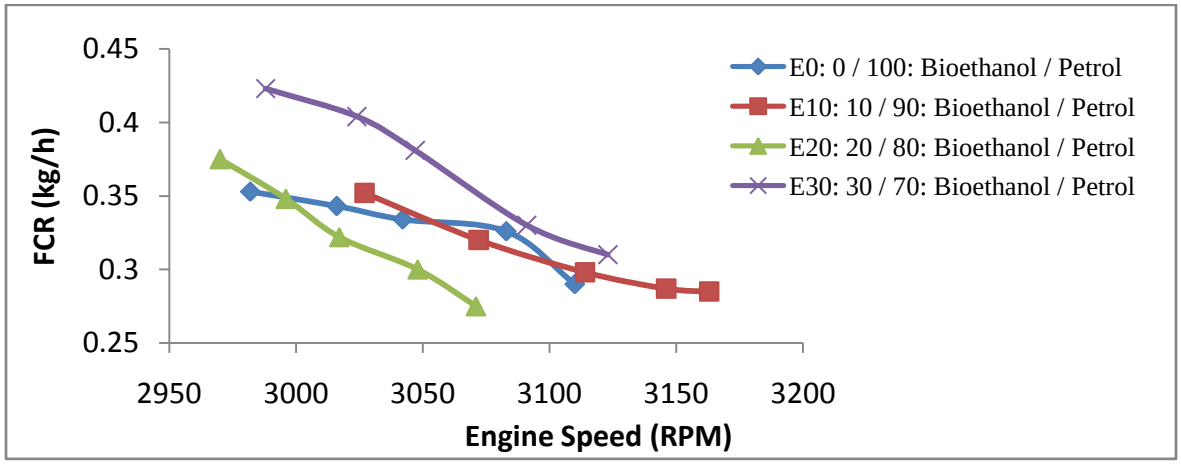

Figure 4.37: Effect of Blends on Fuel Consumption under ½-Load Conditions

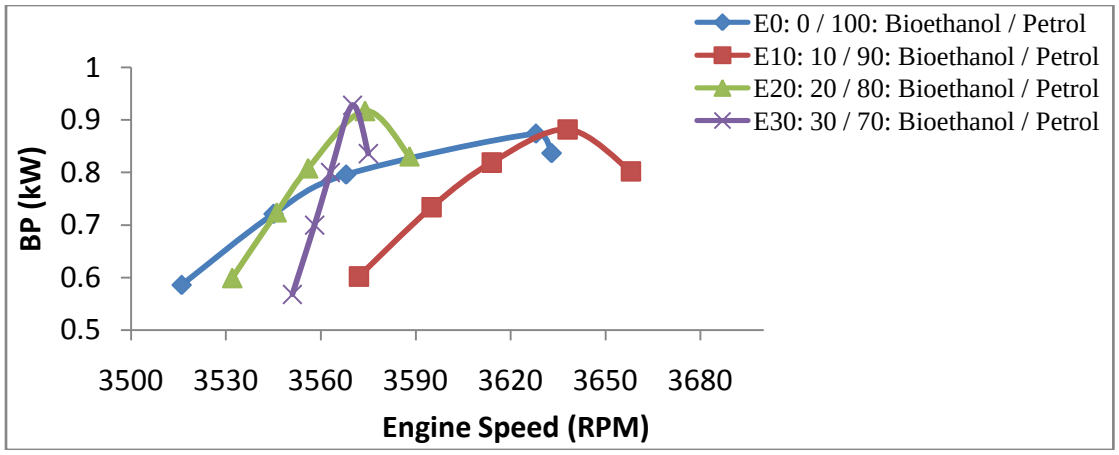

Figure 4.38: Effect of Blends on Brake Power under Full-Load Conditions

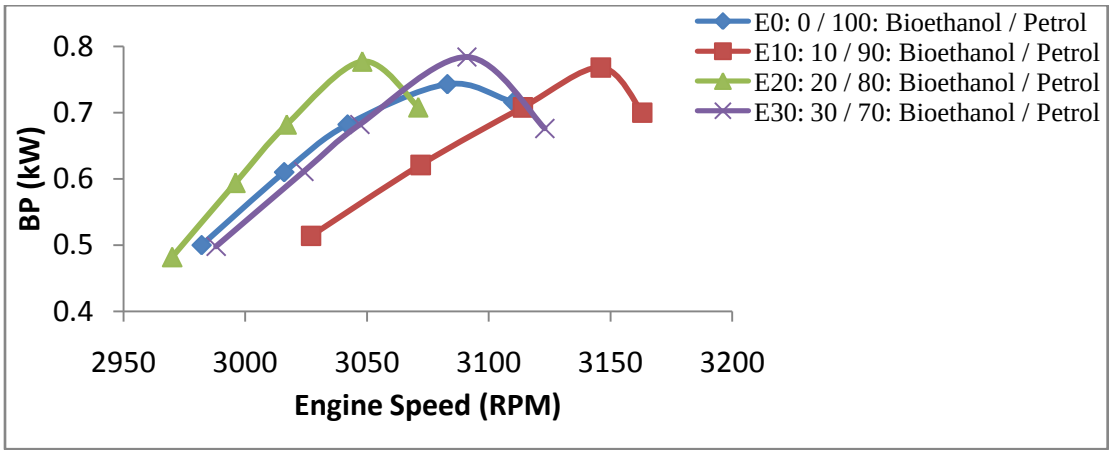

Figure 4.39: Effect of Blends on Brake Power under ¾-Load Conditions

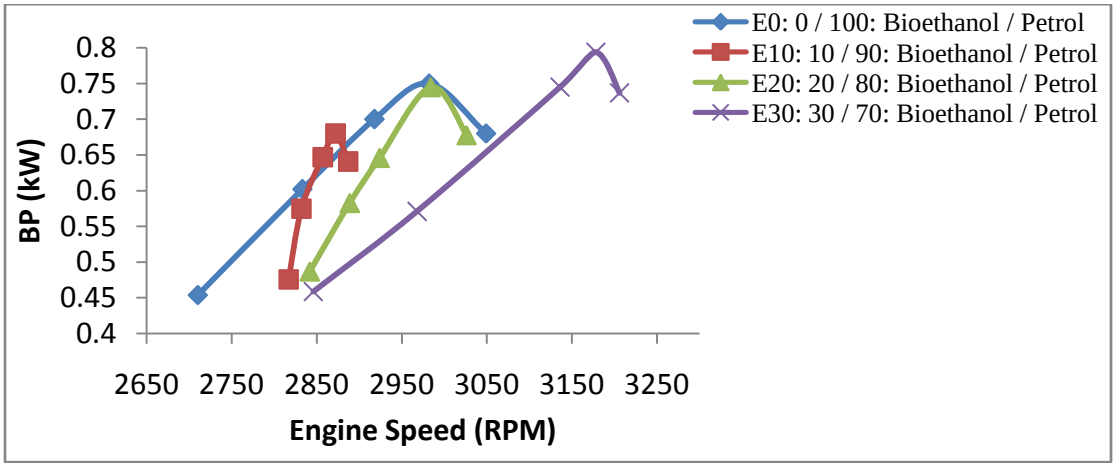

Figure 4.40: Effect of Blends on Brake Power under ½-Load Conditions

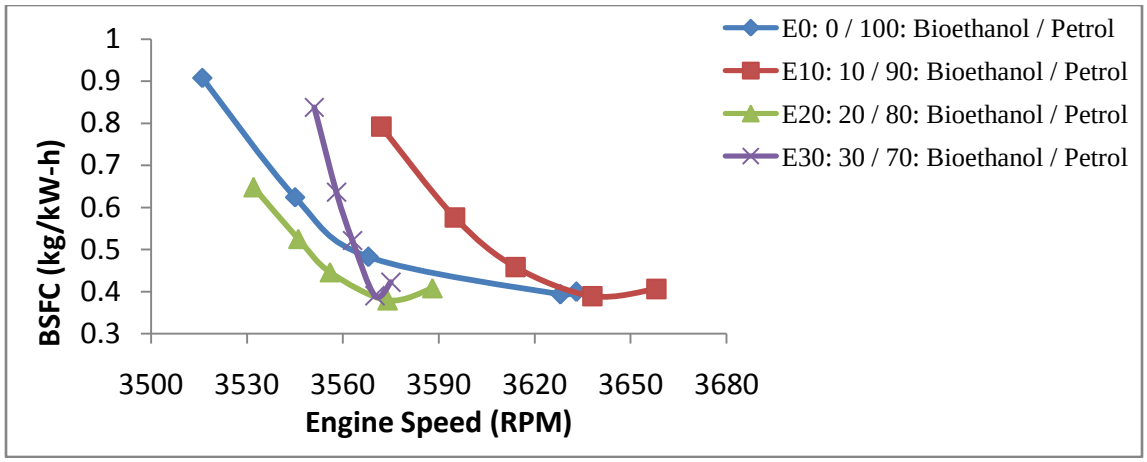

Figure 4.41: Effect of Blends on Brake Specific Fuel Consumption under Full-Load Conditions

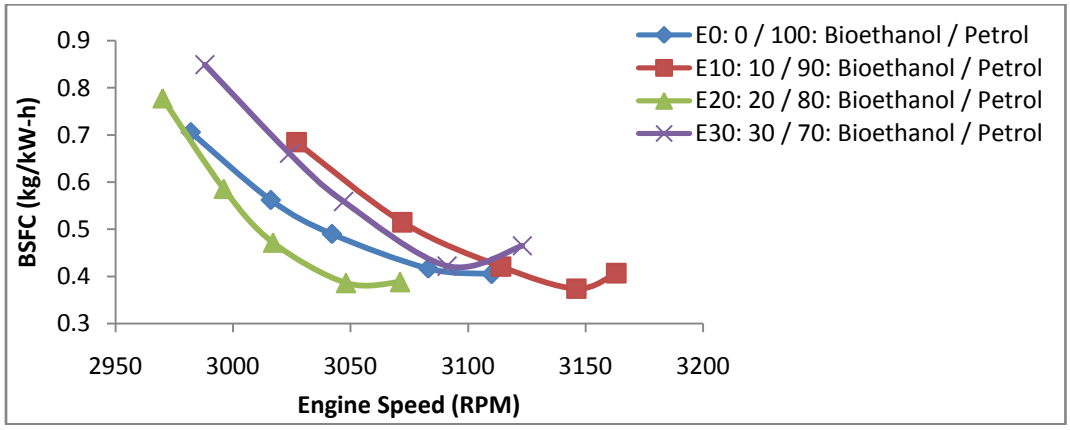

Figure 4.42: Effect of Blends on Brake Specific Fuel Consumption under ¾-Load Conditions

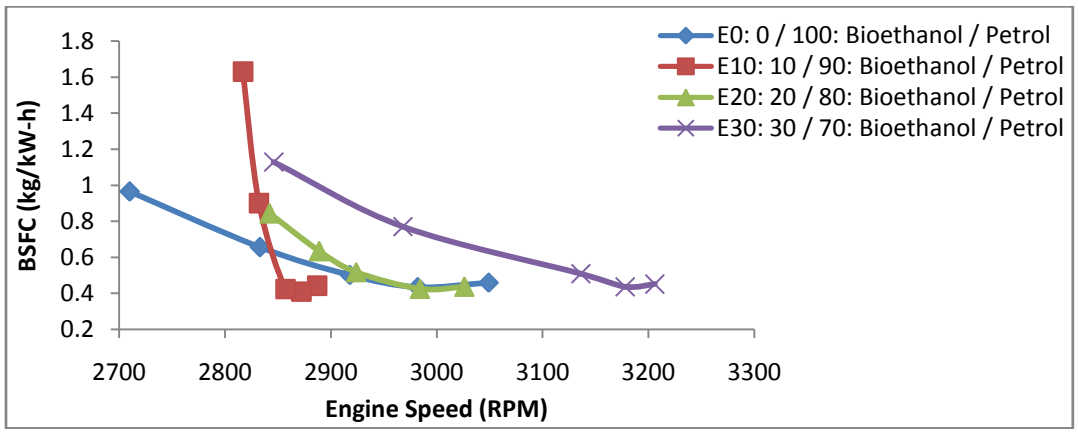

Figure 4.43: Effect of Blends on Brake Specific Fuel Consumption under ½-Load Conditions

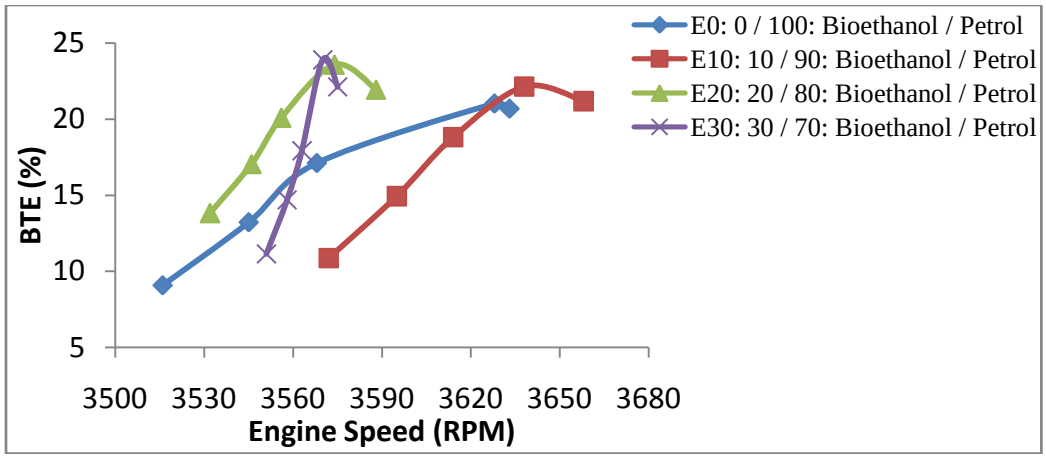

Figure 4.44: Effect of Blends on Brake Thermal Energy under Full-Load Conditions

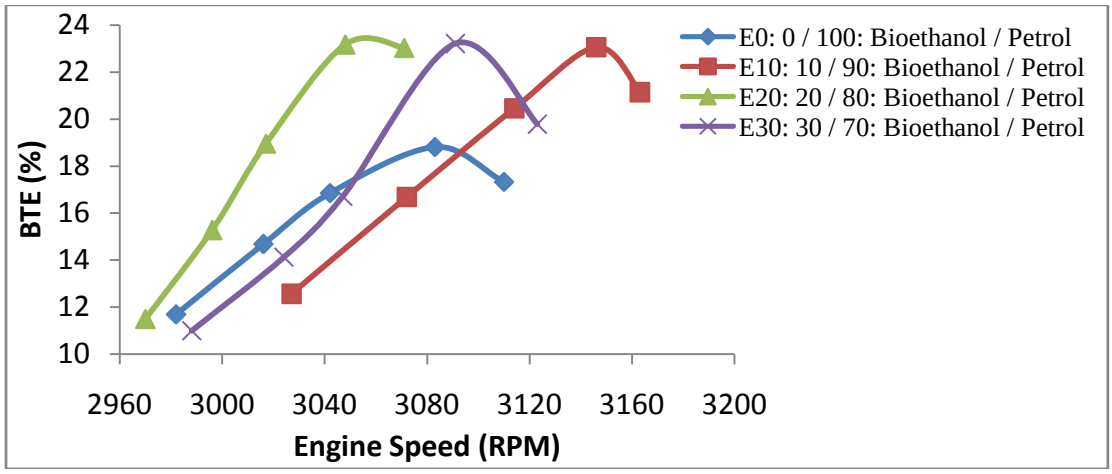

Figure 4.45: Effect of Blends on Brake Thermal Energy under ¾-Load Conditions

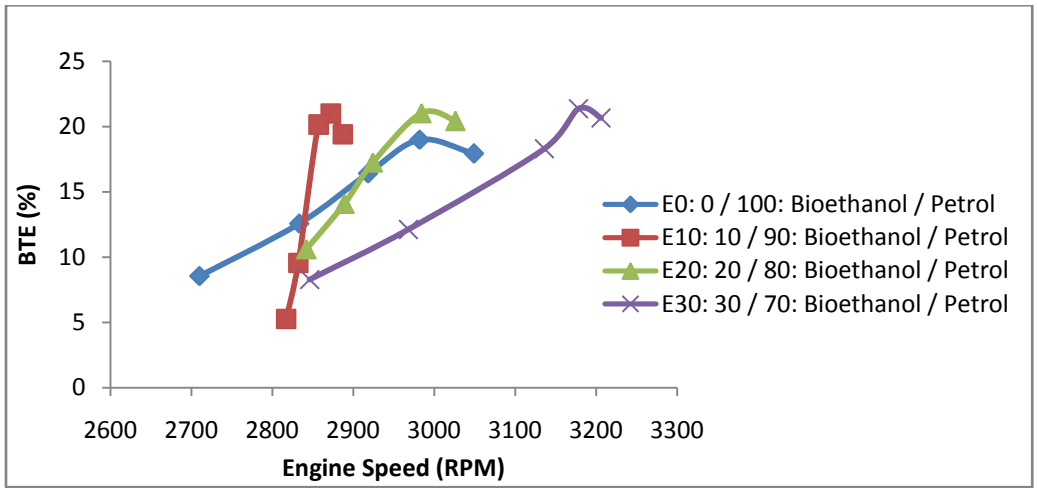

Figure 4.46: Effect of Blends on Brake Thermal Energy under ½-Load Condition

b. Constant Engine Speeds Results

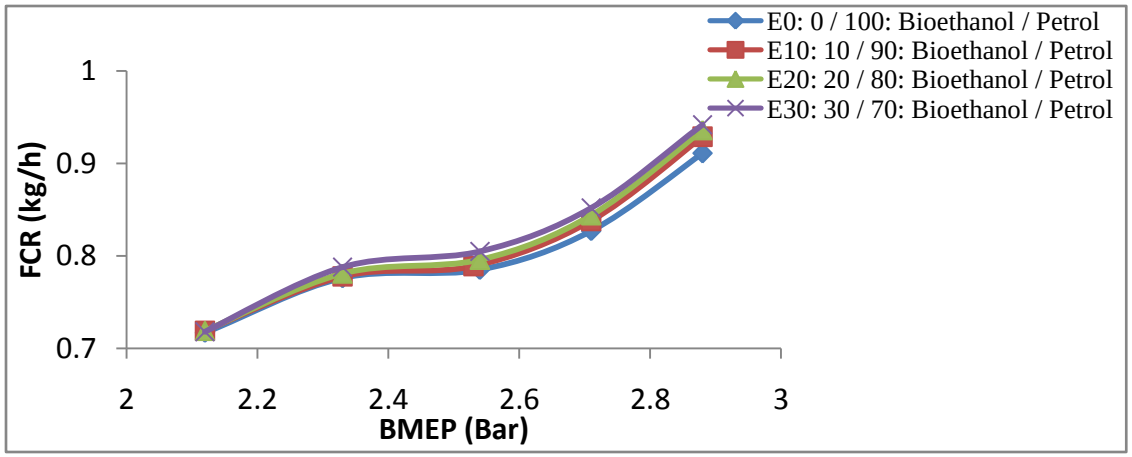

Figure 4.47: Effect of Blends on Fuel Consumption at Engine Speed of 2500 RPM

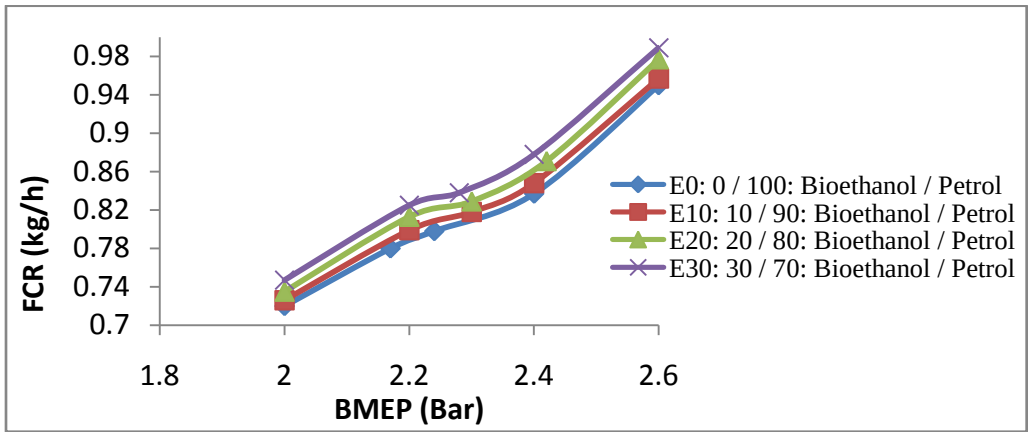

Figure 4.48: Effect of Blends on Fuel Consumption at Engine Speed of 3000 RPM

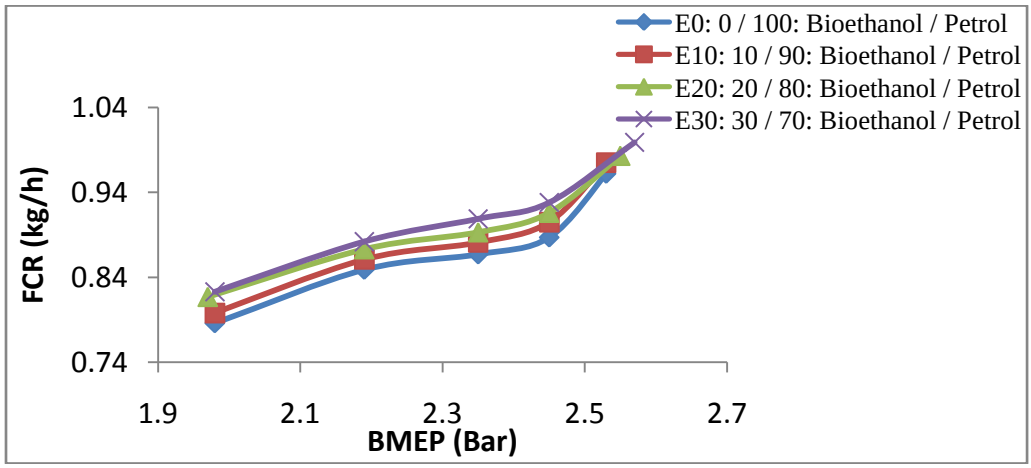

Figure 4.49: Effect of Blends on Fuel Consumption at Engine Speed of 3500 RPM

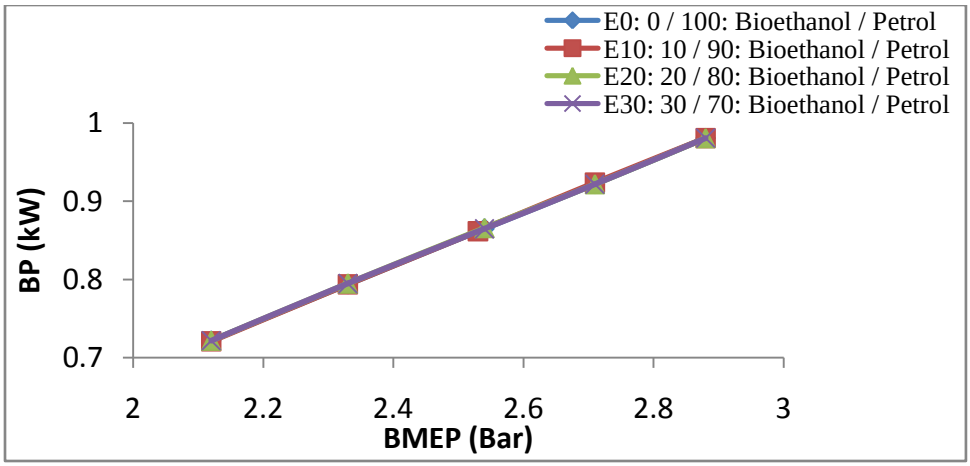

Figure 4.50: Effect of Blends on Brake Power at Engine Speed of 2500 RPM

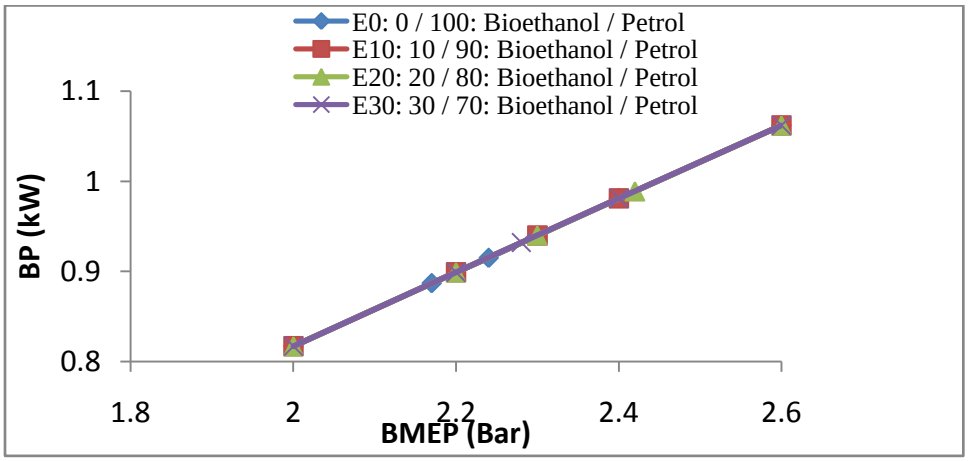

Figure 4.51: Effect of Blends on Brake Power at Engine Speed of 3000 RPM

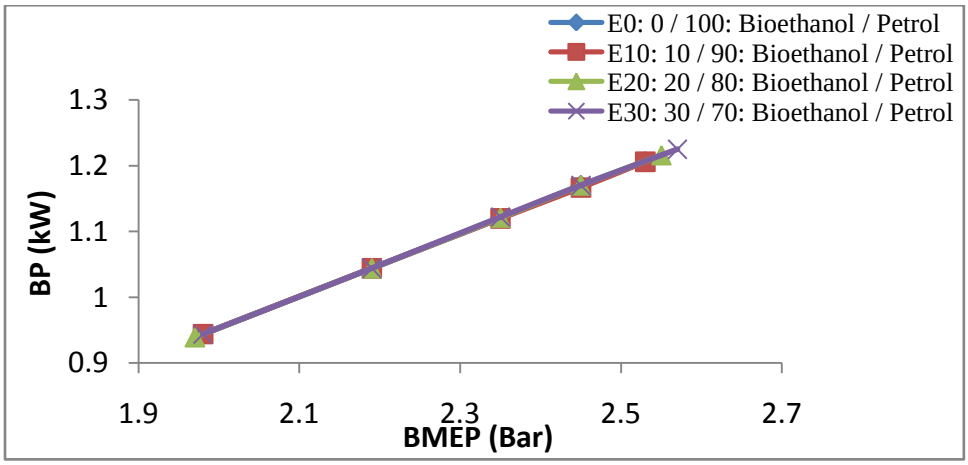

Figure 4.52: Effect of Blends on Brake Power at Engine Speed of 3500 RPM

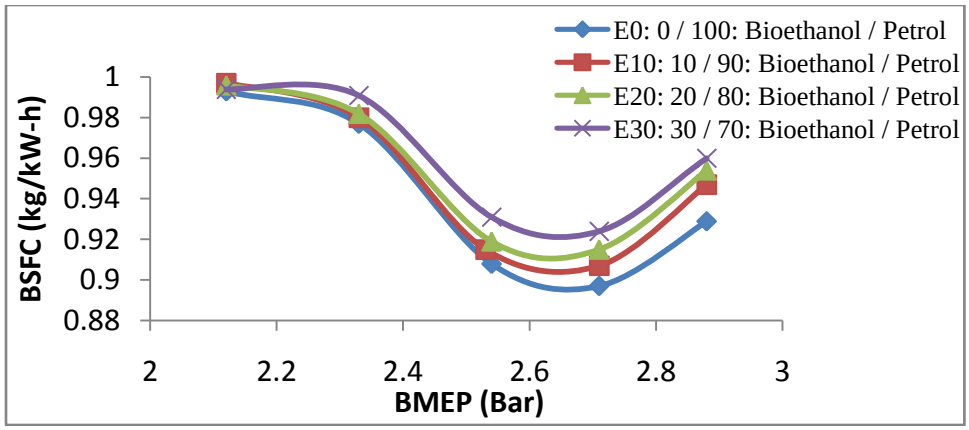

Figure 4.53: Effect of Blends on Brake Specific Fuel Consumption at Engine Speed of 2500 RPM

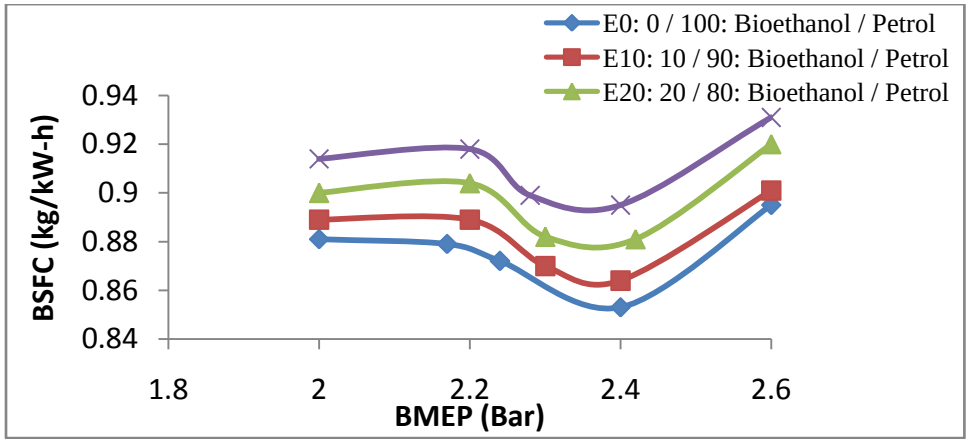

Figure 4.54: Effect of Blends on Brake Specific Fuel Consumption at Engine Speed of 3000 RPM

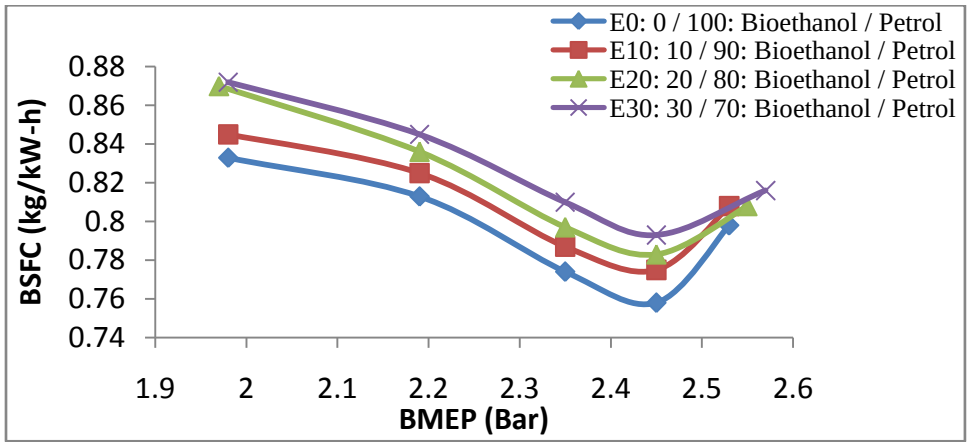

Figure 4.55: Effect of Blends on Brake Specific Fuel Consumption at Engine Speed of 3500 RPM

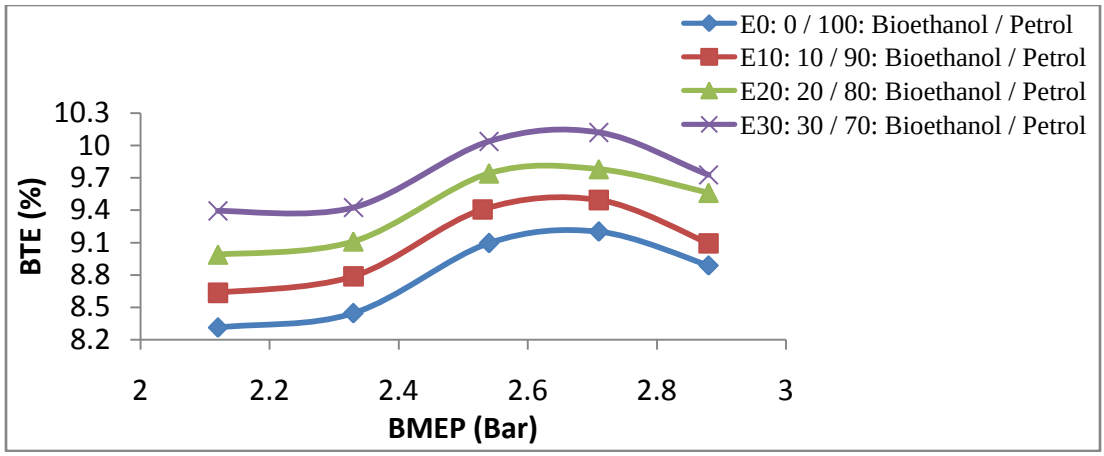

Figure 4.56: Effect of Blends on Brake Thermal Efficiency at Engine Speed of 2500 RPM

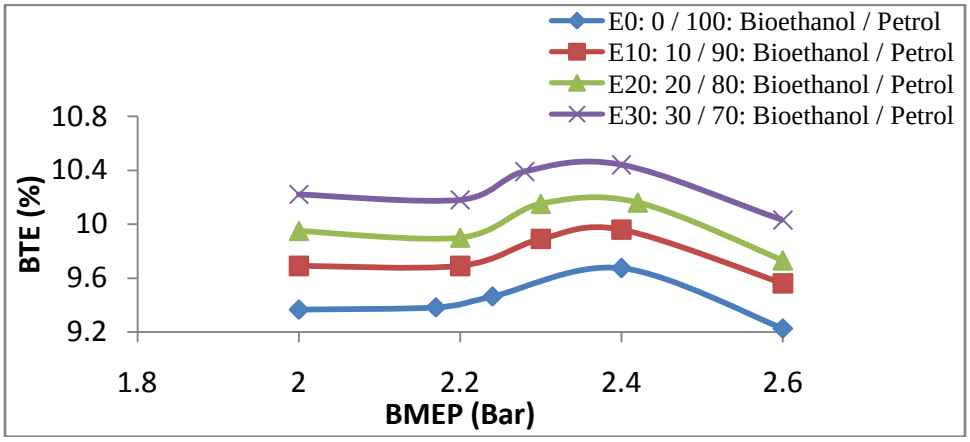

Figure 4.57: Effect of Blends on Brake Thermal Efficiency at Engine Speed of 3000 RPM

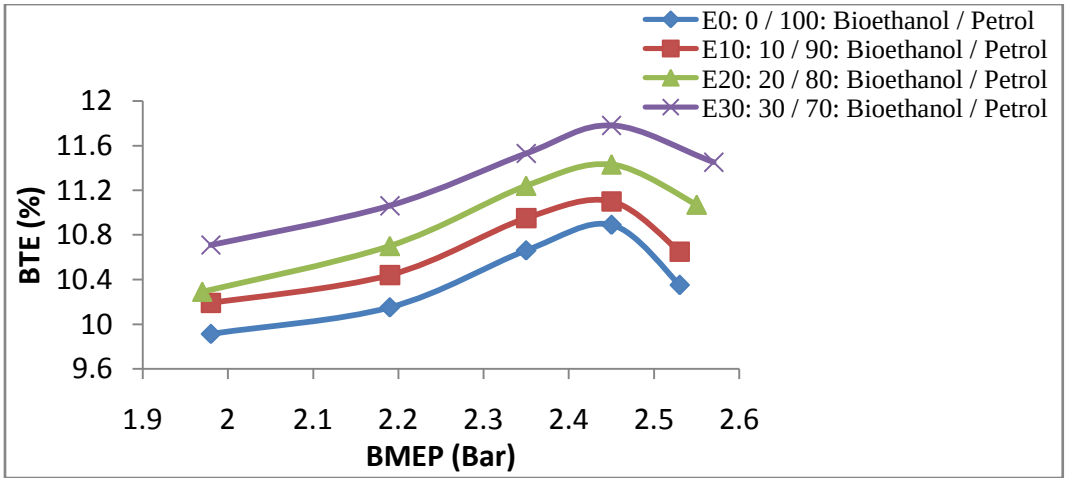

Figure 4.58: Effect of Blends on Brake Thermal Efficiency at Engine Speed of 3500 RPM

4.2 Discussion

4.2.1 Raw Material Pretreatment

The collected sterilized shredded raw material was dried to less than 10 % moisture content and ground to 850 micron powder. It was observed that the dried sample stuck in the machine during grinding until it was scattered and heated to speed up grinding and prevent it from stucking in the grinder. A pair of English blade was used for pulverizing while a pair consisting of the English and Local cast blade was used for final grinding. It was observed that pulverization gave more WPB powder than the final grinding proving that most of the holocellulose were released during pulverization. This justifies the advantage of sterilization which can be seen as a pretreatment step. The ground feedstock was then characterized and used for bioethanol production following the procedures of alcohol production from lignocellulosic materials. The observed results of the followed procedures are analyzed below.

4.2.2 Raw Material Characterization

The chemical compositions of lignocellulosic materials vary depending on plant varieties, geographical condition, harvesting and processing methods. The composition of pretreated WPB was obtained using AOAC (1980) method and presented in Table 4.1. It consists of 74.33 % holocellulose, (57.44 % α-cellulose and 16.89 % hemicelluloses), 15.87 % lignin and 5.57 % ash. This means that, 1 kg ground sample will have 574.4 g cellulose and 168.9 g hemicelluloses while a ton will have 574.4 kg cellulose and 168.9 kg hemicelluloses. Analysis of the WPB shows that theoretical fermentable sugars accounted for more than 62.1 % on a dry matter basis, similar to that of other major lignocellulosic biomass types, such as rice straw, wheat straw, and corn stover, indicating that WPB has a great potential as a bio-fuel feedstock. Sterilization must have increased the release of the 'α-cellulose' a glucose-based polymer which has potential for the conversion into biofuel, break hemicelluloses – lignin bond thereby reducing the need for delignification. Though, it can reduce the hemicellulose content, and more critically, by collapsing the structure of the glucan, it could increase recalcitrance. The holocellulose content agree well with recent analysis data reported by Nor et. al., (2012), Yanni et. al., (2012), Umikalsom et al. (1997), Nuru et. al., (2014), Sarudee and Chayanoot (2013). However, 5.57 % ash content and 15.87 % lignin content are higher than their findings though Richana et. al., (2015) reported 50.03 % ash. Also, the lignin content is high compared with other biomass e.g. 6.3 - 9.8 % in barley straw (Garda et. al., 2006), 17-19 % in rice straw (Prassad et. al., 2007),

14.2 % in oilseed rape and 16.1 % in winter rye (Petersson et. al., 2007). The presence of lignin impedes enzymatic hydrolysis of carbohydrates by blocking access of cellulose and irreversibly binding hydrolytic enzymes. So, chemical hydrolysis was preferred for the undeliginified WPB.

4.2.3 Glucose, Xylose and Bioethanol Standard Analysis

Standard solutions of laboratory grade glucose, xylose and absolute ethanol were prepared with different concentrations which are 0.0, 0.02, 0.04, 0.08, 0.16 and 0.2 g/L for glucose; 0.0, 0.0438, 0.0625, 0.0813, 0.1625 and 0.2438 g/L for xylose, and 0.0, 9.216, 18.432, 27.648, 36.864 and 46.08 g/L for ethanol. Their respective absorbances observed are given in Appendix C but illustrated in Figure 4.1 – 4.3. Absorbances of subsequent analysis were then compared with these standard curves.

4.2.4 Preliminary Hydrolysis

200 g each of ground raw material was hydrolyzed with H_2SO_4 at varying concentration, temperature and time. During acid hydrolysis, many substances are released into the hydrolyzate, of which sugars (hexoses and pentoses) are the main components. From the composition of the used WPB, 200 g of the WPB has 114.88 g cellulose and 33.78 g hemicellulose. Consequently, the theoretical glucose and xylose yield are 127.517 g and 26.87 g respectively. The sample was withdrawn for sugar analysis at 15 minutes intervals. The withdrawn volume of the sample was cooled to room temperature and neutralized to 4.8 pH value to stop the reaction. Table 4.2 presents the observed pH of hydrolyzates before neutralization.

a. Observed pH of Hydrolyzates before Neutralization

From Table 4.2, shows increase pH value with time for a particular temperature. Thus, the acidity of the samples reduces with increase in hydrolysis time for that temperature, confirming trace of alkali content in WPB. For a particular acid concentration, the pH value increases with increase in temperature and decrease in acidity except in hydrolysis condition B_2. The observed absorbance of the hydrolyzates with time, measured on a spectrophotometer at the respective wavelength was converted to glucose and xylose concentration from the standard curve respectively. The recorded xylose and glucose yield monitored every 15 minutes are given in Appendix D while its illustrations are presented below. Glucose, Xylose and bioethanol conversion percentage were calculated with Equation 2.103, 2.104 and 2.113.

b. Glucose Yield of the Hydrolysis Process

Figure 4.4 clearly shows that the six highest glucose yield conditions can only be in B_{12}, B_{21}, C_{11}, C_{12}, C_{21}, and C_{31} with 31.29, 35.735, 28.419, 51.0, 29.097 and 30.323 g/L respectively. Thus, the maximum glucose yield which is 51.0 g/L was achieved with 1.2 % (v/v) H_2SO_4 at 160 ^{0}C, for 30 min, resulting to 40 % cellulose conversion and 102 g/L-h yield rate. These sets of hydrolysis condition are favorable to glucose yield compared to others while condition A_1 is the worst condition for glucose yield as it recorded a low set of glucose yield. The lowest yield is 1.258 g/L at 0.8 % (v/v) H_2SO_4 at 160 ^{0}C, for 15 min reaction condition, corresponding to sample A_{11}. At a particular temperature and concentration, glucose yield increases with time to its peak after which it declines with longer residence time. Longer residence time results to complete degradation of the glucose yield. This result also suggest that in hydrolyzing WPB, mild to high acid concentration within 30 – 45 minutes residence time favors glucose yield. Glucose yield was generally low been less than 50 %, this may be as a result of inhibitors.

c. Xylose Yield of Hydrolysis Process

Figure 4.5 clearly shows that the six highest xylose yield condition can only be in A_2 and C_1. In line with Appendix D, the six highest xylose yield samples are found to be A_{22}, A_{23}, A_{24}, C_{12}, C_{13} and C_{31} with 15.866, 16.144, 15.505, 25.01, 15.732 and 15.103 g/L. The maximum xylose yield which is 25.01 g/L was achieved with 1.2 % (v/v) H_2SO_4 at 160 ^{0}C, for 30 min, resulting to 98.93 % hemicellulose conversion and 50.02 g/L-h yield rate. These sets of hydrolysis condition are favorable to xlyose yield compared to others while condition A_1 recorded the lowest set of xylose yield. The lowest yield is 11.948 g/L for xylose at 1.0 % (v/v) H_2SO_4 at 160 ^{0}C, for 60 min reaction condition, corresponding to sample B_{14}. Long residence time is unfavorable to xylose yield, 45 minutes seems to be a good limit for xylose yield in the WPB. This suggests that the C_5 sugars in the hydrolyzate are mostly lower order oligmers. At 60 minutes xylose yields cluster at a low yield concentration inspite the temperature and acid load. Low xylose yield may be due to xylose degradation as reaction temperature exceeds 140 ^{0}C. It can then be deduce that lower temperature (100 – 140 ^{0}C) is better applied in the hydrolysis of hemicelluloses while higher temperature (180 - 250 ^{0}C) can be applied in cellulose hydrolysis. The result suggest that that for WPB, low and high acid concentration favours xylose yield but at mild and low temperature respectively.

d. Total Sugar Yield from Hydrolysis Process

Figure 4.6 shows that hydrolysis condition 'A' did not favor the WPB as it recorded the lowest set of total sugar yield while condition 'B' and 'C' seems to be better. The low sugar yield may be attributed to the presented of inhibitors from the degradation of glucose and/or xylose at the observed hydrolysis condition. A_{11} has the least total sugar yield with 9.28 % conversion. From Appendix D the six optimum total sugar yields were obtained from sample B_{12}, B_{21}, C_{11}, C_{12}, C_{21} and C_{31} with 30.67, 33.70, 28.72, 51.83, 29.86 and 30.97 % conversion. Hence, the maximum total sugar yield which is 76.01 g/L was achieved with 1.2 % (v/v) H_2SO_4 at 160 ^{0}C, for 30 min while the minimum was 13.609 g/L achieved with 0.8 % (v/v) H_2SO_4 at 160 ^{0}C, for 15 minutes. Observation shows that the higher the temperature and acid loads the lower the resident time needed to obtain maximum total sugar yield. The maximum total sugar yields are more of glucose than xylose thereby justifying the similarity of Figure (4.4) and (4.6). This could be as a result of higher glucose content than xylose in the WPB. As softwood, the sugars in WPB are hexoses. Based on reports of Carvalheiro et. al., (2008); Taherzadeh et. al., (1999); Millati et. al., (2002) and Schell et. al., (1999), Hexoses are usually two to four times higher than that of pentoses, High yield of glucose and xylose are seen not to be favored by high temperature. 160 ^{0}C is clearly the optimum temperature for optimum yield from the WPB. At a lower temperature of 160 ^{0}C, employing lower H_2SO_4 concentration of 0.8 % (v/v), total sugar yield was more of xylose. It may be that hemicelluloses which exist in armorphous form and are easily degraded by chemicals to their monomer components were degraded more above 160 ^{0}C. It was observed that conversion of available cellulose to glucose was low while hemicellulose was considerably converted to xylose. Consequently, total sugar yield from available holocellulose is low. Also, the concentration of sugar in hydrolyzate is relatively low due to high liquid/solid ratio of hydrolysis process. As acid acts as a catalyst, high concentration of acid speeds up the reaction rate while improving the sugar concentration at low resident time and temperature. The effect of temperature and acid concentration on hydrolysis yields is explained below.

e. Effect of Temperature on Total Sugar Yield at different Acid Concentrations

Figure 4.7 shows that at 0.8 % Sugar yield increased with temperature at the low retention time and showed optimum yield at 30 minutes. At longer retention time of 60 minutes, sugar yield decreases. The reason for this could be longer retention time made the sugars to degrade to form

furfural and HMF. This also confirms that 30 minutes are enough to depolymerize cellulose at their corresponding temperature. Since the concentration of H_2SO_4 was higher at 60 minutes, it means that the hemicellulose may be degraded within 30 min. Thus, the optimum retention time can be expected to occur between 15 and 45 min. This could mean that under mild conditions, it is difficult to reduce lignin from the fiber as lignin is the most stable component in lignocellulosic structure. Figure 4.8 shows that at 1.0 % acid load, though 180 ^{0}C has the maximum sugar yield, it has low set of sugar yield compared to 160 ^{0}C. The optimum retention time for all is in 15 - 32 range. Figure 4.9 shows that at 1.2 % acid load, sugar yield improved at 160 ^{0}C compared to in lower acid load. Sugar yield decreased with increasing temperature at 15 min. 180 ^{0}C or 200 ^{0}C seems not to be optimum temperature for WPB hydrolysis inspite of the acid load and retention time. Though 200 ^{0}C gave higher sugar yield than 180 ^{0}C both are having very low yield compared to 160 ^{0}C. Sugar degraded more with 160 ^{0}C at 60 min retention time. The optimum retention time for all is about 30 min for 160 ^{0}C but 15 min for 180 ^{0}C and 200 ^{0}C.

f. **Effect of Concentration on Total Sugar Yield at Temperatures**

Figure 4.10 shows that at 160 ^{0}C, increasing acid load increases sugar yield. 30 minutes seems to be the best retention time for all while 1.2 % acid load gave the highest sugar yield. Figure 4.11 shows that at 180 ^{0}C, beyond 30 min there is no marked improvement in sugar yield for all the acid concentrations, while 15 min favoured 1.0 % and 1.2 %, 30 mins favoured 0.8 %. Sugar yield seems to cluster at 60 minutes. Figure 4.12 shows that at 200 ^{0}C, Optimom residence time increases uniformly with decrease in acid concentration. So, decreasing acid load increases sugar yield at longer residence period thus the optimum period of 15, 30 and 45 min was observed for 1.2, 1.0 and 0.8 % acid load respectively. From Figure 4.10 - 4.12, it can be deduced that the catalyst activity was proportional to H^+ concentration. The more hydrogen ions formed in the solution, the more rapid the hydrolysis process occurred. However, the sugar concentration decreased at high acid concentration at elevated temperatures with longer reaction time; the longer reaction time at high temperature caused deformation of sugar to inhibitors (furfural and hydroxyl methyl furfural). Applying high acid concentration under harsh conditions, the cellulose fraction was disrupted and glucose generated. The breakage of hydrogen bonds in hemicellulose and cellulose fraction occurred rather abruptly in response to temperature.

g. Effect of Temperature on Glucose Yield at different Acid Concentrations

At 0.8 % acid load illustrated by Figure 4.13, applying lower temperature of 160 ^{0}C gave the lowest glucose yield while 180 ^{0}C and 200 ^{0}C favor high glucose yield. Glucose yield decreased with time in the temperatures. Generally, 0.8 % acid load seems low for high glucose quantity. Figure 4.14 shows that at increased acid load of 1.0 % in increasing the temperature above 180 ^{0}C significantly reduced the glucose yield while 180 ^{0}C improved the yield faster in 15 minutes. The optimum time is within 15 – 30 minutes range for 1.0 % acid concentration. For 1.2 % acid load as seen in Figure 4.15, the reaction speeds up at higher temperature of 180 ^{0}C and 200 ^{0}C but records a low yield compared to 160 ^{0}C which is slower. The optimum time is also within 15 – 30 minutes range. Degradation of glucose is observed at long residence time.

h. **Effect of Acid Concentration on Glucose Yield at different Temperature**

At constant temperature of 160 ^{0}C illustrated in Figure 4.16, 1.2 % acid loads were more favorable and any decrease below this reduces glucose yield. So, glucose yield decreases with decrease in acid concentration. 30 min is the observed optimum reaction time. Figure 4.17 shows that at 180 ^{0}C, increasing acid concentration above 0.8 % improves glucose yield and 1.0 % gave a higher yield than 1.2 %. From Figure 4.18, at 200 ^{0}C, optimum retention time decreases with increase in acid load. 1.2 % and 0.8 % have the maximum and minimum glucose yield respectively.

i. **Effect of Temperature on Xylose Yield at Different Acid Concentrations**

Figure 4.19 shows that at 0.8 % acid load and lowest residence time of 15 min, xylose yield increased with temperature. 180 ^{0}C favoured xylose yield while 160 ^{0}C gave the least yield. At increased acid load of 1.0 % illustreated in Figure 4.20, 15 min is the optimum time for all the applied temperatures. 200 ^{0}C gave the best yield while 160 ^{0}C and 180 ^{0}C showed no much difference in xylose yield. Also, from Figure 4.21, at 1.2 % acid load, increase in temperature above 160 ^{0}C markedly decreased xylose yield, also xylose yield seems uniform at the lowest residence time of 15 min. 160 ^{0}C at 30 min residence time seems to be the optimal for xylose yield with 1.2 % acid load. Hemicellulose is degraded at long residence time beyond 30 min. Thus, for WPB, xylose yield decreases with increase temperature and time.

j. **Effect of Concentration on Xylose Yield at Different Temperatures**

At constant temperature of 160 ^{0}C illustrated in Figure 4.22, low acid load was unfavorable to xylose yield. Increase in acid load from 0.8 to 1.0 % slightly improve yield while 1.2 % has a marked improvement on the xylose yield. 45 min which record considerable yield with 1.2 % acid load is the optimum time with 160 ^{0}C. Figure 4.23 shows that at 180 ^{0}C, increasing acid concentration above 0.8 % decreases xylose yield. Optimum retention time is at the range of 15 – 30 min. At 200 ^{0}C in Figure 4.24, low acid load was unfavourable to xylose yield. Increased acid load of 1.0 and 1.2 % has a marked improvement on the xylose yield and have no marked difference in yield within 30 min. For 200 ^{0}C, the optimum time is 15 min for the entire acid load. Generally, it was observed that acid hydrolysis at increased acid load and temperatures degrade xylose to furfural, glucose to HMF and lignin to phenol, and could be the cause of decline in sugars beyond optimum hydrolysis time.

4.2.5 Preliminary Fermentation Result

Samples B_{12}, B_{21}, C_{11}, C_{12}, C_{21} and C_{31} of volume 1.68, 1.58, 1.74, 1.6, 2.02 and 1.495 L respectively were fermentated using 0.1 L (100 ml) of S. cerevisiae innoculum at room temperature for 5 days to maximize bioethanol yield. Base on the theoretical bioethanol yield of the samples, the expected bioethanol yield are 22.985 g/L, 25.257 g/L, 21.52 g/L, 38.84 g/L, 22.375 g/L and 23.213 g/L respectively. Bioethanol production was monitored at 24 h interval of S. cerevisiae cultivation. Increase in broth temperature was observed confirming fermentation an exothermal process. Fermentation ends when the reading became constant. Foam which has been a clear indication of fermentation was noticed within 24 h in $B_{21,}$ C_{12} and C_{21} and within 72 h in others. This means that the yeast cell adapted slowly to all medium but faster in $B_{21,}$ C_{12} and C_{21}. The broth was filtered to separate the feed from the slurry. The absorbances of the samples as read from the spectrophotometer are presented in Appendix E1. Also, the observed readings of bioethanol yield are given in Appendix E2 but illustrated in Figure 4.25.

Figure 4.25 shows higher bioethanol yield for $C_{11,}$ C_{12}, B_{21} and C_{31} from the first 24 h inspite of slow fermentation speed. This proves that fermentation started in all irrespective of the presence of foam. Bioethanol yield started in all media at early stage of fermentation and continuously increased to maximum level of 15.842 g/L, 18.275 g/L within 48 h in $B_{21,}$ and C_{21} respectively. These corresponded to fermentation efficiency of 62.73 % and 81.68 %, respectively. Other

samples recorded maximum bioethanol yield on day 3 which are 10.564, 19.568, 19.999 and 32.01 g/L for $C_{11,}$ B_{12} C_{31} and C_{12} corresponding to fermentation efficiency of 49.09 %, 85.13 % , 86.15 % and 82.42 % respectively. B_{12}, B_{21}, C_{11}, C_{12}, C_{21} and C_{31} made total bioethanol yield of 32.874 g, 25.03 g, 18.38 g, 51.22 g, 36.92 g and 29.9 g respectively. It was observed that samples with higher sugar concentration resulted in higher yield of bioethanol; this confirms carbon source from the sugar as the nutrient for yeast fermentation process. The available total sugar was considerably fermented. The high fermentation efficiency suggests that higher bioethanol yield is better controlled or enhanced at hydrolysis stage to ensure higher quantity of available sugar. After the fermentation optimum time, the cell growth became stagnant and entered the stationary phase while bioethanol production declined slightly thereafter. This might be due to the depletion of carbon source and hence the reverted consumption of the accumulated bioethanol by the organism. Glucose been a growth-limiting factor in fermentation may have hindered the innoculum concentration from having more efficient effect on bioethanol yield.

Inspite of the likely presence of furfural and HMF, the hydrolysate was fermentable by S.cereviciae. One possible explanation for this is that S.cerevicea converted furfural into furfuryl alcohol and furoic acid by emzyme alcohol dehydrogenase and by emzyme aldehyde dehydrogenase, respectively. It also converted HMF into its corresponding alcohol 5-hydroxymethyl-furfural alcohol. The high bioethanol yield and the ability of the yeast to consume furfural and HMF may suggest the concentrations of those inhibitors were relatively low and at tolerable levels for S.cereviciae used in this research. Though innoculum concentration has been proved by Cheng et. al., (2007) not to influence the final amount of bioethanol produced but rather affects the duration of fermentation process. Thus the growth of yeast differs with innoculum concentration; a phenomenon known as diauxic growth which is caused by a shift in metabolic pathway in the middle of growth cycle. To enhance the fermentation in future operation more innoculum concentration could be used, the process to consume the nutrients will become shorter since the growth of yeast becomes dominant against sugar acting as a growth-limiting factor; consequently, efficiency is expected to improve.

It can be concluded 2-3 days, mostly 3 days is actually enough to produce bioethanol by S.cerevisiae. Theoretically, 100 g of glucose will produce 51.4 g of bioethanol and 48.8 g of CO_2. However, in practice, the microorganisms use some of the glucose for growth and the

actual yield was less than 100 %. WPB is a potential and desirable raw material for bioethanol production in Nigeria. The optimum sample C_{12} data was adopted for the distiller design.

4.2.6 Distiller Operation Result

Based on the optimum preparation step as ascertained from the preliminary experiment, 2.5 kg of ground sample was hydrolyzed with 1.2 % H_2SO_4 and 25000 ml H_2O at 160 ^{0}C for 30 minutes. The hydrolyzed sample was neutralized to 4.8 pH with 2M NAOH and then fermented at room temperature for 3 days with 1250 ml innoculum of S.cereviasea to obtain 20 L fermentate which is the boiler feed capacity. Observed change in yield with temperature and time during distillation process is given in Appendix F while the yield curves are given in Figure 4.26 – 4.29.

a. Bioethanol Fuel Yield

It was observed that it took 95 minutes to boil the feed to the boiling point of bioethanol when charcoal fuel was used as heat source as shown in Figure 4.26. From Appendix F, this bubble time corresponded with the observed temperature and vapor pressure of 96 ^{0}C and 2.81 bar respectively. Figure 4.26 shows a progressive yield of bioethanol fuel from 95 minutes to a maximum at 115 minutes after which its yield became constant. 115 and 120 minutes recorded a constant yield while the 3 runs have a very close yield just before 110 minutes. This means that bioethanol yield stopped at 115 minutes. This observation clearly showed that constant and sufficient heat source was used for the distillation process. It also indicated that regression (backward movement) in the distillation process was avoided. Total bioethanol fuel distilled after 20 minutes from the bubble point was 817 ml resulting to 2451 ml per hour of distillation.

b. Time Interval Distillation Rate

It can be deduced from Figure 4.27 that in all the runs, highest yield rate of bioethanol at interval time was observed at 5 min from the bubble point and similar trend were observed up to the 5 min. Beyond 5 min, first and second run showed similar trend slightly different from the third run. Highest yield rate of bioethanol at interval time decrease from 4080, 4104 and 4056 ml/h at 100 min to 744, 660 and 600 ml/h at 115 min for Run 1, 2 and 3 respectively. But, they all have common interval yield rate at about 13 min from the bubble point. This confirms that the distiller showed reasonable consistency throughout the operation.

c. Observed Distillation Productivity

Figure 4.28 gave close maximum and minimum productivity at 105 and 115 min which are 0.0834, 0.084 and 0.083; and 0.0501, 0.05 and 0.0496 for the Run 1, 2 and 3 respectively. This means that distiller showed reasonable consistency in its operation. Maximum productivity was attained at the time corresponding to highest distillation rate. Productivity is the bioethanol yield per period divided by the bioethanol content of feed. It can be deduced from the curve that distillation is a removal process from the boiler point of which material been removed decreases with increase in temperature and time.

d. Observed Distillation Efficiency

Figure 4.29 showed that distillation efficiency increased with time to a maximum at 115 min in all the runs. Comparing productivity and efficiency curves, it can be seen that maximum efficiency occurred at the point of minimum productivity. Thus, this is a case in which increased efficiency justifies decreased productivity. It indicates that the distiller did a quality work though it has small feed capacity, thereby encouraging its adoption and improvement to a larger scale. The distillation efficiency was found to be 99.18 % in the 3rd Run but slightly above 100 % in the 1st and 2nd Run i.e. 100.16 and 100.04 % respectively. Noting that, distillation process is affirmed on the principle of conservation of matter which says that matter can neither be created nor destroyed. Therefore, the excess in the 1st and 2nd run may be as a result of increased fermentation efficiency and/or traces of water. The progressive level of bioethanol yield with time to the observed maximum yield prior to the eventual gradual decrease to no yield as presented in Appendix F, and Figure 4.26 – 4.27 affirmed that bioethanol yield was well regulated by the constructed distiller. Bioethanol yield expressed as g bioethanol per total g of feedstock utilized, using Equation 2.110 is 0.2565 (g g^{-1}), while yield in liters per volume of feed used, calculated with Equation 2.111 is 0.041 (L L^{-1}). This shows that bioethanol concentration was low compared to the volume of feed. Increasing bioethanol concentration in the feed before distillation will increase productivity as well as reducing the production costs.

4.2.7 Distiller Performance

The distiller performed at actual combustion efficiency of 75 %. Distillation process was ascertained to yield 815.67 ml bioethanol quantity in 20 min from bubble point of 99.6 ^{0}C. Heat energy needed to distill the feed was found to be 32212 kJ/h using Equation 2.29. Equation 2.31

gave the reactor power rating required to supply this energy as 8.95 kW. Distiller performance data are presented in Table 4.3. It was observed that it took about 95 min to boil the feed to the bubble point of the bioethanol. Distillation ended in 115 min with 817 ml, 816 ml and 809 ml bioethanol yield for the 3 distillation runs respectively. Distillate was collected as liquid thereby confirming complete condensation and high condensation efficiency.

Table 4.3 showed that ignition of the charcoal was easily achieved within 4 to 7 min with 10 ml kerosene. The combustion zone velocity was actually found to be 0.3043 (cm/min) against 0.583 (cm/min) expected. Apart from possibility of absorbing moisture from the environment and fluctuation in natural air flow, the observed low velocity may be due to charcoal porosity and packing in the reactor which influences pressure draft in terms of air flow channel across the fuel bed. However, complete combustion was achieved, proving good quality of the charcoal specie and sufficient air supply into the fuel column during firing. Smoke emission was clear of soot, all charcoal reduced to ash and foul odor was not observed during the process. The total operating time observed is 115 min which is 55 min more than expected. The extra time may be accounted to the increased yield resulting from increased fermentation efficiency. The operation was stopped at 120 min and reactor consumed 2.2 kg charcoal at the rate of 1.83 kg/h. This is 0.527 kg more than expected which may account for the heat used in heating the boiler material and increase yield and the increase in specific gasification rate. As vapor rises from the mixture, it moves up the apparatus raising the temperature of the apparatus. The distiller was designed at reactor calorific efficiency of 75 % with 8.95 kW power input. In the course of operation, actual calorific efficiency was found to be 55 % with 12.2 kW power input. These also suggest that the purchased charcoal is having a lower calorific value than the design expected, showing that it contains less quantity of acacia specie. Inefficiencies include incomplete combustion as well as heat losses. Boiling temperature of the bioethanol was observed to be a range than a point, taking place at temperature and vapor pressure range of $96 - 98\ ^{0}C$ and 2.81 – 3.01 bars respectively from 95 min. The distiller showed very close performance rate even at 30 L feed/h load. This suggests an optimum capacity range for the boiler to be ½ - ¾ feed of its volume. Below this capacity, the rising vapor will lose energy and cool down before it reaches the condenser, as such the yield will be low. The following observations were also made on the reactor during the design and fabrication of the distiller.

1. The power output of the reactor is highly dependent on the diameter. This may have been due to the fact that the energy released increased as more fuel is expected to be burnt per unit time with increase in diameter.
2. Increase in reactor height will result in increase in operating time. This could be because combustion zone has to move through a longer distance along the reactor height
3. For an inverted down-draft type reactor, the firing of fuel on top was observed to be the best and easiest way. Firing the fuel in this manner minimized smoke emission. However, reloading of fuel in between operation was not easy due to heat radiation. Reloading of fuel during operation will be easier when burning of fuel starts from the bottom of the reactor.
4. Ash layer under the grate helps in drying fresh charcoal for oncoming combustion.

4.2.8 Fuels Characterization Result

In evaluating the suitability of the produced bioethanol as alternative biofuel, blendable with the existing petrol for use in spark ignition engine, it was characterized according to ASTM standard test procedures for bioethanol as explained in chapter three.

a. Elemental Analysis of the Product Fuel

The obtained elemental analysis results are presented in Table 4.4 and compared to ASTM D4806 specification for fuel ethanol. Table 4.4 gave the percentage purity of the produced fuel as 97.68 % making it suitable for blending with pure petrol for use as SI engine fuel. Ash which can result from water soluble metallic compounds, extraneous solids such as dirt and rust was observed to be suitably lower than the maximum value 0.05 % set by the ASTM. Water content is 0.42 % by volume per 100 ml of sample. This is less than the maximum 1.0 % recommended. Noting that some degree of water contamination is practically unavoidable in transport and handling, and bioethanol is miscible with water, the 0.42 % water content can be seen as dissolved moisture of negligible quantity ensuring significant reduction of potential problems caused by water presence in fuels.

Organic acids such as acetic (CH_3COOH) are highly corrosive to many metals and need to be kept at a very low level in fuels. Acidity was found to be 5.05 mg/L and less than the 56 mg/L maximum limit tolerated by the ASTM. When pH is below or above a certain range, fuel pumps can malfunction as a result of film forming between the brushes and commutator, fuel injectors can fail from corrosive wear, and excessive engine cylinder wear can occur; fuel pump plastic

parts can fail. Thus, 6.5 – 9.0 range is recommended. The observed pH falls within this range been '6.61' making the produced bioethanol suitable for wider range blending with petrol. Elemental analysis of the produced bioethanol satisfies the ASTM D4806 specification thereby confirming it blend able with pure petrol for use as spark ignition fuel. Blending bioethanol and pure petrol produces a mixture with its own unique physical characteristics.

b. Fuel Properties of the Sample Fuels

Different blends of the bioethanol and petrol were then formulated and characterized to further determine their conformity with the ASTM D4814 standard specification for automotive SI engine fuel. This was done according to ASTM standard test procedures for gasoline, bioethanol, and gasoline-oxygenated fuels, at NNPC Port Harcourt Refining Company Limited, Elesa-Eleme, Port Harcourt, Rivers State. The fuel properties analysis results obtained are presented in Table 4.5.

i. Effects of Blend Ratios on Viscosity

Kinematic viscosity of the produced bioethanol fuel at 40 ^{0}C is higher at 1.6692 compared to pure petrol which is 0.6097. Adding bioethanol to petrol was observed to increase the viscosity of blends. However, fear of poor atomization and leaks associated with high and low viscosity respectively is ruled out.

ii. Effects of Blend Ratios on Density

Figure 4.30 illustrates the densities of the sample fuels at 15 ^{0}C. It shows that densities of the sample fuels increased from 744.43 kg/m^3 for pure petrol to 782.5 kg/m^3 for E60 while the product fuel E100 has 791.13 kg/m^3 density making 6.23 % increment. The produced bioethanol has higher density than pure petrol and increases the density of its blends with pure petrol. As the percentage of bioethanol increases in the blend the denser the blend becomes. Pure petrol density increased by 0.39, 1.1, 2.04, 3.24, 4.42 and 5.07 % respectively with E10, E20, E30, E40, E50 and E60. Density is the basic gauge of fuel adulteration, and is indirectly related to temperature. Fuel density has the greatest impact of fuel capacity. Hence, it is advice to 'tank up' vehicles in the morning and evening when fuel is denser with small volume, to get more value for your money spent. Since fuel is sold volumetrically, higher density promises greater potential energy.

iii. Effects of Blend Ratios on Flash Point

Observed flash point of produced bioethanol is 12.8 ^{0}C while other blends has flash point below 10 ^{0}C. Flash point indicates the lowest temperature at which the vapor overhead the sample is ignitable with the application of an ignition source under specified conditions. It predicts the temperature at which the vapor pressure reaches the lower flammable limit. The result presented in Table 4.5 shows that all the blends are susceptible to ignition and has the chance of flammability hazard. The flash point of the bioethanol is high compared to -69 ^{0}C for petrol, indicating that it is safer than petrol regarding its handling, transportation and storage. Increase in bioethanol percentage continuously increases the flash point of pure petrol from -69 ^{0}C to -4.8 with 60 % bioethanol. Thereby increasing its safety handling, transportation, storage and flammability limits. Flash point and flammability limits of a fuel describe its flammability. Flammability limits is the maximum and minimum concentrations of combustible vapor in the air and the temperatures at which the vapor occurs, that will propagate a flame after sufficient ignition energy is provided. Thus high flammability limits promotes safety handling of fuel.

iv. Effects of Blend Ratios on Calorific Value

Figure 4.31 illustrates the calorific value of the sample fuels. The calorific value or heat of combustion is a measure of the energy available from a fuel. Knowledge of this value is essential when considering the thermal efficiency of equipment for producing either power or heat. The calorific value of the product bioethanol was found to be 29.16 MJ/kg while pure petrol measured 43.62 MJ/kg on weight basis. The produced fuel (E100) calorific value is 31.73 % less than that of pure petrol. It is deduced from the graph that the calorific value of pure petrol steadly decreased as bioethanol content increased in the blends. It decreased to 33.73 MJ/kg in E60. Product bioethanol has a lower calorific value than pure petrol, which reduced the energy content of the fuel. However this can be partly offset by the higher Octane Number of the bioethanol.

v. Effect of Blend Ratios on Octane Number

Figure 4.32 illustrates the octane number of the sample fuels. The octane number of the bioethanol fuel was measured to be 124 which is higher than 89.2 for pure petrol with 39 % increament. Figure 4.32 shows that the octane number of pure petrol increased continuously and linearly with percentage increase of bioethanol in the blends to 100 in E60. This could be because of higher oxygen content and octane number of the product bioethanol fuel resulting to a

gradual shift from normal heptane (C_7H_{16}) to ideal iso-octane (C_8H_{18}) of the blends. Pure petrol having lower octane number and higher calorific value will burn faster than the bioethanol and its blends having lower calorific value and higher octane number. Notwithstanding, octane number been a measure of the ignition quality of a fuel of which high octane number means more efficient ignition and consequent higher engine performance, proves that the presence of bioethanol in the blends will improve petrol engine performance as the octane number increased with increase in bioethanol in the blends. Therefore fear of auto-ignition and knocking effect could be ruled out in applying these blends. This suggests the produced bioethanol as an effective compound for increasing the value of petrol octane number.

vi. Effect of Blend Ratios on Vapor Pressure

Figure 4.33 illustrates the vapor pressure of the sample fuels. Vapor pressure of the bioethanol was found to be 13.043 kpa which is 72.9 % lower than 48.1 kPa for pure petrol. 10 % bioethanol in pure petrol increased its RVP to a peak value of 53 kPa suggesting that it could reduce the risk for a flammable mixture forming than other blends. Figure 4.33 clearly shows that further increase in the bioethanol above 10 % declines the blend vapor pressure and the decrease is not linear. Product bioethanol has fewer highly volatile components than pure petrol which suggest that it will have less emissions resulting from evaporation. However, when added to pure petrol, the vapor pressure of the blend was increased thereby increasing evaporative emissions. This could be because in its pure form, bioethanol molecules are polar and bond to each other via the hydroxyl (OH) groups. These forces of attraction prevent the molecules from leaving the liquid but in the presence of hydrocarbons, the bonding was weakened. It is expected that at a point addition of bioethanol will not further boost the vapor pressure. It can also be deduced that bioethanol contents higher than 40 % will increase the risk that vapor will form with pressures under the upper flammability limit. However, the blends ensure products of suitable volatility performance.

vii. Effect of Blend Ratios on Distillation Profile

Figure 4.34 presents the distillation profile of the fuel blends from their initial boiling point (IBP) to 90 % distillate, while the profile readings are given in Appendix G. The distillation profile (volatility profile) for the produced bioethanol has IBP of 79 ^oC, 99 ^oC at 90 %vol and EBP of 101 ^oC with total distillate of 97 %vol while petrol has IBP of 44 ^oC, 181 ^oC at 90 %vol and EBP

of 205^{o}C with total distillate of 98 %vol. Temperature of pure petrol when 10 % was distilled is 61^{o}C (i.e. T_{10}), with respect to this temperature E10, E20, E30 and E50 decrease by 6.56 %, 3.28 %, 3.28 %, and 1.64 %, while E40 and E60 increased by 1.64 % and 6.56 % respectively. Decrease of 3.74 %, 36.64 %, 30.84 %, 28.97 %, 28.97 % and 29.91 %, was observed with E10, E20, E30, E40, E50 and E60 respectively for T_{50} (107 ^{0}C), while decrease of 1.1 %, 1.66 %, 3.31 %, 3.87 %, 45.86 % and 56.69 %, respectively at T_{90} (181 ^{0}C). Compared to pure petrol, the distillation curve for each blend was significantly depressed between T_{10} and T_{50} distillate. The curve depression could be attributed to presence of the bioethanol in blends which increased its volatility. This may expect problem with cold starting and vapour lock. The resulting T_{10} is sufficiently low to allow enough fuel to evaporate and form a combustible mixture. T_{50} point associated with engine warm up; is sufficiently low to allow the engine to warm up and gain power quickly without stalling. T_{90} associated with the crankcase dilution and fuel economy; is not expected to be high. If T_{90} is too high, the larger fuel molecule will condensate on the cylinder liners and pass into the lubricating oil in the crankcase instead of burning; this could then be avoided with the blends. Blending pure petrol with the bioethanol increased the volatility, decreases the 50 % distillation point $T_{50,}$ and improved its fuel quality.

viii. **Drivability Index**

This is a measure of the volatility characteristics of a fuel. High DI is normally associated with low volatility. It was calculated based on the relationship between the distillation temperatures of the fuel, cold start and warming up parameters of a vehicle. The driveability index of pure petrol was found to be 723.84 ^{0}C, and reduced with the presence of the bioethanol but not linearly. Pure petrol has the highest DI compared to other fuel samples while E60 has the least with 532.57 ^{0}C. This proves that pure petrol is less volatile and E60 is most volatile. Since low driveability is preferable in an engine, it means the bioethanol improved driveability and volatility of pure petrol; and thus its cold start and warm up performance. High DI causes poor fuel evaporation in cold start, leading to lean A/F ratio, unstable combustion, HC emission, piston and cylinder wear especially in carburetors. This is normally offset by automatic increase in injected fuel or choking in carburetor to achieve a rich mixture which results to more HC emission. Therefore,

engine need to be warmed up for at least 10 – 15 minutes to bring it to its normal operating tempemrature. DI of all the sample fuels ranges from 532.57 ^{0}C - 723.84 ^{0}C in Table 4.45.

ix. Comparison of Fuel Properties with Literature

Comparing with bioethanol from other feedstocks, reported density of product fuel is 767 kg/m^3 while literature has 785 kg/m^3 from Potato waste by Talal et. al., (2012); 789 (kg/m^3) from Sugar cane-palmwine-raffia trunk by Nwufor et. al., (2014), and Maize-raffia wine-palmwine by Tangka et. al., (2011). Reported viscosity '1.6692' is higher than 1.1 reported by Talal et.al., (2012). Reported calorific value '29.16 MJ/kg' is higher than that recorded by Talal et.al., (2012) and Tangka et. al., (2011) but 29.78 MJ/kg from Nwufor et. al., (2014). Octane number '124' is higher than 108.6 and 114 but 129 recorded by Talal et.al., (2012), Nwufor et. al., (2014) and Tangka et. al., (2011) respectively. RVP is 13.043 kPa and higher than 9 and 9.5 but 48 reported by Tangka et. al., (2011), Nwufor et. al., (2014) and Talal et.al., (2012), respectively. Distillation profile 79 - 101 ^{0}C is higher than 55 – 68 reported by Nwufor et. al., (2014). Flash point is 12.5 ^{0}C agrees with Nwufor et. al., (2014) and Tangka et. al., (2011) but Talal et.al., (2012) that reported 14 ^{0}C. Auto-ignition which is 328 ^{0}C is lower than 365 ^{0}C and 336.7 ^{0}C reported by Talal et.al., (2012) and Nwufor et. al., (2014) respectively. Though, the product fuel has lower density and consequent lower potential energy, its high viscosity which rules out poor atomization; and its high octane number which means more efficient ignition and consequent higher engine performance suggests it an effective compound for improving petrol fuel quality and recommends their blends for use in spark ignition engines. The reported results are in conformity with ASTM D4806 and D4814 specifications.

4.2.9 Engine Performance

A single cylinder, 4-stroke petrol engine model IMEX G200 was used for the engine test. Engine performance parameters were obtained at constant load test carried out at full, 3/4 and 1/2 load conditions, and constant speed test conducted at 2500 rpm, 3000 rpm and 3500 rpm respectively. The performance data obtained are tabulated in Appendix H and Appendix I while the results are analyzed and presented in graphical form.

a. Constant Engine Loads Results

SI engines are governed by opening and closing of throttle valve which regulates the mass of charge to the cylinder. Different engine load simply means varying the throttle valve opening which in turn varies quantity of charge flow into the combustion chamber. At constant engine load tests, the performances of the candidate fuels are compared with the results obtained with the baseline fuel, the pure petrol.

i. Effect of Blends on Fuel Consumption under Full-Load Conditions

Figure 4.35 illustrates the fuel consumption of blends under full-load conditions. It was observed that fuel consumption gradually decreased with increase in engine speed in all the blends. This could be due to reduced mass of aspirated air which in turn reduces air charge density. Among the candidate fuels, E20 gave the best fuel consumption followed by E30. Fuel consumption rate is the quantity of blend passing a point per unit time. It is directly dependent on density and volume of blend flow, which differs with the blends. Volume of blends flow differs because their densities differ.

ii. Effect of Blends on Fuel Consumption under ¾-Load Conditions

Figure 4.36 illustrates the fuel consumption of blends under ¾-load conditions. Fuel consumption was observed to gradually decrease as the engine speed increased in all the blends. This could be due to reduced mass of aspirated air which in turn reduces air charge density. Among the candidate fuels, E20 gave the best fuel consumption.

iii. Effect of Blends on Fuel Consumption under ½-Load Conditions

Figure 4.37 illustrates the fuel consumption of blends under ½-load conditions. Fuel consumption gradually decreases as the engine speed increased in all the blends. This could be due to reduced mass of aspirated air which in turn reduces air charge density. The blends gave higher range of speed than pure petrol. Among the candidate fuels, E20 consistently gave the best fuel consumption while E10 showed low fuel consumption from a certain point. Figure (4.35) – (4.37) show that fuel consumption of blends increased as the engine load increased. At the entire engine load, consumption rate of pure petrol is reduced with E20, also with E10 but at ½-load conditions.

iv. Effect of Blends on Brake Power under Full-Load Conditions

Figure 4.38 illustrates the graph of brake power of the blends under full-load conditions. Bioethanol blends show similar trend of brake power with pure petrol. Brake power of pure petrol was slightly increased by the bioethanol blends. The increase in brake power could be due to increase in octane value caused by the bioethanol content in the blends. This is because addition of the bioethanol increased blend octane number which improved anti-knock behavior thereby allowing a more advanced timing that resulted in higher combustion pressure and thus higher torques. Also higher heat of evaporation of bioethanol provides fuel-air charge cooling. This increases the density of the charge, and thus higher power output is obtained. Resulting speed of pure petrol was improved by the bioethanol content. Brake power was observed to increase steadily with increase in speed to a peak value and then decrease with further increase in speed. Decrease in brake power is because at higher speed, engine is unable to induce a full charge of air, so, torque and brake-power decreased. When running the engine on pure petrol, E0, engine speed was observed to be in the range of 2982 – 3110 rpm. Higher speed range, 3027 – 3163 rpm, 2970 – 3071 rpm, and 2988 – 3123 rpm were observed with E10, E20 and E30 respectively. Thus, maximum speed of pure petrol was increased from 3110 rpm to 3163 rpm by E10, to 3071 rpm when running on E20 and to 3123 rpm when running on E30. The observed peak brake power and its corresponding optimum speed are 0.874 kW at 3628 rpm, 0.882 kW at 3638 rpm, 0.917 kW at 3574 rpm and 0.928 kW at 3570 rpm with E0, E10, E20 and E30 respectively. E10 has the highest optimum speed while E30 gave the highest peak brake power.

v. Effect of Blends on Brake Power under ¾-Load Conditions

Figure 4.39 illustrates the graph of brake power of the blends under ¾-load conditions. The curves for bioethanol blends show similar trend of brake power with pure petrol. Brake power of pure petrol was improved by bioethanol content. This is because addition of the bioethanol increased blend octane number which then resulted in higher combustion pressure and thus higher torques. Also higher heat of evaporation of bioethanol provides fuel-air charge cooling and increases the density of the charge, resulting to higher power output. As in Figure (4.38), brake power was observed to increase steadily with increase in speed to a peak value and then decrease with further increase in speed. When running the engine on pure petrol, engine speed was observed to be in the range of 2982 – 3110 rpm. But 3027 – 3163 rpm, 2970 – 3071 rpm and 2988 – 3123 rpm was observed with E10, E20 and E30 respectively. Thus, maximum speed of

pure petrol was increased from 3110 rpm to 3163 rpm by E10, to 3071 rpm when running engine on E20 and to 3123 rpm with E30. The observed peak brake power and its corresponding optimum speed are 0.743 kW at 3083 rpm, 0.768 kW at 3146 rpm, 0.777 kW at 3048 rpm and 0.784 kW at 3091 rpm when running on E0, E10, E20 and E30 respectively.

vi. Effect of Blends on Brake Power under ½-Load Conditions

Figure 4.40 illustrates the graph of brake power of the blends under ½-load conditions. It show similar trend of brake power with that of pure petrol. Brake power of pure petrol was improved by bioethanol content. The increase in brake power could be due to increase in cylinder pressure caused by the bioethanol content in the blends. Also higher heat of evaporation of bioethanol provides fuel-air charge cooling and increases the density of the charge, and thus higher power output is obtained. Brake power was observed to increase steadily with increase in speed to a peak value and then decrease with further increase in speed. Decrease in brake power is because at higher speed engine is unable to induce a full charge of air, so, torque and break power decrease. When running the engine on pure petrol, engine speed was observed to be in the range of 2710 – 3049 rpm. But 2817 – 2887 rpm, 2842 – 3026 rpm and 2846 – 3206 rpm was observed with E10, E20 and E30 respectively. Thus, maximum speed of pure petrol was increased from 3049 rpm to 3206 rpm with E30 while E20 and E10 reduced it to 3026 rpm and 2887 rpm respectively. Observed peak brake power and its corresponding optimum speed are 0.75 kW at 2982 rpm, 0.68 kW at 2872 rpm, 0.745 kW at 2984 rpm and 0.794 kW at 3178 rpm with E0, E10, E20 and E30 blends respectively.

Power output of an engine is largely a function of the amount of heat that can be released in the combustion chamber which is determined by the amount of air available and fuel quality. Figures (4.38) – (4.40) show that both brake power output and its resulting speed of pure petrol and bioethanol blends increased with increase in engine load. Peak brake power of each candidate fuel occurred at different speed indicating variation in the physico-chemical characteristics of the blends. At the entire engine load condtion, the engine developed maximum peak brake power with E30 which are 0.928 kW at 3570 rpm, 0.784 kW at 3091 rpm and 0.794 kW at 3178 rpm under full, 3/4 and ½-load conditions respectively. The addition of 30 % bioethanol might then be the optimal blend for increasing the brake power and be an appropriate blend for the engine compression ratio. Engine speed for all bioethanol blends ranges from 3532 rpm to 3658 rpm under full-load conditions and 2817 rpm to 3206 rpm at ½-load conditions.

vii. Effect of Blends on Brake Specific Fuel Consumption under Full-Load Conditions

Figure 4.41 illustrates variation of brake specific fuel consumption (BSFC) under full-load engine condition. The graphs show similar trend for all the fuels. BSFC was observed to decrease with increase in speed to a minimum value and then increase with further increase in speed. The curves showed minimum BSFC of 0.393 kg/kW-h when engine was running on pure petrol. Minimum BSFC of 0.389 kg/kW-h, 0.379 kg/kW-h and 0.39 kg/kW-h were observed when the engine was running on E10, E20 and E30 respectively. At full-load conditions, running the engine on E20 gave the lowest BSFC of 0.379 kg/kW-h compared to 0.393 kg/kW BSFC obtained with pure petrol.

viii. Effect of Blends on Brake Specific Fuel Consumption under ¾-Load Conditions

Figure 4.42 illustrates variation of brake specific fuel consumption under ¾-load engine load. The graphs showed similar trend for all the fuels. BSFC was observed to decrease with increase in speed to a minimum value and then increased with further increase in speed. The curves showed minimum BSFC of 0.405 kg/kW-h when the engine was running on pure petrol. Minimum BSFC of 0.374 kg/kW-h, 0.386 kg/kW-h and 0.422 kg/kW-h were obtained when the engine was running on E10, E20 and E30 respectively. The curves showed that lowest BSFC of 0.374 kg/kW-h was obtained when running the engine on E10 under 3/4 load condition. Also, E10 and E20 improved the minimum BSFC of pure petrol by 7.65 % and 4.69 % respectively.

ix. Effect of Blends on Brake Specific Fuel Consumption under ½-Load Conditions

Figure 4.43 illustrates variation of BSFC under ½-load conditions. It showed similar trend for all the fuels. BSFC was observed to decrease with increase in speed to a minimum value and then increased with further increase in speed. The curves showed minimum BSFC of 0.435 kg/kW-h when engine was running on pure petrol. Minimum BSFC of 0.41 kg/kW-h, 0.426 kg/kW-h and 0.437 kg/kW-h were observed when the engine was running on E10, E20 and E30 respectively. Lowest BSFC was obtained with E10 under ½-load conditions. E10 and E20 improved the minimum BSFC of pure petrol by 5.75 % and 2.07 % respectively.

Figures (4.41) – (4.43) show that, each fuel BSFC curve has a minimum point which indicates point of maximum fuel economy and thermal efficiency of the particular fuel. It further suggests that BSFC is an inverse of fuel economy. The minimum BSFC lies between different speed

range for different fuel and different engine load indicating that the fuels gave different speed under the engine load conditions. The rise in BSFC at lower and higher speed could be attributed to rising friction losses at high speed and increased time for the heat transfer from the working fluid to the cylinder walls at low speed; both conditions increase fuel consumption. Whatever increases fuel consumption will increase BSFC because they are directly related. BSFC of all the fuel slightly increased as engine load increased. Since the bioethanol reduced the heating value of blends, extra fuel could be consumed with increase in bioethanol content to produce high power output than pure petrol. Though E30 has higher brake power output, E10 and E20 has better fuel economy. It could be deduced that BSFC decreased with increase in bioethanol percentage as engine load increases. This may be a consequence of the behavior of the engine brake thermal efficiency.

x. Effect of Blends on Brake Thermal Energy under Full-Load Conditions

Figure 4.44 illustrates the variation of candidate fuels brake thermal efficiency (BTE) with speed at different full engine load. Brake thermal efficiency of candidate fuels was observed to increase with increase in engine speed to a peak point after which it decreased with further increase in speed. Pure petrol showed maximum brake thermal efficiency of 21.02 % under full engine load. Brake thermal efficiency was higher than those of pure petrol by 5.33 %, 12.18 % and 13.65 % when the engine was operated with E10, E20 and E30 under full load condition. At full load conditions, highest BTE of 23.89 % was achieved when engine was operated with E30.

xi. Effect of Blends on Brake Thermal Energy under ¾-Load Conditions

Figure 4.45 illustrates the variation of candidate fuels brake thermal efficiency with speed at ¾-load conditions. Brake thermal efficiency of candidate fuels was observed to increase with increase in engine speed to a peak point after which it decreased with further increase in speed. Pure petrol showed maximum brake thermal efficiency of 18.81 % under ¾ engine load. Brake thermal efficiency was higher than those of pure petrol by 22.6 %, 23.23 % and 23.44 % when the engine was operated with E10, E20 and E30 under ¾-load conditions. At ¾-load conditions, highest brake thermal efficiency of 23.22 % was achieved when the engine was operated with E30 blend.

xii. Effect of Blends on Brake Thermal Energy under ½-Load Condition

Figure 4.46 illustrates the variation of candidate fuels brake thermal efficiency with speed at 1/2 engine load. Brake thermal efficiency of candidate fuels was observed to increase with increased in engine speed to a peak point after which it decreased with further increase in speed. Pure petrol showed maximum BTE of 18.99 % under ¾ engine load. Brake thermal efficiency was higher than those of pure petrol by 10.64 %, 10.8 % and 12.53 % when the engine was operated with E10, E20 and E30 under ½-load conditions. At ½-load conditions, highest BTE of 21.37 % was achieved when the engine was operated with E30.

Figures (4.44) – (4.46) show that brake thermal efficiency of pure petrol was improved by bioethanol blends in the entire engine load. The increment in brake thermal efficiency could be as a result of decrease in calorific value of the blends caused by bioethanol content. It was observed that brake thermal efficiency of candidate fuels increased with increase in engine speed to a peak point after which it decreased with further increase in speed. Decrease brake thermal efficiency at higher speed could be due to increase in fuel consumption and high friction losses at such points. Increase in engine load seems to increase brake thermal efficiency though the increment is small. Brake thermal efficiency of pure petrol was mostly improved by E30, E20 and E10 under ½-load, ¾-load and full-load conditions respectively. This means that increase in the bioethanol content increases brake thermal efficiency of pure petrol even as engine load increases. This might be due to bioethanol's higher heat of vaporization which provides cooling effect to the cylinder air-fuel charge thereby increasing its density and power output. Added bioethanol produce lean mixture that increased the relative air-fuel ratio to a higher value and make burning more efficient.

b. Constant Engine Speeds Results

The constant speed test was first conducted with pure petrol to establish baseline for the candidate fuels. The performance of the candidate fuels are compared with the baseline results.

i. Effect of Blends on Fuel Consumption at Engine Speed of 2500 RPM

Figure 4.47 illustrates the graphs of fuel consumption of the blends at engine speed of 2500 rpm. It was observed that as bioethanol content in the blend increases so the fuel consumption increased. The fuel consumption gradually increased with increased BMEP to about 2.6 bar and then increased more sharply with further increase in BMEP. At 2500 rpm, fuel consumption of blends is higher than then

that of pure petrol with E10 having closer values to pure petrol. Maximum fuel consumption of 0.942 kg/h was observed when engine was running on E30. This is 3.403 % more than quantity of pure petrol consumed at this same engine operating conditions.

ii. Effect of Blends on Fuel Consumption at Engine Speed of 3000 RPM

Figure 4.48 illustrates the graphs of fuel consumption of the blends at engine speed of 3000 rpm. The graphs show that fuel consumption increased as bioethanol percentage increases in the blends. Fuel consumption increased with increase in BMEP to a point and then sharply increases with further increases in BMEP. Maximum fuel consumption of 0.989 kg/h was obtained when engine was running on E30. This is 4.11 % more than quantity of petrol consumed at this engine operating conditions.

iii. Effect of Blends on Fuel Consumption at Engine Speed of 3500 RPM

Figure 4.49 illustrates the graphs of fuel consumption of the blends at engine speed of 3500 rpm. The fuel consumption increased with increase in BMEP to a point and then increases with further increase in BMEP. The engine consumed more fuel when running on E30 compared to other candidate fuels. However, at higher BMEP rate of candidate fuel consumption started decreasing slowly. The engine when running on E30 consumed maximum fuel of 0.999 kg/h which is 3.85 % more than the quantity of petrol consumed at this same engine condition.

Fuel consumption of the blends is presented as a rate in Figures (4.47) – (4.49). At all speeds, it was observed that FCR increased slowly with increase in BMEP to a point and then increased sharply with further increase in BMEP. This might be attributed to the increase in octane number with reduced knocking which results to increased pressure on the piston. Higher fuel consumption was observed with the blends as bioethanol content increased; that could be due to their lower calorific values which need to be compensated with more volume of the fuel to achieve the same power output. At lower BMEP, consumption value of blends are closer to that of pure petrol but have wider values at higher BMEP. Fuel consumption of the blends and pure petrol increased with increase in speed. At 2500, 3000 and 3500 rpm, FCR of blends are higher than that of pure petrol with E10 followed by E20 having closer values to pure petrol. Blends showed very close fuel consumption rate with E0 at lower BMEP at 2500 rpm, and at higher BMEP at 3500 rpm.

iv. Effect of Blends on Brake Power at Engine Speed of 2500 RPM

Figure 4.50 illustrates the graphs of brake power of the blends at engine speeds of 2500 rpm. Brake power of the entire candidate fuels showed similar trend with that of pure petrol which was observed to increase steadily with increase in BMEP. At engine speed of 2500rpm maximum brake power of 0.981 kW at 2.88 bars was observed with all the fuels.

v. Effect of Blends on Brake Power at Engine Speed of 3000 RPM

Figure 4.51 illustrates the graphs of brake power of the blends at engine speeds of 3000 rpm. Brake power of the entire candidate fuels showed similar trend with that of pure petrol which was observed to increase steadily with increase in BMEP. At engine speed of 3000 rpm maximum brake power of 1.062 kW corresponding to 2.6 bar was observed with all the fuels.

vi. Effect of Blends on Brake Power at Engine Speed of 3500 RPM

Figure 4.52 illustrates the graphs of brake power of the blends at engine speed of 3500 rpm. Brake power of the entire candidate fuels showed similar trend with that of pure petrol which was observed to increase steadily with increase in BMEP. At engine speed of 3500 rpm E30 has the maximum brake power of 1.225 kW which occurred at 2.57 bar. This is 1.575 % higher than that of pure petrol and E10, and 0.74 % higher than that of E20. Figures 4.50 – 4.52 show that brake power of the entire candidate fuels increased steadily with increase in speed. Thus minimum and maximum brake power of each blend increased with speed. At constant speed, it can be deduced from the graphs that the engine has almost the same power output irrespective of the fuel it is running on. However, quantity of fuel needed to achieve this power output may differ with the different fuels.

vii. Effect of Blends on Brake Specific Fuel Consumption at Engine Speed of 2500 RPM

Figure 4.53 illustrates variation of brake specific fuel consumption (BSFC) of the blends at engine speed of 2500 rpm. The BSFC curves superimposed showed small increase in BSFC with the presence of bioethanol compared to pure petrol. At engine speed of 2500 rpm, BSFC of the candidate fuels showed similar trend with pure petrol. It was observed to decrease from low BMEP to a minimum after which it showed gradual increase on increasing BMEP. The minimum BSFC of the candidate fuels lies between the BMEP of 2.6 and 2.8 bar at 2500 rpm. The engine gave 0.897 kg/kW-h minimum BSFC when running on pure petrol. Comparing the

minimum BSFC of blends at 2500 rpm, E10, E20 and E30 consumed 1.115 %, 2.01 % and 3.01 % fuel more than pure petrol respectively.

viii. Effect of Blends on Brake Specific Fuel Consumption at Engine Speed of 3000 RPM

Figure 4.54 illustrates variation of BSFC of the blends at engine speed of 3000 rpm. It showed that BSFC of pure petrol increased with increase in bioethanol percentage in blends. BSFC of the blends showed similar trend with that of pure petrol. It was observed to decrease from low BMEP to a minimum after which it showed gradual increase on increasing BMEP. The observed minimum BSFC of the blends lies between the brakes mean effective pressure of 2.3 and 2.5 bar at 3000 rpm. Minimum BSFC of 0.853 kg/kW-h was obtained when running the engine on pure petrol. Comparing the minimum brake specific fuel consumption of blends at 3000 rpm, E10, E20 and E30 consumed 1.29, 3.28 and 4.92 % fuel more than pure petrol respectively.

ix. Effect of Blends on Brake Specific Fuel Consumption at Engine Speed of 3500 RPM

Figure 4.55 illustrates variation of brake specific fuel consumption of the blends at engine speed of 3500 rpm. The graphs showed that running the engine on E30 consumed more fuel than pure petrol and other bioethanol blends. BSFC of pure petrol increased with increase in bioethanol percentage in the blends. BSFC of blends showed similar trend with that of pure petrol. It was observed to decrease sharply from low BMEP to a minimum and then showed gradual increase on increasing BMEP. The minimum BSFC of the candidate fuels lies between the brakes mean effective pressure of 2.4 and 2.5 bar at 3500 rpm. Minimum BSFC obtained when running the engine on pure petrol is 0.758 kg / kW-h. Comparing the minimum BSFC of blends at 3500 rpm, E10, E20 and E30 consumed 2.24, 3.3 and 4.62 % fuel more than pure petrol respectively. At higher BMEP blends showed very close values of BSFC with pure petrol.

Figures 4.53 – 4.55 showed that there is increase in BSFC with the presence of bioethanol compared to pure petrol. This is expected since theoretical air flow rate of pure petrol is 1.6 times that of the bioethanol. Therefore, BSFC could increase with the increase of bioethanol content. In the entire speed, BSFC was observed to decrease from low BMEP to a minimum after which it showed gradual increase on increasing BMEP. This is because BSFC depends on fuel consumption which increased at high BMEP due to increase in speed and brake power. BSFC is a measure of the ability of the engine in using the fuel supplied to produce work. Thus, the

minimum BSFC of each fuel confirms good fuel economy at that condition. All the blends showed decreased BSFC with increasing engine speed to 3500 rpm. In the entire speed tested, lowest fuel consumption rate per brake power occurred with E0 at 3500 rpm as 0.758 kg/kW-h. Also bioethanol blends ranges as E10, E20, E30 in terms of lowest BSFC at 3500 rpm which are 0.775 kg/kW-h, 0.783 kg/kW-h and 0.793 kg/kW-h i.e 2.24, 3.3 and 4.62 % respectively more than that of pure petrol. This increament in blend's BSFC must be to achieve the same power output with the baseline fuel owing to the lower calorific values of the blends. This indicates that pure petrol gave an engine power with less fuel consumption. At minimum BSFC, maximum fuel economy was obtained which means that enough air was available for complete combustion. Near to that point will give a lean mixture due to oxygen constituent of bioethanol. This means that the maximum fuel economy of pure petrol was improved by bioethanol presence in the blends which could be as a result of the oxygenating effect of bioethanol, and CO emission will decrease tremendously.

x. Effect of Blends on Brake Thermal Efficiency at Engine Speed of 2500 RPM

Figure 4.56 illustrates variation of brake thermal efficiency at engine speed of 2500 rpm. It showed that BTE of bioethanol blends have similar trend with pure petrol. BTE increased to a maximum with increase in BMEP and gradually decreases with further increase in brake mean effective pressure. Brake thermal efficiency of pure petrol increased with increase in bioethanol content of the blends. This could also be as a result of the decrease in the blends calorific value as bioethanol percentage in it increases. Pure petrol showed maximum brake thermal efficiency of 9.201 % at 2500 rpm. Brake thermal efficiency was higher than those of pure petrol by 3.18 %, 6.29 % and 9.99 % when the engine was operated with E10, E20 and E30 at 2500 rpm.

xi. Effect of Blends on Brake Thermal Efficiency at Engine Speed of 3000 RPM

Figure 4.57 illustrates variation of brake thermal efficiency at engine speed of 3000 rpm. The graphs showed that BTE of bioethanol blends have similar trend with petrol. BTE increased to a maximum with increase in BMEP and gradually decreases with further increase in brake mean effective pressure. Brake thermal efficiency of pure petrol increased with increase in bioethanol content of the blends. Pure petrol showed maximum brake thermal efficiency of 9.673 % at 3000 rpm. Brake thermal efficiency was higher than those of pure petrol by 2.97 %, 5.03 % and 7.93 % when the engine was operated with E10, E20 and E30 at 3000 rpm.

xii. Effect of Blends on Brake Thermal Efficiency at Engine Speed of 3500 RPM

Figure 4.58 illustrates variation of BTE at engine speed of 3000 rpm. The graphs showed that BTE of bioethanol blends have similar trend with petrol. BTE increased to a maximum with increase in BMEP and gradually decreases with further increase in brake mean effective pressure. BTE of pure petrol increased with increase in bioethanol content of the blends. Pure petrol showed maximum BTE of 10.89 % at 3500 rpm. BTE was higher than those of pure petrol by 1.93, 4.96 and 8.17 % when the engine was operated with E10, E20 and E30 at 3500 rpm.

BTE is an indication of power output gain from given heat energy input. Fuel with higher calorific value has more heat input potential therefore expected to give better performance. Figures 4.56 – 4.58 showed that the curve for pure petrol is superimposed by that for its blends with bioethanol. This clearly shows that BTE of pure petrol was improved by increase in percentage of bioethanol in the blends. This may be as a result of the higher latent heat of vaporization of bioethanol owing to which the intake fuel gains heat from the cylinder walls thereby reducing heat loss. This prevents knocking effect and increase engine overall efficiency. The figures reveal that BTE of pure petrol was improved in all the petrol-bioethanol blends. This could be as a result of the decrease in the blends calorific value as bioethanol percentage in it increases. Recall that BTE is directly proportional to brake-power and inversely related to fuel consumption rate and heating value of a fuel. Hence, running the engine on the blends resulted to higher efficiency even though more of the blends were consumed than pure petrol to achieve the same brake power. The figures also showed that BTE of candidate fuels increased with speed. For all speed, BTE increased to a maximum with increase in BMEP and gradually decreases with further increase in BMEP. The reduction of BTE at higher BMEP may be due to increase in BSFC caused by speed increase, and decrease in volumetric efficiency and air fuel ratio.

Blending bioethanol and pure petrol produces a mixture with its own unique physical characteristics. One of the noticed differences in the blends against pure petrol is visual difference of the smoke characteristics. The higher the bioethanol in the blends is, the less visible the black smoke from the exhaust pipe. This is because higher bioethanol content has higher oxygen content which shifts combustion towards completion.

c. Validation of the Bioethanol Production Result

Table 4.7: Comparison of Reported Bioethanol Yield with Literature Results

Feed stock	Method	Bioethanol Yield	% Difference	Literature
WPB	Physical Pretreatment: Grinding Acid hydrolysis: dil. 1.2% H_2SO_4, 30 min Fermentation: local strains *S. cerevisiae*, 32ºC, 72h	32.01 g/L (82.42%)	0	Reported
WPB	Alkali pretreatment: NaOH, 140 - 145^{0}C, 30min. Enzymatic hydrolysis: 50 - 52 ^{0}C, pH 4.8-5.5. Fermentation: local strains *S. cerevisiae* Mk, 32 ^{0}C, pH 6 -5, 48 h.	69 %	13.42 %	Yani et. al. (2012),
WPB	Pretreatment: NAOH, 15min. Hydrolysis: incubation in xylanase and cellulase pH 6, 6 days Fermentation: *S.cerevisae*, 48h.	540 – 655 ml (90 %)	-7.58 %	Richana et. al., (2015)
WPB	Acid pretreatment: 1.0% (v/v) dilute H2SO4 at 125°C for 90 min Enzymatic hydrolysis: 1% (w/v) NaOH at 100°C, 60 min. Fermentation: S. cerevisiae, 24 h.	0.99 g/L i.e. 89.1% ,	- 6.68 %	Nuru et. al., (2014)
	Sulfite pretreatment: sodium bisulfite Enzymatically hydrolysis: Glucan, pH 5.5 Fermention: S.cerevisiae	32 g/L	0.01 g/L	Jinlan et. al., (2014)
Oil palm bunch	Alkali pretreatment: 15% NaOH , 40 min, 130°C, Acid hydrolysis: 7% H2SO4, 119 °C, 110 min. Fermention: *baker's yeast* *Loog-Pang*	*8.49 g/l* *56 times lower*	23.52 g/L *lower*	Chayanoot & Sairudee (2013)
Palm pressed fiber	Pretreatment: milling Emzymatic hydrolysis: NaClO2. Fermentation: C. *shehatae* TISTR5843, 30ºC,150 rpm, 24h	11.5 g L^{-1}	0.641 %	Wiboon et. al., (2012)

Table 4.7 compares bioethanol production result to that of literature. 32 g/L optimum bioethanol yield was reported as obtained at 72 h fermentation period and 30 min hydrolysis period. This corresponds to 82.42 % fermentation efficiency. It is 13.42 %, 0.01 g/L and 23.52 g/L higher than that obtained by Yanni et. al., (2014), Jinlan et. al., (2014), and Chayanoot and Sairudee (2013) respectively. This suggests that physical pretreatment followed by acid hydrolysis improves bioethanol production than alkali pretreatment followed by enzymatic or acid hydrolysis. But acid pretreatment followed by enzymatic hydrolysis carried out by Nuru et. al., (2014) yielded 6.68 % more than that reported; while alkali pretreatment before enzymatic hydrolysis using xylanase and cellulase for a long period by Richana et. al., (2015) gave the highest bioethanol yield which is 7.58 % more than that reported.

4.2.10 Trouble Shooting Guide

The problems that may be encountered in the operation of the constructed distiller are listed in Table (4.8), possible causes are identified and their corresponding remedies are given.

Table 4.8: Trouble Shooting

Trouble	Possible cause	Remedy
Pump fails to operate	plugged wrongly	Plug to a convenience outlet
	Faulty circuit	Check circuit
	Low Voltage	Check voltage
charcoal fails to burn or it produces lots of smoke	Wet charcoal	Use dry charcoal
	Small charcoal size	Use big charcoal particles
	Insufficient air supply	Check fan speed; check for possible air leakage
Fuel burning with much flame	Presence of gas due to limited air	increase fan speed
Deficiencies in heat transfer and pressure loss rating	Leakages	Use double tube if necessary
	insuficient heat input	Check design overall heat transfer coefficient and effective temperature difference
	Flow misdistribution	Check coolant velocity
	Fouling	Design with fouling factor, clean HE
Erosion	High fluid velocity, large fluid density	Reduce fluid velocity if possible or interchange fluid location
	Weak metal material	Use hard metals. check system geometry
HE vibration	High fluid velocity	Reduce fluid velocity if possible, fix tubes rigidly

Leakages: The leakage at the condenser seriously affects heat transfer since the stream may have avoided contact with the heat transfer surface and disturbs the particular fluid velocity. As such heat transfer and pressure drop reduce. Deficiencies in heat transfer and pressure loss rating is as well as distiller failure. Also, since the rate of heat transfer Q in HE is determined by the simple relationship in Equation (4.4) derived from Equation (2.79).

$$Q = \int_0^A U_0 \Delta T dA = A_0 U_{0m} \Delta T_m \qquad (4.4)$$

Another reason for failure of heat exchanger to perform heat transfer duty is to be sought in either of the two quantities, the mean overall heat transfer coefficient U_{0m} or the mean effective temperature difference ΔT_m between the heat exchanging streams. Since U_0 and ΔT_m may vary throughout the exchanger, the incorrectly integrated value of their product may be the culprit in a heat transfer deficiency. Leakages must be checked during distiller construction. The value of U_0 and ΔT_m should be based on experiment or on standard given values.

Eddies: Stationary eddies (backwaters) which the stream energizes but does not penetrate or sweep away also causes heat transfer degradation. Such zones are not prevalent except where sedimentary or particulate deposit may block the normal fluid escape routes. Under such circumstances not only the heat transfer coefficient and effective temperature difference suffer but the pressure loss as well. The HE design may be helpful in minimizing such.

Fouling: The presence of fouling deposited on heat transfer surface by any mechanism whatsoever constitute a heat transfer resistance, r_o and/or r_i to the detriment of the overall heat transfer coefficient U_0. Recognition of this effect first took the form of a 'fouling factor', i.e. a multiplier less than unity applied to the overall coefficient for new clean equipment to provide some reasonable operating period before the apparatus will be incapable of handling the specified heat load, and had to shut down and cleaned. Fouling like vapor blanket, when it occurs on the coolant side of high temperature equipment may lead to overheat, then tube failure. The tubular exchanger manufacturers association (TEMA) founded in the late 1930's in an attempt to establish standards for high quality shell and tube exchangers, provided a list of recommended fouling resistances for various services. These should be incorporated in the design process.

Erosion: the rapid removal of metal due to the friction of the fluid flowing in the tube. It often occurs with and accelerates the effect of corrosion by stripping off the protective film formed on certain metals. Erosion rate depends upon the metal (the harder the metal, the less the erosion if other factors are equal), geometry of the system, velocity and density of the fluid. It is usually more severe at the entrance of a tube or in the bend of a U-tube, due to the additional shear stress associated with developing the boundary layer or turning the fluid. Other erosion effect is associated with chemistry of the fluid and the tube metal, especially where corrosion is involved.

Vibration: a very serious problem in the mechanical design of HE is flow-induced vibration of the tubes. For example, fatigue cracking of a tube, loosing of the tube joint, accelerated corrosion and repeated unbalanced forces been applied to the tube causes vibration. There are several possible consequences of the tube vibration. The most common of such forces in HE is the eddying motion of the fluid in the wake of a tube as the fluid flow across the tubes. The unbalance forces are relatively small but they occur several of times a second and their magnitudes increase rapidly with increase velocity. Even so, these forces are ordinarily damped out with no damage to the tube. However, anybody can vibrate much more easily at certain frequencies called natural frequencies, than at others if the unbalanced forces are applied at 'driving frequencies' that are at or near those natural frequencies, resonance occur and even small forces can result in a very strong vibration of the tube. Although progress is been made, the prediction of whether or not a given HE configuration will adequately resist vibration problems are to fix the tubes as rigidly as possible and to keep the velocities low.

Distiller Maintenance

The distiller should be properly taken care of to prolong its durability. It should be cleaned at intervals to prevent corrosion. Frequent flush under high pressure can be used to remove any blockage due to fouling. Obsolete components should be changed with the current economical substitute to ensure its efficiency. Components should be checked for leakage continuously and appropriate changes should be made. Distiller should have a fixed location since less tool handling increases its economical worth. It should not be exposed to moisture, to avoid rusting and anti-rust paints e.g. red oxide should be used when repainting. Production rig should be dry.

4.2.11 Economics Analysis of the WPB Bioethanol Fuel

Economics of producing bioethanol fuel from WPB is base on the cost sum of setting up a production rig, feed cost and the distillation economics. The fabricated distiller was constructed on site. The breakdown of the financial analysis of this research work is given below.

a. Production Rig Cost

This is the cost of preparing a site for distillation machines installation and operation. Thus, it includes the cost of acquiring the site and raising shelter for the operation. This cost is determined from Table (4.9).

Table 4.9: Production Rig Cost Table

Material	Quantity / specification	Unit price (₦)	Total amount (₦)
Site Cost	1/10 plot	-	-
Zinc	2 bundles	5,500	11,000
Wood	25 (2" x 4") 25 (2" x 2")	400 220	10,000 5,500
Cement	4 bags	1,950	7,600
Blocks	150 pcs	100	15,000
Sand	½ trip	12,000	7,000
Rod	4	2,500	10,000
Nails	4 pds weight (3") 2 pds " (4") 4 pds " (zinc nail) 2 pds " (1.5")	130 130 200 130	520 260 800 260
Door	1	8,000	8,000
Extended wire	8 pcs	500	4,000
Paint	2 bkts	850	1,700
Miscellenous			8,000
Labour			33,000
		TOTAL	**122,640**

b. Distiller Feed Cost

This is the cost of producing the boiler feed, which is the cost sum of acquiring and preparing the feedstock. It includes feedstock, pretreatment, hydrolysis and fermentation cost. The evaluation of feedstock costs is a very important issue that is related to the proximity of taking it to the production rig. Zhan et al. (2005) indicated that the costs of the feedstock depend on the plant location, plant size and the procedure for acquiring the feedstock. Feedstock cost is also influenced by its production, harvesting, processing, transportation and by-product disposal. Feedstocks such as WPB produced as by-products of other profitable processes have lower production costs than those produced specifically for bioethanol production e.g. grains. Sometimes industries provide a convenient disposal for waste biomass. In these cases the biomass is transformed from an economic liability to an asset (Holt et. al., 2006). Though palm

mills use WPB as fuel for boilers and as manure for palm trees, using it for bioethanol production is increasing its economic value. Different harvesting methods can have different efficiencies, causing differences in price (Nurmi 2007). The effect of production and harvesting on feedstock cost is zero for WPB as they are already borne by the palm mills. Processing is the third factor; for feedstocks with high moisture contents than needed, drying is a necessary process which increases the quality. Feedstocks which dry naturally will have lower processing costs than those that require a dryer (Tripathi et. al., 1998) especially when time is not a constraint. Drying with waste heat can also reduce drying costs, although this method is not as cost effective as natural drying since new equipment installations may be required (Renström 2006; Wolf et. al., 2006). Processing effect on WPB cost is considered at the pretreatment step.

Transportation of biomass contributes significantly to overall feedstocks cost. Some experts suggest that a 100 km radius should be used to identify sources of biomass (Pari 2001; Strehler 2000). Often densified biomass hold an advantage over less dense materials because of lower transportation cost. The WPB was transported from Ubima in Rivers state to Nekede in Owerri, Imo state which is about 55 km distance. Disposal of resulting by-product from feedstock has its effect on feedstock cost as it may be disposed of a cost; this is zero for this process. Pretreatment cost is the cost of preparing the feedstock for hydrolysis. Hydrolysis cost is the cost of producing the hydrolysate for fermentation while fermentation cost is the cost of producing the bioethanol for distillation. All the chemicals used are supplied by Juceco Enterprises and Company, Owerri. The distiller feed production cost is determined from Table (4.10).

Table 4.10: Distiller Feed Production Cost Table

Description	Quantity	Unit price (₦)	Total amount (₦)
WFB: tranportation	10 bags	1000	10,000
WPB oven drying	3 batches	2,000	6,000
WPB Pretreatment: grinding	10 bags	3,500	35,000
Reagents: H_2SO_4	2.5 L	2,400	6,000
NAOH	1 tn of 500g	4,800	4,800
Distilled H_2Os	300 L	1,000	30,000
Acetic acid	200 ml		
Sodium chlorite	50g	16	800
Whatman filter paper	1pkt	1000	1000
Phloroglucinol	25g	-	7500
Hcl D-xylose Benzoic acid	25g	-	6800
Potassium dichromate	150g	10	1500
D-glucose	100g	12	1200
Phenol	10g	150	1500
Laboratory grade ethanol	500ml	-	850
Innoculum			8,000
Laboratory equipments			26,000
Charcoal	1 bag	2500	2500
Miscellenous			16, 000
		TOTAL	155,450

c. Distillation Economics

The economics of the distillation comprises that of fabricating the distiller and utilizing it.

i. Distillation Unit Setup Cost

Distiller cost is composed of the cost of its components i.e. boiler and reactor cost, condenser cost, reservoir, pump and piping cost. It is the sum of the costs of the materials used, contingency, and fabrication cost of these units. Certain steps can be taken to reduce cost e.g. in condenser, the same total heat transfer area may be put in a small diameter and shorter length shell by coiling the tube. The boiler can be described as having a single distillation column. The investment cost of a distillation column is a function of its diameter (Holland 1997). The cost of

condenser shell often increases very rapidly with diameter but only linearly with length. Therefore, unless space or pressure drop limits dictate otherwise, the most economical exchanger is usually one of relatively large length to diameter ratio. All the materials used for the fabrication were purchased within Owerri, Imo state. Table (4.11) presents the distiller cost.

Table 4.11: Bill of Materials for setting up the Distillation Unit

Description	**Quantity**	**Unit price (₦)**	**Total amount (₦)**
Plate (30 x 30cm)	3 Pcs	3,000	9,000
Pipe (22cm x 160cm)	1	19,000	19,000
Pipe (2" x 61 cm)	2	800	1600
Pipe (4" x 30 cm)	1	1,500	1,500
Pipe (6" x 85 cm)reservior	1	8,500	8,500
PVC Pipe (2")	3	1000	3000
Mesh (30cm x 30cm)	1	1000	3000
Galvanized elbow (2")	2Pcs	450	900
Galvanized valve (2")	2 Pcs	700	1,400
PVC elbow (2")	10 Pcs	300	3000
Angle iron stand (3" x 3")	1	3,500	3,500
Drum	1	6000	6,000
Electrode	1 Pkt	3,500	3,500
Gas cutting		4000	4,000
Discharge pipe	5m	500	2,500
pump	1	10,000	10,000
Thermometer	1 (360^0C)	2,800	2,800
Pressure gauge	1	4,500	4,500
Paint: silver colour	1 tin	3500	3,500
Fabrication cost			20,000
		TOTAL	111,200

* Production of the dryer was sub-contracted so; fabrication cost already includes the costs of labour and consumables.

The selling price per unit of the distiller is determined by providing overhead cost (based on the production cost), margin, and tax. To determine the bill of Materials for setting up a distiller unit the following steps were taken as given in Equation (4.5 – 4.9).

Material Costs = (Unit Cost1 x No. of Units1) + (Unit Cost2 x No. of Units2) +…… …..

. .. . + (Unit Cost n x No. of Units n) (4.5)

Therefore, Material Costs = ₦91,200

Total Material Cost = MC + Contingency (4.6)

∴ Total Material Cost = ₦ (91,200 + 91, 20) = ₦100,320

Contingency is 10 % of the material cost; it was to provide allowance for price increases and for other incidental expenses that might be needed during the fabrication of the distiller.

Production Cost of distiller = Fabrication Cost + Total Material Cost (4.7)

∴ Production Cost of dryer = ₦ (100,320+ 20,000) = ₦120,320

Manufacturing Cost = Production Cost + Overhead + Profit Margin (4.8)

∴ Manufacturing Cost = ₦ (120,320 + 120, 32 + 10,588.16) = ₦142,940.16

To get the manufacturing cost, 10 % of the production cost was allotted as the overhead cost while 8 % of the sum of production cost and overhead was allotted as the margin. Considering all taxes needed to be paid as only 10 % of the manufacturing cost, dryer selling price was calculated with Equation (4.9).

Selling Price per Unit = Manufacturing Cost + Tax (4.9)

∴ Selling Price per Unit = ₦ (142,940.16 + 16,907.616) = ₦157, 234.176

As shown in Table (4.9), total cost for the materials in producing a unit of the distiller is ₦91,200. This includes the costs of metal sheets, pipes, bars, switch and other basic parts. With the additional 10 % contingency, the material cost for the distiller is ₦100,320. The fabrication

cost of the distiller is ₦20,000. With 10 % overhead cost of ₦120, 32, 8 % profit margin of ₦10,588.16, and a 10 % tax of ₦16,907.616, the total selling price of dryer is ₦157, 234.176.

ii. Operating Cost

Operating cost represents the total expenses incurred by the users in operating the distiller. Basically, this includes the fixed cost, which is the cost of owning the distiller, and the variable cost, which is the cost incurred in operating the distiller. The fixed costs basically include depreciation, interest on investment, repair and maintenance, and insurance. On the other hand, the variable costs include the cost of charcoal fuel and electricity consumed in running the blower. The sum of the fixed and variable costs divided by the operating time is the cost of operating the distiller per unit time. To determine the operating cost of the distiller for a minimum of four years life span and 6 hours operating time per day, the following steps in Equation 4.10 - 4.18 are taken while Equation 4.19 gives the amount of savings per year.

Depreciation = (Investment Cost – Salvage Value) / (Life Span expressed in days) (4.10)

∴ Depreciation = ₦ (157, 234.176 – 15,723.418) / (4 x 365) = ₦96.93 per day.

The investment cost IC, for the distiller is the purchase cost of the distiller or the selling price. The salvage value is 10 % of the original cost of the distiller.

Interest on Investment = (Investment Cost x Interest Rate) / 365days (4.11)

∴ Interest on Investment = ₦ (157, 234.176 x 0.21) / 365 = ₦90.463

The interest rate charged by banks on loans is 21 % of IC.

Repair and Maintenance = (Investment Cost x 10 % of IC) / 365days (4.12)

∴Repair and Maintenance = ₦ (157, 234.176 x 0.1) / 365 = ₦43.078

The 10 % of IC is the percentage repair and maintenance.

Insurance = (Investment Cost x 3 % of IC) / 365days (4.13)

∴ Insurance = ₦ (157, 234.176 x 0.03) / 365 = ₦12.923

$$\text{Total Fixed Costs} = \text{Depreciation} + \text{Interest on Investment} + \text{Repair and Maintenance} + \text{Insurance} \quad (4.14)$$

∴ Total Fixed Costs = ₦ (96.93 + 90.463 + 43.078 +12.923) = ₦243.394

$$\text{Fuel Cost per day of operation} = \text{Fuel Consumption Rate per day x Operating Time per day} \quad (4.15)$$

∴ Fuel Cost per day of operation = ₦350 x 1.83 x 6 = ₦3,843

Cost of fueling generator to run the pump per day = ₦500

Total Variable Costs = Total Fuel Cost + Cost of running generator (4.16)

∴ Total Variable Costs = ₦ (3,843 + 500) = ₦ 4,343.

Total Cost = Total Fixed Costs + Total Variable Costs (4.17)

∴ Total Cost = ₦ (243.394 + 4,343) = ₦4,586.394

Operating Cost per hour of operation = Total Cost / Operating Time per day (4.18)

∴ Operating Cost per hour of operation = ₦₦4,586.394/ 6 = ₦ 764.399

Operating cost per hour of operation multiplied with the total operating time in one year i.e [6 x (4/7) x 365] gives the savings per year:

Savings per year = operating cost x Operating time per year (4.19)

∴ Savings per year = ₦764.399 x [6 x (4/7) x 365] = ₦956,590.749

d. Payback Period of the Distillation Unit

Payback period is the period expressed in years, which it will take the distillation unit cash inflows to equal the cash outflows. It was calculated with Equation 4.20.

Payback Period = Investment Cost / Savings per year (4.20)

∴ Payback Period = ₦ (157, 234.176 / 956,590.749) = 0.1 64

The payback period is two months. Decision rules to accept the project with the shortest payback period. The distiller has a short payback period of two months, assuring positive returns over the investment requirements. Thus, the distiller could be generally accepted. Firing the distiller with charcoal resulted to a feasible economical and sustainable design. The distiller provides 532.51 L of the bioethanol i.e. 11235.94 MJ of energy base on the LHV per year. 1000 L feed capacity of such distiller will provide 26625.5 L bioethanol and 561798.05 MJ per year.

Cost of setting up the distillation unit = Production Rig Cost + cost of distiller

= ₦ 122,640 + ₦ 111,200 = ₦ 233,840 (4.21)

Cost of producing distiller feed for this study = ₦ 155,450 (4.22)

Cost of producing the distiller feed for a Liter bioethanol fuel = ₦ 5,200 (4.23)

817 ml bioethanol was produced in 115 minutes using the fabricated distiller.

∴ Time to produce 1L = $\frac{1000\ ml}{817\ ml}\ x\ 115\ min = 140.76\ min = 2.35\ h$ (4.24)

Equation (4.18) gave operating cost per hour of operation as ₦ 764.399 / h.

∴ Distiller Operating Cost per liter Bioethanol

= ₦ 764.399 / h x 2.35 h = ₦ 1,796.34 (4.24)

∴ Total cost of producing a liter of the bioethanol in the distillation unit

= Cost of producing the distiller feed for a Liter bioethanol fuel

+ Distiller Operating Cost per liter Bioethanol

= ₦ 5,200 + ₦ 1,796.34 = ₦ 6,996.34 (4.24)

This study produced a liter of bioethanol fuel from waste palm bunch at the cost of ₦ 6, 996.34. This could lead to a selling price at 5 – 10 % higher than the present price of petrol per liter (i.e. ₦ 145/L). But government intervening through usage enforcement, incentives and subsidy will reduce the price lower than that of pure petrol. Notwithstanding, commercial production scale will reduce the bioethanol price per gallon thereby making it more prices competitive with petrol.

CHAPTER FIVE

CONCLUSIONS AND RECOMMENDATIONS

5.1 Conclusions

This study has successfully produced bioethanol from waste palm bunch which was obtained from Nigeria; recorded hydrolysis with 1.2 % dilute H_2SO_4, at 160 ^{0}C for 30 min and fermention for 72 h with S.scerevisea separated from palm wine as optimum processing conditions.

Physical pretreatment of palm bunch followed by acid hydrolysis improves bioethanol yield. S.cerevisiae isolated from palm wine demonstrated an efficient ethanol production.

A distiller was fabricated and successfully used to distill 817 ml bioethanol in 20 minutes from the bubble point.

The bioethanol satisfies ASTM D4806 specification and thus blend able with pure petrol; it improved fuel quality of pure petrol as it increased octane number, volatility and decreased drivability index of their blends thereby satisfying ASTM 4814 specification.

At entire constant load, the engine developed maximum BP with E30 while E10 recorded lower value; at entire constant speed, the curves showed almost the same power output irrespective of the fuel it is running on.

At entire constant load, minimum BSFC of pure petrol was improved by blends in decreasing order of bioethanol content; but more blends were consumed than pure petrol in increasing order of bioethanol percentage to achieve same brake power at the entire constant speed.

BTE of pure petrol was improved in increasing order of bioethanol content in the blends, at entire constant engine speed and load.

Thus, blending pure petrol with 10 – 30 % of the bioethanol is confidently recommended for SI engines without modification; E30 followed by E20 gave the optimum engine performance.

5.2 Recommendation

The following recommendations are made for consideration in future studies:

i. The distillation process should be modeled for optimization and continuous operation.
ii. Further work should be done to establish the engine performance of blends with higher proportions of the bioethanol; in unmodified SI engine.

5.3 Contribution to Knowledge

This work has successfully changed waste to energy by producing bioethanol from Nigerian waste palm bunch. The waste disposal problems are hereby solved. The study established hydrolysis with 1.2 % H_2SO_4, at 160 ^{0}C for 30 minutes after physical pretreatment as the optimum hydrolysis condition; and fermenting for 72 h with S.scerevisea isolated from palm wine as the optimum fermentation process. This confirms that S.scerevisea isolated from palm wine can economically and efficiently ferment waste palm bunch hydrolyzate. The study developed a distiller which can handle the distillation of biofuels efficiently, within the temperature range of 0 – 3500 ^{0}C. This distiller can be integrated to the down-stream operation of Oil Palm Industries. The study has confirmed that fuel properties of bioethanol produced from Nigerian waste palm bunch met the international standard as established by ASTM for use in SI engine. The work established for optimum performance, the blend ratio of 30 % bioethanol content. It recommends blend ratio of 30 % of bioethanol content, with pure petrol to be confortably used for running SI engines without engine modification. This is an improvement compared to 10 % biethanol content recommended by Altun and Hakan (2009), Seshaiah (2010), Jitendra et. al., (2013), Shyam et. al., (2012) and Gaurav and Nitin (2014) while 20 % was recommended by Al-Hassan (2003), Siddegowda and Venkatesh (2013) and Yanuandri et. al., (2014). This work has clearly proved that bioethanol from Nigerian waste palm bunch is a reliable fuel to improve pure petrol fuel properties and engine performance, and thus can be a perfect replacement for lead compound used as an anti-knock agent.

REFFERENCE

Abdullah, N., Sulaiman, F. and Gerhauser, H. (2011). Characterisation of Oil Palm Empty Fruit Bunches for Fuel Application. Journal of Physical Science, Vol. 22, No 1, Pp. 1–24.

Aden, A., Ruth, M., Ibsen, K., Jechura, J., Neeves, K., Sheehan, J., Wallace, B., Montague, L., Slayton, A. and Lukas, J. (2002). Lignocellulosic Biomass To Ethanol Process Design and Economics Utilizing Concurrent Dilute Acid Prehydrolysis and Enzymatic Hydrolysis For Corn Stover. Technical Report, National Renewable Energy Laboratory, Pp. 143.

Adzimah, K. and Seckley, E. (2009). Improvement on the Design of a Cabinet Grain Dryer. America Journal of Engineering and Applied Science, pp. 217-228.

Akpan, U., Kovo, A., Abdullahi, M. and Ijah, J. (2005). The Production of Ethanol from Maize Cobs and Groundnut Shells. AU J.T. Vol.9, No. 2, Pp. 106 - 110.

Al-Baghdadi, M. (2000). Performance Study of a Four-Stroke Spark Ignition Engine Working with Both of Hydrogen and Ethyl Alcohol as Supplementary Fuel. International Journal of Hydrogen Energy, Vol. 25, Pp. 1005 - 1009.

Al-Hasan, M. (2003). Effect of Ethanol–unleaded Gasoline Blends on Engine Performance and Exhaust Emission Energy Conversion and Management, Vol. 44, Pp. 1547–1561.

Al-Hassan, M., Mujafeta, H. and Al-Shannag, M. (2012). An Experimental Study on the Solubility of a Diesel-Ethanol Blend and on the Performance of a Diesel Engine Fueled with Diesel-Biodiesel - Ethanol Blends. Jordan Journal of Mechanical and Industrial Engineering, Vol. 6, No. 2, Pp.147 - 153.

Altun, S. and Hakan, F. (2009). Exhaust Emissions of Methanol and Ethanol-Unleaded Gasoline Blends in a Spark-ignition Engine. Applied Energy, No. 86, Pp. 630 - 639.

Alvira, P., Tomás-Pejó, E., Ballesteros, M. and Negro, M. (2010). Pretreatment Technologies for an Efficient Bioethanol Production Process Based on Enzymatic Hydrolysis: A Review. Elsevier Bioresource Technology, Vol. 101, Pp. 4851– 4861.

Alvydas, P., Saugirdas, P. and Juozas, G. (2003). Influence of Composition of Gasoline – Ethanol Blends on Parameters of Internal Combustion Engines. Journal of Kones Internal Combustion Engines, Vol. 10, Pp. 3 – 4.

Ananda, S. and Saravanan, C. (2010). Emission Reduction in SI Engine using Ethanol Gasoline Blends on Thermal Barrier Coated Pistons. Vol. 1, Issue 4, Pp.715-726, www.IJEE.IEEFoundation.org.

Andersen, H., Laroche, L. and Morari, M. (1995). Effect of Design on the Operation of Homogeneous Azeotropic Distillation. Comprehensive Chemical Engineering, Vol. 19, No. 1, Pp. 105 – 122.

Anderson, J., DiCicco, D., Ginder, J., Kramer, U., Leone, T., Raney, H., and Wallington, T. (2012). High Octane Number Ethanol−gasoline Blends: Quantifying the Potential Benefits in the United States. Fuel, Vol. 97, Pp. 585-594.

Andy, A. (2008). Biochemical Production of Ethanol from Corn Stover: 2007 State of Technology Model. Technical Report. National Renewable Energy Laboratory.

Anjan, R. (2013). Second-generation Hydrocarbon Fuels from Oil Palm By-products. Journal of Oil Palm & the Environment. Malaysian Palm Oil Council (MPOC), Vol. 4, Pp. 22-28.

Ann, C., Kelly, J. and Jhon, M. (2000). Stillage Characterization and Anaerobic Treatment of Ethanol Stillage from Convectional and Cellulosic Feedstocks. Biomass and Bioenergy, Vol. 19, Pp. 63 - 102.

Anne, J., Robert, C., Pierre, L., Jean, N., Marlène, D. and Bruno, C., (2002). Industrial State - of- the Art of Pervaporation and Vapor Permeation in the Western Countries. Journal of Membrane Science. No 206, Pp. 87-117.

Antoni, J. (2003). Exhaust Emission Reduction Problems of Internal Combustion Engines Fueled with Biofuels. Journal of Kones Internal Combustion Engines, Vol. 10, Pp. 3 - 4.

Antonia, V. H., Timothy, E. L. and Daniel, M. K. (2000). Renewable Energy Sources. Energy and Resources Group. Renewable and Appropriate Energy Laboratory (RAEL). University of California, Berkeley, USA.

Antonius, J., Aaron, A., Marko, K., Wim, T., Johannes, P. and Jack, T. (2007). Development of Efficient Xylose Fermentation in Saccharomyces cerevisiae: Xylose Isomerase as a Key Component. Advance Biochemcal Engineering/Biotechnology, Vol. 108, Pp. 179 – 204.

Apace Research Limited (1998). Intensive Field Trial of Ethanol/Petrol Blend in Vehicles. ERDC Project, No. 2511, Dungog, NSW, Australia.

Archer, D. and Wang, P. (1990). The Dielectric Constant of Water and Debye-Hückel Limiting Law Slopes. Journal of Physical Chemistry, Vol. 19, Pp. 371.

Ashish, S. and Deshmukh, M. (2012). Performance and Emission Characterization of SI Engine using LPG-Ethanol Blends: A Review International Journal of Emerging Technology and Advanced Engineering, Vol. 2, Issue 10. www.ijetae.com.

Ashish, M. and Mohapatra, S. (2013). Biomass-based Gasifiers for Internal Combustion (IC) Engines. Indian Academy of Sciences, Vol. No. 38, Pp. 461– 476.

Asli, U., Hamid, H., Zakaria, Z., Sadikin, A. and Rasit, R. (2013). Fermentable Sugars from Palm Empty Fruit Bunch Biomass for Bioethanol Production. International Journal of Chemical, Molecular, Nuclear, Materials and Metallurgical Engineering Vol. 7, No. 12.

ASTM D 4806-03 (2012). Standard Specification for Denatured Fuel Ethanol for Blending with Gasolines for use as Automotive Spark-Ignition Engine Fuel," ASTM International, http://www.astm.org/cgi-bin/SoftCart.exe/index.shtml/E+mystore

AVL KMA Mobile Fuel Consumption Measuring System: Operating Instructions (2008). Product Guide. Austria: AVL List GmbH, Graz, June 2008, AT2262E, Rev. 02, Pp. 96.

Axtell, B. (2002). Drying Food for Profit: A Guide for Small Business. Intermediate Technology Development Group Publishing Limited. Pp. 85 - 103.

Azapagic, A. and Perdan, S. (2010). Sustainable Development in Practice: Case Studies for Engineers and Scientists, Second Edition, John Wiley & Sons Incorporation.

Azih, I. (2007). Biofuels Demand: Opportunities for Rural Development in Africa (Nigerian case-study). A paper presented at the 2nd European Forum on Sustainable Development, Berlin Germany, June 18-21.

Babu, S. (2005). Observation of the Current Status of Biomass Gasification. Research and Deployment at the Gas Technology Institute, Des Plaines, Illinos USA, Pp. 1-14.

Badal, C., Loren, B., Michael, A. and Victor, Y. (2005). Dilute Acid Pretreatment, Enzymatic Saccharification and Fermentation of Wheat Straw to Ethanol. Process Biochemistry, Vol. 40, Pp. 3693 – 3700.

Bailey, R.and Blankenhorn, P. (1984). Wood Science, Vol. 15, No. 1, Pp. 19 - 18.

Balat, M. (2011). Production of Bioethanol from Lignocellulosic Materials via the Biochemical Pathway: A Review. Energy Conversion and Management, Vol. 52, Pp. 858 – 875.

Baldwin, S.F. (1987). Biomass Stoves: Engineering Design, Development, and Denomination. VITA, USA.

Ballesteros, I., Ballesteros, M. and Manzanares, P. (2008). Dilute Sulfuric Acid Pretreatment of Cardoon for Ethanol Production. Biochemical. Engineering Journal, Vol. 42, PP. 84-91.

Baqui, M.A., M Ahiduzzuman, and Rahman M.M. (1997). Experiences in Installation and Operation of Energy Efficient Rice Parboiling System. Short Course on Energy Efficiency, Pp.108 - 124.

Barnett, J., Payne, R. and Yarrow, D. (1990). Yeasts; Characteristics and Identification, 2nd Edition, Cambridge University Press, Cambridge, UK.

Bauer, M. and Stichlmair, J. (1995). Synthesis and Optimization of Distillation Sequences

for the Separation of Azeotropic Mixtures. Comprehensive Chemical Engineering, Vol. 19, Pp. 15-20.

Bayrok, D. and Ingledew, W. (2001). Chandes in Steady State on Introduction of Lactobacillius Contaminant to a Continuous Culture Ethanol Fermentation. Journal of Industrial Microbiology and Biotechnology, Vol. 27, No. 1, Pp.39 - 45.

Belkacemi, K., Turcotte, G. and Savoie, P. (2001). Aqueous / Steam-Fractionated Agricultural Residues as Substrates for Ethanol Production. Ind. Eng. Chem. Res., Vol. 41, No. 2, Pp. 173 – 179.

Bello, R. S., Adegbulugbe, T. A. and Onilude, M. A. (2015). Characterization of Three Conventional Cookstoves in South Eastern Nigeria. AgricEngInt: CIGR Journal, Vol. 17, No. 2. http://www.cigrjournal.org.

Bello, R. S., Adegbulugbe T. A. and Onyekwere P. S. N. (2010). Comparative Study on Utilization of Charcoal, Sawdust and Rice Husk in heating oven. Agric Eng Int: CIGR, Vol.12, No. 2, Pp. 29－33.

Belonio, Alexis T., (2005). Rice Husk Gas Stove Handbook. Central Phlilippine University Iloilo City Philippines.

Biomass and Bioenergy Research Group, BBRG (2008).

Biodiesel (2009). Methanol Handling Guide. http://www.biodisel.org.pdf_files/methanol_handling_Guide.pdf. Accessed on January 28th 2016.

Bodîrlău, R., Spiridon, I. and Teacă A. (2007). Chemical Investigation of Wood Tree Species in Temperate Forest in East-Northern Romania. Bioresources, Vol. 2, No. 1, Pp. 41-57.

Bolling, C., and Suarez, N.R. (2001). The Brazilian Sugar Industry: Recent Developments. Sugar and Sweetener Situation & Outlook. Economic Research Service, USDA. http://www.ers.usda.gov/briefing/Brazil/ braziliansugar.pdf.

Boullanger, E. (1924). Distilleria Agricole et industrielle. Translation from the French by F. Marc de piolen, Pp. 3 - 8.

Bourne, J. (2007). Green Dreams: Making Fuel from Crops. National Geographic. www.greendreams Accessed 10th July 2015.

Bromberg, L. et al (2006). Calculations of Knock Suppression in highly Turbocharged Gasoline / Ethanol Engines using Direct Ethanol Injection. Cambridge MA: Massachusetts Institute of Technology.

Brooker, D., Bakker, A. and Hal,l C. (1974). Drying of Grains. The AVI Publishing Company, INC Westport, Connecticut.

Browning, B. (1967). Determination of Sugars; Methods of Wood Chemistry, Wiley, New York, Vol. 1, Pp. 598 – 599.

Caputi, A., Ueda, M. and Brown, T. (1968). Spectrophotometric Determination of Ethanol in

Wine. American Journal of Enol. Vitic 19: Pp. 160 – 165.

Cardona, C., Quintero, J.and Paz, I., (2010). Production of Bioethanol from Sugarcane Bagasse: Status and Perspectives. Bioresource Technology, Vol. 101, Pp. 4754–4766.

Carlos, et. al., (2010). Bioethanol from Lignocelluloses: Status and Perspectives in Brazil. Bioresource Technology. Vol. 101, PP. 4820 – 4825.

Caro, J., Noack, M., Kolsch, P. and Schafer, R. (2000). Microporous Mesoporous Mater, Vol. 38, Pp. 3.

Carvalheiro, F., Duarte, L., Lopes, S., Parajó, J., Pereira, H.and Gírio, F., (2005). Evaluation of the Detoxification of Brewery's spent Grain Hydrolysate for Xylitol Production. Process Biochemistry, Vol. 40, Pp. 1215 – 1223.

Carvalheiro, F., Duarte, I. and Girio, F. (2008). Hemicellulose Biorefineries: A Review on Biomass Pretreatments. Journal of Science Industrial Resources, India, Vol. 67, No. 11, Pp. 849 – 864.

Carvalho, W., Silva, S., Converti, A., Vitolo, M., Felipe, M., Roberto, I., Silva M. and Manchilha, I. (2002). Used of Immobilized Candida Yeast Cells for Xylitol Production from Sugarcane Bagasse Hydrolysate. Applied Biochemical Biotechnology, Pp. 489–496.

Chabannes, M., Chabannes, M., Ruel, K., Yoshinaga, A., Chabbert, B., Jauneau, A., Joseleau, P. and Boudet M. (2001). In Situ Analysis of Lignins in Transgenic Tobacco reveals a Differential Impact of Individual Transformations on the Spatial Patterns of Lignin Deposition at the Cellular and Subcellular Levels. Plant Journal, Vol. 28, Pp. 271-282.

Chandel, A., Kapoor, R., Singh, A. and Kuhad, R., (2007). Detoxification of Sugarcane Bagasse Hydrolysate improves Ethanol Production by Candida Shehatae NCIM 3501. Bioresources Technology, Vol. 98, Pp. 1947–1950.

Chandra, R., Bura, R. and Mabee, W. (2007). Substrate Pretreatment, the Key to Effective Enzymatic Hydrolysis of Lignocellulosics. *Advance Biochemical Engineering / Biotechnology*, Vol. 108, Pp. 67 - 93.

Chang, V. and Holtzapple, M., (2000). Fundamental Factors affecting Biomass Enzymatic Reactivity. Applied Biochemistry Biotechnology, Pp. 5 – 37.

Chato, J. C. (1962). Laminar Condensation inside Horizontal and Inclined Tubes. ASHRAE Journal, Vol. 4, Pp. 52.

Chayanoot, S. and Sairudee, D. (2013). Fermentation of Oil Palm Empty Fruit Bunch Hydrolysate to Ethanol by Baker's Yeast and Loog – Pang. PSU-UNS International Conference on Engineering and Technology, No. T.2-2.1, Pp. 1-3.

Chen, H. and Lin, Y. (2001). Case Studies on Optimum Reflux Ratio of Distillation Towers in Petroleum Refining Processes. Tamkang Journal of Science and Engineering, No.2, Vol.4, Pp. 105 -110.

Cheng, K., Cai, B., Zhang, J., Ling, H., Zhou, Y., Ge, J., and Xu J. (2008). Sugarcane Bagasse Hemicellulose Hydrolysate for Ethanol Production by Acid Recovery Process. Biochemical Engineering Journal, Vol. 38, Pp. 105 –109.

Cheng, C., Hajar, H. and Ku, S. (2007). Production of Bioethanol from Oil Palm Empty Fruit Bunch. International Conference Symposium (ICoSM). University of Malaysia Pahang. http://umpir.ump.edu.my/7248/.

Chevron (2009, 2002-2005). Motor Gasoline Technical Review Gasoline and Driving. Performance, and Gasoline Questions and Answers - Oxygenated Gasoline. http://www.chevron.com/prodserv/fuels /gas /oxygen/motorgas/.shtml.

Christos, H., Cynthia, R. and George, P. (1996). Detailed Material Balance and Ethanol Yield Calculations for the Biomass to Ethanol Conversion Process. Applied Biochemistry and Biotechnology, No. 1, Vol. 57 – 58, Pp. 443 – 459.

Chun, S. G., Kok, T. T. and Keat, T. L. (2010). Bioethanol from Lignocellulose: Status, Perspectives and Challenges in Malaysia. Subhash Bhatia Bioresource Technology, Vol. 101, Pp. 4834 – 4841.

Claassen P.A., Lopez C.A., Sijtsma L., Weusthuis R.A., Van Lier J.B., Van Niel E.W., Stams A.J. and De Vries S.S. (1999). Utilisation of Biomass for the Supply of Energy Carriers. Applied Microbiology and Biotechnology, Vol. 52, Pp. 741–755.

CNN (2001). News Broadcast, June 11.

Colburn, A. P. (1951). Problems in Design and Research on Condenser of Vapor and Vapor Mixtures. The Institution of Mechanical Engineering.

Collier, J.G. (1982). Convective Boiling and Condensation. 2nd ed., McGraw Hill.

Cooper, C. and Alley, F. (2002). Air Pollution Control A Design Approach. Third edition, Long Grove, IL: Waveland Press Inc.

Congcong, C., Hou-min, C., Zhijan, L., Hasan, J. and Zeng, Z. (2013). Sugars Analysis of Hydrolyzate: A Method for Rapid Determination of Sugars in Lignocellulose Prehydrolyzate. BioResources, Vol. 8, No. 1, Pp. 172 – 181.

Coronas, J. and Santamaría, J. (1999). Separation Purification Methods, Vol. 28, Pp. 127.

Dahiru, U., Binash, A., Antar, M. and Atia, E. (2014). Performance of Spark Ignition Engine using Gasoline-91 and Gasoline-95. International Journal of Innovative Science, Engineering & Technology, Vol. 1, Issue 6.

Dayo, F. (2008). Clean Energy Investment in Nigeria: The domestic context, Manitoba, International Institute for Sustainable Development. Pp. 59.

De-Menezes, E., Da-Silva, R., Cataluna, R. and Ortega, R. (2006). Effect of Ethers and Ether/Ethanol Additives on the Physicochemical Properties of Diesel Fuel and on Engine Tests. Fuel, Vol.85, Pp. 815–822.

Delmer, D. and Amor, Y. (1995). Cellulose Biosynthesis. Plant Cell, Vol. 7, Pp. 987 – 1000.

Demirbas, A., (2008). Biofuels: Securing the Planet's Future Energy needs. First edition. Springer, Berlin, Germany.

Demirbas, A. (2006). Global Biofuel Strategies. Energy Education Science Technology, Vol. 17, Pp. 27- 63.

Department of agricultural and food (DAF) (2006). Ethanol Production from Grain. Government of Western Australia. May 2006.

Department of Energy (DOE). Hybrid Separations/Distillation Technology: Research Opportunities for Energy and Emissions Reduction. A Study Conducted for the US DOE by the University of Texas.

Dhanapal, B., Periyasamy, G. and Jayaraj, V. (2010). Emission and Combustion of SI Engine Working under Gasoline Blended with Ethanol Oxygenated Organic Compound. American Journal of Environmental Science, Vol. 6, Pp. 495 - 499.

Dheeraj, K., Veeresh, B. and Vijay, K. (2014). Effects of LPG on the Performance and Emission Characteristics of SI Engine. International Journal of Engineering Development and Research, Vol. 2, Issue 3, ISSN: 2321-9939. www.ijedr.org.

Diane, D. S., Charles, E.W. and Karel, G. (1991). The Simultaneous Saccharification and Fermentation of Pretreated Woody Crops to Ethanol. Applied Biochemistry and Biotechnology, Vol. 28 - 29, Pp. 773.

Dirk, M. and Fred, B. (2002). Grain Drying System.

Dong, J., Lin, R. and Yen, W. (1988). Heats of Vaporization and Gaseous Molar Heat Capacities of Ethanol and the Binary Mixture of Ethanol and Benzene. Journal of Chemistry, No. 4, Vol. 66, Pp. 783 – 790.

Douglas, A. (1981). A Rapid Method for the Determination of Pentosans in Wheat Flour. Food Chemistry, Vol. 7, No. 2, Pp. 139 – 145.

Drapcho, C., Nhuan, N. and Walker T., (2008). Biofuels Engineering Process Technology. Mc Graw Hill Companies, Inc.

Dubois, M., Gilles, K., Hamilton, J., Rebers, P. and Smith, F. (1956). Colorimetric Method for Determination of Sugars and Related Substances. Analytical Chemistry, Vol. 28, No. 3, Pp. 350 – 356.

Duff, S. and Murray, W. (1996). Bioconversion of Forest ProductsIindustry Waste Cellulosics to Fuel Ethanol. Bioresource Technology, Vol. 55, No. 1, Pp. 33.

Eastop, T. and McConkey, A. (1993). Applied Thermodynamics for Engineering Technologies. 5th Edition, Prentice hall USA, Pp. 180 – 183.

Edgard, G. (2010). Production and use of Lignocellulosic Bioethanol in Europe: Current Situation and Perspectives. Bioresource Technology Elsevier, Vol. 101, Pp. 4842 – 4850.

Edgard, G. and Arnaud, D. (2011). Technoeconomic Analysis of Lignocellulosic Ethanol. Academic Press, Elsevier. 2011

Eke, A. (1991). Experimental Performance Evaluation of Laboratory and Field Solar and Hybrid Crop Dryer. Msc Thesis, Department of Agricultural Engineering ABU Zaria Nigeria.

Eknath, R., Ramchandra, S., Milind, S. and Purushottam, S. (2011). Performance of Single Cylinder DI Diesel Engine – Varied Compression Ratio Fueled With Blends of Ethanol. Proceedings of the World Congress on Engineering Vol. 3.

Emerhi, E. (2011). Physical and Combustion Properties of Briquettes Produced from Sawdust of Three Hardwood Species and Different Organic Binders. Advance Applied Science Research, Vol. 2, No. 6, Pp. 236 - 246.

Engineering Toolbox (ET), (2016). Theoritical Air for Combustion. www.engineeringtoolbox.com. Accessed 4th September, 2016.

Engineeringtoolbox.com. (2008). Material properties - Density, Heat Capacity, Viscosity and more - for Gases, Fluids and Solids. http://www.engineeringtoolbox.com/material-properties-t_24.html. Accessed 12th November 2016.

ETSAP (2010). Technology Brief, TO6. www.etsap.org. Accessed 19th June, 2015.

Excoffier, G., Toussaint, B. and Vignon, M. (1991). Biotechnology Bioengineering, Vol. 28, Pp. 792 - 801.

Fang, X., Yu, S., Jian, Z., Xiaoming, B. and Yinbo, Q. (2010). Status and prospect of Lignocellulosic Bioethanol Production in China. Bioresource Technology, Elsevier, Vol. 101, Pp. 4814 – 4819.

Farid, T., Dimitar, K. and Irini, A., (2010). Production of Bioethanol from Wheat Straw: An

Overview on Pretreatment, Hydrolysis and Fermentation. Bioresource Technology, Vol. 101, Pp. 4744 – 4753.

Ferreira, V., Mariana, O. F., Sabrina, S. M. and Nei, P. (2010). Simultaneous Saccharification and Fermentation Process of different Cellulosic Substrates using a Recombinant *Saccharomyces cerevisiae* harbouring the β-glucosidase gene. Electronic Journal of Biotechnology. Vol. 13, No. 2, March 15.

Fitriani, K. and Anwar, K., (2013). Hydrolyzate as Raw Material for Bioethanol Production. International journal on advanced science engineering information technology, Vol.3, No. 3.

Food and Agriculture Organization of the United Nations (FAO), (2002): Animal Production Based on Crop Residues: Chinese experiences. Food and Agriculture Organization of the United Nations, Roma, Italy.

Food and Agricultural Organization, (FAO), (1985): Industrial charcoal making. FAO Forestry Paper, Version 63, ISSN 0259-2800, Pp. 1.

Frank Incopera and David DeWitt (2002): Fundamentals of Heat and Mass Transfer. John Wiley & Sons, New York, 5th edition.

Fujii, T., Fang, X., Inoue, H., Murakami, K. and Sawayama S., (2009). Enzymatic Hydrolyzing Performance of *Acremonium cellulolyticus* and *Trichoderma reesei* against three Lignocellulosic Materials. Biotechnology Biofuels, Vol. 2, Pp. 24.

Ganesan, S. and Elango, A. (2013). Performance Analysis of CI Engine using blends of Castor Oil and Ethanol. International Journal of Mining, Metallurgy and Mechanical Engineering, Vol. 1, ISSN 2320–4060.

García, A., Carmona, R., Lienqueo, M. and Salazar, O. (2010). The Current Status of Liquid Biofuels in Chile. Energy, Elsevier, Vol. 30, Pp.1-8.

Garda, M., Ballesteros, I., Gonzalez, A., Oliva, J., Ballesteros, M. and Negro M. (2006). Effect of Inhibitors Released during Steam-Explosion Pretreatment of Barley Straw on Enzymatic Hydrolysis. Applied Biochemistry and Biotechnology, Vol. 129, No. 32, Pp. 278 – 288.

Garrote, G., Domı´nguez, H. and Parajo,´ J.C., (1999). Hydrothermal Processing of Lignocellulosic Materials. European Journal of Wood / Wood Prodion, Vol. 57, No. 3, Pp. 191 – 202.

Gaurav, D., Siddharth, J. and Sharma, M. (2013). Diesel Engine Performance and Emission Analysis using Biodiesel from various Oil Sources. Journal Material Environmental Science, Vol. 4, No. 4, Pp. 434 - 447.

Gaurav, T. and Nitin, S. (2014). Experimental Investigation of Ethanol Blends with Gasoline on SI Engine. International Journal of Engineering Research and Applications, Vol. 4, Pp.108 - 114.

Ghasem, N., AsmidaIi., Sadegh, S. and Mohammad, N. (2007). Acid Hydrolysis of Pretreated Palm Oil Lignocellulosic Wastes. IJE Transactions B: Applications, Vol. 20, No. 2. www.SID. ir. Accessed June 12th 2015.

Ghobadian, B., Rahimi, H., Tavakkoli, H. and Khatamifar, M. (2008). Production of Bioethanol and Sunflower Methyl Ester and Investigation of Fuel Blend Properties. Journal of Agricultural Science Technology, Vol. 10, Pp. 225 - 232.

Gil, I., Uyazán, A., Aguilar, J., Rodríguez, G. and Caicedo, I. (200). Separation of Ethanol and Water by Extractive Distillation with Salt and Solvent as Entrainer. Process Simulation. Brazilian Journal of Chemical Engineering, Vol. 25, No. 01, Pp. 207 – 215.

Givens, L. (1992). A Technical History of the Automobile, Automotive Engineering, SAE International Inc, Vol. 98, No. 6 - 8.

Grassi, G. and Allan, A. (2007). Bioelectricity and Cogeneration. Improvement of Crop Plants for Industrial End Uses, Ranalli P. (Ed.), Springer.

Graves, T., Narendranath, N., Dawson, K. and Power, R. (2006). Effect of pH and Lactic or Acetic Acid on Ethanol Productivity by Saccaromyces Cerevisiae in Corn Mash. *Journal of Industral Microbiology and Biotechnology*, vol. 33, No. 6, Pp. 469 - 474.

Grønli, M. (1996). Theoretical and Experimental Study of the Thermal Degradation of Biomass. Doctoral dissertation. Norwegian University on Science and Technology, Faculty of Mechanical Engineering, Department of Thermal Energy and Hydropower, Norway. Pp. 339.

Grous, W., Converse, A. and Grethlein, H. (1986). Effect on Steam Explosion Pretreatment on Pore Size and Enzymatic Hydrolysis of Popular. *Enzyme Microbiology Technology*, No. 8, Pp. 274 - 280.

Guerreri, G., (1992). Membrane Alcohol Separation Process: Integrated pervaporation and Fractional distillation, Transaction of Institute Chemical Electronics, Part A, Vol. 70, Pp. 501 – 508.

Gutierrez, L., Sanchez, O. and Cardona, C. (2009). Process Integration Possibilities for Biodiesel Production from Palm Oil using Ethanol obtained from Palm Lignocellulosic Residues Oil Palm Industry. Bioresource Technology, Pp. 1227-1237.

Haggin, J., (1988). New Generation of Membranes Developed for Industrial Separations, Chemical and Engineering News, Vol. 66, Pp. 7 – 16.

Hall, D. (1997). Biomass Energy in Industrialised Countries—A View of the Future. For Ecology Management, Vol. 91, No. 1, Pp. 17 – 45.

Hammel-Smith, C., Fang, J., Powders, M. and Aabakken, J. (2002). Issues Associated with the Use of Higher Ethanol Blends, National Renewable Energy Laboratory.

Hansen, A. and Zhang, Q. (2003). Engine Durability Evaluation with E-diesel. An ASAE Meeting Presentation, USA. No: 036033, Pp. 13.

Hansen, A., Zhang, Q. and Lyne, P. (2005). Ethanol–Diesel Fuel Blends – A Review. Bioresource Technology, Vol. 96, Pp. 277–285.

Harr, L., Gallagher, J. and Kell, G. (1984). *NBS/NRC Steam Tables*, Hemisphere Publishing Corporation.

Hassan, S., Nor, F., Zainal, Z. and Miskam, M. (2011). Performance and Emission Characteristics of Supercharged Biomass Producer Gas-Diesel Dual Fuel Engine. Journal of Applied Science, Vol. 11, Pp. 1606 – 1611.

Hayn, M., Steiner, W., Klinger, R., Steinmüller, H., Sinner, M. and Esterbauer, (1993). Basic Research and Pilot Studies on the Enzymatic Conversion of Lignocellulosics. Bioconversion of Forest and Agricultural Plant Residues. Wallingford: CAB International, Pp. 33 – 72.

Health Canada (2003). Potential Health Effects of Ethanol-Blend Gasoline, Health Canada Expert Panel Workshop.

He, B., Shuai, S., Wang, J. and He, H. (2003). The Effect of Ethanol Blended Diesel Fuels on Emissions from Diesel Engine. Atmospheric Environment, Vol. 37, Pp. 4965 – 71.

Héctor, A. R., António, A. V. and José, A. T. (2012). Kinetic Modeling of Enzymatic Saccharification using Wheat Straw Pretreated under Autohydrolysis and Organosolv Process. Industrial Crops and Products. Vol. 36, Pp. 100 – 107.

Heitz, M., Capek, E. and Koeberle, P. (1991). Fractionation of Populus Tremuloides in the Pilot Plant Scale, Optimization of Steam Pretreatment Conditions using STAKE II technology. *Bioresoures. Technology*, Vol. 35, Pp. 23 - 32.

Henley, Ernest J. and Seader, J. (2006). Separation Process Principles. John Wiley & Sons, 2nd Edition, New York.

Helma Krishna R. (2013). Review of Research on Production Methods of Hydrogen: Future

Fuel. European Journal of Biotechnology and Bioscience. Vol. 1, No. 2, Pp. 84 - 93.

Hendriks, A.T. and Zeeman, G., (2009). Pretreatments to enhance the Digestibility of Lignocellulosic Biomass. Bioresour. Technol. Vol. 100, No. 1, Pp. 10 – 18.

Hennepe, C., Bargeman, D., Mulder, V. and Smolders, A. (1988). Permeation through Zeolite filled Silicone Rubber Membranes, Characterization of Porous Solids. Ed. K. Ungen, Elsevier, Amsterdam, Pp. 411– 420.

Highina, B.K., Hashima, I. and Bugaje, I.M.(2011). Optimization of Ethanol Production from Sugar Molasses in Nigeria. Journal of Applied Technology in Environmental Sanitation, Vol. 1, No. 3, Pp. 233 - 237.

Higuchi, T., (1985). Biosynthesis of Lignin, in: Higuchi, T. (Ed.), Biosynthesis and Biodegradation of Wood Components. Academic Press, New York, Pp. 141-160.

Hiregoudar, Y., Manjunatha, K., Chandragowda, M. and Basava, P. (2014a). Performance & Emission of C I Engine Using Diesel & Ethanol Blended with Jatropa Oil. International Journal of Recent Development in Engineering and Technology Website, Volume 2, Issue 6. www.ijrdet.com.

Hiregoudar, Y., Manjunatha, K., Chandragowda, M. and Basavaprakash, B. (2014b). Performance & Emission of CI Engine Using Diesel & Ethanol blended with linseed oil. International Journal of Engineering Science and Innovative Technology, Vol. 3Pp. 735.

Holman, S.P. (1990). Hat Transfer. (McGraw Hill).

Holland, C. (1997). Fundamentals of Multi-Component Distillation. New York: McGraw-Hill.

Holt, G., Blodgett, T. and Nakayama, F. (2006). Physical and Combustion Characteristics of Pellet Fuel from Cotton Gin by-Products Produced by Select Processing Treatments. Industrial Crops and Products, No. 3, Vol. 24, Pp. 294.

Hossein, S., Michael S. and Nelson J. (2006). The Economic Feasibility of Ethanol Production from Sugar in the United States. United States Department of Agriculture.

Hsiao, H., Chiang, L., Chen, L. and Tsao, G. (1982). Enzym Microbiological Technology, Vol. 4, Pp. 25.

Hsieh, W., Chen, R., Wu, T. and Lin, T. (2002). Engine Performance and Pollutant Emission of an SI Engine Using Ethanol-Gasoline Blended Fuels, Atmospheric Environment, Vol. 36, Pp. 403 - 410.

Hsu, T. (1996). Pretreatment of Biomass. Handbook on Bioethanol Production and Utilization. Taylor & Francis, Pp. 179-212.

http,//www.iogenenzymes.com/company/demo_plant/index.html

Hu, Z., Wang, J., Kong, H. and Chai, X. (2008). A Novel Method for Determination of Sugars by UV Spectroscopy. Journal of Chemical Industrial Engineering, Vol. 59, N o. 5, Pp. 1233 – 1237.

Huang, J., Wang, Y., Li, S., Roskilly, A., Hongdong, Y. and Li, H. (2009): Experimental Investigation on the Performance and Emissions of a Diesel Engine Fuelled with Ethanol–Diesel Blends. Applied Thermal Engineering, Vol. 29, No. 11–12, Pp. 2484 –90.

Huseyin, S., Tolga, T., Can, C. and Melih, O. (2006). Effect of Ethanol-Gasoline Blends on Engine Performance and Exhaust Emission in Different Compression Ratio. Applied Thermal Science, Vol. 26, Pp. 2272 - 2278.

Ibrahim, T. (2011). Experimental Study of Gasoline-Alcohol Blend on Performance of Internal Combustion Engine. European Journal of Scientific Research, Vol. 52, Pp. 16 - 22.

Iguaz, A. and Vı´rseda, P. (2007). Moisture Desorption Isotherms of Rough Rice at high Temperatures. Journal of Food Engineering, Vol. 79, Pp. 94-802. www.sciencedirect.com.

Ijagbemi, C., Adepo, S. and Ademola, K. (2014). Evaluation of Combustion Characteristic of Charcoal from Different Tropical Wood Species. International Organization of Scientific Research, Vol. 04, Issue 04, Pp. 50 - 57.

Inderwildi, O.R. (2008). Energy and Environmental Science. Vol. 2, Pp. 343.

International Energy Agency (2007). World Energy Outlook. Paris: IEA-OECD, 2007 Edition.

International Energy Agency (2006). World Energy Outlook, 2006 Edition.

International Fuel Quality Center, IFQC, (2004). Setting a Quality Standard for Fuel Ethanol. Report Presented to: Department of the Environment and Heritage. DEH Ethanol Standard, 18 / 2004.

International Rice Research Institute (IRRI). Paddy Drying. Agricultural Engineering Unit. www.irri/paddy drying/org. (Accessed 13th August 2010).

James, D. K. and John, K. L. (2001). Wheat Straw for Ethanol Production in Washington: A Resource, Technical, and Economic Assessment. Washington State University Cooperative Extension Energy Program. WSUCEEP201084. Sept. 2001.

James, E. and David, F. (1986). Biochemical Engineering Fundamentals. Second Edition Pp. 38 - 42.

Jie, L., Xuezhi, L., Jian, Z. and Yinbo, Q. (2012). Emzymatic Saccharification and Ethanol Fermentation of Reed Pretreated with Liquid Hot Water. Journal of Biomedicine and Biotechnology, Article ID 276278.

Jim Clark (2005). Non Ideal Mixture of Liquids. www.chemguide.co.uk/physical/phaseeqia/nonideal.html. Accessed 18th June, 2015.

Jinlan, C., Shao, Y., Zhu, J. and Thomas, W. (2014). Ethanol Production from Non-Detoxified

Whole Slurry of Sulfite-Pretreated Empty Fruit Bunches at a Low Cellulase Loading. Bioresource Technology, Vol. 164, Pp. 331–337.

Jitendra, k., Ansari, N., Vikas, V. and Sanjeev, K. (2013). Exhaust Gas Analysis and Parametric Study of Ethanol Blended Gasoline Fuel in Spark Ignition Engine. American Journal of Engineering Research (AJER), Vol. 2, Pp.191-201.

John, B. H. (1988). Internal Combustion Engine Fundamentals First Edition.

John, W. (2006). Journal on the World Watch Institute and Center for American Progress. Vol. 100, Pp. 30.

Jonsson, A. and Bengt, H. (2006). Planning for Increased Bioenergy use - Evaluating the Impact on Local Air Quality. Biomass and Bioenergy, No. 6, Vol. 30, Pp. 543.

Jones, J. and Dugan, R. (1998). Engineering Thermodynamics. Prentice Hall India Limited. Published by New Delhi-110001.

Josef, L. (2006). The use of Bioethanol in Engine Fuels in the Czech Republic. Research Center for Engine and Vehicle Technology II. Josef.laurin@jslib.cz.

Joseph, K. K. and Oliver, H. (2016). Experimental Evaluation of Bulk Charcoal Pad Configuration on Evaporative Cooling Effectiveness. CIGR Journal. Vol. 18, No. 4, Pp. 11. http://www.cigrjournal.org.

Joseph, B., Sankarganesh, P., Edwin, B., Raj, S. and Jeevitha, M. (2011). Sustainable Energy Resources from Chicken. Asian Journal of Applied Science, Vol. 4, Pp. 355 – 361.

Julia´n, A. Q., Luis, E. R. and Carlos, A. C., (2011). Production of Bioethanol from Agro Industrial Residues as Feedstocks. Academic Press, Elsevier. 2011.

Jungho, Cho and Hwayong, Kim (2015). Comparison of Extractive with Azeotropic Distillation in Ethanol Dehydration. Dealim Engineering Company Limited. www.lnk.kstudy.com/others/web.

Jun-Seok K, Soon-Chul, P., Jin-Woo, K., Jae Chan, P., Sung-Min, P. and Jin-Suk, L., (2010). Production of Bioethanol from Lignocellulose: Status and Perspectives in Korea. Bioresource Technology. Vol. 101, Pp. 4801– 4805.

Karimi, K., Emtiazi, G. and Taherzadeh, M., (2006). Ethanol Production from Dilute-Acid Pretreated Rice Straw by Simultaneous Saccharification and Fermentation with Mucor Indicus, Rhizopus Oryzae, and Saccharomyces Cerevisiae. Enzyme Microbiology Technology, Vol. 40, Pp. 138 –144.

Karl, E., Magnus, H., Björn, R., Mats, W. and Roger, W. (2005). Blending of Ethanol in Gasoline for Spark Ignition Engines. AVR, MTC. www.avlmtc.com.

Kass, M., Thomas, J., Storey, J., Domingo, N., Wade, J. and Kenreck, G. (2001). Emissions

from a 5.9 Liter Diesel Engine Fueled with Ethanol Diesel Blends. SAE Technical, Pp.1632.

Katamanee, A. (2006). Appropriate Technology Evaluation for Oil Palm Product Utilization in Krabi Province. *Mahidol University*, www.mahidol.ac.th/thesis/2549/cd388/4637145.pdf

Kays, W. M. and Perkins, H. C. (1972). Chapter 7. In Handbook of Heat Transfer, ed. W. M. Rohsenow and J. P. Hartnett. New York: McGraw-Hill.

Kent, H. S., Amber, B., Curtis, R., Eric, C. and Mani, N. (2012). Review of Biodiesel Composition, Properties, and Specifications. Renewable and Sustainable Energy Reviews. Vol. 16, Pp.143 – 169.

Khurmi, R. S. (2005). Hydraulics, Fluid Mechanics and Hydraulic Machines. S.Chand and Company Limited, Rom, Nagar, New Delihi – 110 - 025.

Khurmi, R. and Gupta, J. (2006). Thermal Engineering. Chand and Company Limited, Two Colour Edition.

Kim, T. and Lee, Y., (2005). Pretreatment of Corn Stover by Soaking in Aqueous Ammonia. Applied Biochemistry Biotechnology, Vol. 124, No. 1, Pp. 1119 –1131.

Kim, T.H. and Lee, Y.Y., (2007). Pretreatment of Corn Stover by Soaking in Aqueous Ammonia at Moderate Temperatures. Applied Biochemistry Biotechnology, Vol. 136, No. 140, Pp. 81– 92.

Kister, H. (1992). Distillation Design. New York: McGraw-Hill.

Kister, H. (2008). Equipment for Distillation. Gas Absorption, Phase Dispersion and Phase Separation. Section 14: Perry's Chemical Engineers Handbook, 8th Edition, New York: McGraw-Hill.

Klavina, K., Cinis, A. and Zandeckis, A. (2014). A Study of Pressure Drop in an Experimental Low Temperature Wood Chip Dryer. Agronomy Research, Vol. 12, No. 2, Pp.511–518.

Knauf, M. and Moniruzzaman, M., (2004). Lignocellulosic Biomass Processing: A Perspective. International Sugar Journal, Vol. 106, Pp. 147–150.

Kojima, M. and Johnson, T. (2005). Potential for Biofuels for Transport in Developing Countries. Energy Sector Management Assistance Programme (ESMAP), World Bank Publication.

Kongdej, L. and Songchai, W. (2009). Drying Kinetics of Steamed Glutinous Rice with a Free Convective Solar Dryer. Walailak Journal of Science and Technology, Vol. 6, No. 2, Pp. 217 - 229.

Koonin, S. (2006). Getting Serious about Biofuels. Science, Vol. 311, Pp. 435.

Koyuncu, T. and Pinar, Y. (2007). The Emissions from a Space-Heating Biomass Stove. Biomass and Bioenergy, No. 31, Vol. 1, Pp. 73.

Kris, A. (2004). Artisan Distilling. A Guide for Small Distilleries. Electronic Edition 1.0.0

Kristina, B., Haide, B., Ulrika, F. and Ulf, L. (2008). Technical Guidance to Biofuels SenterNovem and ICLEI European Secretariat, Netherlands. www.biofuel.cities.eu.

Kujawski, W. (2000). Application of Pervaporation and Vapor Permeation in Environmental Protection. Polish Journal of Environmental Studies, Vol. 9, No. 1, Pp.13 - 26.

Kumar, S., Sing, S., Mishra, I. and Adhikari, (2009). Recent Advances in Production of Bioethanol from Lignocellulosic Biomass. Chemical Engineering & Technology, Vol.32, No 4, Pp. 517-526.

Kyoto Protocol: http://unfccc.int/kyoto_protocol/items/2830.php.

Lalit, K., Gaurav, ,C., Majumderb, C. and Sanjoy, G. (2011). Utilization of Hemicellulosic Fraction of Lignocellulosic Biomaterial for Bioethanol Production. Advances in Applied Science Research, Vol. 2, No. 5, Pp. 508-521. www.pelagiaresearchlibrary.com

Lapuerta, M., Armas, O. and Garcı´a-Gontreras, R. (2007). Stability of Diesel–Bioethanol Blends for Use in Diesel Engines. Fuel, Vol. 86, Pp. 1351–1357.

Laws of Federation of Nigeria (2004). Companies Income Tax Act A (Cap C 21, Laws of Federation of Nigeria, 2004), Value Added Tax Act (Cap V 1, Laws of Federation of Nigeria, 2004), Petroleum Profit Tax Act (Cap P 13, Laws of Federation of Nigeria, 2004).

Lee, D., Owens, N., Boe, A. and Jeranyama, P., (2007). Composition of Herbaceous Biomass Feedstocks. http://agbiopubs.sdstate.edu/articles/SGINC1-07.pdf

Leland, M. V. (2005). A Review of Pervaporation for Product Recovery from Biomass Fermentation Processes. Journal of Chemical Technology and Biotechnology. Vol. 80, Pp. 603 – 629.

Li, D., Zhen, H., Xingcai, L., Wu-gao, Z. and Jianguang, Y. (2005). Physico-Chemical Properties of Ethanol-Diesel Blend Fuel and its Effect on Performance and Emissions of Diesel Engines. Renewable Energy, Vol. 30, Pp. 967- 976.

Li, X., Qiao, X., Zhang, L., Fang, J., Huang, Z. and Xia, H. (2005). Combustion and Emission Characteristics of a Two-Stroke Diesel Engine Operating on Alcohol. Renewable Energy, Vol. 20, Pp. 1-10.

Lin, C. and Huang, J. (2003). An Oxygenating Additive for Improving the Performance and Emission Characteristics of Marine Diesel Engines. OCEAN Engineering, Vol. 30, No. 13, Pp. 169 –715.

Liu, C. and Wyman, C.E., (2003). The Effect of Flow Rate of very Dilute Sulfuric Acid on

Xylan, Lignin, and Total Mass Removal from Corn Stover. Industrial Engineering Chemistry Research. Vol. 43, No. 11, Pp. 2781 – 2788.

Liu, R. and Shen, F (2008). Impacts of Main Factors on Bioethanol Fermentation from Stalk Juice of Sweet Sorgum By, Immorbilized Saccharomyces Cerevisiea (CICC 1308). Bioresources Technology, Vol. 99, Pp. 847 - 854.

Luyna, U., Hay, S., Sophiak, S. and Sar, C. (2009). Status and Potential for the Development of Biofuels and Rural Renewable Energy. Cambodia. Asian Development Bank.

Lynd, L., Larson E., Greene, N., Laser, M., Sheehan, J. and Dale, B. (2009). The Role of Biomass in America's Energy Future: Framing the Analysis. Biofuels Bioprod. Bioref. Vol. 3, Pp. 113 – 123.

Lynd, L., Lase,r M., Bransby, D., Dale, B., Davison, B. and Hamilton, R. (2008). How Biotech can Transform Biofuels. National Biotechnology, Vol. 26, Pp. 169 –172.

Lynd, L. (1996). Overview and Evaluation of Fuel Ethanol from Cellulosic Biomass: Technology, Economics, the Environment, and Policy. Annual Review of Energy and the Environment, Vol. 21, Pp. 403 – 465.

Mabee, W.E. and Saddler, J.N. (2010). Bioethanol from Lignocellulosics: Status and Perspectives in Canada. Bioresource Technology, Vol. 101, Pp. 4806 – 4813.

Madamba, P. S; Driscoll, R. H. and Buckle, K. A. (1996). The Thin Layer Drying Characteristics of Garlic Slices. Journal of Food Engineering, Vol. 37, Pp. 437 – 449.

Mochamad, A. (2011). Engineering Design Guidelines: Distillation Column Selection and Sizing. KLM Technology Group. www.klmtechgroup.com.

MacLean, H., and Lave, L. (2003). Evaluating Automobile Fuel/Propulsion System Technologies, Progress in Energy and Combustion Science, Vol. 29, Pp. 1- 69.

Majer, V. and Svobodo, V. (1985). Enthalpies of Vaporization of Organic Compouds: A Critical Review And Data Compilation. Blackwell scientific publications, oxford, Pp. 300.

Małgorzata, L. and Wojciech, K. (2007). Ethanol Production from Lactose in a Fermentation/Pervaporation System. Journal of Food Engineering, Vol. 79, Pp.430 – 437.

Mařík, J., Pexa, J., Kotek, M. and Hönig, V. (2014). Comparison of the Effect of Gasoline – Ethanol E85 – Butanol on The Performance and Emission Characteristics of the Engine Saab 9-5 2.3 L Turbo. Agronomy Research, Vol. 12, No. 2, Pp. 359 – 366.

Marsh, K. (1987). Recommended Reference Materials for the Realization of Physicochemical Properties, Blackwell Scientific Publications, Oxford.

Martinez, A., Rodriguez, M.E., Wells, M.L., York, S.W., Preston, J.F. and Ingram, L.O. (2001). Detoxification of Dilute Acid Hydrolysates of Lignocellulose with Lime.

Mathewson, S.W. (1980). The Manual for the Home and Farm Production of Alcohol Fuel. Ten Speed Press J.A. Diaz Publications, USA.

Mayote, S., Lindhjem, C., Rao, V. and Sklar, M. (1994). Reformulated Gasoline Effects on Exhaust Emissions: Phase 1: Initial Investigation of Oxygenate, Volatility Distillation and Sulfur Effect, SAE Technical Paper, Pp. 941 - 973.

Mcdougall, G. (1991). The Physical Nature and Manufacture of Activated Carbon. Journal South African Institute of Mineral Metal, Vol. 91, No. 4. Pp. 109 - 120.

Milani, S. (1999). Optimization of Solvent Feed Rate for Maximum Recovery of High Purity Top Product in Batch Extractive Distillation. Trans. IChemical Engineering, Vol. 77, Pp. 469 – 470.

Milindi, P. (2009). Experimental Study for Improving Energy Efficiency of Charcoal Stove. Journal of Scientific and Industrial Research, Vol. 68, Pp.412 – 416.

Millati, R., Wikandari, R., Trihandayani, E., Cahyanto, M., Taherzadeh, M. and Niklasson, C. (2011). Ethanol from Oil Palm Empty Fruit Bunch via Dilute-acid Hydrolysis and Fermentation by Mucor Indicus and Saccharomyces Cerevisiae. Agriculture Journal, Vol. 6, No. 2, Pp. 54–59.

Millati, R., Nikklasson, C., and Taherzadeh, M. (2002). Effect of pH, Time and Temperature of Overliming on Detoxification of Dilute Acid Hydrolyzates for Fermentation by S. Cerevisiae. Process Biochemistry, Vol. 38, No. 4, Pp. 515 – 522.

Miller, G. (1959). Use of Dinitrosalicylic Acid Reagent for Determination of Reducing Sugar. Analytical Chemistry, Vol. 31, No. 3, Pp. 426 – 428.

Mingjia, Z., Fang, W., Rongxin, S., Wei, Q. and Zhimin, H., (2010). Ethanol Production from High Dry Matter Corncob using Fed-Batch Simultaneous Saccharification and Fermentation after Combined Pretreatment. Bioresource Technology, Vol. 101, Pp. 4959 – 4964.

Mohd, A., Loh, SOh K., Nasrin, A. and Astimar, A. (2011). Bioethanol Production from Enzymatically Saccharified Empty Fruit Bunches Hydrolysate using Saccharomyces Cerevisiae, ISSN 1819-3412.

Moran and Shapiro (1995). Fundamentals of Engineering Thermodynamics Third Edition.

Moran, J. and Howard, N. (2000). Fundamentals of Engineering Thermodynamics. 4th

Edition, New York: John Wiley & Sons, Inc.

Morris, D. and Brondum, J. (2000). Does Ethanol Result in More Air Pollution? Institute for Local Self- Reliance, USA.

Mosier, N., Ladisch, C. and Ladich, M., (2002). Characterization of Acid Catalytic Domains for Cellulose Hydrolysis and Glucose Degradation. Biotechnology and Bioengineering, Vol. 6, No. 79, Pp. 610 - 618.

Mujtaba, I. (1999). Optimization of Batch Extractive Distillation Processes for Separating Close Boiling and Azeotropic Mixtures. Trans. IChemical Engineering, Vol. 77, Pp. 588 – 596.

Murali, M., Seshagiri, V., Murthy, P. and Reddy, T. (2011). Performance Evaluation of A Low Heat Rejection Diesel Engine with Carbureted Ethanol and Crude Jatropha Oil. Indian Journal of Engineering and Materials Sciences. Vol. 18, Pp. 293 - 302.

Mustafa, K., Yakup, S., Tolga, T. and Huseyin, S. (2009). The Effect of Ethanol-Unleaded Gasoline Blends on Engine Performance and Exhaust Emission In A Spark-Ignition Engine. Renewable Energy, 34, Pp. 2101 - 2106.

Nair, S., Lai, Z., Nikolakis, V., Xomeritakis, G., Bonilla, G. and Tsapatsis, M. (2001). Microporous Mesoporous Mater. Vol. *48*, Pp. 219.

Nakorn, T., Nakarin, S., Ekarin, C. and Narawut, S. (2010). Production of Charcoal from Woods and Bamboo in A Small Natural Draft Carbonizer. International Journal of Energy and Environment, *Vol.1, Issue 5, Pp. 911 - 918.*

National Institute for Occupational Safety and Health (NIOSH). Pocket Guide to Chemical Hazards.

National Renewable Energy Laboratory (NREL) (2002): Issues Associated with the Use of Higher Ethanol Blends. http://www.nrel.gov/docs/fy03osti/32206.pdf.

Nebraska Ethanol Board (2011). Ethanol Blended Fuels. Clean Fuel Development Coalition. www.cleanfuelsdc.org.

Negro, M., Manzanares, P. and Oliva, J. *(*2003). Changes in Various Physical/Chemicals Parameters of *Pinus Pinaster* Wood after Steam Explosion Pretreatment. *Biomass Bioenergy*, Vol. 25, Pp. 301-308.

Negro, M., Manzanares, P. and Ballesteros, I. (2003). Hydrothermal Pretreatment Conditions to Enhance Ethanol Production from Popular Biomass. *Applied Biochemical Biotechnology*, Vol. 105, Pp. 87 - 100.

Neureiter, M., Herbert, D., Christiane, T., Bamusi, S. and Rudolf, B. (2002). Dilute Acid Hydrolysis of Sugarcane Bagasse at Varying Conditions. Applied Biochemistry and Biotechnology, Vol. 98 -100, No. 1 - 9.

Nigeria Tribune Newspaper (16/09/2008). Africa's First Ethanol Refinery Flagged off in Ekiti. Available at http://www.tribune.com.ng/16092008/ biznes.html.

Nigerian National Petroleum Corporation, NNPC (2005). Draft Nigerian Biofuel Policy and Incentives. NNPC Approved Ethanol Policy. NNPC, 2007.

Niven, R. (2005). Ethanol in Gasoline: Environmental Impacts and Sustainability Review Article, Renewable and Sustainable Energy Reviews, Vol. 9, Pp. 535 - 555.

Nomura, M., Bin, T., Nakao, S. I., (2002). Selective Ethanol Extraction from Fermentation Broth using a Silicate Membrane, Separation Science and Technology, Vol. 27, Pp. 59 – 66.

Nor, A., Mailin, M., Roslindawati, H., Mohd, F., Wan, N. and Kok-Giap, H. (2012). Bio-oils and Diesel Fuel derived from Alkaline treated Empty Fruit Bunch (EFB). International Journal of Biomass and Renewable Energy, Vol. 1, Pp. 6 – 14.

Norhisam, M., Suhairi, R., Aravind, V., Nashiren, F., Hanamoto, T., Yamada, H. and Shirai, Y. (2011). Performance Improvement of a Portable Electric Generator Using an Optimized BioFuel Ratio in a Single Cylinder Two-Stroke Engine. *Energies* 2011, Vol. *4*, www.mdpi.com/journal/energies.

Nurmi, J. and Kari, H. (2007). The Characteristics of Whole-Tree Fuel Stocks from Silvicultural Cleanings and Thinnings. Biomass and Bioenergy, No. 31, Vol. 6, Pp. 381.

Nurul, A., Nasrin, A., Loh, S. and Choo, Y. (2014). Bioethanol Production by Fermentation of Oil Palm Empty Fruit Bunches Pretreated with Combined Chemicals. Journal of Applied Environmental and Biological Sciences, Vol.4, No.10, Pp. 234 - 242.

Nyachaka, C., Yawas, D. and Pam, G. (2013). Production and Performance Evaluation Of Bioethanol Fuel from Groundnuts Shell Waste. American Journal of Engineering Research (AJER), Vol. 02, Issue-12, Pp. 303 - 312.

Oak Ridge National Laboratory (2002). Fuel Specifications and Fuel Properties issues and their Potental Impact on the Use of Ethanol as a Transportation Fuel. Phase III Project Deliverable Report Ethanol Project, http://biodiesel.pl/uploads/media/pdf.

Obernberger, I., Thomas, B. and Georg, B. (2006). Chemical Properties of Solid biofuels-

Significance and Impact. Biomass and Bioenergy, No. 11, Vol. 30, Pp. 973-82.

Ohe, S. (1979). Correlation and Prediction of Salt Effects in Vapor–Liquid Equilibrium in Alcohol–Water–Salt Systems, Advances in Chemistry Series, No. 155.

Oil World (2012). Oil World. http://www.oilworld.biz/app.php?ista. http://www.rspo.org/ Accessed December 18th 2013.

Ojolo, S., Abolarin, S. and Adegbenro, S. (2012). Development of a Laboratory Scale Updraft Gasifier. International Journal of Manufacturing Systems, Vol. 2, Pp. 21 - 42.

Oliver, C. and William, H. (2010). Medium Scale Solar Crop Dryers for Agricultural Products. Centre for Resource Management and Environmental Studies, University of the West Indies, Cave Hill Campus. www.dryer/annex3/pdf. (Accessed August 13th 2010).

Olsson, L., Linde´n, T. and Hahn-Ha¨Gerdal, B., (1992). Performance of Microorganisms in spent Sulfite Liquor and Enzymatic Hydrolysate of Steam-Pretreated Salix. Applied Biochemistry Biotechnology, Vol. 34-35, No.1, Pp. 359 – 368.

Onwuka, G. (2005). Food Analysis and Instrumentation (Theory and Practice). First Edition.

Ophardt, P. (2003). Chemistry of Hydrogen Bond. Journal of Applied Chemistry, Vol. 73, Pp.18 – 24.

Orbital Engine Company (2002). A Literature Review Based Assessment on the Impacts of A 10% and 20% Ethanol Gasoline Fuel Blend on Non- Automotive Engines, Environment Australia.

Oscar, J. and Carlos, A. (2008). Trends in Biotechnological Production of Fuel Ethanol from Different Feedstocks. Bioresource Technology, Vol. 99, Pp. 5270 – 5295.

Oyeleke, S., Dauda, B., Oyewole, O., Okoliegbe, I. and Ojobode, T. (2012). Production of Bioethanol from Cassava and Sweet Potato Peels. Advanced in Environmental Biology, Vol. 6, Pp. 241-245.

Ozer, C., Smet, E. and Nazim, U. (2004). Effects of Ethanol Addition on Performance and Emissions of A Turbocharged Indirect Injection Diesel Engine Running at Different Injection Pressures. Energy Conversion and Management, Vol. 45, Pp. 2429 – 40.

Pal, A., Maji. S., Sharma, O. and Babu, M. (2004). Vehicular Emission Control Strategies for the Capital City of Delhi, India. No. 28, Pp.16 - 18.

Pang, X., Shi, X., Mu, Y., He, H., Shuai, S., Chen, H. and Li, R. (2006). Characteristics of Carbonyl Compounds from A Diesel-Engine using Biodiesel–Ethanol–Diesel As Fuel. Atmospheric Environment, Vol. 40, Pp. 7057 – 7065.

Paola, A., Iván, D. and Gerardo, R. (2010). Comparison of the Main Ethanol Dehydration Technologies through Process Simulation. 20th European Symposium on Computer Aided Process Engineering – ESCAPE20, © 2010 Elsevier B.V.

Parameswaran, B., Raveendran, S., Reeta, R., Surender, V., Lalitha, D., Satya, N., Noble, K., Rajeev, K. and Ashok, P., (2010). Bioethanol Production from Rice Straw: An Overview. Bioresource Technology, Vol. 101, Pp. 4767 – 4774.

Parameswaran, B., Janu, K.U., Raveendran, S. and Ashok, P. (2011). Hydrolysis of Lignocellulosic Biomass for Bioethanol Production. Academic Press, Elsevier.

Pari, L. (2001). Energy Production from Biomass: The Case of Italy. Renewable Energy, Vol. 1-3, No. 22, Pp. 21-30.

Peng, M., Vane, L. and Liu, S. (2003). Recent Advances in VOCs removal from Water by Pervaporation. Journal of Hazardous Material, Vol. 98, Pp. 69 – 90.

Pereira Ramos L. (2003). The Chemistry involved in the SteamTreatment of Lignocellulosic Materials. Quimica Nova. Vol. 26, No. 6, Pp. 863 – 871.

Perry's Chemical Engineers' Handbook, McGraw-Hill, Inc., 8th Edition, 1997.

Perry's Chemical Engineers' Handbook, McGraw-Hill Companies, 7th Edition, 1997.

Perry, Clinton and Kirkpatrick (1963). Chemical Engineer's Handbook. Fourth edition, McGraw-Hill, Pp. 13 – 18.

Peter, K. and Gbenga, S. (2007). The Nigerian Biofuel Policy and Incentives: A Need To Follow the Brazilian Pathway. International Association for Energy Economics, Pp. 35.

Petersson, A., Thomsen, M., Hauggaard, H. and Thomsen, A. (2007). Potential Bioethanol and Biogas Production using Lignocellulosic BiomassfFrom Winter Rye, Oilseed Rape and Faba Bean. Biomass and Bioenergy, Vol. 31, Pp. 812 – 819.

Peterson Thokozani Ngema (March 2010). Separation Processes for High Purity Ethanol Production. Department of Chemical Engineering, University of Technology Durban.

Phillips, A.O., Mary, A. O. and Egelioglu, F. (2011). Bioethanol Derivation from Energy Crop in Nigeria: A Path to Food Scarcity or Biofuel Advancement. Proceedings of the World Congress on Engineering (WCE), London, U.K. 3

Phillips, A.O. and Mary, A.O. (2011). Nigeria's Bioethanol: Need for Capacity Building Strategies to Prevent Food Crises. World Renewable Energy Congress, Sweden. Bioenergy Technology (BE).

Piarpuza´n, D., Quintero, J.A. and Cardona, C.A., (2011). Empty Fruit Bunches from Oil Palm as a Potential Raw Material for Fuel Ethanol Production. Biomass and Bioenergy. Vol. 35, No. 3, Pp. 1130–1137.

Piotr, O., Przemyslaw, L., Jens, H., Anne, B.T. and Mette, H. T. (2007). Ethanol Production from Maize Silage as Lignocellulosic Biomass in Anaerobically Digested and Wet-Oxidized Manure. Bioresource Technology.

Practical Action Technical Brief (PATB). Solar Drying: Technology Challenging Poverty. The Schumacher Centre for Technology and Development. Warwickshire CV23 9Q2 United Kingdom. www.practicalaction.org. Accessed August 13th 2010.

Pradeep, C.M. and Samir, K. K. (2011). Biomass-Derived Syngas Fermentation into Biofuels. Academic Press, Elsevier. 2011.

Prassad, S., Singh, A. and Joshi, H. (2007). Ethanol as an Alternative Fuel from Agricultural, Industrial and Urban Residues. Resources Conservation and Recycling, Vol. 50, Pp. 1–39.

Pulkrabek (1997). Engineering Fundamentals of the Internal Combustion Engine First Edition.

Punnapayak, H. and Emert G. (1986). Use of Pachysolen Tannophilus in Simultaneous Saccharification and Fermentation (SSF) of Lignocellulosics. Biotechnology Letter, Vol. 8, Pp. 63 – 66.

Quintero, J.A., Cardona, C.A. and Triana, C., (2010). Analysis of Sugarcane Bagasse and Coffee Cut. 32nd Symposium on Biotechnology for Fuels and Chemicals. Clearwater Beach, USA.

Quintero, J.A. and Cardona, C.A., (2011). Process Simulation of Fuel Ethanol Production from Lignocellulosics using Aspen Plus. Industrial & Engineering Chemistry Research. In Press, Corrected Proof.

Rakopoulos, D., Rakopoulos, C., Kakaras, E. and Giakoumi, E. (2008). Effect of Ethanol Diesel Fuel Blends on the Engine Performance and Emissions of Heavy Duty DI Diesel Engine. Energy Conversion and Management, Vol. 49, No. 11, Pp. 3155 – 62.

Rajeev, K., Vikram, J., Raveendran, S., Parameshwaran, B., Kanakambaran, U, Kuttavan, V., Kuni, P. and Ashok, P. (2010). Lignocellulosic Ethanol in India: Prospects, Challenges and Feedstock Availability. Bioresource Technology, Elsevier, Vol. 101, Pp. 4826 – 4833.

Rajvir, S., Maheshwari, R. and Ojha, T. (1980). Development of Husk fired furnace. Journal of Agricultural Engineering Resources, Vol. 25, Pp.109-120.

Rathore, N., Panwar, N. and Vijay, C. (2009). Design and Techno Economic Evaluation of Biomass Gasifier for Industrial Thermal Applications. African Journal of Environmental Science and Technology, Vol. 3, No. 1, Pp. 006 - 012.

Raneses, A., Hanson, K. and Shapouri, H. (1998). Economic Impacts from Shifting Cropland

Use from Food to Fuel. Biomass Bioenergy, Pp. 15.

Regmi, A. and Mark, G. (2001). New Directions in Global Food Market. United State. Department of Agricultural Economic Research Service, Vol. iv, Pp. 794.

Renewable Fuels Association (RFA), (2002). Fuel Ethanol Industry Guidelines Specifications, and Procedures. RFA Publication. http://www.pei.org/FRD/rfa_pub.pdf.

Renström, R. (2006). The Potential of Improvements in the Energy Systems of Sawmills when Coupled Dryers are used for Drying of Wood Fuels and Wood Products. Biomass and Bioenergy, No. 30, Vol. 5, Pp. 452 - 60. .

Ria, M., Rachma, W., Elisabeth, T., Muhammad, N., Mohammad, J. and Claes, N. (2011). Ethanol from Palm Oil Empty Fruit Bunch via Dilute Acid hydrolysis and Fermentation by *Mucor indicus and Saccharomyces Cerevisiae*. Agricultural journal, Vol. 6, No. 2, Pp. 54 – 59.

Richana, N., Winarti, C., Hidayat, T. and Prastowo, B. (2015). Hydrolysis of Empty Fruit Bunches of Palm Oil (Elaeis Guineensis Jacq.) by Chemical, Physical, and Enzymatic Methods for Bioethanol Production. International Journal of Chemical Engineering and Applications, Vol. 6, No. 6.

Rivers, D. and Emert, G. (1987). Lignocellulose Pretreatment, Acomparison of Wet and Dry ball Attrition. *Biotechnology Lett*er, No. 9, Pp. 365 - 368.

Robert, E. T. (1981). Mass Transfer Operations. McGraw-Hill, Inc., 3rd Edition.

Rohsenow, W. M., Webber, J. H. and Ling, A. T. (1956). Effect of Vapor Velocity on Laminar and Turbulent Film Condensation. Trans. Asme Vol. 78, Pp. 1637-1643.

Rollma, L. and Valyocsik, E. (1983). Compounds Miscellaneous Solid-State: Zeolite Molecular Sieves. Inorganic Synthesis, Nol. 30, No. 22, Pp. 61.

Rong, H., Li-Bin, C., Chung, C. and Ta-Hui, L. (2011). Cold-start Emission of an SI Engine using Ethanol-Gasoline Blended Fuel. Applied Thermal Science, Vol. 31, Pp. 1463-1467.

Rudkin, E., (2002). Bioethanol as a Transport Fuel. http://www.maf.govt.nz/mafnet/publications/rmupdate/rm10/rm-update-june-2002-04.htm

Ruth, L. (2008). Bio or Bust? The Economic and Ecological Cost of Biofuels. EMBO Reports, Vol. 9, No.2, Pp.130-133.

Rutz, D., Janssen, R. (2008). Biofuel Technology Handbook, WIP Renewable Energies, München, Germany.

Ryu, D., Lee, S. and Tassinari, T. (1982). Effect of Compression Milling on Cellulose Structure

and Enzymatic Hydrolysis Kinetics. *Biotechnology Bioeng*ineering, Vol. 24, Pp. 1047 - 1067.

Sarkanen, V., Ludwig, H. (1971). Lignins: Occurrence, Formation, Structure, and Reactions. John Wiley & Sons Inc., New York.

Schell, D., Ruth, M. and Tucker, M. (1999). Modeling the Enzymatic Hydrolysis of Dilute Acid Pretreated Douglas Fir. Applied Biochemistry Biotechnology, Vol. 77, No 1 – 3, Pp. 67 – 81.

Schifter, I., Vera, M., Diaz, L., Guzman, E., Ramos, F. and Lopez-Salinas, E. (2001). Environmental Implications on the Oxygenation of Gasoline with Ethanol in the Metropolitan Area of Mexico City, Environmental Science and Technology, Vol. 35, No. 10, Pp. 1893 - 1901.

Scott, (2013). Experimental Evaluation of Alternative Fuels for Internal Combustion Engines. Conference for Industry and Education Collaboration, American Society for Engineering Education, Session ETD 445.

Seider, E.N and Tate, G.E (1936). Heat Transfer and Pressure Drop of Liquids in Tubes. Industrial and Engineering Chemistry, Vol. 28.

Sener, A., Cnabas, A. and Unal, M. (2007). The Effect of Fermentation Temperature on the Growing Kinetics of Wine Yeast Species. Turkish Journal Agricultural Forestry, Vol. 31, Pp. 349 - 354.

Sengers, J. and Watson, J. (1986). Improved International Formulations for the Viscosity and Thermal Conductivity of Water Substance, *J. Physical Chemistry, Vol.* 15, Pp. 1291.

Seshaiah, N. (2010). Efficiency and Exhaust Gas Analysis of Variable Compression Ratio Spark Ignition Engine Fuelled with Alternative Fuels. International Journal of Energy and Environment. Vol. 1, Issue 5, Pp. 861- 870.

Sheng, C. and Azevedo, J. (2005). Estimating the Higher Heating Value of Biomass Fuels from Basic Analysis Data. Biomass and Bioenergy, No. 5, Vol. 28, Pp. 499-507.

Shi, X., Yu, Y., He, H., Shuai, S., J. Wang, J. and Li, R. (2005). Emission Characteristics using Methyl Soyate–Ethanol–Diesel Fuel Blends on A Diesel Engine. Fuel, Vol.84, Pp. 1543 – 1549.

Shyam, P., Amit, S. and Sahoo, P. (2012). Experimental Investigation on the Performance and Emission Characteristics of a Diesel Engine Fuelled with Ethanol, Diesel and Jatropha Based Biodiesel Blends. International Journal of Advances in Engineering & Technology, ISSN: 2231-1963.

Siddegowda, K. and Venkatesh, J. (2013). Effect of Ethanol-Gasoline Blends on MPFI Engine Performance, Emission and Lubricating oil Properties. International Journal of Innovative Research in Science, Engineering and Technology, Vol. 2, Issue 10. www.ijirset.com.

Siddegowda, K. and Venkatesh, J. (2013). Performance and Emission Characteristics of MPFI Engine by Using Gasoline-Ethanol Blends. International Journal of Innovative Research in Science, Engineering and Technology, Vol. 2, Issue 9, www.ijirset.com.

Siew, H., Kok, T. and Keat, T. (2008). Oil Palm Biomass as A Sustainable Energy Source: A Malaysian Case Study. International Conference on Environment. chktlee@eng.usm.my.

Simarani, K., Hassan, A., Abdaziz, S., Wakisaka, M. and Shirai, Y. (2009). Effect of Palm Oil Mill Sterilization Process on the Physicochemical Characteristics and Enzymatic Hydrolysis of Empty Palm Bunch. Asian journal biotechnology, No. 1, Pp. 57 – 66.

Simetric & Co. (2009). Biofuel Energy. http://www.simetric.co.uk. Accessed on November 12th 2015.

Singh, S. (2008). Mechanical Engineers Handbook. Khanna Publishers, New Delhi India.

Sinnott, R. and Towler, G. (2009). Chemical Process Design. Fifth Edition. Elsevier Limited, ISBN 978-0-7506-8551-1.

Sinnott, R., Coulson and Richardson (1999). Chemical Engineering: Chemical Engineering Design. Butterworth-Heinemann, Vol. 6, 3rd Edition.

Sjöström, E. (1993). Wood Chemistry: Fundamentals and Applications, Second Edition, Academic Press, Orlando.

Skotnicki, M.L. (1983). High-Productivity Alcohol Fermentations using Zymomonas Mobilis. Biochemistry Social Symposium, Vol. 48, Pp. 53 – 86.

Smith, R., (1995). Chemical Process Design. McGraw-Hill, Inc.

Smith, J. M., Van, Ness, H. C. and Abbott, M. M. (2001). Introduction to Chemical Engineering Thermodynamics, Sixth Edition, McGraw-Hill International Edition

Sombat, M. and Wittaya, P. A. (2009). Rice Dryer using Either Solar Energy or Fuel from Agricultural Waste: Case Study of Tumbol Bankrang, Amphur Muang, Phitsanulok Province, Thailand

Somchart, S., Thanit, S., Adisak, S., Somboon, W. and Boonrueng, S. (2000). Cylonic Rice Husk Furnace and Its Application on Paddy Rice Drying. www.paddydryer.pdf.com. Accessed 22nd June. 2010.

Somerville, C. (2006). The Biofuels Conundrum. *Science, Vol.* 312, Pp. 1277.

Spindler, D., Wyman, C., Mohagheghi, A. and Gorhmann K. (1988). Thermotolerant Yeast for

Simultaneous Saccharification and Fermentation of Cellulose to Ethanol. Applied Biochemistry Biotechnology, Vol. 17, Pp. 279 –293.

Sreenivasulu, P., Durga, B., Naga, G. and Sudhakar, S. (2013). Importance and Role of Additives for Estimating Performance and Emissions In CI Engines using Alcohol as Fuels. International Journal of Innovative Research in Science, Engineering and Technology, Vol. 2, Issue 8, www.ijirset.com.

Srinivasa, S. G. and Murali, K. M. (2016). Performance Evaluation of High Pressure Down Draft Biomass Gasifier for BIG/GT Applications. International Journal of Engineering Research, Vol. 5, Issue Special 2, Pp: 499 -505.

Steenblik, R. (2007). Biofuels – At What Cost? Government Support for Ethanol and Biodiesel in Selected OECD Countries. Geneva, Switzerland: The Global Subsidies Initiative of the International Institute for Sustainable Development.

Stephen, I., Hinrich, U. and Birgitte, K. (2013). Comparing Oxidative and Dilitute Acid Wet Explosion and Preatment of Cocksfoot Grass at High Dry Matter Concentration For Cellulosic Ethanol Production. Journal of the Society of Chemical Industry. No. 1, Vol. 1, Pp. 1 – 10.

Stone (1992). Introduction to Internal Combustion Engines Second Edition.

Souder, M. and Brown, G. (1934). Design of Fractionating Columns, Entrainment and Capacity. Industrial and Engineering Chemistry. No. 1, Vol. 38, Pp. 98 – 103.

Strehler, A. (2000). Technologies of Wood Combustion. Ecological Engineering Supplement, No. 16, Vol. 1, Pp. 25-40.

Sudheer, N. (2013). Performance of C.I Engine by using Biodiesel-Mahua Oil. American Journal of Engineering Research (AJER), Vol. 2, Issue 10, Pp-22-47.

Sugiyama, M., Suthee, B., Auesukaree, C., Asavarak, T., Kaneko, Y., Boonchird, C. and Harashima, S. (2008). Yeast Carbon Neutral Biotechnology, High Temperature and Acid Tolerant Strain for High Level Bioethanol Production. Thailand-Japan Joint Symposium on Biotechnology by Efficient Utilization of Thai Biosciences, Thailand.

Sukumaran, R. K., Singhania, R. R., Mathew, G. M. and Pandey, A. (2009). Cellulase Production using Biomass Feed Stock and its Application in Lignocellulose Saccharification for Bioethanol Production. Renewable Energy, Vol. 34, No. 2, Pp, 421-424

Sun, Y. and Cheng, J., (2002). Hydrolysis of Lignocellulosic Materials for Ethanol Production. Bioresource Technology Vol. 83, Pp. 1 – 11.

SUN NEWS (2014). Allied Atlantic Distilleries Limited Invests #5bn in Ethanol Plant. 3 / 2 / 2014.

Syafwina, Y., Honda, T., Watanabe and Kuwahara M. (2002). Pretreatment of Palm Oil Empty Fruit Bunch by White-Rot Fungi for Enzymatic Saccharification. Wood Research, Vol. 89, Pp. 19 – 20.

Syarief, A. M; Morey, R. V. and Gustafson, R. J. (1984). Thin Layer Drying Rates of Sun Flower Seed. Transactions of the ASAE, Vol. 27, Pp. 195 – 200.

Taherzadeh, M., Gustafsson, C., Niklasson and Liden, G. (1999). Conversion of Furfural in Aerobic and Anaerobic Batch Fermentation of Glucose by Saccharomyces Cereviciae. Journal of Biosciences Bioengineering, Vol. 87, Pp. 169 – 174.

Taherzadeh, M., Niklasson, C. and Liden, G. (1999). Conversion of Dilute Acid Hydrolyzates of Spruce and Birch to Ethanol by Fed-Batch Fermentatation. Bioresource Technology, Vol. 69, No. 1, Pp. 59 – 66.

Taherzadeh, J. M., Gustaffson, L., Niklasson, C. and Liden, G. (2000). Physiological Effects of 5-Hydroxymethylfurfural (HMF) on Saccharomyces Cerevisiae. Applied Microbiological Biotechnology, Vol. 53, Pp. 701 – 708.

Taherzadeh, J. M. and Karimi, K. (2007). Enzyme Based Hydrolysis Processes for Ethanol from Lignocellulosic Materials: A Review. Bioresources, Vol. 2, No. 4,Pp. 707-738.

Taherzadeh, M.J. and Karimi, K. (2008). Pretreatment of Lignocellulosic Wastes to Improve Ethanol and Biogas Production. International Journal Mol. Science, Pp. 1621–1651.

Talal, Y., Najafi, G. and David, B. (2012). Theoretical and Experimental Investigation of SI Engine Performance and Exhaust Emissions using Ethanol-Gasoline Blended Fuels. University of Southern Queensland, 4350 Toowoomba, QLD Australia. yusaft@usq.edu.au.

Tan, K., Lim, S., Low, C. and Chang, S. (2014). Engine Emission Analysis and Performance Test with Ethanol-Gasoline Blended Fuel. European International Journal of Science Technology, Vol. 3 No. 7.

Tangka, J., Berinyuy, J., Tekounegnin and Okale, A. (2011). Physico-Chemical Properties of Bioethanol / Gasoline Blends and The Qualitative Effect of Different Blends on Gasoline Quality and Engine Performance. Journal of Petroleum Technology and Alternative Fuels Vol. 2, No. 3, Pp. 35 - 44.

Tassinari, T. and Macy, C. (1977). Differential Speed Two Roll Mill Pretreatment of Cellulosic Materials for Enzymatic Hydrolysis. Biotechnology Bioengineering, Vol. 19, Pp. 1321-1330.

Thallada, B., Balagurumurthy, B., Rawel, S., Desavath, V.N., Ajay, K. and Hari, B. G. (2011). Thermochemical Conversion of Biomass to Biofuels. Council of Scientific and Industrial Research (CSIR). Academic Press, Elsevier. 2011.

Tham, M. (1997). Distillation, An Introduction. Pp. 1997 – 2006. http://lorien.ncl.ac.uk/ming/distil/distil0.htm.

Theraja, B.L., Theraja, A.K. (2001). Electrical Technology in S.I Systems of Units. Fourth Edition.

Thermal Fluidpedia (2010). Thermophysical Properties of Ethanol.

Thiam, L. and Bhatia, S. (2008). Catalytic Processes towards the Production of Biofuels in a Palm Oil and Oil Palm Biomass-based Biorefinery. Bioresource Technology, Vol. 99, Pp. 7911–7922.

Thomas, N. (2003). Combustion and Co-combustion of Biomass: Fundamentals, Technologies, and Primary Measures for Emission Reduction. Energy & Fuels, No. 3, Vol. 17, Pp. 1510 -1521.

Torija, M. Rozes, N, Poblet, M. Guillamon, J. and Mas, A. (2003). Effect of Fermentation Temperature on The Strain Population of Saccharomyces Cerevisea. International Journal of Food Microbiology, Vol. 80, Pp. 47-53.

Tripathi, K., Iyer, P. and Tara, K. (1998). A Techno-Economic Evaluation of Biomass Briquetting in India. Biomass and Bioenergy, No.14, Vol. 5-6, Pp. 479 - 982.

Ullmann (1990). Encyclopedia of Industrial Chemistry. Ethanol, A9.

Ullmann (1990). Encyclopedia of Industrial Chemistry. Ethanol, A1.

Um, B. and Hanley, T. (2008). High-Solid Enzymatic Hydrolysis and Fermentation of Solka Floc into Ethanol. Journal Microbiology Biotechnology, No. 7, Vol. 18, Pp. 1257-1265.

Umikalsom, M., Ariff, B., Zulkifli, H., Tong, C., Hassan, M. and Karim, M. (1997). The Treatment of Oil Palm Empty Fruit Bunch for Subsequent as Substratefor Cellulose Production by Chaetomium Globosum. Bioresourse Technology, Vol. 62, Pp. 1- 9.

United Nations Development Programme (UNDP) (2007). Malaysia Generating Renewable Energy from Palm Oil Wastes. Malaysia Report, UNDP, Malaysia.

United States Department of Agriculture (USDA), (2007). Agricultural Baseline Projections. Economic Research Service, http://www.ers.usda.gov/briefing/baseline

Van, G., Shanks, B., Prisszko, R., Clements, D. and Knothe, G. (2004). Biodiesel Analytical

Methods. National Renewable Energy Laboratory. NREL/SR-510-36240.

Vane, L. M. (2005). A Review of Pervaporation for Product Recovery from Recovery from Biomass Fermentation Processes. Journal Chemical Technology, Biotechnology, Vol. 80, Pp. 603 – 629.

Vargaftik, N. et al., (1983). International Tables of the Surface Tension of Water. Journal Physical Chemistry Vol. 12, Pp. 817

Verônica, F., Mariana, O.F., Sabrina, S. M. and Pereira, J. (2010). Simultaneous Saccharification and Fermentation Process of Different Cellulosic Substrates using a Recombinant *Saccharomyces cerevisiae* Harbouring the β-glucosidase gene. Electronic Journal of Biotechnology, Vol. 13, No. 2.

Viele, E., Uyigue, L. and Chukwuma, F. (2013). Production of Anhydrous Bioethanol from Palm Wine Suitable for Biodiesel Synthesis. International Journal of Application or Innovation in Engineering & Management (IJAIEM), Vol. 2, No 10, Pp 180 -185.

Viele, E., Chukwuma, F. and Uyigue, L. (2014). Production and Characterization of Biodiesel from crude Palm Kernel Oil and Bio-ethanol using Potash from Ash of Empty Oil Palm Bunch Residue as Catalyst. International Journal of Application or Innovation in Engineering & Management (IJAIEM), Vol. 3, issue 1.

Von Braun (2007). The World Food Situation: New Driving Force and Required Action. International Food Policy Research Institute, Washington. Dec. 2007.

Wallner, T., Miers, S. and McConnell, S. (2009). A Comparison of Ethanol and Butanol as Oxygenates Using a Direct-Injection, Spark-Ignition Engine. Journal of Engineering for Gas Turbines and Power, Vol. 3, Pp. 131.

Wang, Y. and LeVan, M. (2009). Absorption Equilibrium of Carbon Dioxide and Water Vapor on Zeolites 5A and 13X and Silica Gel. Journal Chemical Engineering, Vol. 54, Pp. 2839 - 2844.

Wanrosli, W., Zainuddin, Z., Lawb, K. and Asro, R. (2006). Pulp from Oil Palm Fronds by Chemical Processes. Industrial Crops and Products, Vol. 25, Pp. 89 - 94.

Weil, J., Sarikaya, A. and Rau, S. *(*1997). Pretreatment of Yellow Popular Sadust by Pressure Cooking in Water. Applied Biochemical Biotechnology, Vol. 68, Pp. 21- 40.

Wiboon, R., Maneewan, S. and Poonsuk, P. (2012). Application of Palm Pressed Fiber as a carrier for Ethanol Production by *Candida shehatae* TISTR5843. Electronic Journal of Biotechnology. http://www.ejbiotechnology.info.

Wingren, A., Galbe, M. and Zacchi, G. (2003). Techno-economic Evaluation of Producing Ethanol from Softwood - A Comparison of SSF and SHF and Identification of Bottlenecks. Biotechnology Programme, Vol. 19, Pp. 1109 - 1117.

Wikipedia (2012a). American Coalition for Ethanol. http://www.ethanol.org. Accessed January 22th 2012.

Wikipedia (2011b). Cellulose Ethanol Commercialization. http://en.wikipedia.org/wiki/Cellulosic_ethanol. Accessed Nov. 8th 2011.

Wikipedia (2012c). The Current Fuel Ethanol Industry-Transportation, Marketing, Distribution, and Technical Considerations. http://en.wikipedia.org/wiki/ ethanol market Accessed Jan. 22th 2012.

Wikipedia (2012d). Ethanol Distillation. http://en.wikipedia.org/wiki/ ethanol distillation Accessed Jan. 22th 2012.

Wikepedia (2015). Bioplastic. http://en.wikipedia.org/wiki/Bioplastic. Accessed August 27th 2015.

Wladyslaw, K., Joanna, M. and Agnieszka, C. (2008). Renewable Energy Source - Dehydrated Ethanol. Chemical Engineering Journal, Vol. 135, Pp. 95 – 102.

Woehrle, W. (1995). A History of the Passenger Car Tire: Part I, Automotive Engineering, Vol. 103, No.9, Pp. 71-75.

Wolf, A., Anna, V. and Eva, A. (2006). Energy-Efficient Pellet Production in the Forest industry - A Study of Obstacles and Success Factors. Biomass and Bioenergy, No. 30, Vol. 1, Pp. 38 - 45.

Won, C., Ji-Yeon, P., Joon, L., You-Kwan, O., Yong, P., Jun, K., Jang, M, Chul, K. and Jin, L. (2013). Optimization of NaOH-catalyzed Steam Pretreatment of Empty Fruit Bunch. Biotechnology for Biofuels, Vol. 6, No. 1, Pp. 170.

World Energy (2008). Publication and Report on Energy Crop. http://www.worldenergy.org/wecgeis/publications/reports/ser/wood/wood.asp. Accessed on November 12th 2015.

World Ethanol Markets (WEM), (2006). The Outlook to 2015.

World -Wide Fuel Charter (WWFC) (2002). Fuel Quality. http://www.oica.net/htdocs/fuel%20quality/WWFC_Dec2002_Brochure.pdf.

Wright, J. (1988). Ethanol from biomass by enzymatic hydrolysis. Chemical Engineering Programme, Vol. 84, Pp. 62-74.

Wusana, A. W., Sunu, H. P., Juli, N. S. and Doyok, P. (2014). Effect of Biomass Feed Size and Air Flow Rate on the Pressure Drop of Gasification Reactor. Jurnal Teknologi.

Wyman, C. E. (1996). Handbook on Bioethanol: Production and Utilization, Washington DC, Taylor & Francis.

Xiang, Q., Kim, J. and Lee, Y. (2003). A Comprehensive Kinetic Model for Dilute Acid Hydrolysis of Cellulose. Applied Biochemical Biotechnology, Vol. 105, No. 108, Pp. 337-352.

Yanni, S., Dyah, S., Eka, T., Sudiyarmanto, Kiky, C., Yosi, A., Haznan, A. and Min, H. (2013). Utilization of Biomass Waste Empty Fruit Bunch Fiber of Palm Oil for Bioethanol Production using Pilot – Scale Unit. Energy Procedia, Vol. 32, Pp. 31 – 38.

Yanni, S., Syarifah, A. and Kiky, C. (2008). Alkali Pretreatment and Enzymatic

Saccharification of Oil Palm Empty Fruit Bunch Fiber for Production of Ethanol. Proceeding of the International Seminar on Chemistry, Pp. 643 - 647.

Yanuandri, P., Haznan, A., Achmad, P., Arifin, N., Yan, I. and Sabar, P. (2014). Experimental Investigation of 2nd Generation Bioethanol derived from Empty-fruit-bunch (EFB) of Oil-palm on Performance and Exhaust Emission of SI Engine. Mechatronics, Electrical Power, and Vehicular Technology, Vol. 05, Pp. 9-16. www.mevjournal.com.

Yong, T., Lee, K., Mohamed, A. and Subhash, B. (2007). Potential of Hydrogen from Oil Palm Biomass as a Source of Renewable Energy Worldwide. Energy Policy, Vol. 35, Pp. 5692 - 5701.

Yoshida, M., Liu, Y. and Uchida, S. (2008). Effects of Cellulose Crystallinity, Hemicellulose, and Lignin on the Enzymatic Hydrolysis of *Miscanthus Sinensis* to Monosaccarides. Bioscience Biotechnology Biochemistry, Vol. 72, Pp. 805 - 810.

Yuelei, Y., Kevin, B. and Dan, Z. (2012). A Sustainable Ethanol Distillation System. Sustainability, Vol. 4, Pp. 92 - 105. www.mdpi.com/journal/sustainability.

Yuksel, F. and Yuksel, B. (2004). The Use of Ethanol-Gasoline Blend as a Fuel in an SI Engine, Renewable Energy, Vol. 29, pp. 1181-1191.

Yusoff, S. (2006). Renewable Energy from Palm Oil – Innovation of Effective Utilization of Waste. Journal of Cleaner Production, Vol. 14, Pp. 87 - 93.

Zetty, A., Mohd, J., Tan, P., Osman, H. and Mohamad, Y. (2014). Effect of Direct Pretreatment using Steam on the Properties of Oil Palm Empty Fruit Bunch. Der Pharma Chemica, Vol. 6, No. 5, Pp. 1- 6. *www.scholarsresearchlibrary.com*.

Zhang, W., Liang, M. and Lu, C. (2007). Morphological and Structural Development of Hardwood Cellulose during Mechanochemical Pretreatment in Solid State through Pan Milling. Cellulose, Vol. 14, Pp. 447-456.

Zheng, Y., Lin, H.M. and Tsao, G.T., (1998). Pretreatment for Cellulose Hydrolysis by Carbon Dioxide Explosion. Biotechnol Programme, Vol. 14, No. 6, Pp. 890 – 896.

APPENDICES

Appendix A 1

Table A1: Common Azeotropes

Azeotrope	Composition	Boiling point (^{0}C)	Type
Ethanol-water	95.6%C_2H_5OH, 4.4%H_2O	78.2	Minimum
Benzene – water	91.1%C_6H_6, 8.9%H_2O	69.4	Minimum
Benzene-water-ethanol	74.1%C_6H_6, 7.4%H_2O, 18.5% C_2H_5OH	64.9	Minimum
Ethanol-benzene	32.4% C_2H_5OH, 67.6%C_6H_6,	67.8	Minimum
Methanol-toluene	72.4% CH_3OH, 27.6% C_6H_5 CH_3	63.7	Minimum
Isopropanol-water	87.8% $(CH_3)_2CHOH$, 90.8%H_2O,	80.4	Minimum
Phenol-water	9.2%C_6H_5OH, 90.8%H_2O	99.5	Minimum
Acetone-chloroform	20.0%CH_3COCH_3, 80.0% $CHCl_3$	64.7	Maximum
HCL-water	20.2% HCl, 79.8% H_2O	108.6	Maximum
Acetic acid-dioxane	77.0%CH_3COOH, 23.0% $C_4H_8O_2$	119.5	Maximum
Benzaldehyde-phenol	49.0% C_6H_5CHO, 51.0% C_6H_5OH	185.6	Maximum
Nitric acid-water	68.0%HNO_3, 32.0%H_2O	120.5	Maximum

Three types of azeotrope are:

Minimum or Positive Azeotrpoes: These have slight repulsion which leads to a higher than expected combined vapor pressure that causes a lower boiling point for the mixture than is observed for the pure components e.g. ethanol-water mixture.

Maximum or Negative Azeotrpoes: These have slight attraction between components molecules which leads to lower combined vapor pressure than expected in the solution, that causes a higher boiling point than what would be characteristics for the components.

Zeotropes: These are mixtures that do not show a maximum or minimum boiling point.

Appendix A2

<u>Table A2:</u> Gas Composition of Commercial Wood and Charcoal (FAO 1986)

Component	Wood gas (vol %)	Charcoal gas (vol %)
Nitrogen	50 – 54	55 – 65
Carbon monoxide	17 – 22	28 – 32
Carbon dioxide	9 – 15	1 – 3
Hydrogen	12 – 20	4 – 10
Methane	5 - 3	0 - 2
Heating value (MJ/m^3)	5 – 5.9	4.5 – 5.6

Data is obtained on low to medium moisture content fuels (Wood 20 %, Charcoal 7 %).

Appendix A3

Comparative Utilization of Charcoal, Sawdust and Rice Husk as Fuel in Biomass Furnace Dryer (Segun & Adegbulugbe 2010)

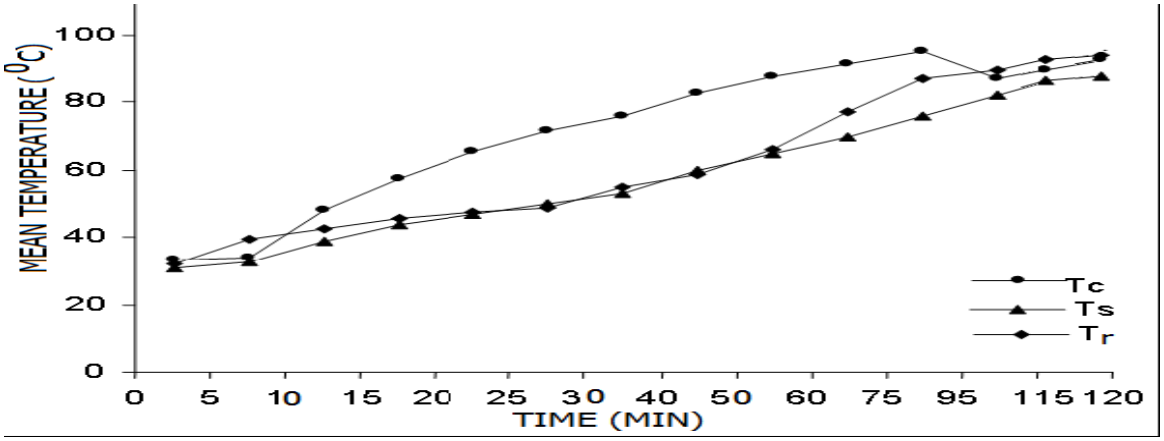

Figure 1: The Mean Temperature at Intervals for each Fuel in the Drying Chamber.

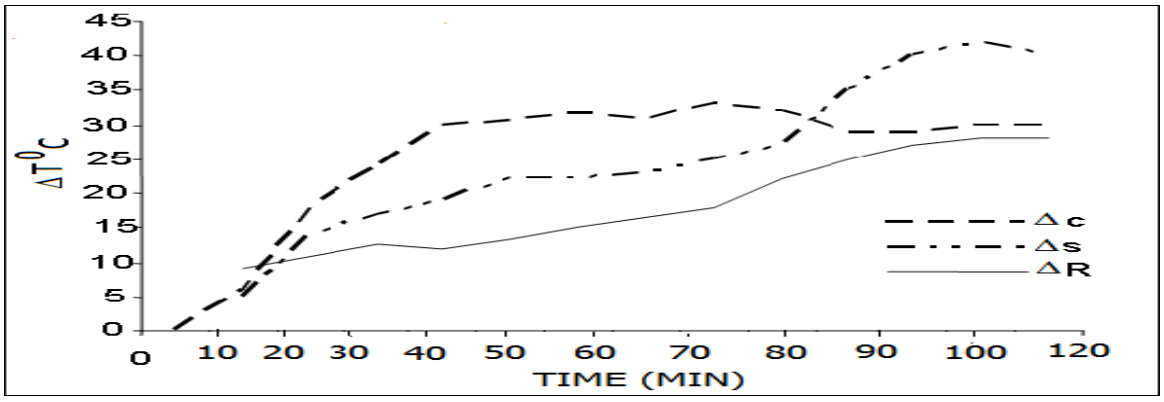

Figure 2: Differential Temperature in the Drying Chamber.

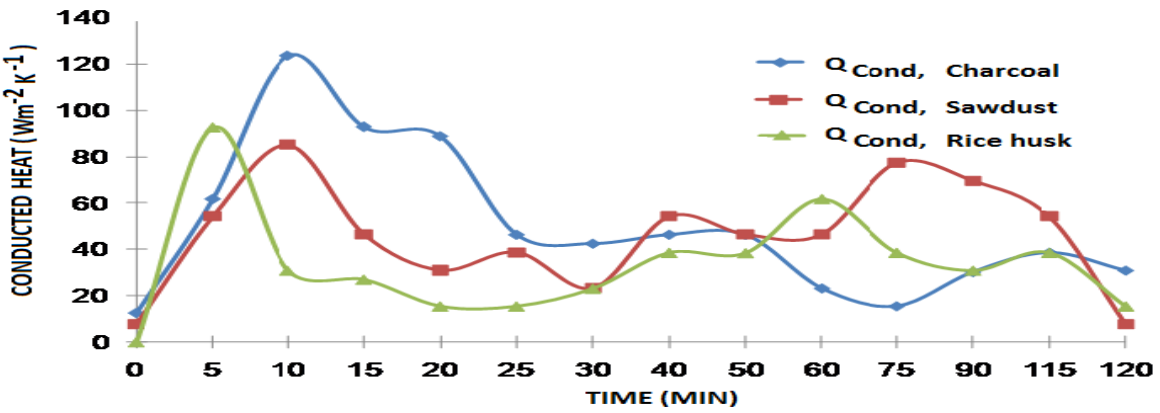

Figure 3: Heat Conducted to the Drying Chamber by each Fuel per Unit Time.

Appendix A4

Table A3: Thermal Physical Properties of Water

T °C	Sat.P (10^5Pa)	Lat.Heat (kJ/kg)	Liquid density (kg/m^3)	V. density (kg/m^3)	Liquid viscosity (N-S/m^2)	V. viscosity (N-S/m^2)	L . thermal conductivity (W/m-K)	V. thermal conductivity (W/m-K)	Liquid spec. Heat (kJ/kg . k)	Vapor spec. Heat (kJ/kg . k)
0	0.023368	2453.8	999.0	0.01729	10015	88.5	0.602	0.0188	4.182	1.874
20	0.073749	2406.5	993.05	0.0511	6513	96.6	0.630	0.0201	4.179	1.894
40	0.19919	2358.4	983.28	0.1302	4630	105.0	0.653	0.0216	4.185	1.924
60	0.47359	2308.9	971.82	0.2932	3510	113.0	0.669	0.0231	4.197	1.969
80	1.01325	2251.2	958.77	0.5974	2790	121.0	0.680	0.0248	4.216	2.034
100	1.9854	2202.9	943.39	1.121	2300	128.0	0.685	0.0267	4.245	2.124
120	3.6136	2144.9	925.93	1.9656	1950	135.0	0.687	0.0288	4.285	2.245

Ref: Thermal – Fluidpedia Atom Feed, Thermal Fluid Central Encyclopedia (2016).

Table A4: Enthalpy of Vaporization of Water (Marsh 1987)

T (^{0}C)	$\Delta_{vap}H$ (kJ/mol)	T (^{0}C)	$\Delta_{vap}H$ (kJ/mol)
0	45.054	200	34.962
25	43.990	220	33.468
40	43.350	240	31.809
60	42.482	260	29.930
80	41.585	280	27.795
100	40.657	300	25.300
120	39.684	320	22.297

Table A5: Antnoine Constant for Water and Ethanol

Component	A	B	C	T (^{0}C)
Water	8.07131	1730.63	233.426	1 – 100
Ethanol	7.68117	1332.04	199.2	77 - 243

Table A6: Thermal Physical Properties of Ethanol

T °C	Sat. P (10^5Pa)	Lat. Heat (kJ/kg)	Liquid density (kg/m^3)	V. density (kg/m^3)	Liquid viscosity (N-S/m^2)	V. viscosity (N-S/m^2)	L. thermal conductivity (W/m-K)	V. thermal conductivity (W/m-K)	Liquid spec. Heat (kJ/kg.k)	V. Spec.Heat (kJ/kg . k)
0	0.012	1048.4	0.901	0.036	1.7990	0.774	0.183	0.0117	2.27	1.34
20	0.058	1030.0	0.800	0.085	1.1980	0.835	0.179	0.0139	2.4	1.40
40	0.180	1011.9	0.789	0.316	0.8190	0.900	0.175	0.0160	2.57	1.48
60	0.472	988.9	0.770	0.748	0.5880	1.959	0.171	0.0179	2.78	1.54
80	1.086	960.0	0.757	1.430	0.4320	1.030	0.169	0.0199	3.03	1.61
100	2.260	927.0	0.730	3.410	0.3180	1.092	0.167	0.0219	3.30	1.68
120	4.290	885.5	0.710	6.010	0.2430	1.157	0.165	0.0238	3.61	1.75

Ref: Thermal – Fluidpedia Atom Feed, Thermal Fluid Central Encyclopedia (2016).

Appendix A5

Table A7: Nusselt Nuber for Lainar Flow in a Circular Annulus

D_i / D_o	Nu_i	Nu_o
0.00	_	3.66
0.05	17.46	4.06
0.10	11.56	4.11
0.25	7.37	4.23
0.50	5.74	4.43
1.00	4.86	4.86

Ref: Kays and Perkins (1972).

Nusselt Number for fully developed laminar flow in a circular annulus with one surface insulated and the other isothermal.

Appendix A6: Types of Fuel Additives

Alcohol Base Oxygenates: methanol, ethanol, isopropyl alcohol, n-butanol, and gasoline grade t-butanol.

Ethers Base Oxygenates: methyl tert-butyl ether, ethyl tertiary butyl ether, diisopropylether, tertiary amyl methyl ether, tertiary hexyl methyl ether.

Antioxidants: Butylated hydroxytoluene, 2,4-Dimethyl-6-tert-butylphenol, Di-tert-butylphenol-Phenylene diamine and Ethylene diamine.

Antiknock Agents: is a gasoline additive that works to reduce engine knocking while trying to increase the octane rating of the fuel.

Antiknock Agents: Tetra-ethyl lead, Methylcyclopentadienyl manganese tricarbonyl, Ferrocene, Iron pentacarbonyl, Toluene and Isooctane

Metal Deactivator for Petrol: N,N'-disalicylidene-1,2- propanediamine.

Elmulsifiers: n-butanol, 1-octylamino-3octyloxy-2propanol and N-octyl nitramine.

Corrosion Inhibitors: sodium nitrite hexamine, and phenylenediamine.

Others outside the given categories are:

•**Acetone:** this is a vaporization additive. It is used, together with methanol, to improve vaporization when the engine starts up.

• **Nitromethane:** is used to up the engine power – commonly referred to as 'nitro'.

• **Ferrous picrate:** is used to improve combustion and increase mileage.

• **Ferox:** this is a catalyst additive used to increase fuel efficiency, clean the engine, and extend the life of the engine, lower emission.

Appendix B1

Table B1: Density Specific Weight of Air at Standard ATM Pressure

T °C	Density (kg/m^3)	Spec. weight (N/m^3)	Spec. heat kJ/kg K	Thermal conductivity, W/m K	Dynamic viscosity, x 10^{-6} m^2/s	Expansion coefficient, x 10^{-3} L/K	Prandtl number
0	1.293	12.67	1.005	0.0243	13.30	3.67	0.715
20	1.205	11.81	1.005	0.0257	15.11	3.43	0.713
40	1.127	11.05	1.005	0.0271	16.97	3.20	0.711
60	1.067	10.40	1.009	0.0285	18.90	3.00	0.709
80	1.000	9.803	1.009	0.0299	20.94	2.83	0.708
100	0.9461	9.278	1.009	0.0314	23.06	2.68	0.703

Ref: The Engineering Tool Box. www.engineeringtoolbox.com

Appendix B2

Table B2: Some Properties of Metal Materials

Metal	Thermal Cond. ($J/m.s.^0C$)	Sp. heat (kJ /kg^0C)	Density (kg/m^3)	Thermal Diffusivity at Room Temp. (mm^2/s)	Temp. (^0C)
Aluminium	220	0.87	2640	85	0
Brass	97	0.38	8650		0
Cast iron	55	0.42	7210		0
Copper	388	0.38	8900	115	0
Steel, mild	45	0.47	7840	13	18
Steel, stainless	21	0.48	7950		20
Non-Metals					
Brick	0.7	0.92	1760	0.45	20
Wood shavings	0.09	2.5	1.50		0
Wood	0.28	2.5	700		30
Cork	0.043	1.55	160		30
Cotton wool	0.04	1.26	80		30
Celluloid	0.21	1.55	1400		30

Appendix B3

Glossary

Down-Draft Combustion – It is a fixed bed type of combustion where the combustion zone is at the bottom, the air enters through lateral air inlets and moves downward, with the hot gases exiting at the bottom. The fuel supply is above and keeps dropping down into the combustion zone.

Equivalence Ratio - It is the percentage ratio of the air needed for gasification to the stoichiometric air requirement of rice husks.

Fixed Bed Reactor - It is a major type of reactor where the fuel is burnt while it is held in place inside the reactor.

Gasification – It is the process of converting rice husks fuel into combustible gases by using limited amount of air during combustion process.

Inverted Down Draft combustion – It is a method of gasifying fuel by starting the ignition on top of the reactor as the air is introduced at the bottom of the reactor, either naturally or with forced air.

Reactor – It is a component of the boiler system where the fuel is burned. It is also called combustion chamber.

Specific Gasification Rate – It is the amount of rice husk fuel consumed per unit area of the reactor.

Stoichiometric Air - It is the air needed to completely burn rice husks and convert it to ash.

Top Lit Up Draft (T-LUD) Combustion– It is similar to the inverted down draft combustion where the ignition of fuel is started on top of the fuel bed while the air is introduced at the bottom of the bed.

Up-Draft Combustion– It is fixed bed type combustion where the fire zone is at the bottom and the air moves upward through the hot char and usually exits laterally. The fuel supply, which is above the gasification and combustion zone, continually drops into the combustion zone.

Appendix C

Table C1: Standard Solutions and Absorbance

Glucose Conc. (g/L)	Absorbance	Xylose Conc. (g/L)	Absorbance	Ethanol Conc. (g/L)	Absorbance
0.0	0.912	0.0	0.026	0.0	0.808
0.02	0.9127	0.0438	0.031	9.216	1.102
0.04	0.9134	0.0625	0.0326	18.432	1.453
0.08	0.9146	0.0813	0.0345	27.648	1.837
0.16	0.9172	0.1625	0.0422	36.864	2.15
0.2	0.9184	0.2438	0.0502	46.08	2.5

Appendix D

Table D1: Preliminary Chemical Hydrolysis Result for 0.8 % Acid Concentration.

Acid conc. 0.8 (%, v/v)									
Temp. (°C)	Time (min)	Sample	Xylose yield ($g\ L^{-1}$)	Yield Rate ($g\ L^{-1}h^{-1}$)	Hemi-cellulose conversion (%)	Glucose yield ($g\ L^{-1}$)	Yield Rate ($g\ L^{-1}\ h^{-1}$)	Cellulose conversion (%)	Total Sugar (gL^{-1})
160	15	A_{11}	12.35	49.4	48.85	1.258	5.032	0.99	13.609
	30	A_{12}	12.474	24.948	49.34	7.613	15.226	5.96	20.087
	45	A_{13}	12.722	16.963	50.32	10.00	13.3	7.84	22.722
	60	A_{14}	12.515	12.515	49.50	5.419	5.419	4.25	17.934
180	15	A_{21}	14.65	58.6	57.95	8.258	33.032	6.47	22.908
	30	A_{22}	15.866	31.732	62.76	22.161	44.322	17.36	38.027
	45	A_{23}	16.144	21.472	63.86	11.742	15.617	9.2	27.886
	60	A_{24}	15.505	15.505	61.33	6.226	6.226	4.88	21.731
200	15	A_{31}	14.299	57.196	56.56	8.645	34.58	6.77	22.944
	30	A_{32}	13.876	27.752	54.89	12.355	24.71	9.68	26.231
	45	A_{33}	13.784	18.333	54.52	22.548	29.988	17.67	36.332
	60	A_{34}	13.742	13.742	54.36	6.742	6.742	5.28	19.484

Table D2: Preliminary Chemical Hydrolysis Result for 1.0 % Acid Concentration

Acid conc 1.0 (%, v/v)									
Temp. (°C)	Time (min)	Sample	Xylose yield (gL^{-1})	Yield Rate ($gL^{-1}h^{-1}$)	Hemi-cellulose conversion (%)	Glucose yield (gL^{-1})	Yield rate ($gL^{-1}\ h^{-1}$)	Cellulose conversion (%)	Total sugar (gL^{-1})
160	15	B_{11}	13.845	55.38	54.76	8.742	34.968	6.85	22.587
	30	B_{12}	13.691	27.382	54.16	31.29	62.58	24.52	44.981
	45	B_{13}	12.979	17.262	51.34	20.903	27.801	16.38	33.882
	60	B_{14}	11.948	11.948	47.26	12.387	12.387	9.71	24.335
180	15	B_{21}	13.691	54.764	54.16	35.735	142.94	28.0	49.426
	30	B_{22}	13.144	26.288	52.0	25.226	50.452	19.76	38.37
	45	B_{23}	13.103	17.427	51.83	14.871	19.778	11.65	27.974
	60	B_{24}	12.773	12.773	50.52	11.323	11.323	8.87	24.096
200	15	B_{31}	15.021	60.084	59.42	11.742	46.968	9.20	26.763
	30	B_{32}	15.010	30.02	59.37	24.903	49.806	19.51	39.913
	45	B_{33}	14.392	19.141	56.93	11.290	15.016	8.85	25.682
	60	B_{34}	13.959	13.959	55.22	9.290	9.290	7.28	23.249

Table D3: Preliminary Chemical Hydrolysis Result for 1.2 % Acid Concentration

Acid conc 1.2 (%, v/v)									
Temp. (°C)	**Time (min)**	**Sample**	**Xylose yield ($g\ L^{-1}$)**	**Yield Rate ($gL^{-1}h^{-1}$)**	**Hemi-conversion (%)**	**Glucose yield (gL^{-1})**	**Yield Rate ($gL^{-1}\ h^{-1}$)**	**Cellulose conversion (%)**	**Total sugar (gL^{-1})**
160	15	C_{11}	13.701	54.804	54.19	28.419	113.676	22.27	42.12
	30	C_{12}	25.01	50.02	98.93	51.00	102	40.00	76.01
	45	C_{13}	15.732	20.924	62.21	18.226	24.241	14.28	33.958
	60	C_{14}	12.536	12.536	49.59	9.71	9.71	7.61	22.246
180	15	C_{21}	14.691	58.764	58.11	29.097	116.388	22.80	43.788
	30	C_{22}	14.763	29.526	58.4	15.032	30.064	11.78	29.795
	45	C_{23}	14.67	19.511	58.03	11.323	15.06	8.87	25.993
	60	C_{24}	13.866	13.866	54.85	9.032	9.032	7.08	22.898
200	15	C_{31}	15.103	60.412	59.74	30.323	121.292	23.76	45.426
	30	C_{32}	15.00	30.00	59.33	14.677	29.354	11.5	29.677
	45	C_{33}	14.45	19.219	57.16	10.71	14.244	8.39	25.555
	60	C_{34}	14.381	14.381	56.88	6.129	6.129	4.8	20.51

Table E1: Preliminary Fermentation Samples Absorbances.

Sample	**24h**	**48h**	**72h**	**96h**	**120h**
B_{12}	0.8359	1.0802	1.5090	1.5090	1.5089
B_{21}	0.9687	1.3712	1.3712	1. 3712	1. 3712
C_{11}	0.8976	1.0513	1.1759	1. 1759	1. 1759
C_{12}	0.9941	1.4083	1.9694	1. 9694	1. 9694
C_{21}	0.8629	1.4612	1.4612	1. 4612	1. 4610
C_{31}	0.9116	1.1637	1.5249	1. 5249	1. 5249

Appendix E2

Table E2: Preliminary Fermentation Results

Sample B_{12}					
Hour	24	48	72	96	120
Ethanol yield (g L^{-1})	1.379	7.979	19.568	19.568	19.566
Ethanol/day	1.379	6.60	11.589	0	-0.002
Ethanol Productivity (g L^{-1} h^{-1})	0.058	0.275	0.483	0	~ 0
Fermentation Efficiency (%)	6.0	34.714	85.13	85.13	85.13

Sample B_{21}					
Hour	24	48	72	96	120
Ethanol yield (g L^{-1})	4.966	15.842	15.842	15.842	15.842
Ethanol/day	4.966	10.876	0	0	0
Ethanol Productivity (g L^{-1} h^{-1})	0.207	0.453	0	0	0
Fermentation Efficiency (%)	19.66	62.73	62.73	62.73	62.73

Sample C_{11}					
Hour	24	48	72	96	120
Ethanol yield (g L^{-1})	3.043	7.197	10.564	10.564	10.564
Ethanol/day	3.043	4.154	3.367	0	0
Ethanol Productivity (g L^{-1} h^{-1})	0.127	0.173	0.1402	0	0
Fermentation Efficiency (%)	14.14	33.44	49.09	49.09	49.09

Sample C_{12}					
Hour	24	48	72	96	120
Ethanol yield (g L^{-1})	5.651	16.847	32.01	32.00	32.0
Ethanol/day	5.651	11.196	15.163	- 0.01	0
Ethanol Productivity (g L^{-1} h^{-1})	0.2355	0.4665	0.6318	~0	0
Fermentation Efficiency (%)	14.53	43.33	82.33	82.33	82.33

Sample C_{21}					
Hour	24	48	72	96	120
Ethanol yield (g L^{-1})	2.108	18.275	18.275	18.275	18.269
Ethanol/day	2.108	16.167	0	0	-0.006
Ethanol Productivity (g L^{-1} h^{-1})	0.0878	0.6736	0	0	0
Fermentation Efficiency (%)	9.42	81.68	81.68	81.68	81.65

Sample C_{31}					
Hour	24	48	72	96	120
Ethanol yield (g L^{-1})	3.423	10.235	19.999	19.999	19.699
Ethanol/day	3.423	6.812	9.764	0	0
Ethanol Productivity (g L^{-1} h^{-1})	0.1426	0.2838	0.4068	0	0
Fermentation Efficiency (%)	14.75	44.09	86.15	86.15	86.15

Appendix F

Appendix F Table F1: Distiller Distillation Readings

Time (min)	BP	100	105	110	115	120
Run 1						
Temp. (^oC)	96.4	97.3	98	98	98	98.8
V. pressure (bar)	2.85	2.94	3.012	3.012	3.012	na
Bioethanol fuel (ml)	0	340	632	759	817	817
Bioethanol fuel at time interval (ml)	0	340	292	127	62	0
Distillation rate (ml/h)	0	4080	3792	3036	2451	2451.8
Distillation rate at time interval (ml/h)	0	4080	3504	1524	744	0
Productivity	0	0.0834	0.0775	0.062	0.0501	0
Distillation efficiency (%)	0	41.68	77.48	93.05	100.16	100.16
Run 2						
Temp. (^oC)	96	97	98	98	98	98.5
V. pressure (bar)	2.81	2.91	3.012	3.012	3.012	na
Bioethanol fuel (ml)	0	342	642	765	816	816
Bioethanol fuel at time interval (ml)	0	342	300	123	55	0
Distillation rate (ml/h)	0	4104	3852	3060	2448	2448.4
Distillation rate at time interval (ml/h)	0	4104	3600	1476	660	0
Productivity	0	0.084	0.079	0.0625	0.05	0
Distillation efficiency (%)	0	41.93	78.71	93.79	100.04	100.04
Run 3						
Temp. (^oC)	95.7	97.8	98	98	98	98.9
V. pressure (bar)	2.78	2.99	3.012	3.012	3.012	na
Bioethanol fuel (ml)	0	338	646	763	809	809
Bioethanol fuel at time interval (ml)	0	338	308	117	50	0
Distillation rate (ml/h)	0	4056	3876	3052	2427	2427.2
Distillation rate at time interval (ml/h)	0	4056	3696	1404	600	0
Productivity	0	0.083	0.079	0.0624	0.0496	0
Distillation efficiency (%)	0	41.44	79.2	93.54	99.18	99.18

na = not available

Appendix G

Table G1: Sample Fuels Distillation Profile

	E0 (ºC)	**E10 (ºC)**	**E20 (ºC)**	**E30 (ºC)**	**E40 (ºC)**	**E50 (ºC)**	**E60 (ºC)**	**E100 (ºC)**
IBP	44	46	45	48	52	47	55	79
10 ml	61	57	59	59	62	60	65	79
20 “	70	63	62	64	63	67	69	80
30 “	79	78	65	69	72	71	72	80
40 “	91	90	67	72	74	74	74	80
50 “	107	103	71	74	76	76	75	81
60 “	121	121	114	75	78	77	76	81
70 “	141	138	131	90	78	78	77	82
80 “	158	158	170	152	80	79	78	83
90 “	181	179	178	175	174	98	78.4	99
EBP	205	201	200	202	196	102	183	101
TD	98	98.5	82	97.6	96	93	99	97

Appendix H

Engine Performance Parameters Readings at Constant Load

Table H1: Engine Performance of E0 at Constant Engine Load Conditions

Load (N)	Speed (rpm)	FC (ml)	T (sec)	Volume Rate (ml/s)	FCR (kg/h)	B.P (kW)	BSFC (kg/kW-h)	BMEP (bar)	Fuel P. (kW)	BTE (%)
E0 under Full Engine Load Condition										
9.81	3633	20	156	0.128	0.334	0.837	0.399	1.692	4.05	20.68
19.62	3628	20	152	0.132	0.343	0.874	0.393	1.87	4.16	21.02
29.43	3568	20	136	0.147	0.384	0.796	0.482	1.638	4.65	17.11
39.24	3545	20	116	0.172	0.45	0.721	0.624	1.493	5.45	13.22
49.09	3516	20	98	0.204	0.532	0.586	0.908	1.224	6.446	9.09
E0 under 3/4 Engine Load Condition										
9.81	3110	20	153	0.111	0.29	0.716	0.405	1.69	3.51	20.37
19.62	3083	20	160	0.125	0.326	0.743	0.417	1.86	3.95	19.77
29.43	3042	20	156	0.128	0.334	0.682	0.49	1.646	4.05	16.85
39.24	3016	20	152	0.132	0.343	0.61	0.562	1.485	4.16	14.68
49.09	2982	20	148	0.135	0.353	0.5	0.706	1.231	4.28	11.69
E0 under 1/2 Engine Load Condition										
9.81	3049	20	166.8	0.12	0.313	0.68	0.46	1.637	3.79	17.93
19.62	2982	20	160	0.125	0.326	0.75	0.435	1.847	3.95	18.99
29.43	2918	20	148.15	0.135	0.352	0.7	0.503	1.761	4.27	16.41
39.24	2833	20	132	0.152	0.395	0.602	0.656	1.56	4.79	12.58
39.24	2710	20	119	0.168	0.438	0.454	0.965	1.23	4.11	11.05

Table H2: Engine Performance of E10 at Constant Engine Load Conditions

Load (N)	Speed (rpm)	FC (ml)	T (sec)	Vol. Rate (ml/s)	FCR (kg/h)	B.P (kW)	BSFC (kg/kW-h)	BMEP (bar)	FP (kW)	BTE (%)
E10 under Full Engine Load Condition										
9.81	3658	20	161	0.124	0.326	0.802	0.406	1.61	3.79	21.18
19.62	3638	20	152.95	0.131	0.343	0.882	0.389	1.78	3.98	22.14
29.43	3614	20	140	0.143	0.375	0.819	0.458	1.664	4.36	18.81
39.24	3595	20	124	0.161	0.423	0.734	0.576	1.5	4.91	14.94
49.09	3572	20	110	0.182	0.477	0.602	0.792	1.237	5.54	10.87
E10 under 3/4 Engine Load Condition										
9.81	3163	20	184.1	0.1086	0.285	0.7	0.407	1.625	3.31	21.15
19.62	3146	20	182.79	0.1094	0.287	0.768	0.374	1.792	3.33	23.06
29.43	3114	20	168	0.119	0.298	0.708	0.421	1.669	3.46	20.46
39.24	3072	20	160	0.125	0.32	0.621	0.515	1.484	3.72	16.69
49.09	3027	20	149	0.134	0.352	0.514	0.685	1.247	4.09	12.57
E10 under 1/2 Engine Load Condition										
9.81	2887	20	184.72	0.108	0.284	0.641	0.443	1.63	3.3	19.42
19.62	2872	20	188	0.106	0.279	0.68	0.41	1.744	3.24	21.01
29.43	2857	20	190.76	0.105	0.275	0.647	0.425	1.669	3.19	20.26
39.24	2832	20	101.5	0.197	0.518	0.575	0.901	1.49	6.02	9.55
49.09	2817	20	67.34	0.297	0.778	0.476	1.63	1.237	9.04	5.27

Table H3: Engine Performance of E20 at Constant Engine Load Conditions

Load (N)	Speed (rpm)	FC (ml)	T (sec)	Vol. Rate (ml/s)	FCR (kg/h)	B.P (kW)	BSFC (kg/kW-h)	BMEP (bar)	FP (kW)	BTE (%)
E20 under Full Engine Load Condition										
9.81	3588	20	156	0.128	0.339	0.831	0.408	1.7	3.79	21.94
19.62	3574	20	152	0.132	0.348	0.917	0.379	1.884	3.89	23.58
29.43	3556	20	148	0.135	0.36	0.808	0.446	1.668	4.02	20.09
39.24	3546	20	140	0.143	0.38	0.724	0.525	1.499	4.25	17.05
49.09	3532	20	136	0.147	0.388	0.599	0.648	1.245	4.33	13.82
E20 under 3/4 Engine Load Condition										
9.81	3071	20	198	0.1	0.275	0.708	0.388	1.693	3.07	23.04
19.62	3048	20	176	0.114	0.300	0.777	0.386	1.872	3.35	23.18
29.43	3017	20	164	0.122	0.322	0.682	0.472	1.66	3.6	18.96
39.24	2996	20	152	0.132	0.348	0.594	0.586	1.456	3.89	15.28
49.09	2970	20	141	0.142	0.375	0.482	0.778	1.192	4.19	11.5
E20 under 1/2 Engine Load Condition										
9.81	3026	20	200	0.1	0.297	0.678	0.438	1.645	3.32	20.43
19.62	2984	20	166.67	0.12	0.317	0.745	0.426	1.833	3.54	21.04
29.43	2924	20	157.48	0.127	0.335	0.646	0.519	1.622	3.74	17.26
39.24	2889	20	142.86	0.14	0.37	0.583	0.635	1.482	4.13	14.10
49.09	2842	20	128.56	0.156	0.411	0.487	0.844	1.258	4.59	10.61

Table H4: Engine Performance of E30 at Constant Engine Load Conditions

Load (N)	Speed (rpm)	FC (ml)	T (sec)	Vol. Rate (ml/s)	FCR (kg/h)	B.P (kW)	BSFC (kg/kW-h)	BMEP (bar)	FP (kW)	BTE (%)
E30 under Full Engine Load Condition										
9.81	3575	20	151	0.132	0.353	0.836	0.422	1.717	3.78	22.12
19.62	3570	20	147.36	0.136	0.362	0.928	0.390	1.91	3.86	23.89
29.43	3563	20	128	0.156	0.417	0.8	0.521	1.649	4.46	17.92
39.24	3558	20	120	0.167	0.445	0.7	0.636	1.444	4.76	14.69
49.09	3551	20	112	0.179	0.476	0.568	0.838	1.174	5.1	11.15
E30 under 3/4 Engine Load Condition										
9.81	3123	20	167.23	0.12	0.319	0.676	0.465	1.589	3.42	19.79
19.62	3091	20	161.7	0.124	0.330	0.784	0.422	1.862	3.53	23.22
29.43	3047	20	140	0.143	0.381	0.682	0.559	1.643	4.08	16.72
39.24	3024	20	132	0.152	0.404	0.611	0.661	1.483	4.33	14.13
49.09	2988	20	126	0.159	0.423	0.498	0.849	1.224	4.53	11
E30 under 1/2 Engine Load Condition										
9.81	3206	20	160.2	0.125	0.333	0.737	0.452	1.688	3.56	20.67
19.62	3178	20	153.73	0.13	0.347	0.794	0.437	1.834	3.53	21.37
29.43	3136	20	140.38	0.142	0.380	0.745	0.51	1.744	4.07	18.31
39.24	2968	20	121.24	0.165	0.440	0.571	0.771	1.413	4.71	12.12
49.09	2846	20	102.98	0.194	0.518	0.459	1.129	1.184	5.55	8.28

Appendix I

Engine Performance Parameters Readings at Constant Speed

Table I1: Engine Performance of E0 at Constant Engine Speeds

Load (N)	FC (ml)	T (sec)	Volume Rate (ml/s)	FCR (kg/h)	B.P (kW)	BSFC (kg/kW-h)	BMEP (Bar)	FP (kW)	BTE (%)
E0 at 2500 rpm Engine Speed									
9.81	20	72.73	0.275	0.717	0.722	0.993	2.12	8.69	8.31
19.62	20	67.23	0.297	0.776	0.794	0.977	2.33	9.40	8.44
29.43	20	66.47	0.301	0.785	0.865	0.908	2.54	9.512	9.094
39.24	20	63.09	0.317	0.827	0.922	0.897	2.71	10.021	9.201
49.09	20	57.28	0.349	0.911	0.981	0.929	2.88	11.038	8.887
E0 at 3000 rpm Engine Speed									
9.81	20	72.47	0.276	0.72	0.817	0.881	2.0	8.724	9.365
19.62	20	66.9	0.3	0.78	0.887	0.879	2.17	9.451	9.385
29.43	20	65.39	0.306	0.798	0.915	0.872	2.24	9.669	9.463
39.24	20	63.0	0.317	0.837	0.981	0.853	2.4	10.142	9.673
49.09	20	54.92	0.364	0.95	1.062	0.895	2.6	11.511	9.226
E0 at 3500 rpm Engine Speed									
9.81	20	66.34	0.301	0.786	0.944	0.833	1.98	9.524	9.912
19.62	20	61.46	0.325	0.849	1.044	0.813	2.19	10.287	10.15
29.43	20	60.18	0.332	0.867	1.12	0.774	2.35	10.505	10.66
39.24	20	58.83	0.34	0.887	1.17	0.758	2.45	10.748	10.89
49.09	20	54.24	0.369	0.962	1.206	0.798	2.53	11.656	10.35

Table I2: Engine Performance of E10 at Constant Engine Speeds

Load (N)	FC (ml)	T (sec)	Volume Rate (ml/s)	FCR (kg/h)	B.P (kW)	BSFC (kg/kW-h)	BMEP (Bar)	FP (kW)	BTE (%)
E10 at 2500 rpm Engine Speed									
9.81	20	72.96	0.274	0.719	0.721	0.997	2.12	8.35	8.63
19.62	20	67.44	0.297	0.778	0.794	0.98	2.33	9.04	8.79
29.43	20	66.49	0.301	0.789	0.862	0.915	2.53	9.16	9.41
39.24	20	62.60	0.314	0.838	0.924	0.907	2.71	9.73	9.5
49.09	20	56.47	0.354	0.929	0.981	0.947	2.88	12.5	9.09
E10 at 3000 rpm Engine Speed									
9.81	20	72.26	0.277	0.726	0.817	0.889	2.0	8.432	9.69
19.62	20	65.66	0.305	0.799	0.899	0.889	2.2	9.28	9.69
29.43	20	64.13	0.312	0.818	0.94	0.87	2.3	9.5	9.89
39.24	20	61.86	0.323	0.848	0.981	0.864	2.4	9.85	9.96
49.09	20	54.82	0.365	0.957	1.062	0.901	2.6	11.11	9.56
E10 at 3500 rpm Engine Speed									
9.81	20	65.74	0.304	0.798	0.944	0.845	1.93	14.19	10.19
19.62	20	60.93	0.328	0.861	1.044	0.825	2.19	13.49	10.44
29.43	20	59.55	0.336	0.881	1.12	0.787	2.35	13.18	10.95
39.24	20	57.97	0.345	0.905	1.167	0.775	2.45	12.83	11.1
49.09	20	53.81	0.372	0.975	1.206	0.808	2.53	11.91	10.65

Table I3: Engine Performance of E20 at Constant Engine Speeds

Load (N)	FC (ml)	T (sec)	Volume Rate (ml/s)	FCR (kg/h)	B.P (kW)	BSFC (kg/kW-h)	BMEP (Bar)	FP (kW)	BTE (%)
E20 at 2500 rpm Engine Speed									
9.81	20	73.47	0.272	0.719	0.722	0.996	2.12	8.03	8.99
19.62	20	67.64	0.3	0.781	0.795	0.982	2.33	8.73	9.11
29.43	20	66.36	0.301	0.796	0.866	0.919	2.54	8.89	9.74
39.24	20	62.59	0.32	0.844	0.922	0.915	2.71	9.43	9.78
49.09	20	56.44	0.354	0.936	0.981	0.954	2.88	10.46	9.56
E20 at 3000 rpm Engine Speed									
9.81	20	71.87	0.278	0.735	0.817	0.9	2.0	8.212	9.95
19.62	20	64.97	0.308	0.813	0.899	0.904	2.2	9.083	9.9
29.43	20	63.72	0.314	0.829	0.94	0.882	2.3	9.262	10.15
39.24	20	60.65	0.33	0.871	0.989	0.881	2.42	9.731	10.16
49.09	20	54.06	0.37	0.977	1.062	0.92	2.6	10.92	9.73
E20 at 3500 rpm Engine Speed									
9.81	20	64.66	0.309	0.817	0.939	0.87	1.95	9.128	10.29
19.62	20	60.51	0.331	0.873	1.044	0.836	2.19	9.753	10.7
29.43	20	59.15	0.338	0.893	1.121	0.797	2.35	9.977	11.24
39.24	20	57.67	0.347	0.916	1.17	0.783	2.45	10.234	11.43
49.09	20	53.74	0.372	0.983	1.216	0.808	2.68	10.982	11.07

Table I4: Engine Performance of E30 at Constant Engine Speeds

Load (N)	FC (ml)	T (sec)	Volume Rate (ml/s)	FCR (kg/h)	B.P (kW)	BSFC (kg/kW-h)	BMEP (Bar)	FP (kW)	BTE (%)
E30 at 2500 rpm Engine Speed									
9.81	20	74.3	0.269	0.718	0.722	0.994	2.12	7.69	9.393
19.62	20	67.7	0.295	0.788	0.795	0.991	2.33	8.436	9.424
29.43	20	66.27	0.302	0.805	0.865	0.931	2.54	8.618	10.037
39.24	20	62.61	0.314	0.852	0.922	0.924	2.71	9.12	10.12
49.09	20	56.63	0.353	0.942	0.981	0.96	2.88	10.085	9.728
E30 at 3000 rpm Engine Speed									
9.81	20	71.41	0.28	0.747	0.817	0.914	2.0	7.997	10.22
19.62	20	64.66	0.309	0.825	0.899	0.918	2.2	8.832	10.18
29.43	20	63.66	0.314	0.838	0.932	0.899	2.28	8.971	10.39
39.24	20	60.76	0.329	0.878	0.981	0.895	2.4	9.4	10.44
49.09	20	53.94	0.371	0.989	1.062	0.931	2.6	10.59	10.03
E30 at 3500 rpm Engine Speed									
9.81	20	64.82	0.309	0.823	0.944	0.872	1.98	8.81	10.71
19.62	20	60.48	0.331	0.882	1.044	0.845	2.19	9.44	11.06
29.43	20	58.69	0.341	0.909	1.122	0.81	2.35	9.73	11.53
39.24	20	57.48	0.348	0.928	1.17	0.793	2.45	9.935	11.78
49.09	20	53.39	0.375	0.999	1.225	0.816	2.68	10.69	11.45

Appendix J
Conversion Constants

Length

1 ft = 12 in.

1 cm = 0.3937 in.

1 in. = 2.54 cm

1 m = 3.28 feet

Area

1 ft^2 = 144 $in.^2$

1 m^2 = 10.76 ft^2

1 ft^2 = 929 cm^2

1 $in.^2$ = 6.452 cm^2

Volume

1 liter = 1000 cm^3

= 0.2642 gal

= 61.025 $in.^3$

1 ft^3 = 144 $in.^3$

= 7.482 gal

= 28.317 liter

= 28,317 cm^3

1 gal = 3.7854 liter

Mass and force

1 lb mass = 4.535 x 10^{-3} (m/s)

lb force = 4.448 (N)

dyne = 1 x 10^{-5} (N)

Density

1 $lb/in.^3$ = 1728 lb/ft^3

1 lb/ ft^3 = 16.018 kg/m^3

1 gm/cm^3 = 1000 kg/m^3

Speed

1knott/h = 0.4469 m/s

1 fps = 0.3048 m/s

1 fpm = 5.08 x 10^{-3} (m/s)

1 in/sec = 2.54 x 10^{-2} (m/s)

Force, Mass

1 lb = 4.4482 N

= 453.6 g

1 kg = 2.205 lb

= 9.80665 N

1 metric ton = 1000 kg

Pressure

1 atm = 1.033 bar

= 14.7 psi

= 101,325 N/m^2

= 29.921 in. Hg (0°C)

= 760 mm Hg (O°C)

= 1.0332 kg/cm^2

1 pound force/in^2 (psi)

= 27.684 in. of water

= 2.036 in. of Hg

= 51.715 mm Hg (0°C)

= 0.0731 kg/cm^2

1 in. H_20 = 0.0361 psi

= 0.0736 in.of Hg

Energy

1 Btu = 251.98 cal

= 1.055 kJ

1 kw-hr = 3412.2

Btu= 3600 kJ

1 kJ = 1 kw-s

1 kw-min = 56.87 Btu

1 kcal = 4.1668 kJ

1 wt-hr = 860 cal

Power

1 BTU/hr = 0.2931 W

1 BTU/sec = 1.0551 kW

Foot pound-force/min=$2.260x10^{-2}$ watt =J/s

Horsepower (550 ft-lb/sec.) = 7.457×10^2 watt

Specific Heat

1 BTU/lb-F = 4.1868 kJ/kg-K

1 Kcal/kg-K = 1 cal/g-°C

Heat Capacity

1 BTU/hr-F = 0.5274 W/°C

1 W/C = 1.8961 BTU/hr-F

Btu/lb mass= 2.326×10^3 (J/kg)

Btu/lb mass $^oF = 4.187 \times 10^3$ (J/kg.^oC)

Heat Flow

1 BTU/hr = 0.2931 W

1 watt = 3.411 BTU/hr

Btu-in/hr-ft^2-^oF =$1.441x10^{-1}$(W/m ^oC)

=1.441×10^1(W-cm/$m^{2o}C$)

1 Kcal/(m.hr.K) = 1.1630 W/(m.K)

1W/(m.K) = 0.859845 Kcal/(m.hr.K)

Heat transfer coefficient

1 Kcal/(m^2.hr.K) = 1.1630 W/(m^2.K)

1 W/(m^2.K) = 0.859845 Kcal/(m^2.hr.K)

Diffusivity

$Ft^2/hr = 2.58 \times 10^{-5}$ (m^2/s)

Temperature

°F = 1.8°C + 32

°C = [°F – 32] / 1.8

Appendix K

Different Views of the Distiller

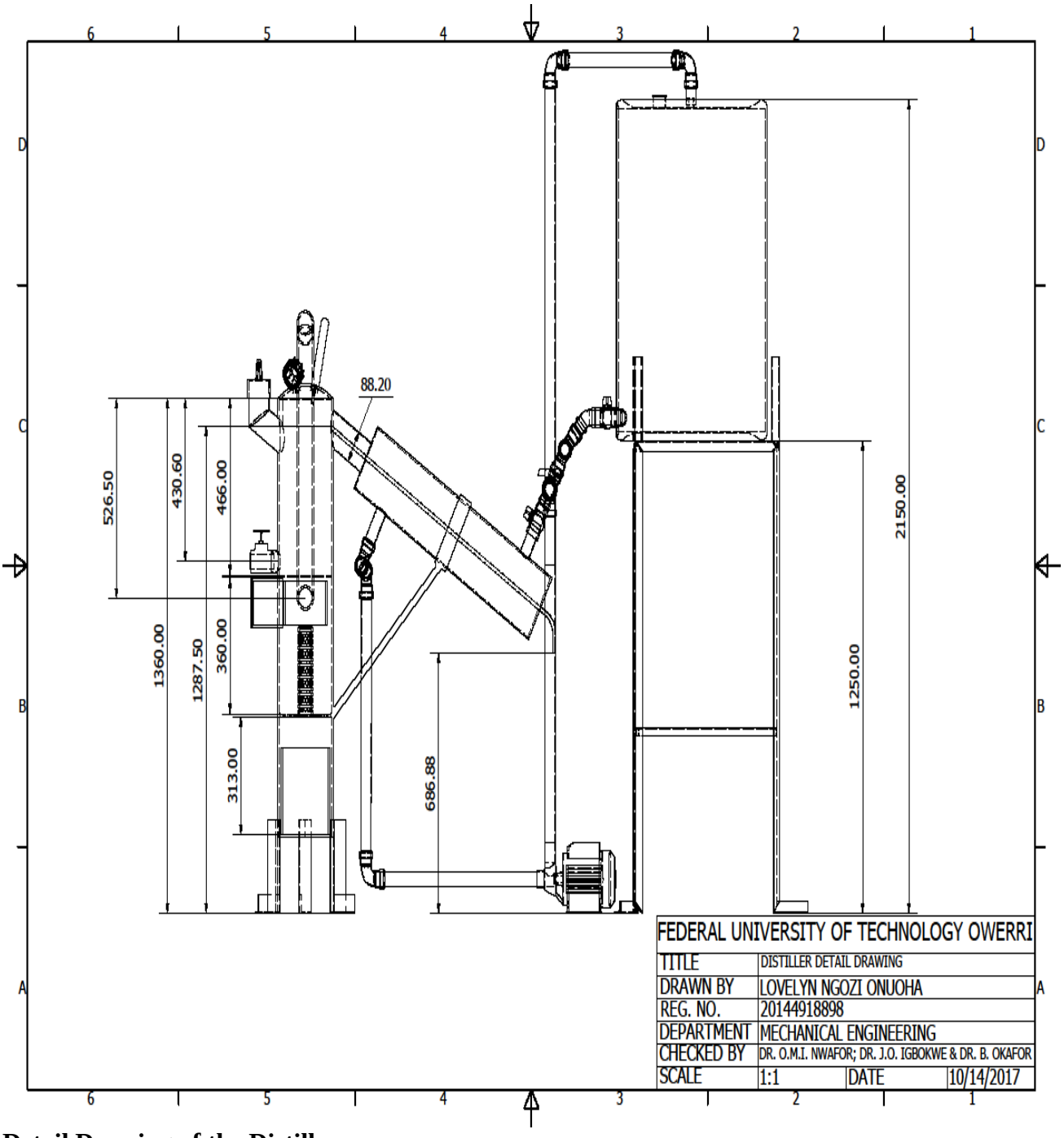

Detail Drawing of the Distiller

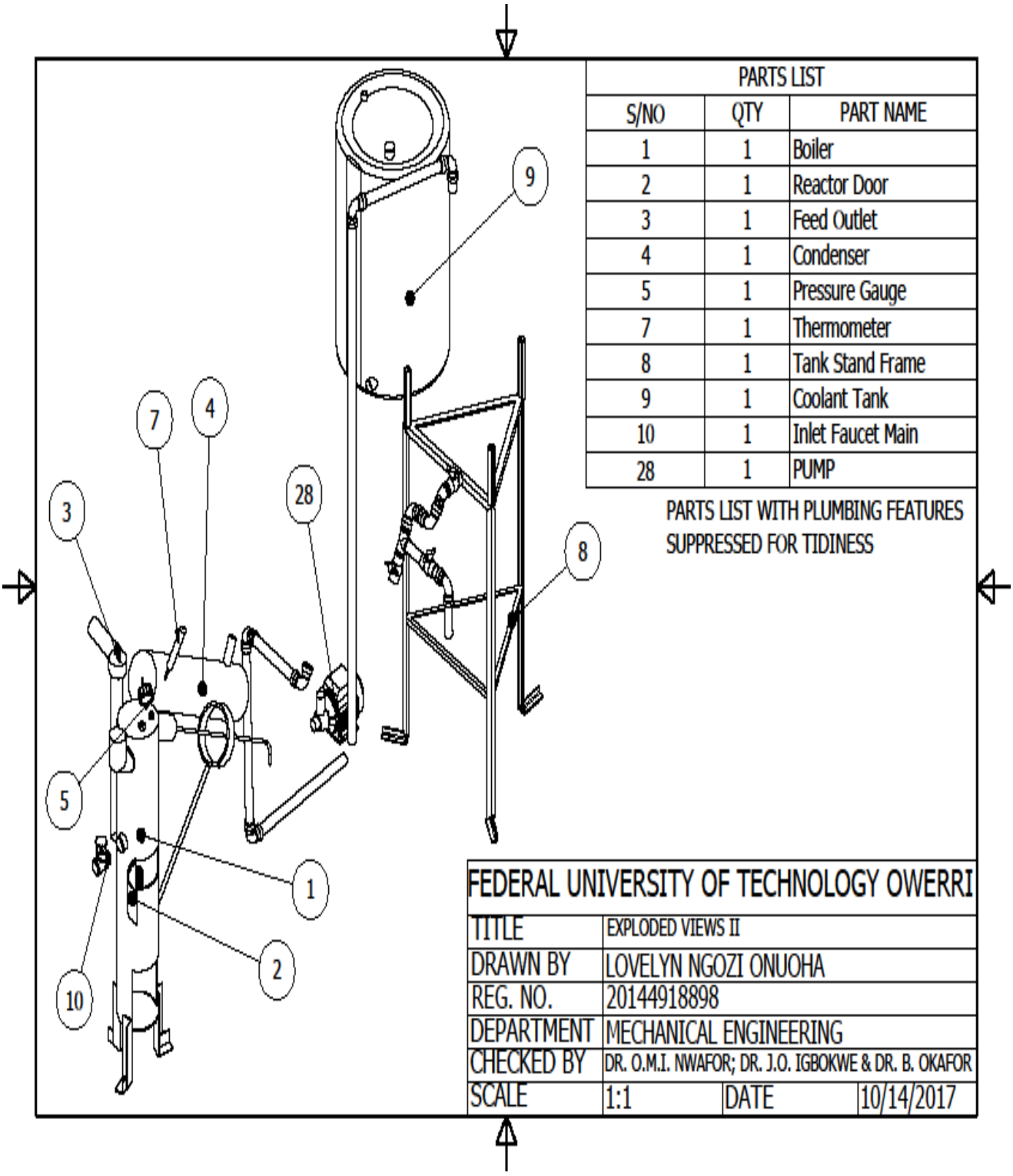

PARTS LIST		
S/NO	QTY	PART NAME
1	1	Boiler
2	1	Reactor Door
3	1	Feed Outlet
4	1	Condenser
5	1	Pressure Gauge
7	1	Thermometer
8	1	Tank Stand Frame
9	1	Coolant Tank
10	1	Inlet Faucet Main
28	1	PUMP

PARTS LIST WITH PLUMBING FEATURES SUPPRESSED FOR TIDINESS

FEDERAL UNIVERSITY OF TECHNOLOGY OWERRI			
TITLE	EXPLODED VIEWS II		
DRAWN BY	LOVELYN NGOZI ONUOHA		
REG. NO.	20144918898		
DEPARTMENT	MECHANICAL ENGINEERING		
CHECKED BY	DR. O.M.I. NWAFOR; DR. J.O. IGBOKWE & DR. B. OKAFOR		
SCALE	1:1	DATE	10/14/2017

Exploded View of the Distiller

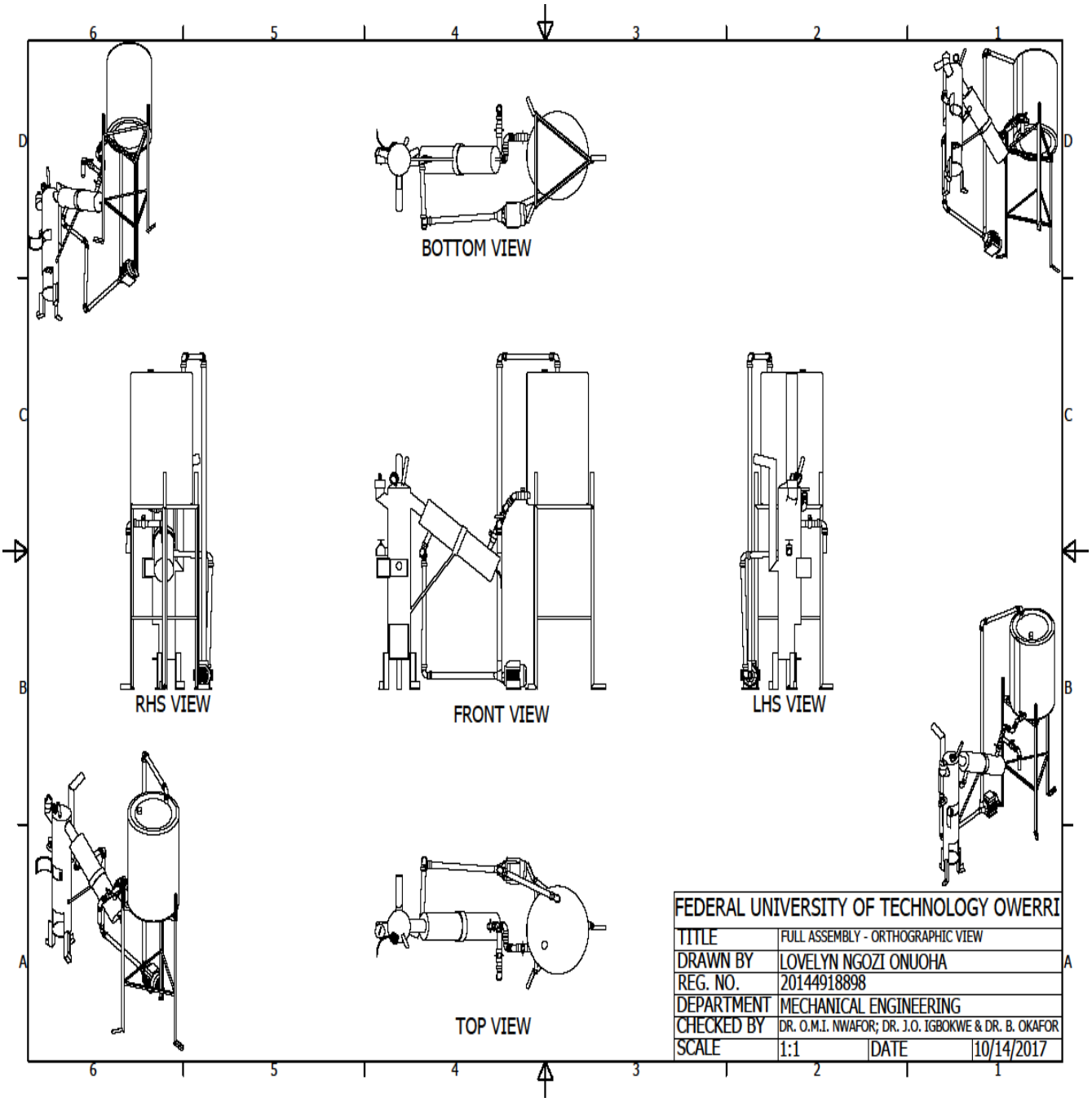

Orthographic Views of the Distiller

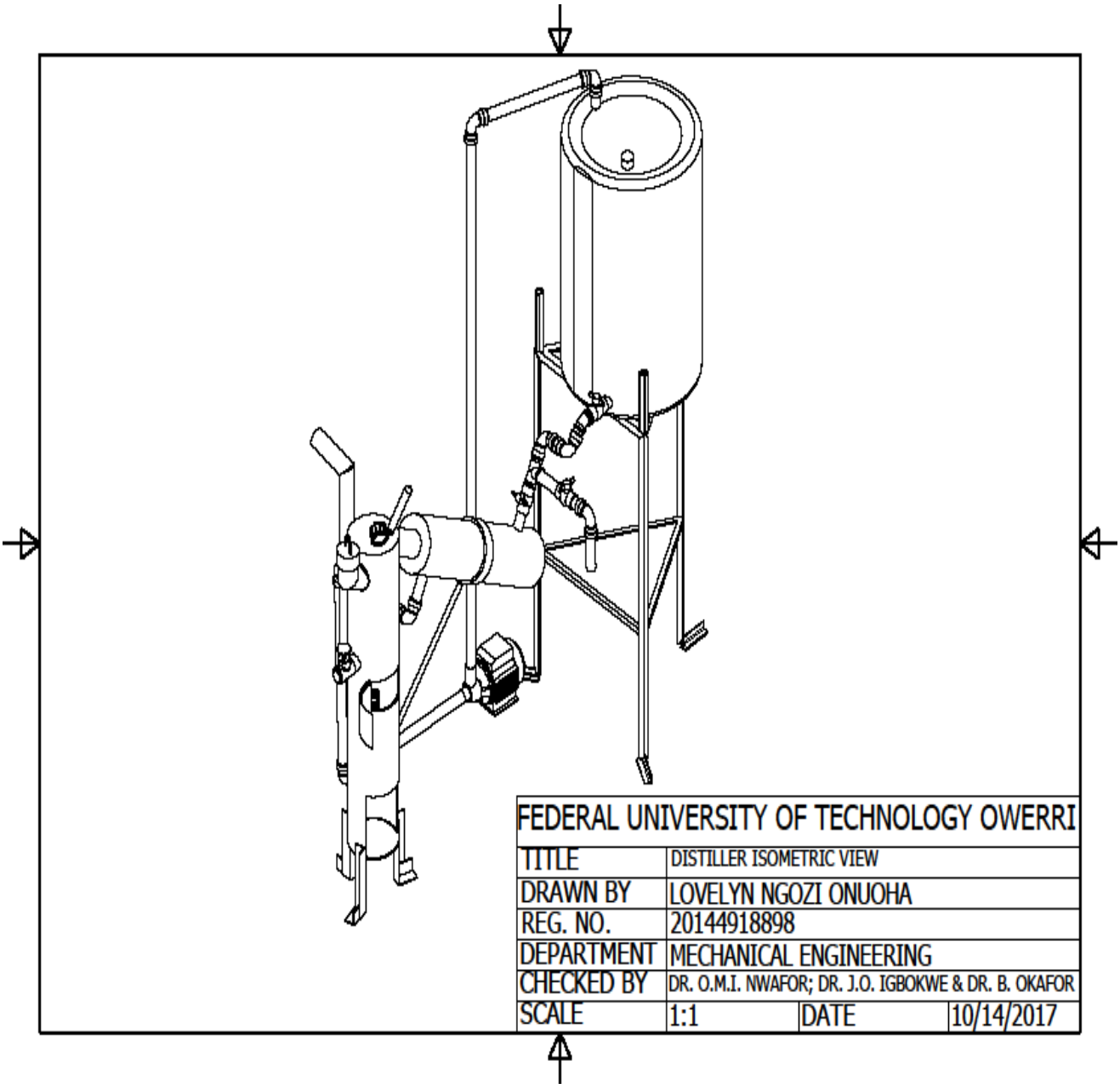

Isomeric View of the Distiller